

Observation of infectious *Legionella pneumophila*  
in host model *Caenorhabditis elegans*

by

Jacqueline Rene Hellinga

A thesis submitted to the Faculty of Graduate Studies of  
The University of Manitoba

In partial fulfillment of the requirements for the degree of

Master of Science

Department of Microbiology

University of Manitoba

Winnipeg, MB

Copyright © 2014 by Jacqueline Rene Hellinga

## Abstract

The Gram-negative bacterium *Legionella pneumophila* is an intracellular parasite of aquatic protozoa. It exhibits a distinct dimorphic lifecycle that alternates between vegetative replicative form (RF) and infectious cyst-like form (CLF). Inadvertent inhalation of aerosolized CLFs by immunocompromised individuals leads to an infection in alveolar macrophages causing Legionnaires' disease characterized by atypical pneumonia. *Legionella* uses its Dot/Icm type IV protein secretion system to secure effectors to establish a replication niche in the host cell. To date more than 300 effector molecules have been identified to alter host trafficking pathways such as programmed cell death (PCD) and phagosome-lysosome fusion pathway. To further study a *Legionella* infection the use of the multicellular organism *Caenorhabditis elegans* was done. Due to the *C. elegans* multiple innate immune pathways activated upon a response to pathogenic bacteria in the intestine and their ability to elicit germline apoptosis as an immune defense, these organisms could potentially further the understanding of *Legionella* infections in multicellular organisms. *C. elegans* share homology with core innate immune defense molecules of mammals. Here we show by counts of apoptotic cells in the gonad arm that Dot/Icm secreted effector molecules interact with the *C. elegans* PCD pathway. Differential Interference Contrast (DIC) microscopy of live *L. pneumophila* infected nematodes shows Legionella-containing vacuoles (LCVs) with motile forms. Observed by DIC, the locations of LCVs, outside of the intestine, are in the pseudocoelomic cavity and gonadal tissues. Transmission Electron Microscopy (TEM) has defined the ultrastructure of *L. pneumophila* forms found in the primary infection site of the intestinal lumen along with the secondary infection site in the gonadal tissues. The LCVs in the pseudocoelom found by DIC could not be identified by TEM. These findings suggest the

possible intracellular replication cycle of *Legionella* occurring in the gonadal tissues of the nematode. Providing an insight and a plausible evolutionary origin of the ability of *L. pneumophila* to manipulate the macrophage innate immune system.

## **Acknowledgements**

I would like to thank my supervisor, Dr. Brassinga for her support and mentorship.

A special thanks to my committee members, Dr. Kormish for her guidance on *C. elegans* anatomy and microscopy techniques; and Dr. Sparling for his valuable guidance throughout the course of my studies.

Thank you to Dr. Garduño in the Department of Microbiology and Immunology at Dalhousie University for his time in consulting, guidance, and the use of his Electron Microscope.

I would also like to thank André Dufresne in the Department of Biological Sciences at University of Manitoba for technical microscopic support; Mary Ann Trevors at the Department of Electron Microscope Services and Microbiology and Immunology at Dalhousie University for helping to cut EM grids; those at the Terebiznik lab in the Department of Biological Sciences at the University of Toronto in Scarborough for their help in cell culture staining.

Lastly, I would like to thank Miss Jennifer Tanner, Mr. Aniel Moya-Torres, and Mr. Palak Patel for all of their help and support in the lab.

This work was supported by the Manitoba Health Research Council (MHRC) and University of Manitoba Graduate Studies, Faculty of Science (UMGS).



## Table of Contents

<b>Abstract .....</b>	<b>i</b>
<b>Acknowledgements .....</b>	<b>iii</b>
<b>List of Tables .....</b>	<b>ix</b>
<b>List of Figures .....</b>	<b>x</b>
<b>List of Copyrighted Material for which Permission was Obtained.....</b>	<b>xvi</b>
<b>List of Abbreviations .....</b>	<b>xvii</b>
<b>Chapter 1: Introduction .....</b>	<b>1</b>
<b>1.1 <i>Legionella pneumophila</i>.....</b>	<b>1</b>
<b>1.2 <i>Legionella pneumophila</i> infection cycle in Alveolar Macrophages .....</b>	<b>6</b>
1.2.1 Alveolar Macrophage Innate Immune response .....	8
<b>1.3 <i>C. elegans</i> .....</b>	<b>11</b>
1.3.1 General Information .....	11
1.3.2 Innate Immune System .....	16
1.3.3 Germline Apoptosis.....	23
1.3.4 Oocyte Endocytosis Pathway .....	27
1.3.5 <i>Legionella pneumophila</i> infection characteristics in <i>C. elegans</i> .....	31
<b>1.4 Study Aims.....</b>	<b>33</b>
<b>Chapter 2: Materials and Methods .....</b>	<b>34</b>
<b>2.1 Bacterial strains .....</b>	<b>34</b>
<b>2.2 Nematode strains .....</b>	<b>36</b>
<b>2.3 Culture Conditions .....</b>	<b>37</b>

2.3.1 <i>E. coli</i> culture conditions .....	37
2.3.2 <i>S. enterica</i> serovar Typhimurium culture conditions .....	37
2.3.3 <i>L. pneumophila</i> culture conditions .....	37
2.3.4 Heat-Killed <i>L. pneumophila</i> culture conditions .....	38
2.3.5 Heat-Killed <i>E. coli</i> OP50 culture conditions .....	39
<b>2.4 Maintenance of Nematode Strains .....</b>	<b>39</b>
2.4.1 Nematode Propagation .....	39
2.4.2 Nematode Propagation from frozen stock .....	40
2.4.3 RNAi Nematode Propagation .....	40
2.4.4 Synchronization of Nematode Population .....	41
2.4.5 Freezing Nematode Population .....	42
<b>2.5 Survival Assays.....</b>	<b>43</b>
<b>2.6 Nomarski optics of <i>C. elegans</i> infected with <i>L. pneumophila</i> .....</b>	<b>44</b>
<b>2.7 Fluorescent Imaging of <i>C. elegans</i> infected with <i>L. pneumophila</i> .....</b>	<b>44</b>
<b>2.8 Assessment of Infected <i>C. elegans</i> Tissues.....</b>	<b>45</b>
<b>2.9 Germline Apoptotic Counts Assays .....</b>	<b>46</b>
2.9.1 MD701 strain.....	46
2.9.2 RNAi on MD701 strain .....	47
<b>2.10 Transmission Electron Micrographs .....</b>	<b>47</b>
<b>2.11 Immunogold .....</b>	<b>49</b>
2.11.1 Preparation of Immunogold Electron Micrograph grids .....	49
2.11.2 Immunogold Tagging of Electron Micrograph grids .....	50

<b>Chapter 3: Results</b>	<b>53</b>
<b>3.1 Assessing Virulence of <i>L. pneumophila</i> in <i>C. elegans</i></b>	<b>53</b>
<b>3.2 Morphology changes in <i>C. elegans</i></b>	<b>54</b>
3.2.1 Morphology of the posterior tail region	56
3.2.2 Morphology of the vulva and uterus region	60
3.2.3 Morphology of the intestinal tract	64
<b>3.3 <i>C. elegans</i> Intestinal tract colonization and morphology</b>	<b>70</b>
3.3.1 Colonization of the intestinal tract	70
3.3.2 Constipation and swelling of the intestinal tract	73
3.3.3 Manipulation of the intestine apical membrane	75
<b>3.4 <i>L. pneumophila</i> secondary infection sites</b>	<b>82</b>
3.4.1 <i>L. pneumophila</i> presence in the pseudocoelomic cavity	82
3.4.2 <i>L. pneumophila</i> growth in the gonadal tissue	86
3.4.3 <i>L. pneumophila</i> forms expelled from the <i>C. elegans</i>	90
3.4.4 Assessment of infected tissues by wild-type <i>L. pneumophila</i>	93
3.4.5 <i>L. pneumophila</i> chromosomal GFP expression in <i>C. elegans</i> gonadal tissues	96
<b>3.5 <i>L. pneumophila</i> observed bacterial morphology in <i>C. elegans</i></b>	<b>99</b>
<b>3.6 Infection characteristics of <i>C. elegans</i> fed <i>L. pneumophila</i> <math>\Delta dotA</math> and <math>\Delta sdhA</math> mutant strains</b>	<b>106</b>
3.6.1 Survival curves of <i>C. elegans</i> fed <i>L. pneumophila</i> $\Delta dotA$ and $\Delta sdhA$ mutant strains	107
3.6.2 Phenotypical evaluation of <i>C. elegans</i> fed <i>L. pneumophila</i> $\Delta dotA$ mutant strain	109

3.6.3 Phenotypical evaluation of <i>C. elegans</i> fed <i>L. pneumophila</i> $\Delta dotA$ complemented strain.....	112
3.6.4 Phenotypical evaluation of <i>C. elegans</i> fed <i>L. pneumophila</i> $\Delta sdhA$ mutant strain..	114
3.6.5 Phenotypical evaluation of <i>C. elegans</i> fed <i>L. pneumophila</i> $\Delta sdhA$ complemented strain.....	116
<b>3.7 Germline Apoptosis</b> .....	116
3.7.1 Germline apoptosis assay of known apoptotic <i>L. pneumophila</i> mutant strains .....	119
3.7.2 Germline Apoptosis assay of <i>L. pneumophila</i> Dot/Icm component mutant strains .....	124
3.7.3 Germline Apoptosis assay of CED-3 .....	126
3.7.4 Germline Apoptosis assay of SEK-1 .....	129
3.7.5 Germline Apoptosis assay of VHP-1 .....	131
<b>3.8 Effects of the Oocyte Endocytosis pathway during an <i>L. pneumophila</i> infection</b> .....	133
3.8.1 Survival Proportion of $\Delta rme-1(b1045)$ <i>C. elegans</i> during infection with various <i>L. pneumophila</i> strains .....	135
3.8.2 Phenotype of $\Delta rme-1(b1045)$ <i>C. elegans</i> during a wild-type <i>L. pneumophila</i> infection .....	138
3.8.3 Survival Proportions of RME-2 knockdown gene expression in <i>C. elegans</i> .....	141
3.8.4 Germline Apoptosis assay of RNAi RME-2 .....	143
<b>Chapter 4: Discussion</b> .....	146
<b>4.1 Pathology of <i>L. pneumophila</i>-infected nematodes</b> .....	147
<b>4.2 <i>Legionella pneumophila</i> infection affects on Germline PCD</b> .....	149
<b>4.3 Secondary <i>L. pneumophila</i> Infection Sites in <i>C. elegans</i></b> .....	152
4.3.1 Effector protein and component involved in intracellular replication.....	156

4.3.2 Oocyte Endocytosis proteins involved in intracellular replication.....	157
<b>4.4</b> Proposed Lifecycle of <i>Legionella pneumophila</i> in <i>C. elegans</i> .....	158
<b>4.5</b> Conclusions .....	159
<b>4.6</b> Future Directions.....	161
<b>References</b> .....	<b>163</b>

## List of Tables

<b>Table 1.1</b> Ultrastructure of various <i>L. pneumophila</i> forms .....	5
<b>Table 2.1</b> Catalogue of Bacteria Strains used.....	29
<b>Table 2.2</b> Catalogue of Nematode Strains used .....	31
<b>Table 3.1</b> Assessment of CLFs found in <i>C. elegans</i> pseudocoelomic cavity and tail during various <i>L. pneumophila</i> strain infections.....	83
<b>Table 3.2</b> Assessment of CLFs found in <i>C. elegans</i> gonad and gonad arm tissues during various <i>L. pneumophila</i> strain infections.....	88
<b>Table 3.3</b> Assessment of CLFs in <i>C. elegans</i> vulva and expelled from vulva during various <i>L. pneumophila</i> strain infections.....	91

## List of Figures

<b>Figure 1.1</b> Ultrastructure of various <i>L. pneumophila</i> forms .....	2
<b>Figure 1.2</b> Intracellular Lifecycle of <i>L. pneumophila</i> in macrophage cells and Non-pathogenic intracellular trafficking of non-pathogenic bacteria .....	4
<b>Figure 1.3</b> <i>L. pneumophila</i> affect on Macrophage Apoptotic pathways .....	9
<b>Figure 1.4</b> <i>C. elegans</i> lifecycle by developmental states at 22°C .....	13
<b>Figure 1.5</b> <i>C. elegans</i> adult anatomy .....	15
<b>Figure 1.6</b> The innate immune system of <i>C. elegans</i> .....	18
<b>Figure 1.7</b> The components of the various Innate Immune pathways in <i>C. elegans</i> .....	19
<b>Figure 1.8</b> Germline Apoptosis in <i>C. elegans</i> .....	24
<b>Figure 1.9</b> Oocyte Endocytosis in <i>C. elegans</i> .....	28
<b>Figure 3.1</b> Kaplan-Meier survival curve of wild-type <i>L. pneumophila</i> in wild-type N2 Bristol <i>C. elegans</i> .....	55
<b>Figure 3.2</b> Observed morphology of the tail region of N2 <i>C. elegans</i> fed <i>E. coli</i> OP50 on NGM .....	57
<b>Figure 3.3</b> Observed morphology of the tail region of N2 <i>C. elegans</i> fed heat-killed <i>E. coli</i> OP50 on BCYE .....	58

<b>Figure 3.4</b> Observed morphology of the tail region of N2 <i>C. elegans</i> fed heat-killed wild-type <i>L. pneumophila</i> .....	59
<b>Figure 3.5</b> Observed morphology of the vulva and uterus region of N2 <i>C. elegans</i> fed <i>E. coli</i> OP50 on NGM .....	61
<b>Figure 3.6</b> Observed morphology of the vulva and uterus region of N2 <i>C. elegans</i> fed heat-killed <i>E. coli</i> OP50 on BCYE.....	62
<b>Figure 3.7</b> Observed morphology of the vulva and uterus region of N2 <i>C. elegans</i> fed heat-killed wild-type <i>L. pneumophila</i> .....	63
<b>Figure 3.8</b> Observed morphology of the anterior intestinal region of N2 <i>C. elegans</i> fed <i>E. coli</i> OP50 on NGM .....	66
<b>Figure 3.9</b> Observed morphology of the anterior intestinal region of N2 <i>C. elegans</i> fed heat-killed <i>E. coli</i> OP50 on BCYE.....	67
<b>Figure 3.10</b> Observed morphology of the anterior intestinal region of N2 <i>C. elegans</i> fed heat-killed wild-type <i>L. pneumophila</i> .....	68
<b>Figure 3.11</b> Transmission electron micrographs in the intestine of heat-killed wild-type <i>L. pneumophila</i> fed <i>C. elegans</i> .....	69
<b>Figure 3.12</b> Observed morphology of the anterior intestinal lumen region of N2 <i>C. elegans</i> fed <i>L. pneumophila</i> .....	72



<b>Figure 3.13</b> Transmission electron micrographs of <i>L. pneumophila</i> in intestinal lumen of <i>C. elegans</i> .....	74
<b>Figure 3.14</b> Observed morphology of the intestinal region of <i>C. elegans</i> fed <i>L. pneumophila</i> .....	76
<b>Figure 3.15</b> Transmission electron micrographs of <i>L. pneumophila</i> forms in various components of the brush boarder and supporting components of the intestine .....	78
<b>Figure 3.16</b> Transmission electron micrographs of <i>L. pneumophila</i> manipulating the apical membrane and microvilli of the intestine of <i>C. elegans</i> .....	80
<b>Figure 3.17</b> Transmission electron micrographs of <i>L. pneumophila</i> forms leaving the lumen of the intestine in tight vacuoles .....	81
<b>Figure 3.18</b> Observed morphology of the pseudocoelomic (body) cavity of <i>C. elegans</i> fed <i>L. pneumophila</i> .....	85
<b>Figure 3.19</b> Observed morphology of the gonadal tissues of <i>C. elegans</i> fed <i>L. pneumophila</i> .....	87
<b>Figure 3.20</b> Observed morphology of the vulva region and expelled LCVs of <i>C. elegans</i> fed <i>L. pneumophila</i> .....	92
<b>Figure 3.21</b> Transmission electron micrographs of <i>L. pneumophila</i> LCVs in various <i>C. elegans</i> tissues .....	94

<b>Figure 3.22</b> Infection day 6 epifluorescent image of $\Delta glo-3(kx94)$ <i>C. elegans</i> gonadal tissue fed GFP-tagged <i>L. pneumophila</i> .....	98
<b>Figure 3.23</b> Infection day 8 epifluorescent image of $\Delta glo-3(kx94)$ <i>C. elegans</i> gonadal tissue fed GFP-tagged <i>L. pneumophila</i> .....	100
<b>Figure 3.24</b> Transmission electron micrographs of replicative <i>L. pneumophila</i> in various <i>C. elegans</i> tissues .....	102
<b>Figure 3.25</b> Transmission electron micrographs of transitioning <i>L. pneumophila</i> forms in various <i>C. elegans</i> tissues. ....	105
<b>Figure 3.26</b> Kaplan-Meier survival curve of <i>L. pneumophila</i> wild-type, $\Delta dotA$ and $\Delta sdhA$ mutant strains survival assay in WT N2 <i>C. elegans</i> .....	108
<b>Figure 3.27</b> Observed morphology of the intestinal region of <i>C. elegans</i> fed <i>L. pneumophila</i> $\Delta dotA$ mutant strain.....	110
<b>Figure 3.28</b> Observed morphology of the secondary infection sites of <i>C. elegans</i> fed <i>L. pneumophila</i> $\Delta dotA$ mutant strain.....	111
<b>Figure 3.29</b> Observed morphology of secondary infection sites of <i>C. elegans</i> fed <i>L. pneumophila</i> $\Delta dotA$ complement strain.....	113
<b>Figure 3.30</b> Observed morphology of secondary infection site of <i>C. elegans</i> fed <i>L. pneumophila</i> $\Delta sdhA$ mutant strain .....	115

<b>Figure 3.31</b> Observed morphology of secondary infection sites of <i>C. elegans</i> fed <i>L. pneumophila</i> $\Delta$ <i>sdhA</i> complement strain.....	117
<b>Figure 3.32</b> Timeline of Apoptotic cell counts in CED-1::GFP nematodes infected with various bacterial strains .....	120
<b>Figure 3.33</b> Germline apoptotic counts of infected transgenic CED-1::GFP <i>C. elegans</i> with various <i>L. pneumophila</i> effector molecule mutant strains at 24 hour time point.....	122
<b>Figure 3.34</b> Germline apoptotic cell counts of infected transgenic CED-1::GFP <i>C. elegans</i> with various <i>Dot/Icm L. pneumophila</i> mutant strains at 24 hour time point .....	125
<b>Figure 3.35</b> Germline apoptotic cell counts of RNAi <i>ced-3</i> CED-1::GFP <i>C. elegans</i> infected with various <i>L. pneumophila</i> strains at 24 hour time point .....	128
<b>Figure 3.36</b> Germline apoptosis cell counts of RNAi <i>sek-1</i> CED-1::GFP <i>C. elegans</i> infected with various <i>L. pneumophila</i> strains at 24 hour time point .....	130
<b>Figure 3.37</b> Germline Apoptosis Cell Counts of RNAi <i>vhp-1</i> CED-1::GFP <i>C. elegans</i> infected with various <i>L. pneumophila</i> strains at 24 hour time point .....	132
<b>Figure 3.38</b> Kaplan-Meier survival curve of $\Delta$ <i>rme-1(b1045)</i> <i>C. elegans</i> infected with wild-type <i>L. pneumophila</i> .....	136
<b>Figure 3.39</b> Kaplan-Meier survival curve of $\Delta$ <i>rme-1(b1045)</i> nematodes infected with wild-type $\Delta$ <i>dotA</i> and $\Delta$ <i>sdhA</i> mutant <i>L. pneumophila</i> strains .....	137

<b>Figure 3.40</b> Observed morphology of intestinal region of $\Delta rme-1$ (d1045) <i>C. elegans</i> fed wild-type <i>L. pneumophila</i> .....	139
<b>Figure 3.41</b> Observed morphology of intestinal region and secondary infection sites of $\Delta rme-1$ (d1045) <i>C. elegans</i> during a wild-type <i>L. pneumophila</i> infection .....	140
<b>Figure 3.42</b> Observed morphology of secondary gonad infection site of $\Delta rme-1$ (d1045) <i>C. elegans</i> fed wild-type <i>L. pneumophila</i> .....	142
<b>Figure 3.43</b> Kaplan-Meier survival curve of RNAi <i>rme-2</i> knockdown <i>C. elegans</i> infected with wild-type <i>L. pneumophila</i> .....	144
<b>Figure 3.44</b> Germline apoptotic cell counts of RNAi <i>rme-2</i> CED-1::GFP <i>C. elegans</i> infected with various <i>L. pneumophila</i> strains at 24 hour time point .....	145
<b>Figure 4.1</b> Schematic of <i>L. pneumophila</i> movement in the <i>C. elegans</i> host model .....	160

List of copyrighted material used in this study

<b>Section</b>	<b>Reference</b>	<b>Licence ID</b>
Figure 1.2	Isberg, <i>et al.</i> , 2009	3400891506630
Figure 1.5	Sifri, <i>et al.</i> , 2005	3401090485713
Figure 1.6	Millet, and Ewbank, 2004	3400940506970
Figure 1.7	Schulenburg, <i>et al.</i> , 2008	3400960023227

## List of Abbreviations

63X	magnification 63X 1.4 oil DIC objective lens
ABC	ATP-binding cassette
AM	apical membrane of <i>C. elegans</i> intestinal lumen
Amp	ampicillin
Ant. bulb	Anterior bulb
$\beta$	beta
BCYE	buffered charcoal yeast extract
BYE	buffered yeast extract
CaCl <sub>2</sub>	calcium chloride
<i>C. elegans</i>	<i>Caenorhabditis elegans</i>
CLF	cyst-like form
CO <sub>2</sub>	carbon dioxide
°C	degrees Celsius
$\Delta$	inactivation of gene
d	days
DAF-2/DAF-16	Insulin-like DAF-2/DAF 16 pathway
DBL	Dmp/Bpp-like
DNA	deoxyribonucleic acid
DNA-J	Chaperone DnaJ or Hsp40
<i>Dod</i>	downstream of DAF-16

Dot/icm	Dot/icm type four secretion system
<i>E. coli</i>	<i>Escherichia coli</i>
<i>E. coli</i> OP50	<i>Escherichia coli</i> OP50 benign <i>C. elegans</i> food source
<i>E. faecalis</i>	<i>Enterococcus faecalis</i>
ER	endoplasmic reticulum
ERK	extracellular signal-regulated kinase
ETR	effector-triggered response
g	gram
GFP	green fluorescent protein
h	hour
HeLa	Henrietta Lacks
IC	intestinal cell
IL	intestinal lumen
Inc	inclusion of poly- $\beta$ -hydroxybutyrate
JNK	c-Jun N-terminal kinase pathway
KOH	potassium hydroxide
L	liter
L1	larval stage 1
L2	larval stage 2
L2d	larval stage 2 dauer
L3	larval stage 3
L4	larval stage 4

<i>L. pneumophila</i>	<i>Legionella pneumophila</i>
<i>Legionella spp.</i>	<i>Legionella species</i>
LB	Luria-Bertani
LCV	<i>Legionella</i> -containing vacuole
LDL	low-density lipoprotein
MAPK	mitogen-activated protein kinase
MEK	mitogen/extracellular signal-regulated kinase
µg	microgram
µm	micrometer
µM	micromolar
mg	milligram
min	minute
mL	milliliter
mm	millimeter
mM	millimolar
MgCl	magnesium chloride
N2	Wild-Type Bristol <i>C. elegans</i>
NaCl	sodium chloride
NF-κB	nuclear factor kappa-light-chain-enhancer of activated B cells
ng	nanogram
nm	nanometer
OD	optical density



p38	p38 mitogen activated protein kinase
<i>P. aeruginosa</i>	<i>Pseudomonas aeruginosa</i>
PB	posterior bulb
PCD	Programmed Cell Death
PHBA	poly- $\beta$ -hydroxybutyrate
RF	replicative form
RNAi	ribonucleic acid interference
rpm	revolutions per minute
RT	room temperature
s	second
SAPK	stress-activated protein kinase pathway
<i>S. enterica</i>	<i>Salmonella enterica</i>
SL1344	<i>Salmonella enterica</i> Serovar Typhimurium SL1344
<i>S. Typhimurium</i>	<i>Salmonella enterica</i> Serovar Typhimurium SL1344
T4SS	type four-secretion system
Term. bulb	Terminal bulb
TGF- $\beta$	Transforming Growth Factor-beta
Thy	thymidine
TS	Transition state
WT	Wild Type
YP170	VIT-2 gene, vitellogenin structural gene

## Chapter 1: Introduction

### 1.1 *Legionella pneumophila*

The environmental *Legionella pneumophila* is a Gram-negative, gamma-proteobacterium intracellular parasite of aquatic protozoa (Berk *et al.*, 1998; Fields, 1996; Molofsky and Swanson, 2004). *L. pneumophila* is incapable of replicating extracellularly in the environment due to their obligate requirement for L-cysteine and other essential nutrients (Ewann and Hoffman, 2006). In infected aquatic protozoa, *L. pneumophila* exhibits a distinct dimorphic lifecycle that alternates between the vegetative replicative form (RF) and the infectious cyst-like form (CLF) (Garduño *et al.*, 2002) (Figure 1.1).

The *L. pneumophila* RF is a rod-shaped, typical Gram-negative ultrastructure, length between 1.5 µm to 3.0 µm, non-motile and non-infectious (Garduño *et al.*, 2002). Once taken in the protozoa host cell, *L. pneumophila* will form a *Legionella*-containing vacuole (LCV), which will divert host trafficking pathways and recruit host organelles such as mitochondria and ribosomes. In the LCV *L. pneumophila* will undergo multiple rounds of replication dependent on the concentration of nutrients in the host cell, specifically L-cysteine. Various amino acids are utilized as a source of carbon and energy by *L. pneumophila* in the protozoan host cell; the RF is prevalent (Faulkner and Garduño, 2002). Then when nutrients from the protozoa start to deplete the *L. pneumophila* replicative form receives a series of intracellular signals and enters into a transition state (TS) (Faulkner *et al.*, 2008) (Figure 1.1).

In the transition state, *L. pneumophila* develops characteristics of the infectious CLFs. During this state, there is a thickening of the outer membrane due to the production of multiple

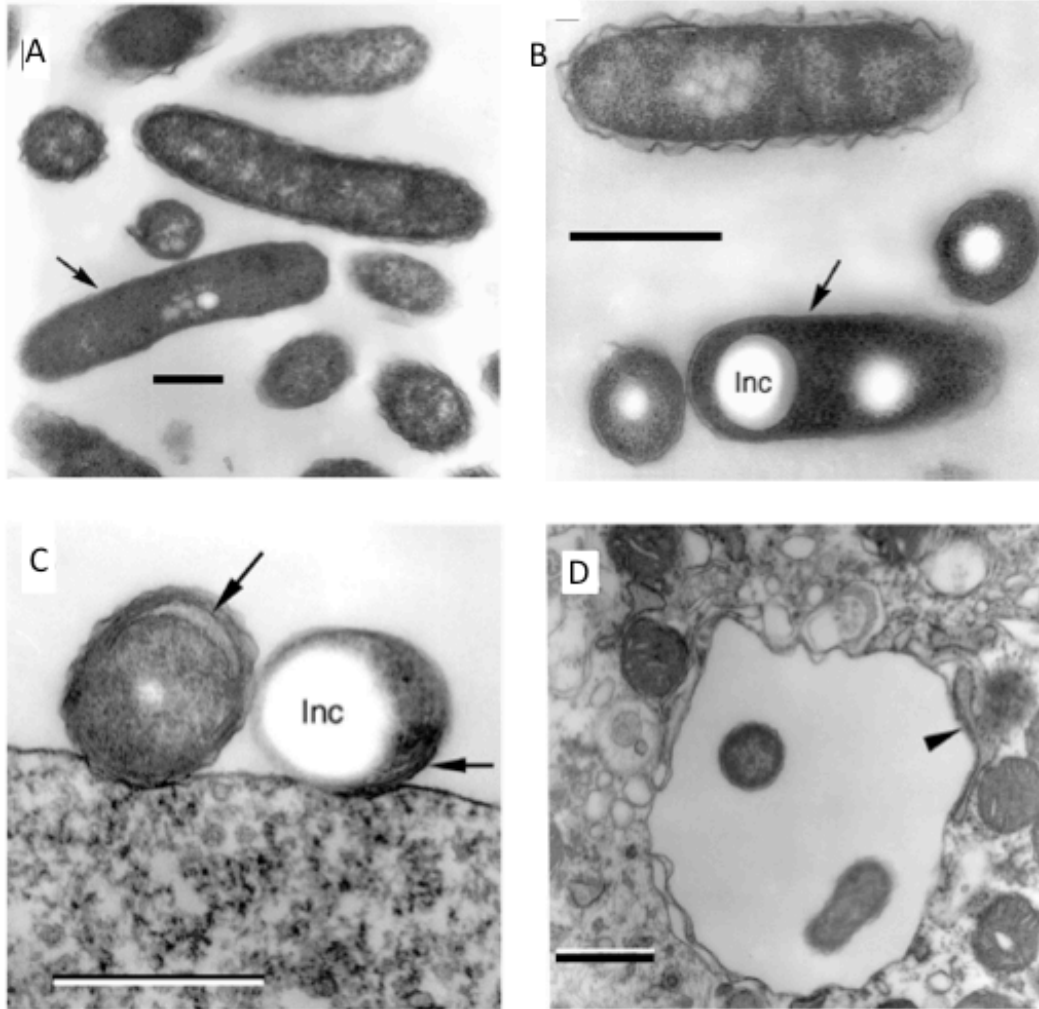


Figure 1.1 Ultrastructure of various *L. pneumophila* forms. A) The arrow indicates a transitioning form with its smooth outer membrane. Above and to the left is a typical replicative form with Gram-negative cell qualities. B) Other types of transitioning forms, arrow indicates the smooth membrane, note the inclusion as well. Above is a form with a wavy membrane. C) CLF forms, the arrow indicates the thick outer membrane that is pulling away. The second arrow indicates an inclusion and an electron dense area. D) An early LCV in the HeLa cells, note the recruitment of organelles around it. Also, the thin electron dense membrane is seen surrounding the non-replicative forms. Scale bars: 500 nm. Images obtained from Faulkner and Garduño, 2002.

inner leaflets of the outer membranes giving the bacteria an ultrastructural characteristic of multiple wavy outer membranes (Garduño *et al.*, 2002). The bacteria generally shorten and length ranges anywhere between 2 µm to 0.5 µm with dense cytoplasm (Faulkner and Garduño, 2002). When the nutrients are completely depleted from the host cell environment *L. pneumophila* enters into a CLF.

The CLF is 0.5 µm in length, has distinct morphological characteristics of a thickened cell wall, intracytoplasmic membranes and poly-β-hydroxybutyrate inclusions (PHBA) (Garduño *et al.*, 2002) (Figure 1.1). Other characteristics of the CLFs are their metabolic dormant state, motility, and their resistance to osmotic shock, chlorine, heat, detergent and antibiotics (Garduño *et al.*, 2002; Koubar *et al.*, 2011). CLFs are expelled from the protozoan host through cell lysis into the water environment (Berk *et al.*, 1998). *L. pneumophila* then repeats its dimorphic lifecycle by infecting new protozoan hosts (Figure 1.2, part A).

*L. pneumophila* also exhibits a distinct intracellular and extracellular lifecycle. In the intracellular lifecycle, *L. pneumophila* has the described structures detailed in the infection process in the protozoan host. In the extracellular life cycle, *L. pneumophila* will alternate between the exponential phase and the stationary phase (Table 1.1). The stationary phase is often referred to as the post-exponential phase and is the virulent form in the extracellular life cycle. The exponential phase is the replicative form of *L. pneumophila* in the environment. The ultrastructure of the replicative form is of typical Gram-negative bacteria (Table 1.1). The exponential phase will differentiate to the stationary phase when the alarmone ppGpp is present indicating a decrease in nutrient concentration. The stationary phase has an ultrastructure similar to Gram-negative bacteria but with slight modifications including bacteria cells seen with

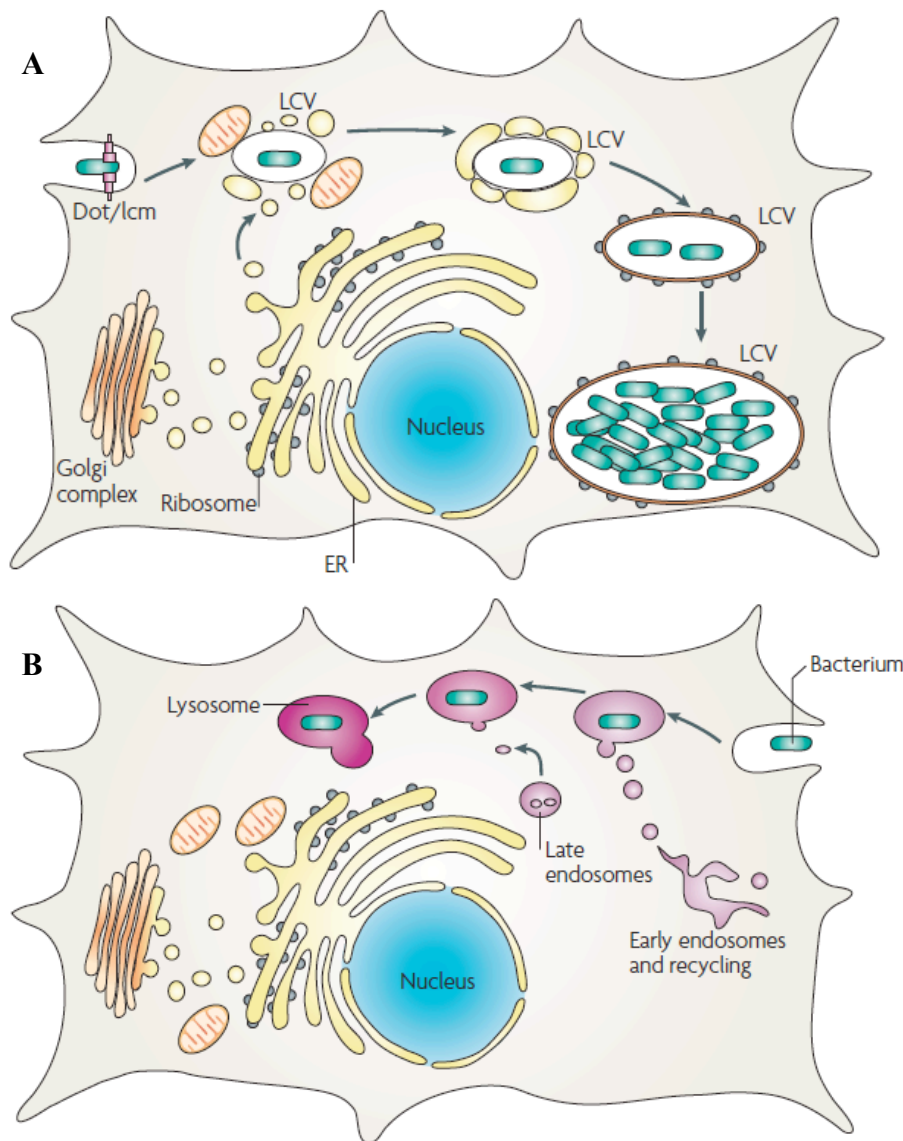

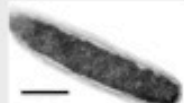


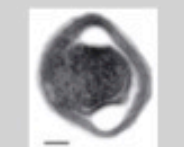


Figure 1.2 Comparison of the Intracellular lifecycle of *L. pneumophila* in macrophage cells and non-pathogenic bacteria intracellular trafficking. (A) Formation of the replication vacuole. The Dot/Icm secretion system secretes effector molecules to modify the host cells for bacterial replication. After uptake into the cell the LCV evades the phagosome-lysosomal fusion pathway through use of effector molecules. Within minutes vesicles from ER and mitochondria appear in close proximity to the LCV surface. The vesicles about the LCV appear docked and extend out, and eventually the membranes surrounding the bacterium closely resemble rough ER. Within the compartment the bacterium replicates to high numbers and lyses the host cell. (B) Cell phagosome-lysosome pathway with non-pathogenic bacteria. Notice the difference of the vacuoles at the late endosome phase and the non-avoidance of the phagosome-lysosomal fusion pathway. Isberg *et al.*, 2009.

Table 1.1. Ultrastructure of various *L. pneumophila* forms. Forms are found in intracellular or extracellular environments. Information obtained from Faulkner and Garduño, 2002<sup>1</sup>; Garduño *et al.*, 2002<sup>2</sup>; Garduño, 2008<sup>3</sup>; and Brassinga *et al.*, 2010<sup>4</sup>.

Bacteria form name	Synonym names	Intracellular or Extracellular	Ultrastructure	Characteristics	Found in Host/ Environment	Image
Replicative	Exponential or vegetative <sup>3</sup>	Intracellular <sup>1,3</sup>	Slender rods, typical gram-negative cell envelope <sup>1,2</sup>	Sensitive to chemicals and detergents <sup>2</sup>	All known hosts <sup>3,4</sup>	
Exponential	Replicative, vegetative <sup>3</sup>	Extracellular <sup>2,3</sup>	Slender rods, typical gram-negative cell envelope <sup>1,2</sup>	Sensitive to chemicals and detergents <sup>2</sup>	Biofilm environments <sup>3</sup>	
Stationary	Post-exponential, Virulent <sup>3</sup>	Extracellular <sup>2,3</sup>	typical of gram-negative bacteria, with a wavy outer membrane, darkening outer membrane and the presence of internal membranes defining pseudo-compartments, and presence of inclusions <sup>1,3</sup>	survival in ddH <sub>2</sub> O, resistant to osmotic shock and proteinase K treatments; thermal tolerance; flagellum <sup>2</sup>	Biofilm environments <sup>3</sup>	
Transitional	Intermediate <sup>3</sup>	Intracellular <sup>1,3</sup>	Longer wavelength outer membrane ripples, very smooth/straight outer membrane, well-defined membranes and an incipient thick layer, irregular form, Some inclusions of poly- β-hydroxybutyrate (PHBA) <sup>1</sup>	Unknown	Protozoan hosts, HeLa cells, <i>C. elegans</i> <sup>1,3,4</sup>	
MIF (CLF)	Dormant; post-replicative, infectious <sup>3</sup>	Intracellular <sup>1,2,3</sup>	Short, stubby rods, containing cytoplasmic inclusions of (PHBA) and a unique electron-dense layer associated with the outer membrane and/or multiple layers of intracytoplasmic membranes <sup>1</sup>	infectious (10-fold higher than SP); environmentally resilient (alkaline pH, high temperature, osmotic shock, freezing, proteinase K, or starvation in ddH <sub>2</sub> O); has a low respiration rate <sup>2</sup>	Protozoan hosts, HeLa Cells and Environment Possible in <i>C. elegans</i> host <sup>1,3,4</sup>	

inclusions of PHBA, invaginations of the cytoplasmic membrane, and have flagellum synthesis (Table 1.1). Other characteristics of the stationary phase that they are resistant to osmotic shock and proteinase K treatments, they are able to survive in ddH<sub>2</sub>O, and have thermal tolerance (Table 1.1). A difference between the stationary phase and the CLF is that the CLF has a 10-fold higher rate of infectivity for both protozoan cells and macrophage cell lines as observed in vitro (Garduño *et al.*, 2002). Also it is believed that CLFs are not formed in the environment because it is hypothesized that the differentiation needs additional signals that are unique to the infected host (Table 1.1). Thereby, the free floating stationary phase could potentially differentiate straight into the infectious CLF if infected in a host as observed in other bacteria such as the stationary phase bacteria of *Azotobacter vinelandii* that are seen to fully differentiate upon treatment with PHBA, which is seen as an enducer to lead to encystment (Garduño, *et al.*, 2002).

Inadvertent inhalation of aerosolized *L. pneumophila*-laden water droplets by immunocompromised individuals has lead to infection of alveolar macrophages causing the atypical pneumonia Legionnaires' disease (Berk *et al.*, 1998; Cianciotto *et al.*, 2001; Garduño *et al.*, 2002; Molofsky and Swanson, 2004; Steinert *et al.*, 2002). Susceptible individuals include immunocompromised individuals such as the elderly, transplant/cancer patients, heavy smokers and/or drinkers (Fields *et al.*, 2002).

## **1.2 *Legionella pneumophila* infection cycle in Alveolar Macrophages**

The first recognized outbreak of Legionnaires' disease occurred in Philadelphia, PA in 1976 in which 29 individuals died among the 180 people attending the American Legion convention (Kwaik *et al.*, 1998; Fields *et al.*, 2002). Susceptible individuals that inhale *L.*

*pneumophila* water droplets are capable of contracting Legionnaires' disease, which has a characteristic infection of atypical *pneumophila* in their alveolar macrophages. *L. pneumophila* is found in man-made water sources including air conditioners, water heaters, hot tubes and humidifiers (Palmer *et al.*, 1993; Woo *et al.*, 1992).

*L. pneumophila* secretes various effector molecules that have the ability to manipulate cellular host pathways to create a favorable environment for bacterial replication in the alveolar macrophages (Ensminger and Isberg, 2009). There are greater than 300 effector molecules and proteins released into the host cell that allow *L. pneumophila* to manipulate the cell (de Felipe *et al.*, 2008; Richards *et al.*, 2013). These effectors are secreted into the cell by the Dot/Icm Type-IV secretion system (T4SS) (de Felipe *et al.*, 2008; Ensminger and Isberg, 2009). The functions of the effectors include the establishment of an infection site and remodeling of the host cell environment to allow bacterial replication (Isberg *et al.*, 2009).

Key survival characteristics of *L. pneumophila* during the macrophage infection process are the evasion of the phagosome-lysosome fusion pathway as well as the evasion of the activated innate immune defenses of the cell (Horowitz *et al.*, 1983). Evasion of the phagosome-lysosome fusion pathway is done by covering the LCV with small smooth vesicles that originate from the ER within minutes of internalization by the cell. Small vesicles are recruited to the LCV to help the bacteria vacuole resemble the membrane found on the ER and mitochondria. The LCV becomes studded with ribosomes thereby taking on properties of an ER-like membrane and evade identification as a foreign body by immune system and cell. Mitochondria are often recruited close to the LCV reasons behind this recruitment of mitochondria are not specifically known. Another characteristic of the vacuole is the absence of resident proteins of the late



endosome and lysosome such as LAMP-1 (Figure 1.2). Thus, the LCV provides the bacteria a safe place to replicate (Shin and Roy, 2008). *L. pneumophila* must also evade the host's cell innate immune pathways, which includes the apoptotic pathway or the Programmed Cell Death (PCD) pathway (Abu-Zant *et al.*, 2007; Isberg *et al.*, 2009) (Figure 1.3). Bypassing both of these pathways, phagosome-lysosome fusion and PCD pathways, allows successful replication of *L. pneumophila* in the host cell (Shin and Roy, 2008; Isberg *et al.*, 2009). However, while replicating in the macrophage *L. pneumophila* is not able to enter into the CLF state like in the environmental protozoan host cell (Garduño *et al.*, 2002). *L. pneumophila* is unable to reach the CLF state because the macrophage cell lyses before *L. pneumophila* completes its transition to CLF (Isberg *et al.*, 2009). Thus, *L. pneumophila* is not considered to be communicably transmissionable and the macrophage cell is considered a “dead end” for the bacterium (Garduño *et al.*, 2002).

### **1.2.1 Alveolar Macrophage Innate Immune Response**

During the early stages of macrophage infection, *L. pneumophila* is able to avoid the host's PCD pathways through various effector molecules that interact with host PCD proteins (Isberg *et al.*, 2009) (Figure 1.3). One of the *L. pneumophila* effectors that has recently been studied is SidF. SidF prevents the function of the host proapoptotic proteins BNIP3 and Bcl-2 in the macrophage PCD pathway (Banga *et al.*, 2007; Hsu *et al.*, 2012). Both of these host proteins belong to the proapoptotic BCL-2 protein family. The interaction between SidF and the BCL-2 proteins is through direct binding to the proteins in a similar in mechanism to a cell-death inhibiting 19-kDa protein from adenovirus (Banga *et al.*, 2007). Interestingly, the direct binding

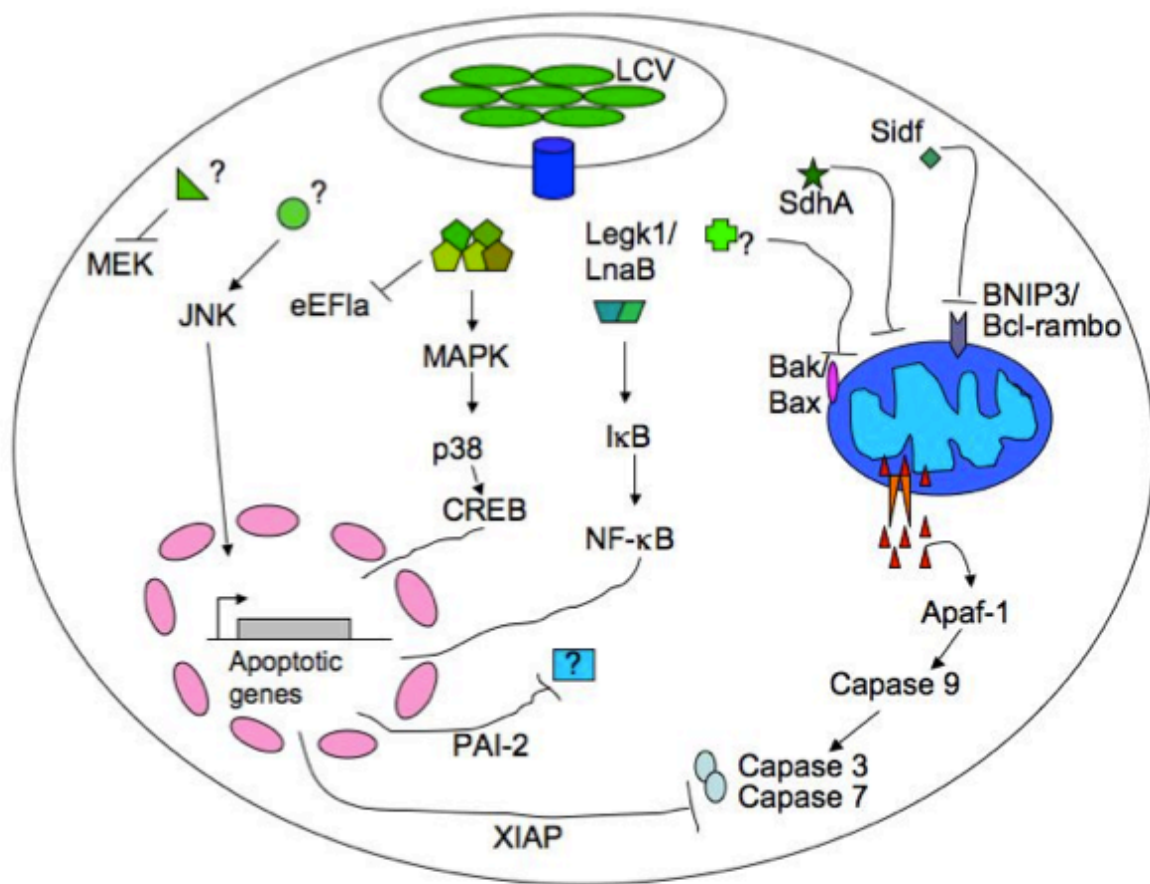


Figure 1.3 *L. pneumophila* effects on macrophage apoptotic pathways. Schematic of the apoptosis pathways manipulated in a macrophage cell to delay cell death in order for bacteria replication to occur; and what is the known interaction between the effector molecules and the pathways. LCV releases the effectors (green shapes) through its T4SS secretion system, *Legionella* effector SidF is seen to interact with the host proteins BNIP3 and Bcl-rambo receptor of the Bcl-2 family, inhibiting the release of cytochrome c, which activates Apaf-1 then activates the caspases that activate the apoptotic genes. Legk1/LnaB delays apoptosis by degrading and binding to the IκB inhibitor of NF-κB. The five-effector molecules known as ETR (Effector Trigger response) are seen to interact with the p38 MAPK pathway. Activation of JNK and MEK is through unknown effector molecules.

to BNIP3 and Bcl-2 rambo does not destabilize the structure of either protein (Banga *et al.*, 2007) (Figure 1.3). Another *L. pneumophila* effector characterized to affect the host's apoptosis pathway during infection is SdhA. SdhA appears to act as a cell death protection protein, with severe intracellular growth defects in strains carrying a mutation in *sdhA* (Laguna *et al.*, 2006) (Figure 1.3). SidF interacts downstream of SdhA by targeting branched death pathways triggered by *L. pneumophila* infection giving the manipulation of host PCD a range of control from major pathways to inhibition of specific pro-death proteins (Banga *et al.*, 2007). Recently, it has been found that SdhA also functions to maintain the integrity of infected cells (Harding *et al.*, 2013) (Figure 1.3).

Other pathways affected and controlled by effector molecules are the NF- $\kappa$ B and the host mitogen activated protein kinase (MAPK) pathways. Both of these pathways have a PCD activation overlap with Toll-Like Receptors (TLRs) and Nod1/Nod2 (Banga *et al.*, 2007). However, TLRs and Nod1/Nod2 present a minimal affect on the overall host immune response and a MAPK response can be activated independently (Newton *et al.*, 2010). MAPK is activated by five *L. pneumophila* effectors (Lgt1, Lgt2, Lgt3, SidI, SidL), which in turn inhibits host translation through the inactivation of the host elongation factor eEF1a (Fontana *et al.*, 2012). The five-effector molecules that generate the MAPK response are known as the effector-triggered response (ETR) (Banga *et al.*, 2007). The ETR also activates the pro-apoptosis NF- $\kappa$ B for the efficient production of cytokine protein and the transcription of a subset of stress response and proinflammatory genes (Banga *et al.*, 2007). The NF- $\kappa$ B pathway can also be activated outside of the ETR activation pathway by two other effector molecules: LegK1 and LnaB. These two effector molecules are involved in the degradation of the NF- $\kappa$ B inhibitor I $\kappa$ B (Ge and Shao,

2011). LegK1 is not required to be phosphorylated to be activated unlike the host molecule IKK thereby *L. pneumophila* is able to achieve a host-independent activation of the NF- $\kappa$ B signaling (Ge *et al.*, 2009).

Less well-characterized pathways in the macrophage that are affected by a *L. pneumophila* infection include the upregulation of stress-activated protein kinase (SAPK)/c-Jun N-terminal kinase (JNK) pathway leading to the mediation of proapoptotic events through unknown *L. pneumophila* effectors (Welsh *et al.*, 2004). In addition, there is a down regulation of the ERK kinase (MEK) pathway, which leads to anti-apoptotic events also observed by unidentified *L. pneumophila* effectors (Welsh *et al.*, 2004). The effectors known to directly interact with these pathways are not identified but there is a general interaction observed between the pathways and *L. pneumophila* (Figure 1.3). Thus, various effectors of *L. pneumophila* can delay PCD and interact with various macrophage cell innate immune system pathways. There is no main pathway immune pathway in the host cell of interest but rather how the various host pathways collaborate to inhibit pathogen replication in the alveolar macrophage. There are still more effectors yet to be determined that can directly inhibit and interact with the host PCD pathway.

### **1.3 *C. elegans***

#### **1.3.1 General information**

*C. elegans* have been utilized for various purposes in the laboratory setting to study numerous processes. *C. elegans* are a relatively easy host model to work with due to their small

size, large population production, transparent bodies and easily maintained population (Brenner, 1974) *C. elegans* possesses homology to other eukaryotic organisms including *Caenorhabditis briggsae*, *Drosophila melanogaster* and *Homo sapiens sapiens* (*C. elegans* Sequencing Consortium, 1998).

The life cycle of *C. elegans* is dependent upon temperature, as in warmer environments their development cycle proceeds at a faster rate (Wood, 1988) (Figure 1.4). At a temperature of 20°C *C. elegans* have a generation time, from embryo to adult, of 3 days and then have a lifespan of 3 weeks (Hope 1999, Wood 1988). Development from embryo to adult includes four larval stages before the nematode molts into a young adult and matures into a reproductive gravid (egg-laying) adult (Wood, 1988; Sulston and Horvitz, 1977). A gravid adult is able to produce up to 300 progeny. Each of the larval stages is completed with the molting of the nematode during which a new stage- specific cuticle is synthesized and the old one is shed (Sulston and Horvitz, 1977) (Figure 1.4). During molting, the pharyngeal pumping ceases and the nematode enters a brief lethargic state (Sulston and Horvitz, 1977).

If the environment is not substantial for the population than after the second larval stage, L2, the nematodes can enter into a dauer stage. The nematodes assess the environmental conditions at the middle of L1 stage and at signals of a pheromone as an indicator of population density, absence of food, and high temperatures act to trigger the L2 to molt into a dauer stage, L2d (Riddle, 1988). The persistence of the environmental conditions dictates whether the nematode retains the L2d stage or can enter into the L3 larvae stage. In the dauer larvae state the nematode is non-aging because its lifespan is not affected by the time spent in the dauer state,

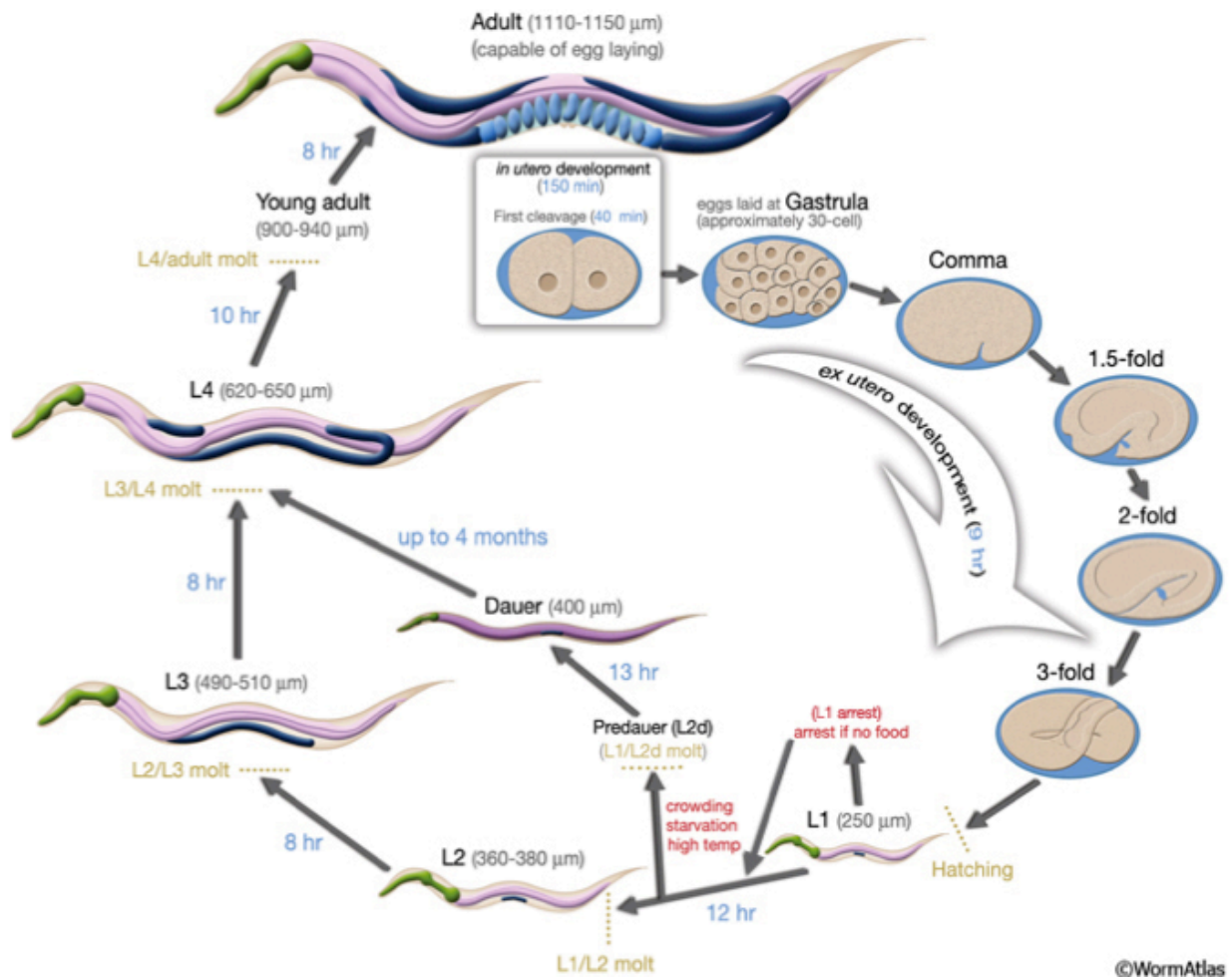


Figure 1.4 *C. elegans* lifecycle by developmental states at 20°C. The fertilization is at time point 0. The first divide occurs at forty minutes past first fertilization. All other length of times for each stage are in blue. The molt states are indicated in gold. With measurements in average size of the nematodes in black. The lifecycle of *in utero* development as the cell division continues to gastrula stage where they are expelled and laid where they further develop. At the L1 stage the nematode then can enter into a normal development cycle or into a dauer state (L2d), in unfavorable conditions. The dauer only enters back into the normal development cycle if favorable environments. Image acquired from *WormAtlas*

this state can last up to several months. Also the dauer nematode has feeding arrested indefinitely and locomotion is reduced greatly (Riddle, 1988). The morphology of a dauer nematode is their very thin (length-width ratio of 30:1) and has a thick altered cuticle. Their buccal cavity is sealed, the gut cells have a dark appearance and the pharyngeal and intestinal lumens are shrunken, and their gonad is also arrested at the L2 stage (Cassada and Russell, 1975). When the dauer nematode senses favorable environmental conditions, they are able to exit out of the dauer stage within an hour, then start feeding in 2-3 hours and enter the L4 stage after approximately 10 hours (Riddle, 1988) (Figure 1.4).

*C. elegans* have two sexes; a self-fertilizing hermaphrodite, and a male (Brenner, 1973). In a hermaphrodite population, a male is present from a spontaneous (0.1%) non-disjunction of the X chromosome in the hermaphrodite germ line (Brenner, 1973). However, with successful mating, male frequency can increase in occurrence to 50% (Wood, 1988). The self-fertilizing hermaphrodites are homozygous and a single worm can establish a colony (Figure 1.5). *C. elegans* have a genome of six chromosomes with five somatic chromosomes (I, II, III, IV, and V) and one sex chromosome (X) (*C. elegans* Sequencing Consortium, 1998; Brenner, 1974). The genome of *C. elegans* has been fully sequenced and annotated (*C. elegans* Sequencing Consortium, 1998). The anatomical description of the nematode has been completed at the electron microscopy level (Woods, 1988; Hall, 1999). The completed cell lineage of the embryo, larvae and adult has been established (Brenner, 1973; Byerly *et al.*, 1976; Sulston *et al.*, 1983; Wood, 1988; Lewis and Fleming 1995).

*C. elegans* have a simple anatomy and a transparent cuticle and an unsegmented, cylindrical body shape that is tapered at the ends (Figure 1.5). *C. elegans* are composed of an

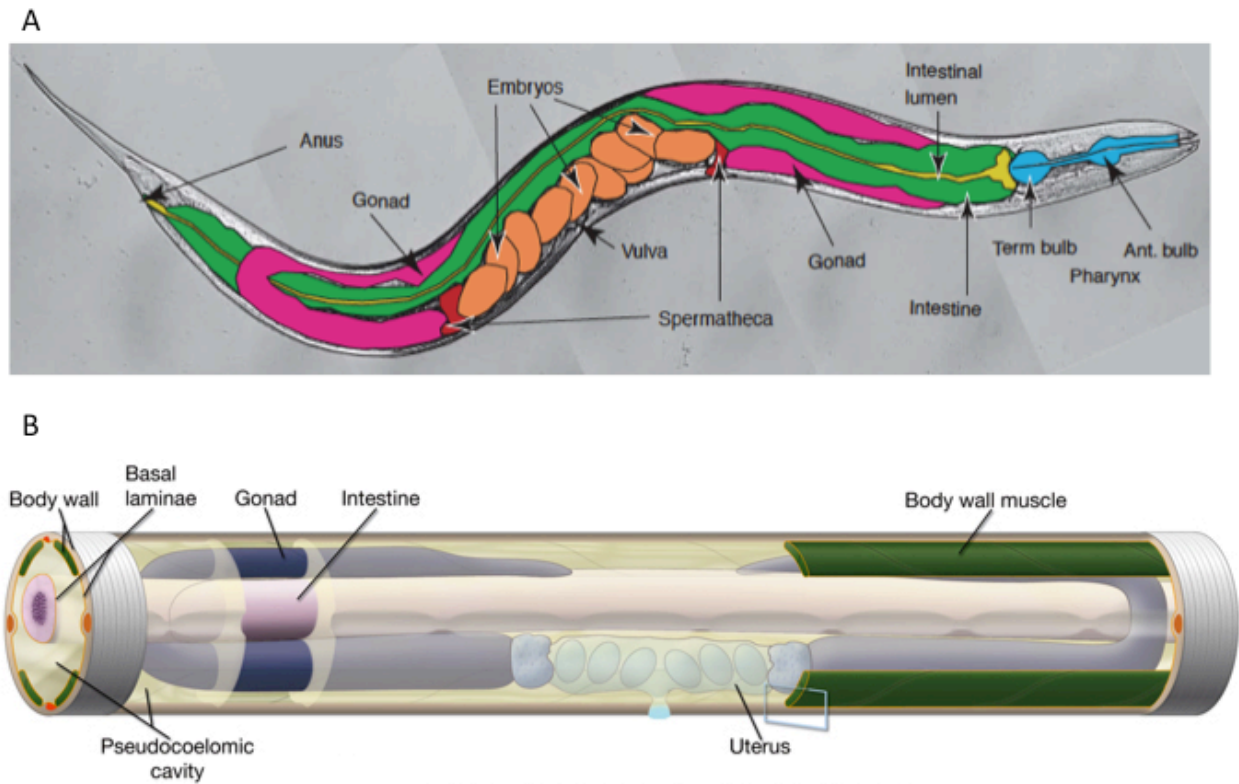


Figure 1.5 *C. elegans* adult anatomy. A) Basic structures of the adult hermaphrodite *C. elegans*. Ant. bulb is the anterior bulb, Term. bulb is the terminal bulb, of the pharynx. The gonad arm is the distal portion of the U-shaped gonad. B) Pseudocoelomic cavity in the adult *C. elegans*. The cavity is seen to cover the internal organs of the nematode with an internal fluid. Images acquired from *WormAtlas* Pericellular Structures (Altun and Hall, 2009).



outer and inner tube that is separated by the pseudocoelomic space. The outer tube consists of the cuticle, hypodermis, excretory system, neurons and muscles (Wood, 1988). The inner tube is made up of the pharynx, intestine, and the adult gonad (Wood, 1988). The nematode is under an internal hydrostatic pressure that is regulated by the excretory system, which is responsible for osmoregulation (Woods, 1988). All of the organs are easily imaged using microscopy. This is a great advantage of using *C. elegans* in the laboratory because of the real-time imaging that can be performed on the nematode (Woods, 1988). There is no circulatory system present in *C. elegans* but they have a primitive central nervous system consisting of a ventral nerve cord and nerve ring (Crofton, 1966; Sulston and Horvitz, 1977). Instead the nematode is highly vacuolated and nutrients move between tissues using various endocytosis and exocytosis pathways (White, 1988) (Figure 1.5, part B). The nutrients are able to move between tissues through the pseudocoelomic cavity that surrounds the internal tube of the nematode (Grant and Hirsh, 1999).

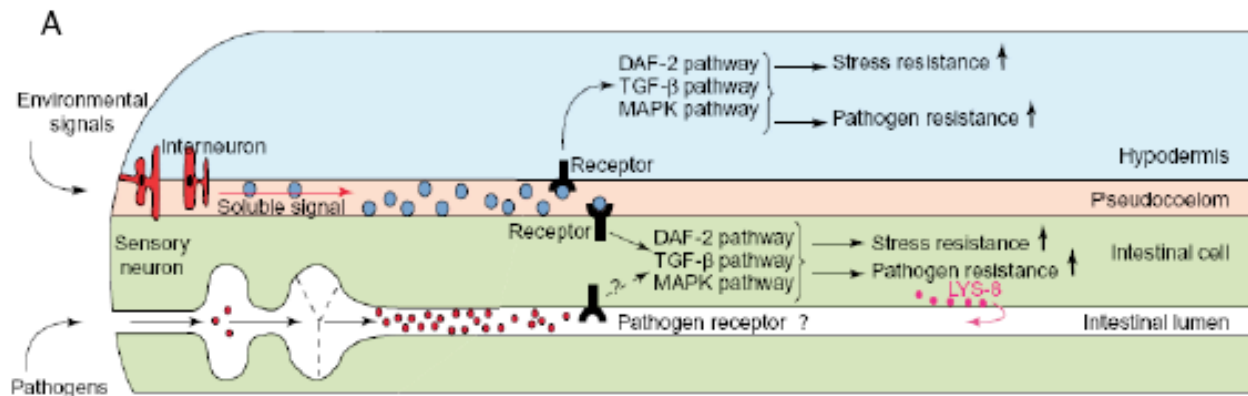
### **1.3.2 Innate Immune System**

The genetically tractable microbivorous *C. elegans* soil nematode has been well established as a host model for immunopathogenesis studies on a variety of human bacterial pathogens. Pathogens of study include *Pseudomonas aeruginosa*, *Staphylococcus aureus*, *Staphylococcus epidermidis*, and intracellular pathogens *Salmonella enterica* and *Listeria monocytogenes* (Ermolaeva, and Schumacher, 2014; Sifri *et al.*, 2005). *Pseudomonas aeruginosa* was the first human pathogen shown to be infectious to *C. elegans* (Sifri *et al.*, 2005). Its method of killing the *C. elegans* is described either by a fast toxin induced death or through a slow colonization of the intestinal lumen (Irazoqui *et al.*, 2010; Sifri *et al.*, 2005). The natural

pathogen of the *C. elegans*, *Microbacterium nematophilum*, is known to form a dense biofilm on the cuticle of the nematode (Sifri *et al*, 2005). To date there are five distinct methods of infections of the nematode: colonization in the lumen of the intestine, a persistent infection in the lumen of the intestine, invasion of tissues, biofilm production, and toxin mediated killing (Sifri *et al.*, 2005). Each pathogen observed in *C. elegans* appears to have unique killing properties of *C. elegans* both genetically and phenotypically.

*C. elegans* do possess a rudimentary innate immune system found on the apical surface of the intestine (Millet and Ewbank, 2004). Bacteria ingested by the nematode pass through a mechanical grinder to be broken up but some bacteria form remains intact after the mechanical shearing of the grinder (Avery and Thomas, 1997). Pathogenic bacteria that can pass through the grinder intact can interact with the host's intestine and possibly other tissues. Pathogenic bacteria have the ability to evoke the *C. elegans* innate immune system by binding to one of the nematode's various receptors in the lumen of the intestine (Millet and Ewbank, 2004) (Figure 1.6). The innate immune system is centered on three pathways: the TGF- $\beta$ , MAP kinase, and DAF-2/DAF-16 pathways (Schulenburg and Ewbank, 2004).

The DBL-1 is one of four TGF- $\beta$  (Transforming Growth Factor) ligands in *C. elegans*. It is the receptor of the DBL-1/TGF- $\beta$  (Dpp/Bmp-Like) pathway (Ewbank, 2006). DBL-1 is shown to regulate the expression of genes associated with mounting an effective innate immune response (Figure 1.7). These genes encode lectins, digestive enzymes such as lysozymes and lipases, the PGP (P-glycoprotein) subclass of ATP-binding cassette (ABC) transporter family proteins and a caenacin (*cnc*) antimicrobial peptide gene cluster (Ewbank, 2006) (Figure 1.6). The activation and control of the antimicrobial gene expression is through DBL-1 binding to the



**B**

Protein family	Proposed function	Pathway regulation	Chromosome location <sup>±</sup>
Lysozymes ( <i>lys-1</i> → <i>lys-8</i> )	Peptidoglycan cleavage	p38-MAPK, TGF-β, DAF-2	<b>I, II, IV, V</b>
Antimicrobial peptides ( <i>nlp-29</i> , <i>nlp-31</i> )	Antibacterial	p38-MAPK	<b>IV, V</b>
C-type lectins (>180)	Antibacterial	p38-MAPK, TGF-β, DAF-2	<b>I, II, IV, V, X</b>
CUB-like proteins	Extracellular proteases	p38-MAPK	<b>I, II, IV, V</b>
Saposin-like proteins ( <i>spp-1</i> → <i>spp-20</i> )	Pore forming toxins	p38-MAPK	<b>I, II, IV, V, X</b>

\* Chromosomes that contain the majority of the genes are in bold font.

Figure 1.6 The innate immune system of *C. elegans*. A) The innate immune signaling response to pathogenic bacteria in the intestinal lumen and binding to the cuticle of *C. elegans*. An example is the secretion of LYS-8, an antimicrobial, by the intestinal cells in a defense response to pathogenic bacteria. (Millet and Ewbank, 2004). B) Possible proteins that are secreted in a response to pathogens and which pathways secrete the proteins. Also indicated is the location of the proteins on the *C. elegans* chromosome. Data obtained and adapted from O'Rourke *et al.*, 2006; Troemel *et al.*, 2006; Alper *et al.*, 2007.

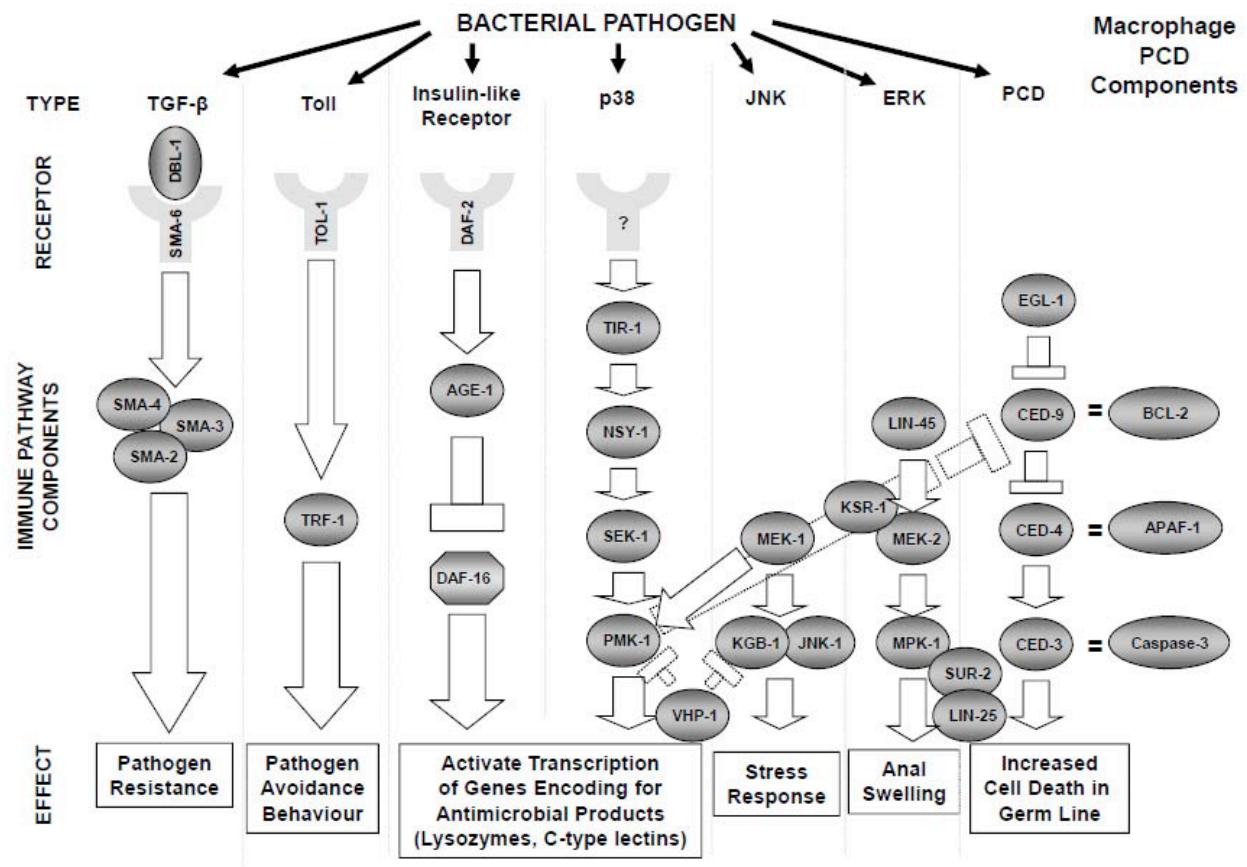


Figure 1.7 The components of the various innate immune pathways in *C. elegans*. Pathogenic bacteria present in the intestinal lumen activate the innate immune pathways. The pathway activated is characterized by the bacteria and is the best pathway to combat the infection. Some pathways have been identified to overlap and interact with each other. Others may function in similar areas in *C. elegans*. Schulenberg *et al.*, 2008.

heterodimeric DAF-4/SMA-6 receptor and acting *via* the SMAD complex (Savage-Dunn, 2005) (Figure 1.7). The SMD complex is composed of SMA-2/SMA-3/SMA-4, and the function of this complex is to regulate the expression of transcription of various lysozyme proteins (Nicholas and Hodgkin, 2004). A *dbl-1* loss of function mutant, and the inactivation of the SMAD complex leads to sensitivity to various pathogens including *E. coli*, *E. faecalis*, *P. aeruginosa* strain PA14, *S. enterica*, *S. typhimurium* strain SL1344, and *Se. marcescens* (Nicholas and Hodgkin, 2004; Ewbank, 2006). The different SMAD pathways are used to regulate distinct sets of immune effectors to provide resistance to specific pathogens. Any loss of function of the *sma-2*, *sma-3*, *sma-4* and *sma-6* genes alone results in a hypersensitive nematode to infection (Ewbank, 2006; Savage-Dunn, 2005). A functional loss of *dbl-1* leads to an increase in infection sensitivity because the nematode fails to effectively kill and digest pathogenic bacteria (Ewbank, 2006). The role of DBL-1/TGF- $\beta$  is conserved for its immune response as seen in the *Drosophila* homolog DBL-1 which possesses the same function observed in the *C. elegans* model (Savage-Dunn, 2005).

The second central pathway of the innate immune system is the MAP (mitogen-activated protein) kinase pathway. This pathway involves the NSY-1/SEK-1/PMK-1 cascade, which has homology to the mammalian MAP3K/MAP2K/MAPK cascade (Schulenburg *et al.*, 2008) (Figure 1.7). It was found that alleles of *nsy-1* and *sek-1* act together upstream of *pmk-1* (Ewbank, 2006). In the nematode, this pathway is used to protect against infection that includes damage from the pore-forming toxins of *Bacillus thuringiensis* (Schulenburg *et al.*, 2008). MAPK is known to activate various antimicrobial products such as lysozymes, C-type lectins, antimicrobial peptides, CUB-like proteins and saposin-like proteins (Ewbank, 2006) (Figure 1.6).

The lysozymes and the C-type lectins activated by MAPK are largely different than the ones activated by the TGF- $\beta$  pathway (Ewbank, 2006). However, there is a slight overlay between the two pathways in activation of these products. Thus, *C. elegans* has a pathogen-specific interpretation and a system-level response when presented with pathogenic bacteria in order to achieve the most effective response (Ewbank, 2006). The MAP kinase overlaps with various other pathways including the JNK pathway and the DAF-2/DAF-16 pathway (Ewbank, 2006). VHP-1 acting on KGB-1 and PMK-1 inhibits the JNK pathway and MAP kinase pathway, respectively (Schulenburg *et al.*, 2008). PMK-1 is also activated by MEK-1, a gene component of the JNK pathway, a MAPK pathway (Ewbank, 2006). Thus, there is crosstalk between various pathways to achieve an appropriate response to pathogens.

The third central pathway of the innate immune system is the DAF-2/DAF-16 pathway. This pathway has been linked to longevity in the nematode and plays a key aspect into the control of dauer state in *C. elegans* (Ewbank, 2006). Any knockdown of the *daf-2* gene expression leads to resistance to both Gram-negative and Gram-positive bacteria (Ewbank, 2006). DAF-2 acts as a receptor that mediates the activation of *age-1* gene expression that in turn inhibits *daf-16* gene expression (Figure 1.7). The function of DAF-16 is to activate transcription of genes encoding for antimicrobial products, including lysozymes, and C-type lectins as well as other antimicrobial products (Ewbank, 2006) (Figure 1.6). Any pathogen that is able to effect activate DAF-2 expression/function during infection will inhibit the activity of DAF-16 protein from activating expression of genes encoding antimicrobial products. The gene targets of DAF-16 are poorly characterized and are considered members of the DOD (downstream of DAF-16) gene group (Ewbank, 2006). An example of the DOD gene group is *lys-7*, which encodes

saposins, non-enzymatic glycoproteins that are ubiquitously present in lysosomes (Ewbank, 2006). Of interest, the expression of LYS-1 and LYS-2, SPP-3 and SPP-18 are also strongly upregulated during a *P. aeruginosa* infection (Kurz and Tan, 2004).

There is significant cross talk between the three central innate immune pathways of *C. elegans* as well as with the non-central, stress response pathways that interact with the central innate immune pathways. Recent work has identified the MAPK phosphatase VHP-1 as an integrator of the stress response pathway (MAPK and JNK) when provoked by the presence of heavy metals or infection (Kim *et al.*, 2004). It was revealed that the MAP2K MEK-1 is required for the full activation of PMK-1 (Mizuno *et al.*, 2004). There is also a link between a MAPK pathway and the DAF-2/DAF-16 pathway, as oxidative stress-induced activation of DAF-16 requires SEK-1. However, normal activation of DAF-16 was observed in *sek-1* mutant nematodes in heat shock or starvation conditions (Ewbank, 2006). On the other hand under heat shock, the nuclear translocation of DAF-16 does require *jnk-1*. Indeed DAF-16 appears to be a direct target of JNK-1 phosphorylation (Ewbank, 2006). Resistance to infection with *E. faecalis* requires the generation of reactive oxygen species (ROS) in the intestine, while DAF-16-mediated induction of the ROS-detoxification genes *sod-3* and *ctl-2* protects the tissues from the ensuing oxidative stress (Ermolaeva, and Schumacher, 2014). In addition, PMK-1-dependent anti-oxidant response *via* activation of SKN-1 might also enable the worms to withstand the dual oxidase Duox1/BLI-3-mediated ROS production during pathogen infection (Ermolaeva, and Schumacher, 2014). These results clearly indicate that different pathways intervene in the response to distinct types of stress. Thus, stress response to infection and the innate immune

response is interconnected and gives the nematode the best possible chance to fight off infection and protect its tissues.

### 1.3.3 Germline Apoptosis

The *C. elegans* germ cells are a unique tissue in variety of ways. First, as with all metazoan, the germ cells are both pluripotent and immortal in that they give rise to all cell types in the next generation and produce all subsequent generations, respectively (Gartner *et al.*, 2008). Second, the germline is the only adult tissue in *C. elegans* that is maintained by stem cells that constantly replenish the population (Gartner *et al.*, 2008). The number of germ cells and their progression through maturation to gametes is tightly spatially and temporally regulated (Sulston *et al.*, 1983). This characteristic makes the tissue similar to self-renewing mammalian tissues than to the other tissues within the adult *C. elegans*. Lastly, the germline is the only tissue in which apoptosis is not controlled by developmentally programmed cell death detailed by the invariant cell lineage (Sulston *et al.*, 1983). Rather germline apoptosis is an intrinsic part of the oogenesis process. However, apoptosis can also be activated by DNA damage or various environmental stresses or pathogenic infection (Gartner *et al.*, 2000) (Figure 1.8).

In the embryo the cells Z2 and Z3 will generate all of the germ cells in the adult hermaphrodite (Kimble and Hirsh, 1979). The gonad arm consists of distinct regions (Figure 1.8). At the distal end of the gonad contains the stem cell population known as the distal tip cell (Sulston *et al.*, 1983). The distal tip cell forms a tight fitting cap over the distalmost 6-10 germ cells. As germ cells move away from the distal end they enter into meiosis I continuing to



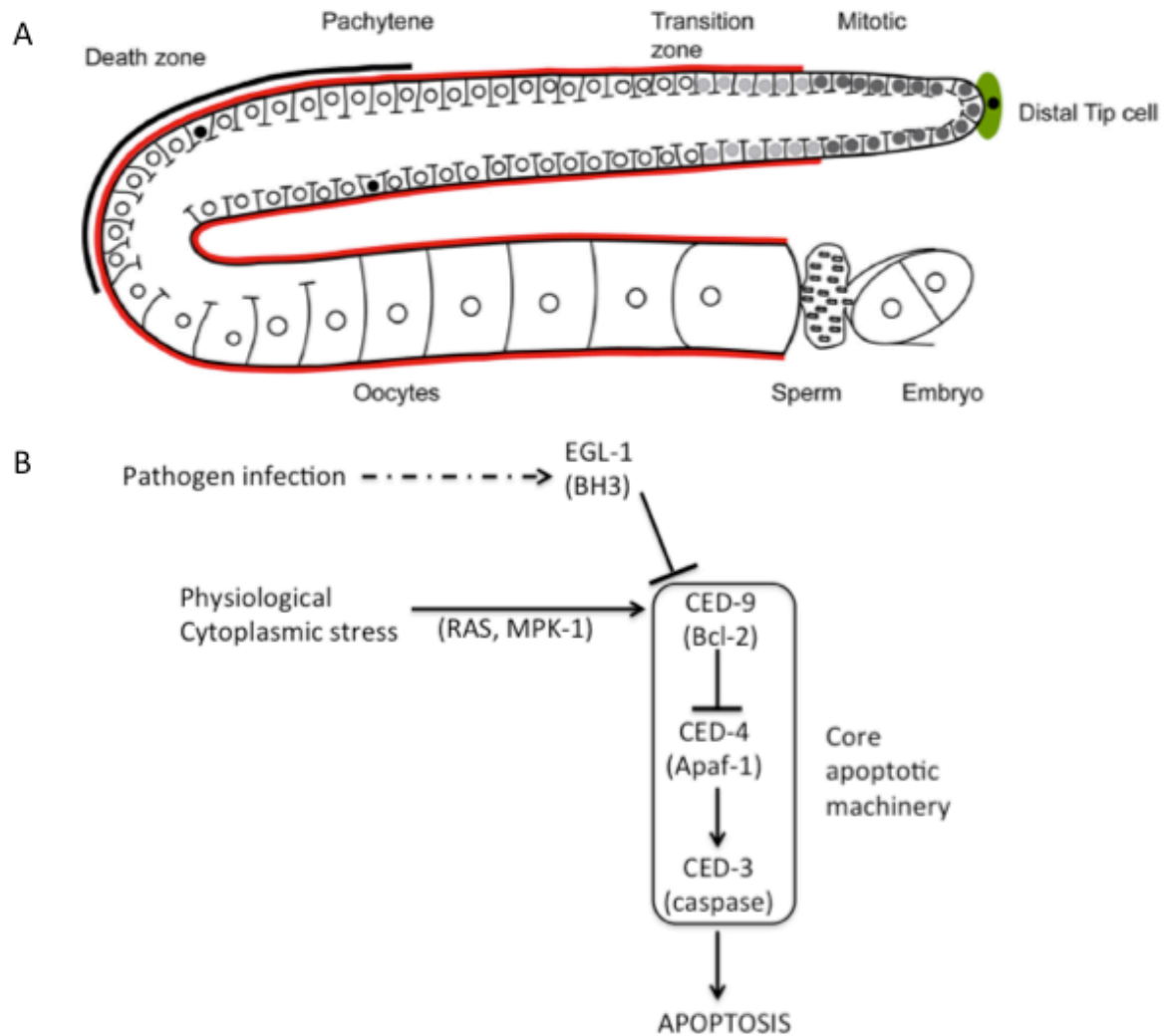


Figure 1.8 Germline Apoptosis in *C. elegans*. A) Schematic of possible apoptotic sites in the gonad arm as indicated by the black line during an infection. B) The core apoptotic machinery as well as the pathways that can activate or inhibit the pathway in the presence of physical stimuli. Adapted from Gartner *et al.*, 2008 under Creative Commons Attribution License.

prophase I and stop at diakinesis (Hirsh *et al.*, 1976). The transition zone is characterized by germ cells entering the early stages of meiotic prophase; almost half of the potential oocytes are eliminated through PCD before the cells enter into prophase I (Gumienny, *et al.*, 1999). After the transition zone germ cells progress into the pachytene region and grow in size. Cells in the pachytene area are characterized by a bowl of spaghetti nucleus morphology (Austin and Kimble, 1987). An exit from the pachytene region requires activation of the MAPK pathway, which is triggered by a signal from the overlaying gonadal sheath cells (Church *et al.*, 1995). The germline cells then progress through the gonad loop region where the nuclei transition into diplotene and where more cells undergo PCD (Figure 1.8). However, the cells that undergo PCD in the loop region often become nurse cells and provide proteins and cytoplasmic components to the surviving cells (Gumienny *et al.*, 1999). In the loop region the cells are organized into a single file as they enter into the proximal arm. In the proximal arm the cells undergo diakinesis and cell division arrests until oocyte maturation is complete (Lints and Hall, 2009). The oocytes enlarge to fill the entire space within the gonad arm by increasing their cytoplasmic contents and size of nucleus (Figure 1.8). Also observed in the oocytes is the increasing number of organelles. The oocytes closest to the spermatheca, proximal oocytes, begin to swell with yolk granules formed by endocytosis of yolk protein from the pseudocoelomic cavity that has transversed the sheath cells through sheath pores (Hall *et al.*, 1999).

The core apoptotic machinery consists of the CED-9/CED-4/CED-3 cascade, which has homology to the mammalian Bcl-2/Apaf-1/caspase cascade (Horvitz, 2003) (Figure 1.8). CED-9 is an anti-apoptotic protein whereas both CED-4 and CED-3 are considered to be proapoptotic proteins (Ellis and Horvitz, 1986; Horvitz, 2003; Salinas *et al.*, 2006). Upstream of CED-9,

EGL-1 acts to induce cell death through binding of CED-9. CED-9 acts upstream of CED-4 to inhibit cell death; CED-4 acts upstream of CED-3 to activate apoptosis of the cells (Horvitz, 2003). Therefore, EGL-1, CED-4, and CED-3 induce cell death whereas CED-9 protects the cells during development. To get rid of the apoptotic cell *ced-1* and *ced-2* are required for the engulfment of dying cells by their neighbors (Hedgecock *et al.*, 1983). Both CED-1 and CED-2 are required for the engulfment of the cell and are not involved in the killing of the cell (Hedgecock *et al.*, 1983). A mutation in *ced-1* results in the prevention of engulfment of dead cells and greatly prolongs the high refractile stage of cell death (Hedgecock *et al.*, 1983). CED-1 transmembrane receptor is related to the human SREC scavenger receptor and is seen clustering on the cell membrane of neighboring cells to the cell undergoing apoptosis (Zhou *et al.*, 2001). CED-1 has motifs in its intracellular domain that interact with PTB and SH2 domains that are necessary for engulfment but not for clustering, further suggesting that it recognizes the apoptotic cell (Zhou *et al.*, 2001). CED-1 is seen to be involved in the engulfment of apoptotic germ cells and is not observed to be involved in the engulfment of apoptotic somatic cells (Zhou *et al.*, 2001). The characteristics of CED-1 in germline apoptosis specifically the engulfment of dead cells has led to the development of an assay by Horvitz lab that utilizes the *ced-1::GFP* transgene (Conradt and Horvitz, 1999). Since CED-1 is expressed on cells engulfing the apoptotic cell *ced-1::GFP* accumulates at the surface of somatic sheath cells when they surround apoptotic germ cells during the engulfment process (Schumacher *et al.*, 2005). The assay is to provide a highly sensitive method to visualize early-stage germ cell apoptotic corpses that are often undetectable by DIC optics (Gartner *et al.*, 2004). However, this method proves to be less sensitive when a large number of germ cells are undergoing apoptosis and the fluorescence is

diluted making individual detection of cells undergoing apoptosis difficult (Gartner *et al.*, 2008). Further some time lapse analyses have indicated that some cells surrounded by *ced-1::GFP* may not end up forming apoptotic corpses (Aymeric Bailly and Anton Gartner, unpublished; Gartner *et al.*, 2008).

The apoptotic cascade can also be acted upon by other innate immune pathways such as the JNK/ERK and the p38 MAPK pathways (Schumacher *et al.*, 2005). The JNK/ERK pathway affects apoptosis through SEK-1 and MEK-1 when the nematode is under various environmental stressors (Schumacher *et al.*, 2005). The MAPK pathway is capable of activating the PCD pathway in the gonad when itself is activated by bacterial presence in the intestinal lumen (Salinas *et al.*, 2006) (Figure 1.8). This affect is done through PMK-1, which is a proapoptotic factor that binds to CED-9. During environmental stresses cell death in the gonad is more prevalent than in well-fed young nematodes (Salinas *et al.*, 2006). Various environmental stresses include salt concentration, starvation, age of nematode, and heat shock (Salinas *et al.*, 2006) (Figure 1.8). During a *S. Typhimurium* SL1344 infection colonization of the intestinal lumen is observed, but also there is a reported increase in apoptotic gonad cells (Aballay and Ausubel, 2001). To date, this bacterium is not found outside of the intestinal lumen of wild-type N2 nematodes. Thus, it is hypothesized that there are receptors in the lumen of the intestine that signal to the gonad tissues to increase apoptosis in response to pathogenic infections.

### **1.3.4 Oocyte Endocytosis Pathway**

The pathway responsible for transporting nutrients from the intestinal lumen to the growing embryos is the endocytosis pathway for oocytes. Grant *et al.*, 2001 describe this

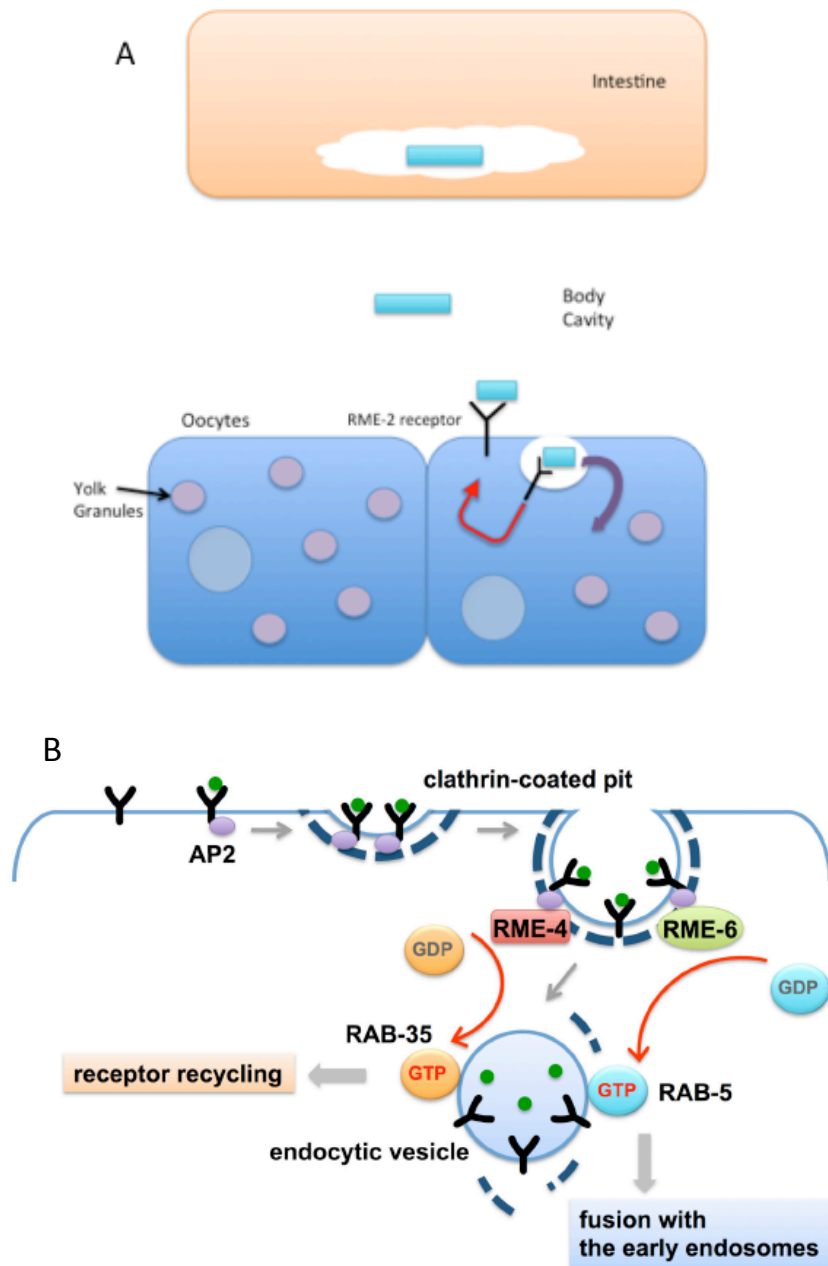


Figure 1.9 Oocyte Endocytosis in *C. elegans*. A) Schematic of the particles moving from the intestine to the oocytes. B) Schematic of the pathway taken inside of the oocytes. The receptor is still the RME-2 receptor seen in part A. Adapted from Grant and Sato, 2006 (A); from Sato *et al.*, 2014 (B) under Creative Commons Attribution License.

pathway as the movement of nutrients from the intestine to the oocytes. This pathway focuses on internalization of huge quantities of yolk proteins and associated lipids through a clathrin-mediated endocytosis (Grant and Sato, 2006) (Figure 1.9). One of the proteins that helped define and identify the factors involved in the pathway was YP170. YP170 is characterized as an endogenous yolk and a cholesterol binding/transport protein that is related to human ApoB-100 (Grant and Hirsh, 1999). It was concluded that YP170 is synthesized in the intestine of the adult hermaphrodites and is secreted basolaterally into the body cavity (Grant and Sato, 2006) (Figure 1.9). YP170 was fused to GFP and used to identify mutants defective in YP170-GFP uptake by oocytes (Grant and Hirsh, 1999). This YP170-GFP screen identified 11 *rme* (receptor-mediated endocytosis defective) genes required for various steps in endocytic transport (Grant and Hirsh, 1999). A genome wide RNAi screen using the same YP170-GFP screen identified hundreds of candidate endocytosis and secretion genes that contribute to all polarity and intracellular trafficking (Balklava *et al.*, 2007). The oocyte receptor RME-2, identified in the YP170-GFP screens, binds to YP170 and is specifically expressed in oocytes (Grant and Sato, 2006). RME-2 is a LDL-receptor related molecule that contains a typical NPXY internalization motif in its intracellular domain. The NPXY intracellular domain is known to direct other members of the LDL-receptor family into clathrin-coated pits (Grant and Sato, 2006) (Figure 1.9). Other factors that play a role in the movement of the endocytosis pathway are endocytic Rab proteins RAB-5, RAB-7 and RAB-11 as well as other RME proteins (Grant and Sato, 2006).

Two of the most studied and best-characterized regulators of the oocyte endocytosis pathway are RME-1 and RME-8. Both of these proteins are found in the cytoplasm of most *C. elegans* cells and are associated with limiting the membranes of endosomes. RME-1 is an EH

domain protein that is associated with later steps in recycling endosome receptors and is a similar protein to the mechanoenzyme dynamin (Grant *et al.*, 2001). Dynamin polymerizes to form spirals around the neck of clathrin-coated pits on the plasma membrane where it constricts the neck of the pit and strongly promotes fission and the release of a free vesicles (Grant and Caplan, 2008). Any mutation in RME-1 results in a phenotype of progressive vacuolation of the intestine beginning in the L4 stage and vacuoles become enlarged to be visualized on the dissecting microscope causing a the *C. elegans* to swell (Grant *et al.*, 2001). The phenotype is based on the *C. elegans* intestine's inability to efficiently recycle oocyte endosome receptor in multiple rounds of endocytosis (Grant *et al.*, 2001). *rme-1* mutants have secondary defects in the endocytosis by coelomocytes and in basolateral endocytic traffic in the intestine (Grant and Caplan, 2008). Interestingly, it was observed that defects in endocytosis (i.e. the RME-1 mutant) do not severely affect the organization or morphology of the germ line or oocytes as seen by Nomarski optics (Grant and Sato, 2006).

Another component of oocyte endocytosis pathway determined in the YP170-GFP screens was RME-8. RME-8 is a large DNA-J domain protein and the exact function of RME-8 in the endocytosis pathway is still not known but it appears to participate in the localization of factors to the early and/or late endosomes (Zhang *et al.*, 2001). A significant portion of RME-8 is its J-domain; this domain belongs to a J-domain family that mediates interactions with heat shock protein 70 family members (Zhang *et al.*, 2001). Recent work done in *Drosophila* indicates that a similar protein, DmRME-8, is required for endocytosis throughout the flies. The *Drosophila* studies of the *rme-8* mutant flies also indicate an interaction between RME-8 and with Hsc70 and clathrin. Further evidence that RME-8 interacts with the clathrin-coated vesicles

is that Hsc70 can uncoat the clathrin-coated vesicles through a cytoplasmic action (Zhang *et al.*, 2001; Brodsky *et al.*, 2001). Other components of interest in the oocyte endocytosis pathway to be further studied in the *C. elegans* under a pathogenic infection with *L. pneumophila* would be RME-2, RME-4, RAB-5 and RAB-35 due to their function in endocytosis as indicated by their work in the priming of endosome fusion and the recycling at the clathrin-coated pit process (Brodsky *et al.*, 2001). Thereby the already determined steps in endosome-lysosome fusion in macrophages and protozoa can be related to various *C. elegans* tissues such as the oocytes.

### **1.3.5 *Legionella pneumophila* infection characteristics in *C. elegans***

Past findings in the study of *L. pneumophila* infections in *Caenorhabditis* spp. have led to the conclusion of a predator (host)-prey (pathogen) relationship (Brassinga *et al.*, 2010). It was found that *L. pneumophila* is able to differentiate and multiply extracellularly within the lumen of the intestine (Brassinga *et al.*, 2010). It was presumed that the nutrients that *L. pneumophila* required to survive and differentiate could be found in the intestinal lumen of *C. elegans* (Brassinga *et al.*, 2010). Other phenotypic changes that occur during a *L. pneumophila* infection include a shortened lifespan, marked intestinal distension, and vulva extrusion of viscera upon nematode death (Brassinga *et al.*, 2010). *L. pneumophila* forms described in the intestinal lumen were both replicative and the intracellular infectious CLF. The replicative form had similar Gram-negative ultrastructural characteristics to those described in the protozoan host model. Also it was noted that the CLF forms were visible in the intestinal lumen could be defecated through the rectum (Brassinga *et al.*, 2010). Through defecation of the CLFs, it was thought that *L. pneumophila* could potentially infect other nearby hosts such as other nematodes.



Infection with *L. pneumophila* and *L. longbeachae* also triggered an innate immune response in *C. elegans*. *nsy-1* and *sek-1* mutant nematodes evoked an immunocompromised phenotype during infection (Brassinga *et al.*, 2010). Conversely, *daf-2* mutants are hyper-resilient to infection due to the DAF-16 regulating stress and antimicrobial gene expression. This is a similar affect observed in other pathogenic bacteria with *daf-2* mutant nematodes (Sifri *et al.*, 2006). Consistent with the increase survival rate of the *daf-2* mutants is the return of the mortality rate observed in wild-type N2 *C. elegans* in the *daf-16* mutant *C. elegans* upon *L. pneumophila* infection (Brassinga *et al.*, 2010). To further confirm the *daf-16 daf-2* genetic interaction double mutant nematodes were analyzed and revealed a similar mortality rate to the *daf-16* mutant nematodes.

Lastly, it was observed that a *L. pneumophila* infection can affect germline apoptosis counts, in a similar fashion to a *S. Typhimurium* infection. Survival assays done with mutant nematodes on the core nematode apoptotic machinery, null mutations in *ced-4: ced-4 (n1894)*, *ced-4 (n1162)*, lead to significant changes in the survival rate of hermaphrodite during *L. pneumophila* infection (Pinette, 2011). All nematodes with mutations of  $\Delta ced-4 (n1894)$ ,  $\Delta ced-4 (n1162)$  lead to a decrease in longevity during the infection process. The decrease in survival rate with the  $\Delta ced-4 (n1894)$ ,  $\Delta ced-4 (n1162)$  is consistent with the survival rates of the same *ced-4* mutant *C. elegans* infected with *S. Typhimurium* (Aballay and Ausubel, 2001). There was no significant difference in longevity in either CED-3 or CED-9 mutant *C. elegans* infected with *L. pneumophila* (Pinette, 2011). There was also a decrease in apoptosis compared to nematodes fed benign *E. coli* OP50 (Brassinga *et al.*, 2010; Pinette, 2011).

#### **1.4 Study aims**

The study aims are to (1) observe and further characterize the life cycle of *L. pneumophila* in *C. elegans* (2) understand the affect of *L. pneumophila* infection on the germline PCD. The working hypotheses of the study are 1) CLFs are formed in *C. elegans* and move between tissues through endocytosis pathways and 2) *C. elegans* survival depends on core apoptotic genes during infection.

## **Chapter 2: Materials and Methods**

### **2.1 Catalogue of Bacteria Strains used**

Strain	Genotype or Strain description	Source (Reference)
<i>Escherichia coli</i>		
OP50	Uracil auxotroph	CGC
HT115 pL4440:: <i>unc-22</i>	F-, <i>mcrA</i> , <i>mcrB</i> , IN( <i>rrnD-rrnE</i> )1, <i>rnc14</i> ::Tn10(DE3 lysogen: <i>lavUV5</i> promoter	Brassinga Laboratory
HT115 pL4440:: <i>ced-3</i>	Caspase, cysteine-aspartate protease	Brassinga Laboratory (Pinette)
HT115 pL4440:: <i>rme-2</i>	Low-density lipoprotein (LDL) receptor	Brassinga Laboratory
HT115 pL4440:: <i>vhp-1</i>	MAP kinase phosphatase	Brassinga Laboratory
<i>Legionella pneumophila</i>		
Lp02	StrR, Thy-, HsdR- derivative of Philadelphia-1 strain	M. Swanson (Berger and Isberg, 1993)
Lp03 $\Delta dotA$	StrR, Thy, derivative of Philadelphia-1 strain	R. R. Isberg (Berger and Isberg, 1993)
Lp03 $\Delta dotA$ pKB9	StrR, <i>dotA</i> complement	A.K.C. Brassinga
JV918	Lp02 $\Delta dotB$ mutant strain	Vogel (Sexton <i>et al.</i> , 2004)
JV3579	Lp02 $\Delta dotF$ mutant strain	Vogel (Luo and Isberg, 2004)
JV3559	Lp02 $\Delta dotG$ mutant strain	Vogel (Vincent <i>et al.</i> , 2006)
JV3563	Lp02 $\Delta dotH$ mutant strain	Vogel (Andrew <i>et al.</i> ,

---

		1998)
JV4044	Lp02 $\Delta dot/icm$ super deletion	Vogel (Vincent <i>et al.</i> , 2006)
Lp02 $\Delta sidF$	Lp02 $\Delta sidF$ mutant strain	Z.-Q. Luo (Banga <i>et al.</i> , 2007)
Lp02 $\Delta sidF$ ( <i>psidF</i> )	Lp02 $\Delta sidF$ complement	Z.-Q. Luo (Banga <i>et al.</i> , 2007)
Lp02 $\Delta sdhA$	Lp02 $\Delta sdhA$ mutant strain	Isberg (Laguna <i>et al.</i> , 2006)
Lp02::GFP	Lp02 <i>magA::gfpmut-3</i>	Brassinga Laboratory (Buchko)
Lp02::GFP	Lp02 <i>magA::gfpmut-3</i>	Brassinga Laboratory (Buchko)
Lp02 $\Delta sdhA$ ( <i>psdhA</i> )	Lp02 $\Delta sdhA$ complement	Brassinga Laboratory (Buchko)
Lp02 pBH6119:: <i>flaA</i> promoter	GFP	Brassinga Laboratory
pBH6119:: <i>htpAB</i> promoter GFP	GFP	Brassinga Laboratory

---

## 2.2 Catalogue of Nematode Strains Used

Strain	Genotype	Strain Description	Reference
N2	<i>C. elegans</i> wild isolate	WT <i>C. elegans</i> var Bristol	CGC (This study)
MD701	<i>bclIs39</i> V.	CED-1::GFP fusion protein in the sheath cells	CGC (This study)
DH1201	<i>rme-1(b1045)</i> V.	Endocytosis defects in oocytes and coelomocytes	CGC (This study)
GH403	<i>glo-3(kx94)</i> X.	Complete loss of gut granules (birefringence) in intestinal cells	CGC (This study)
GH383	<i>glo-3(zu446)</i> X.	Partial loss of gut granules (birefringence) in intestinal cells	CGC (This study)

## **2.3 Culture conditions:**

### **2.3.1 *E. coli* culture conditions**

The media used for all *E. coli* cultures was Luria-Burtani (LB) agar (per Litre: 10 g tryptone, 5 g Yeast extract, 10 g NaCl, 15 g agar). The broth used was LB broth (same recipe minus the agar). Strains were struck out onto LB agar plates with the appropriate antibiotics. Plates were incubated overnight at 37°C. A well isolated colony was selected and inoculated into a test tube containing 3 mL of LB broth and the appropriate antibiotics. Test tubes were incubated overnight with aeration at 37°C. Where appropriate, antibiotics were added to the indicated final concentrations: ampicillin (100 µg/mL).

### **2.3.2 *S. enterica* serovar Typhimurium culture conditions**

The media used for all *S. typhimurium* cultures was Luria-Burtani (LB) agar (per Litre: 10 g tryptone, 5 g yeast extract, 10 g NaCl, 15 g agar). The broth used was LB broth (same recipe minus the agar). Strains were struck out onto LB agar plates containing the appropriate antibiotics. Plates were incubated overnight at 37°C. A well isolated colony was selected and inoculated into a test tube containing 3 mL of LB broth and the appropriate antibiotics. Test tubes were incubated overnight with aeration at 37°C.

### **2.3.3 *L. pneumophila* culture conditions**

The medium used for all *L. pneumophila* cultures was Buffered Charcoal Yeast Extract (BCYE) (per Litre: 10 g bacto yeast extract, 1 g  $\alpha$ -ketoglutaric acid, 1 g ACES (N-(2-acetamido)-2-aminoethanesulfonic acid, N-(carbamoylmethyl)-2-aminoethanesulfonic acid,

(carbamoylmethylamino)ethanesulfonic acid, N-(carbamoylmethyl) taurine), 1.5 g activated charcoal, 15 g agar). The broth used was BYE (10 g bacto yeast extract, 1 g  $\alpha$ -ketoglutaric acid, 1 g ACES). For both the media and broth, the pH was adjusted to 6.6-6.7 via 6 M KOH and after being autoclaved. The medium was cooled to 55°C where the following supplements were added aseptically: 0.2 g L-cysteine and 0.5 mL 25% Fe-pyrophosphate.

L-cysteine was freshly prepared ~1 h prior to addition by measuring out 0.6 g and placed into a test-tube where 5 mL of dH<sub>2</sub>O was added. 6M KOH was used to adjust the pH of the solution to 6.6 – 6.7. The solution was then topped up to 6mL and underwent sterilization via membrane filtration (0.2mm). 25% Fe-pyrophosphate was prepared by adding 10 g of Fe-pyrophosphate and bringing the volume up to 40 mL of dH<sub>2</sub>O in a 50 mL falcon tube. The solution was vortexed, sterilized via 0.2  $\mu$ m syringe membrane filtration, and stored at 4°C in 5 mL aliquots in sterile 15 mL conical tubes covered in aluminum foil.

Strains were streaked out onto BCYE plates, and placed in a 5% CO<sub>2</sub> humid 37°C incubator 48 – 72 h. Where appropriate, antibiotics and supplements were added to the indicated final concentrations: kanamycin (25  $\mu$ g/mL), gentamycin (10  $\mu$ g/mL), streptomycin (100  $\mu$ g/mL) and thymidine (100  $\mu$ g/mL).

#### **2.3.4 Heat-Killed *L. pneumophila* culture conditions**

Wild-Type *L. pneumophila* was struck from frozen stock and grown for 3 days on BCYE with 100  $\mu$ g/mL of thymidine at 37°C+5%CO<sub>2</sub>. A well-isolated colony was picked and incubated with constant agitation in 30 mL of BYE broth overnight at 37°C. The broth was autoclaved for a 20 minute liquid cycle at 121°C. The bacteria were allowed to cool to room temperature then

concentrated by centrifugation 13,000 rpm for 1 minute. The pellet was then resuspended in 10 mL of BYE broth and divided into 1.5 mL eppendorff tubes. 20 µL of suspension was spotted onto BCYE with thymidine supplements and incubated for 48 hours at 37°C+5% CO<sub>2</sub>.

### **2.3.5 Heat-Killed *E. coli* OP50 culture conditions**

Benign *E. coli* OP50 was struck from stock and grown overnight on LB agar at 37°C. A well-isolated colony was picked and incubated with constant agitation in 30 mL of LB broth overnight at 37°C. The broth was autoclaved for a 20 minute liquid cycle at 121°C. The bacteria were allowed to cool to room temperature then concentrated by centrifugation at 13,000 rpm for 1 minute. The pellet was resuspended in 10 mL of LB broth and divided into 1.5 mL eppendorff tubes. 20 µL of suspension was spotted onto BCYE and incubated overnight at 37°C.

## **2.4 Nematode Strain Maintenance:**

### **2.4.1 Nematode Propagation**

3 to 5 gravid (egg-laying) nematodes were seeded onto NGM plates (1 Liter: 3 g of NaCl, 2.5 g of bacto peptone, 17 g of agar. Autoclaved for 20 minutes and cooled for 30 minutes at 55°C. Added aseptically sterile 25 mL of 1 M KPO<sub>4</sub> buffer pH 6.0, 1 mL of 1 M CaCl<sub>2</sub>, 1 mL of 1 M MgSO<sub>4</sub>, 1 mL of 5 mg/mL cholesterol in 95% ethanol) with a 50 µl bacteria lawn of *E. coli* OP50 (An isolated *E. coli* colony was cultured in 25 mL of LB broth overnight at 37°C and properly aerated). The nematodes were allowed to lay their eggs overnight. When the egg population was to be between 30 to 300, the gravid nematodes were removed from the plate and



destroyed by flame. This process of placing new gravids on new NGM media was repeated everyday. Populations would be started from frozen stock once every six months.

#### **2.4.2 Nematode Propagation From Frozen Stock**

From a frozen -80°C 1 mL cryogenic vial of a given nematode strain was allowed to sit at room temperature (21°C) until thawed. At such a time, the nematodes were remixed by a glass 1 mL pasture pipette and 6 drops of nematode suspension were dispensed on a new NGM media plate with a lawn of OP50. The drops were allowed to absorb into the media. The plates were then incubated at 16°C for 3-4 days. The young L1-L2 nematodes were then transferred from the plate to a fresh of NGM. These worms were allowed to grow into a gravid stage. At this point the nematodes were propagated on a daily basis until no longer needed or for 6 months.

#### **2.4.3 RNAi Nematode Propagation**

The RNAi bacteria were prepared by primer design of the desired target gene. Phusion PCR of the *C. elegans* genome was done to prepare the amplicon. The amplicon was digested and ligated into pL4440. The ligation was transformed into *E. coli* DH5α cells. Colony PCR was completed to verify successful insertion of the plasmid into the cell. The plasmid was then extracted from the cell and transformed into *E. coli* HT115 competent cells. A single colony was selected and frozen to create the working stock. When prepared for assay, the strain was struck on LB Amp100 plates and incubated for 37°C overnight. A single colony was selected and placed in a 3 mL LB broth with Amp100 and allowed to grow at 37°C, overnight. 50 µL of solution was spotted onto NGM plates with 12.5 µg/mL carbenicillin and 8 µM IPTG and

allowed to grow overnight at 37°C. One to three gravid (egg-laying) nematodes were seeded onto NGM plates for RNAi (1 Liter: 3 g of NaCl, 2.5 g of bacto peptone, 17 g of agar. Autoclaved for 20 minutes and cooled for 30 minutes at 55°C. Added aseptically sterile 25 mL of 1 M KPO<sub>4</sub> buffer pH 6.0, 1 mL of 1 M CaCl<sub>2</sub>, 1 mL of 1 M MgSO<sub>4</sub>, 1 mL of 5 mg/mL cholesterol in 95% ethanol, 500 µL of 25 mg/mL carboxycillin, 4 mL of 2 mM IPTG). The seeded nematodes were allowed to lay eggs overnight, and were removed in the morning. The plates were incubated at 20°C. 3 days later, the nematode population was at an L4 stage and ready to be used for infection.

#### **2.4.4 Synchronization of Nematode Population**

Adapted from synchronization via bleaching (egg prep) (Sulston, and Hodgkin, 1988). 1-2 propagation plates with 1 to 2 day gravid worms with lots of eggs and gravids were used. 5 mLs of M9 (1 Liter: 3 g KH<sub>2</sub>PO<sub>4</sub>, 6 g NaHPO<sub>4</sub>, 5 g NaCl, 1 mL 1 M MgSO<sub>4</sub>) was poured onto each plate. Gently swirled the buffer around to dislodge eggs from the agar. Used a glass pipette to transfer the nematodes to a 15 mL capped conical tube, if a large amount of eggs were left on the plate the process of adding M9 and swirling was repeated. Centrifuged the nematodes at 1000 rpm for 1 minute to pellet the nematodes, and aspirated the M9 off without disturbing the worm pellet. Added 15 mLs of the 20% alkaline hypochlorite solution (8.25 mL of ddH<sub>2</sub>O, 3.75 mL of 1 M NaOH, 3.0 mL of 6% sodium hypochlorite active agent). The tube was mixed by gently inverting it until all the tissues of gravid adult dissolved into the solution, or for approximately 5 minutes. Once hermaphrodites were dissociated the remaining eggs were centrifuged for 1 minute at 1000 rpm the supernatant was aspirated and replaced with 15 mL of M9 buffer. The

eggs were washed similarly 3 more times. Then after the final centrifuge the M9 buffer was aspirated off and the conical tube was filled with M9 buffer and parafilm and set on a rotor at room temperature overnight to allow the eggs to hatch into L1 nematodes. M9 is a minimal media and the nematodes will halt at L1 stage due to the lack of food. Next day, the L1 nematodes were centrifuged at 1000 rpm for 1 minute. The M9 solution was aspirated off until 1 mL of the solution remained. The pellet was remixed into this solution by a glass pipette. 1 drop of solution was placed onto a new NGM plate with *E. coli* OP50 lawn. These nematodes were grown to L4 stage at 16°C, taking roughly 3 days.

#### **2.4.5 Freezing a Nematode Population**

15 gravid nematodes were seeded onto fresh NGM media with a lawn of *E. coli* OP50. These nematodes were allowed to lay eggs overnight before being burned off. The eggs were allowed to grow at 16°C to a freshly starved L1-L2 state. 2-3 mLs of S buffer (for 1 Liter: 129 mL of 0.05M K<sub>2</sub>HPO<sub>4</sub>, 871 mL of 0.05M KH<sub>2</sub>PO<sub>4</sub>, 5.85g of NaCl. Sterilize by autoclaving.) was poured onto each plate. The buffer was gently swirled to dislodge the nematodes from the agar. A glass pasture pipette was used to transfer the nematodes to a 15 mL capped conical tube. If a large population of the nematode remained 2-3 mLs was applied again to the plate and the process was repeated. The nematodes in the conical tube were allowed to sediment by gravity, 10-15 minutes. The volume of S buffer was removed so that only 3 mLs including the pellet of nematodes remained. 3 mLs of S buffer +30% glycerol (for 1 Liter: 129 mL of 0.05M K<sub>2</sub>HPO<sub>4</sub>, 871 mL of 0.05M KH<sub>2</sub>PO<sub>4</sub>, 5.85g of NaCl, 30% glycerol, sterilized by autoclaving) was added to the conical tube. The population was mixed and 1 mL of the mixture was placed into labeled 1

mL cryogenic tubes, making 6 tubes total. The cryogenic tubes were tightened and placed in the center of a large styrofoam container. The styrofoam container was placed in the -80°C freezer for at least 12 hours.

To test for strain viability after freezing, one test vial was thawed the next day at room temperature and spotted onto an NGM plate with *E. coli* OP50. If worm tracks were visible within 48 hours than freezing was deemed successful and the population was placed in a permanent holding container at -80°C and also placed in the nematode strain database.

## 2.5 Survival Assay

30 wild-type Bristol N2 *C. elegans* were seeded at larval stage L4 onto triplicate Buffered Charcoal Yeast Extract (BCYE) agar plates with a corresponding 48 hour grown *L. pneumophila* bacterial lawn. (*Legionella pneumophila* strains were grown 3 days on BCYE with required supplements, 1 mL BYE broth cultures were inoculated with a loopful of bacteria, then vortexed. 10 µl of bacterial suspension was spotted onto 35 mm BCYE plates with required supplements.) Nematodes were inoculated at 25°C for the entire assay. On the 2<sup>nd</sup> and 4<sup>th</sup> day of the assay the nematodes were transferred to fresh bacterial lawns to remove possible progeny contamination.

Nematodes were assessed daily by prodding with a platinum wire nematode pick. The worms were considered dead when they didn't respond to touch and lacked pharyngeal pumping. Statistical analysis was done using Graph Pad Prism 5.0. Assays were completed for various different *L. pneumophila* strains. All assays were done in biological triplicate and each biological assay was done in technical triplicate.

## **2.6 Nomarski optics of *C. elegans* infected with *L. pneumophila***

30 wild-type Bristol N2 *C. elegans* were seeded at larval stage L4 onto BCYE agar plates in triplicate with a corresponding 48 hour grown *L. pneumophila* bacterial lawn. At 24 hour intervals after the initial seeding 10-20 nematodes were collected *via* a platinum wire pick and transferred to an agar plate with 1 mL of M9 buffer. Nematodes were allowed to swim in the M9 buffer for up to 5 minutes to remove all extracellular bacteria attached to their cuticle. Nematodes were picked up and placed on an 1 mm thick 2% agarose pad on a 3"x 1"x 1 mm microscope slide. The nematodes were paralyzed and hydrated with 10 µl 10 mM levamisole (Sigma Aldrich, Oakville ON) in M9 buffer. Once all desired nematodes were added, a perimeter of silicon grease was applied along the sides of the agarose pad. A coverslip was then mounted making contact with both the agarose pad and the silicon grease (Maddox and Maddox, 2012). Imaging was completed through DIC by Zeiss Observer ZI Inverted Microscope. All assays were done in biological and technical triplicate.

## **2.7 Fluorescent Imaging of *C. elegans* infected with *L. pneumophila***

30 Wild-type Bristol N2, GH403 ( $\Delta$ *glo-3(kx94)* X), GH383 ( $\Delta$ *glo-3(zu446)* X) *C. elegans* were seeded at larval stage L4 BCYE agar plates in triplicate with a corresponding 48 hour grown *Legionella pneumophila* bacterial lawn. At 24 hour intervals after the initial seeding 10-20 nematodes were collected *via* a platinum wire pick and transferred to an agar plate with 1 mL of M9 buffer. Nematodes were allowed to swim in the M9 buffer for up to five minutes to remove all extracellular bacteria attached to their cuticle. Nematodes were picked up and placed on an 1 mm thick 2% agarose pad on a 3"x 1"x 1 mm microscope slide. The nematodes were paralyzed

and hydrated with 10  $\mu$ l 10 mM levamisol (Sigma Aldrich, Oakville ON) in M9 buffer. Once all desired nematodes were added, a perimeter of silicon grease was applied along the sides of the agarose pad. A coverslip was then mounted making contact with both the agarose pad and the silicon grease (Maddox and Maddox, 2012). Imaging was completed through DIC and GFP fluorescent filter set at 488 nm on the Zeiss Observer ZI Inverted Microscope. All assays were done in biological and technical triplicate.

## **2.8 Assessment of Infected *C. elegans* Tissues**

30 Wild-type Bristol N2 nematodes were seeded at larval stage L4 onto nine BCYE agar plates with a lawn of 48 hour grown *Legionella pneumophila* bacterial lawn. At 24 hour intervals after the initial seeding all nematodes on one BCYE plate (approx. 30 nematodes) were collected via a platinum wire pick and transferred to an agar plate with 1 mL of M9 buffer. Nematodes were allowed to swim in the M9 buffer for up to five minutes to remove all extracellular bacteria attached to their cuticle. Nematodes were picked up and placed on an 1 mm thick 2% agarose pad on a 3''x 1''x 1 mm microscope slide. The nematodes were paralyzed and hydrated by 10  $\mu$ l 10 mM levamisol (Sigma Aldrich, Oakville ON) in M9 buffer.

Once all desired nematodes were added, a perimeter of silicon grease was applied along the sides of the agarose pad. A coverslip was then mounted making contact with both the agarose pad and the silicon grease (Maddox and Maddox, 2012). Imaged through DIC by Zeiss Observer ZI Inverted Microscope. The nematodes were visualized over the 8-day infection cycle. Each time point was 24 hours after the initial infection, and a total number of 100 nematodes were observed for each time point. The tissue was determined to be infected if LCVs or CLFs were

observed in the tissue of interest. The number of nematodes with infected tissues was counted. The sum of infected tissues was divided by the total worms counted. The numbers reflect a percentage of the nematode population infected. All assays were done in biological triplicate with each biological triplicate done in technical triplicate.

## **2.9 GermLine Apoptotic Counts Assay:**

### **2.9.1 MD701 strain**

20-30 MD701 (*ced-1::GFP*) nematodes were seeded at larval stage L4 onto BCYE agar plates in duplicate with a corresponding 48 hour grown *Legionella pneumophila* bacterial lawn, or onto BCYE agar plates in duplicate with 24 hour grown *S. enterica* SL1344 bacterial lawn (10 µl of a 1 in 10 dilution of overnight culture was spotted on BCYE plates with streptomycin). At 24 hours the nematodes were collected via a platinum wire pick and transferred to an 1 mm thick 2% agarose pad on a 3"x 1"x 1 mm microscope slide. The nematodes were paralyzed and hydrated with 10 µl 10 mM levamisole (Sigma Aldrich, Oakville ON) in M9 buffer. Once all desired nematodes were added, a perimeter of silicon grease was applied along the sides of the agarose pad. A coverslip was then mounted making contact with both the agarose pad and the silicon grease (Maddox and Maddox, 2012). The number of apoptotic cells was observed as single cell haloed by GFP in each *C. elegans* gonad arm. The number of cells was counted through use of the GFP fluorescent filter set at 488 nm on the Zeiss Observer ZI Inverted Microscope. Data was analyzed by Prism Pad v 5. Assay was completed for various *L.*

*pneumophila* strains. All assays were done in biological triplicate with each biological triplicate done in technical triplicate.

### **2.9.2 RNAi on MD701 strain**

1-3 MD701 (*ced-1::GFP*) nematodes were seeded at gravid stage onto RNAi NGM. The genes studied are *ced-3*, *vhp-1*, and *rme-1*. *E. coli* HT115::*unc-22* was fed to *C. elegans* as a control to ensure proper knockdown of RNAi genes in assay. Next day the nematodes were burned-off, leaving the eggs to grow on the RNAi NGM at 20°C. 3 days later the L4 larval stage nematodes on the RNAi NGM were seeded onto BCYE agar plates in duplicate with a corresponding 48 hour grown *Legionella pneumophila* bacterial lawn. At 24 hours the nematodes were collected via a platinum wire pick and transferred to an 1 mm thick 2% agarose pad on a 3"x 1"x 1 mm microscope slide. The nematodes were paralyzed and hydrated with 10 µl 10 mM levamisol (Sigma Aldrich, Oakville ON) in M9 buffer. Once all desired nematodes were added, a perimeter of silicon grease was applied along the sides of the agarose pad. A coverslip was then mounted making contact with both the agarose pad and the silicon grease (Maddox and Maddox, 2012). The number of apoptotic cells was observed as single cell haloed by GFP in each *C. elegans* gonad arm. The number of cells was counted through the GFP fluorescent filter set at 488 nm on the Zeiss Observer ZI Inverted Microscope. Data was analyzed by Prism Pad v 5. All assays were done in biological triplicate with each biological triplicate done in technical duplicate.

### **2.10 Transmission Electron Microscopy**



Based on the conventional two step fixation for EM procedure (Hall, 1995). 30 wild-type Bristol N2 *C. elegans* were seeded at larval stage L4 onto BCYE agar plates with a 48 hour grown bacteria lawn of wild-type *Legionella pneumophila*. The nematodes were transferred to fresh bacterial lawns every 48 hours. Six days after the initial seeding nematodes were collected via a platinum wire pick and washed in M9 buffer and paralyzed with 10 mM levamisole (Sigma Aldrich, Oakville ON). The modified Karnovsky Fixative (100 mL: 25 mL 8% Paraformaldehyde in H<sub>2</sub>O, 10 mL 25% glutaraldehyde, 50 mL 0.2M phosphate buffer pH 7.4, fill to 100 mL with dH<sub>2</sub>O.) was applied and allowed to sit overnight at 4°C. The samples were washed with 0.2M phosphate buffer pH 7.4 three times. A postfix of 1% osmium tetroxide (in 0.2M phosphate buffer) for 1 hour was applied at room temperature, then washed with distilled water three times. The nematodes were allowed to sit in the distilled water until further processing. Worms were placed in blocks of 3% agarose by transferring the nematodes *via* water droplets onto a bed of agarose where they were lined up. Molten agarose was gently added via 1 mL pipette overtop of the nematodes sealing them into a block of agarose. The agarose blocks underwent a series of ethanol dehydration steps: 50% ethanol for 3 times 5-minute incubation time, 75% for 3 times with 5-minute incubation time, 95% for 3 times with minute incubation time. Lastly, the blocks were dehydrated in 100% ethanol 3 times with 10-minute incubation time. The blocks were finally dehydrated with propylene oxide in which the first dehydration step was 10 minutes with 1 part propylene oxide and 2 parts 100% ethanol. The second dehydration step was 10 minutes with 2 parts propylene oxide and 1 part 100% ethanol. The last dehydration was only propylene oxide for 10 minutes. The blocks were then emerged in fresh Embed 812 resin. The blocks were exposed to 1 part resin and 2 parts propylene oxide for

10 minutes. Then exposed to 2 parts resin and 1 part propylene oxide for 10 minutes. Lastly, they were exposed to 100% resin. The blocks then went under resin changes every two to five hours for the next 48 hours. The samples were placed in aluminum foil pie dishes, the nematodes were arranged to lay parallel to the bottom of the dish. Fresh resin was then added and the samples were cured at 60°C in an oven for 3 days. Ultrathin sections approximately 70 nm in thickness, were obtained with a diamond knife and collected on mesh copper grids. The grids were examined in a Hitachi TM-1000 Electron Microscope. Images were acquired using an AMT CCD camera model 1600 M with software AMT Image Capture Engine V601. Images were further processed using ImageJ software.

## **2.11 Immunogold:**

### **2.11.1 Preparation of Immunogold Electron Micrograph grids**

Based on the conventional two step fixation for EM procedure by (Hall, 1995) and the Immunogold procedure by (Faulkner and Garduño, 2013). 30 Wild-type Bristol N2 *C. elegans* were seeded at larval stage L4 onto 6 BCYE agar plates with a 48 hour lawn of wild type *Legionella pneumophila* and on 12 BCYE agar plates with heat-killed Lp02 and 12 BCYE agar plates with heat-killed *E. coli* OP50, and 6 NGM plates with *E. coli* OP50. The nematodes were transferred to fresh bacterial lawns every 48 hours. The Heat-Killed strains were transferred every 24 hours. Six days after the initial seeding worms were collected via a platinum wire pick and washed in M9 buffer and paralyzed with 10 mM levamisole (Sigma Aldrich, Oakville ON). Half of the worms were prepared by a primary fix of 2.5% glutaraldehyde in 0.1 M sodium

cacodylate pH 7.0, at room temperature for 2 hours. A postfix of 1% osmium tetroxide (in 0.1 M sodium cacodylate buffer) for 1 hour at room temperature, then washed with distilled water three times. The other half of the nematodes were fixed with freshly depolymerized paraformaldehyde (4% formaldehyde-0.25% glutaraldehyde in 0.1 M cacodylate buffer). The paraformaldehyde samples were washed three times with 0.1 M cacodylate buffer, then with distilled water. The nematodes were allowed to sit in the distilled water until further processing. Worms were placed in blocks of 3% agarose by transferring the nematodes *via* water droplets onto a bed of agarose where they were lined up. Gently hot agarose was added *via* 1 mL pipette overtop the nematodes to make a solid block of agarose. The agarose blocks underwent a series of ethanol dehydration steps: 50% ethanol for 3 times 5 minutes incubation time, then 75% for 3 times with 5 minute incubation time, followed by 95% for 3 times with 1-minute incubation time. Lastly, the blocks were dehydrated in 100% ethanol 3 times with 10-minute incubation time. The blocks were sealed airtight in 1 mL cryogenic tubes and sent to Mrs. Trevors, Electron Microscope Technician at Dalhousie University in Halifax for further processing.

### **2.11.2 Immunogold Tagging of Electron Micrograph grids**

Based on the Immunogold procedure stated for *Legionella* (Faulkner and Garduño, 2013). Sodium Borohydride 1 mg/mL (weigh 1-2 mg of Sodium Borohydride powder and dissolve in the corresponding amount of distilled water) was made fresh for each experiment. 50 µL drops of the sodium borohydride solution was applied to a piece of parafilm attached to a glass petri plate. The grids were picked up and floated on corresponding drops of sodium borohydride so that the sections with nematodes made contact with the solution. These were allowed to sit

still for 10 minutes. The grids were then transferred to 50  $\mu$ L drops of glycine in borate buffer (30 mM in 0.1 M borate buffer, was prepared by 2.3 mg of glycine in 1 mL of borate buffer, and the borate buffer was made by dissolving 62 mg of boric acid in 10 mL of water, pH to 9.6 by 4M NaOH) this was allowed to sit for 10 minutes. The grids were then moved to 50  $\mu$ L drops of the blocking buffer consisting of TBS buffer, 1 % Skim Milk and 1% BSA (10 mL of TBS buffer: Tris 10mM, NaCl 0.2 M, BSA 0.2% and pH to 8.1, made by adding 100  $\mu$ L of Tris 1M pH 8.0, 1.3 mL of 1.5M NaCl, bring to 10mL with ddH<sub>2</sub>O), 1% Skim Milk (10mg Milk powder), 1% BSA (10 mg BSA) this was allowed to sit for 45 minutes at room temperature. The grids were then washed quickly with TBS buffer by allowing the grids to float on 50  $\mu$ L drops of TBS buffer. The grids were then moved to the primary antibody, Ip-1 antibody (anti-rabbit, polyclonal, at a dilution of 1 in 10,000) 100  $\mu$ L drops and allowed to sit overnight at 4°C. The grids were then moved to a series of 2 mL washing buffer (10mM Tris, 0.3M Tris, 0.1% BSA, pH 8.1 prepared by 0.5 mL of 1M Tris pH 8 and 10 mL of 1.5 M NaCl then bring the volume to 50 mL with distilled H<sub>2</sub>O) washes each wash lasting for 15 minutes with 3 washes total. The washes were completed in 24 well plates on a rotator at room temperature. The grids were then moved to secondary antibody solution (conjugated gold particle attached to antibody used at a dilution of 1 in 300 in sterile TBS buffer solution) this was allowed to sit at room temperature for 1 hour. The grids underwent another series of washing in the 2 mL of washing buffer in the 24 well plates on a rotator at room temperature with each wash lasting for 15 minutes with 3 washes in total. The grids were then floated onto 50  $\mu$ L 2.5% Gluteraldehyde drops for 15 minutes. The grids were then washed in distilled water for 3 minutes with 3 washes total. The grids were then removed from the drops by tweezers and allowed to dry on a kimwipe before imaging.

The primary antibody used for *L. pneumophila* was rabbit anti-Lp1 (Edelstein and Edelstein, 1993) the secondary rabbit, gold-tagged antibody was supplied by Dr. Rafael Garduño (Sigma Aldrich, Oakville ON). The nickel grids were imaged by the Hitachi TM-1000 Electron Microscope. Images were acquired using an AMT CCD camera model 1600 M with software AMT Image Capture Engine V601. Images were further processed using ImageJ software.

## Chapter 3: Results

### 3.1 Assessing Virulence of *L. pneumophila* in *C. elegans*

Brassinga *et al.*, in 2010 established *C. elegans* as a host model to understand the infection process of *L. pneumophila*. It was found that the nematodes fed live *L. pneumophila* had a shortened lifespan when compared to nematodes fed heat-killed *L. pneumophila* (Brassinga *et al.*, 2010). Also of significance is that several strains of *Legionella spp.* assessed in the nematode model with each *Legionella spp.* resulted in a different survival rate. This indicates a species variation with regards to the *Legionella spp.* virulence and in the *C. elegans* host model. To confirm the previously observed phenotype, a survival assay was performed to assess the lifespan of the infected nematode. Even though multiple strains of *Legionella spp.* are able to kill the nematode, the focus of all past studies has been on the type strain *L. pneumophila* Philadelphia-1. To confirm the survival rate of the nematode, the lab strain *L. pneumophila* Lp02, a derivative of *L. pneumophila* Philadelphia-1, was assessed for virulence. Even though the survival rate of the nematodes fed *L. pneumophila* was previously reported, the infection process needed to be detailed further. The controls used in this study focused on the bacteria and not the assay media itself. For example, when benign *E. coli* OP50 is grown on the *Legionella* growth media (BCYE) it becomes pathogenic to the nematode due to the nutrient rich media because it creates an anaerobic condition.

Overnight cultures from freshly streaked OP50 and *L. pneumophila* were grown at 37°C for 20h. The cells were then autoclaved to achieve complete killing of the virulence factors in both strains. The autoclaved bacterial suspension was concentrated to eliminate the chance of

starvation during infection. To overcome the starvation factor, the nematodes were transferred daily to fresh assay plates with spotted bacterial lawns. As a viable double-check of the heat-killed bacteria's growth rate the strains were incubated for the standard assay time on the assay media that was established for the synonymous live bacteria growth time.

The heat-killed *L. pneumophila* and heat-killed *E. coli* OP50 was used to assess the survival rate of live *L. pneumophila* on the *C. elegans* host model (Figure 3.1). The heat-killed *E. coli* OP50 represents the benign food source. As mentioned before live *E. coli* OP50 becomes pathogenic on nutrient rich media such as BCYE (Garsin *et al.*, 2001). Therefore, the heat-killed *E. coli* OP50 was used to assess the natural aging process of the nematodes at 25°C.

The heat-killed *L. pneumophila* was to represent the effect of live *L. pneumophila* without the virulence factors. Importantly, the nematodes fed heat-killed *E. coli* OP50 did not demonstrate infection characteristics of ingestion/colonization commonly associated with pathogenic bacteria. Thus the demise of the nematode population was due to natural causes (Figure 3.1). In addition, the heat-killed *L. pneumophila* followed the same survival pattern as live *L. pneumophila* observed as a constant slow rate (Figure 3.1). However, it appears that heat-killed *L. pneumophila* is not as nutritionally beneficial as heat-killed *E. coli* OP50 as the survival rate for heat-killed *L. pneumophila* was significantly lower than heat-killed *E. coli* OP50. As observed in a previous study (Brassinga *et al.*, 2010), the lifespan of nematodes fed live *L. pneumophila* was substantially shortened indicating that the death of the population is due to active colonization and infection in *L. pneumophila*.

### **3.2 Morphology changes in *C. elegans***

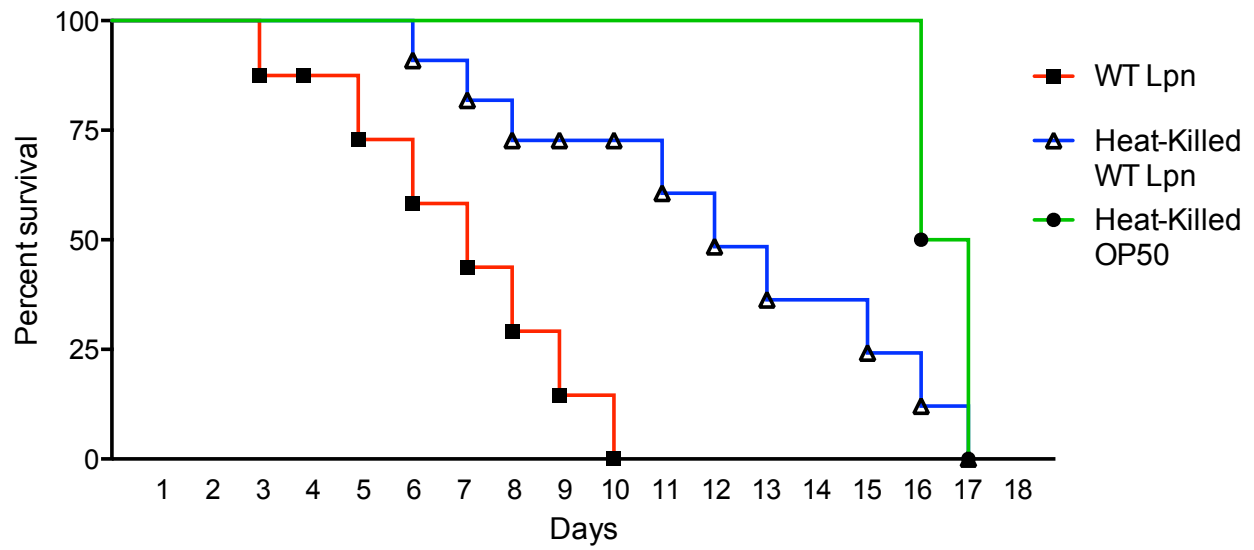


Figure 3.1 Kaplan-Meier survival curve of *L. pneumophila* in wild-type N2 Bristol *C. elegans*. Log-rank analysis p value between all three strains is  $<0.0001$ .  $n=30$  nematodes counted for each strain in assay. Strain designations are *L. pneumophila* Lp02 (WT Lpn), *E. coli* OP50 (OP50). Note that nematodes fed the heat-killed strains, especially heat-killed *E. coli* OP50 were able to survive till the end of the natural lifespan.



### 3.2.1 Morphology of the posterior tail region

To assess the growth and development of the nematodes, they were grown under standard conditions and to determine a baseline of *C. elegans* morphology under infection conditions. The nematodes were visualized over a standard 8-day period. The food source for controls was either live benign *E. coli* OP50 grown on standard NGM media, heat-killed *E. coli* OP50 on BCYE media or heat-killed *L. pneumophila* on BCYE media. Analysis of the controls side by side over the course of the infection allows a confirmation of the survival assay results seen previously. One of the areas of change is in the tail of the nematode. As with any animal, the aging process includes the degradation of the tissues, which is observed in the *C. elegans* model. Over the course of the infection period it was always questioned whether the phenotypic morphology was the cause of the nematode's age or of the bacterial infection.

In the posterior portion of the intestine, there is the defecation of material from the intestine through the rectum. The defecation cycle consists of a series of muscular contractions that are coordinated by neural activity and acuminate in expulsion of digested bacteria material (Avery and Thomas, 1997). It was observed that as the nematode ages this defecation process is altered in correlation to age. The defecation cycle in a healthy hermaphrodite nematode is one that repeats every 45s (Collins *et al.*, 2008). The normal defecation cycle was not quantitatively assessed for the controls. However, the defecation of bacteria was assessed by microscopy to see if the terminal portion of the intestine was swollen with bacteria. If there was swelling, than it was assumed that defecation of bacteria was slowed and that the cycle could not repeat as frequently causing constipation. As observed with live *E. coli* OP50, the intestinal tube is of

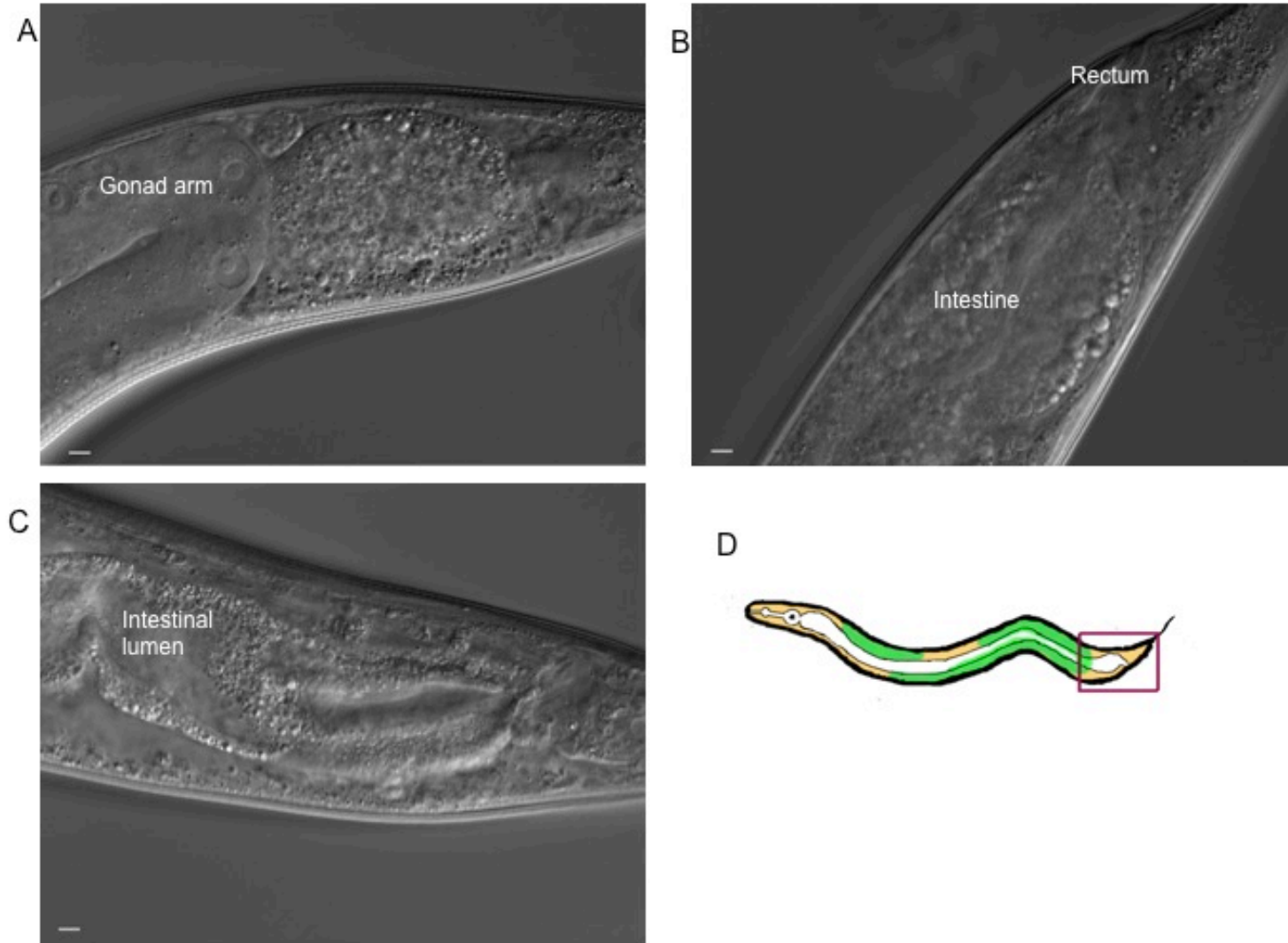


Figure 3.2 Observed morphology of the tail region of N2 *C. elegans* fed *E. coli* OP50 on NGM. Morphology observed over a period of 8 days, images taken on 1, 3 and 6 days post-infection, for A, B, and C respectively. The nematodes were incubated at 25°C on NGM with benign *E. coli* OP50 as a food supplement. D) Schematic of nematode; box indicates region of interest. Scale bar is 5  $\mu$ m.

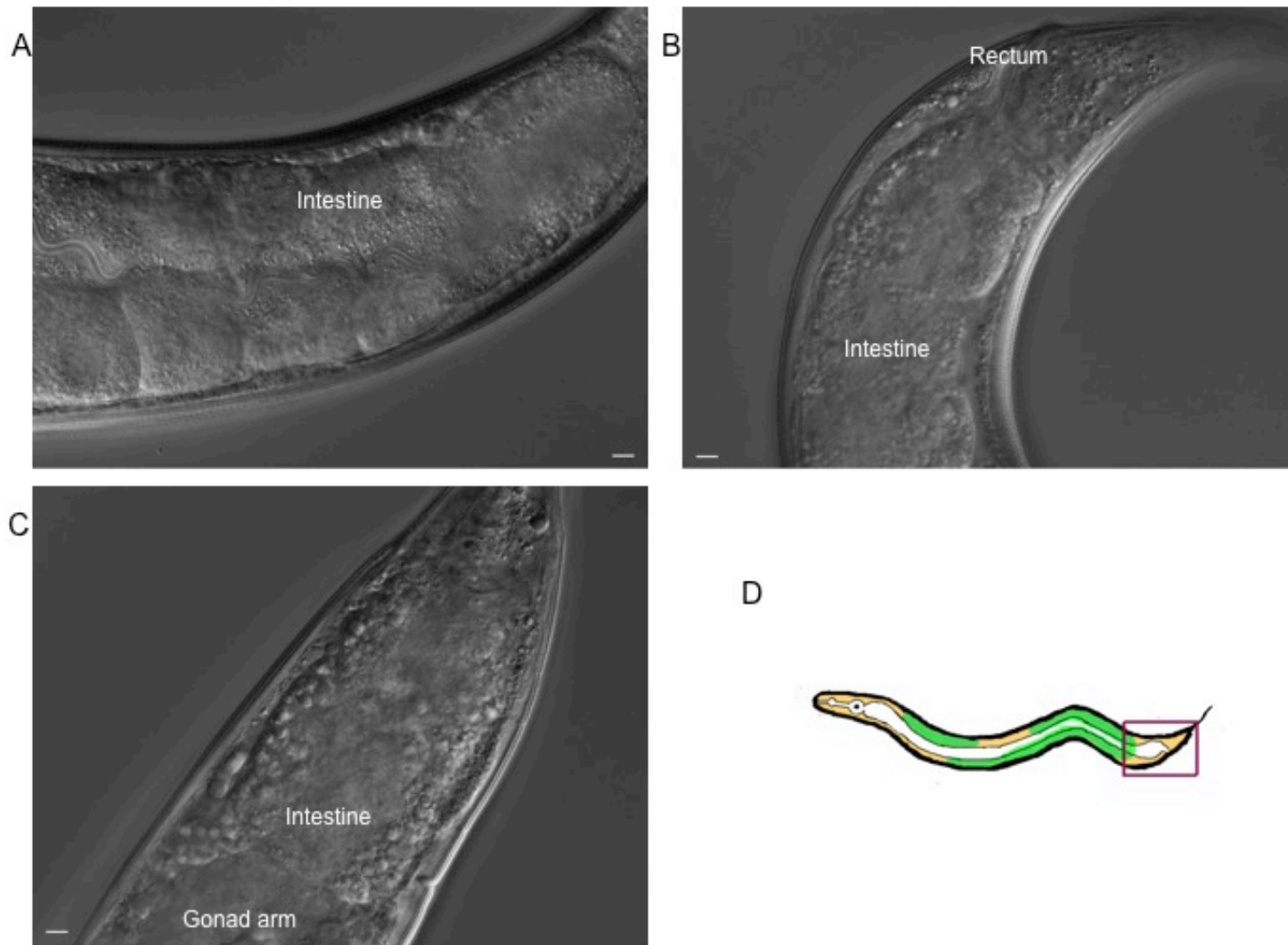


Figure 3.3 Observed morphology of the tail region of N2 *C. elegans* fed heat-killed *E. coli* OP50 on BCYE. Morphology observed over a period of 8 days, images taken on 1, 3 and 6 days post-infection, for A, B, and C respectively. The nematodes were incubated at 25°C on BCYE with heat-killed benign *E. coli* OP50 as a food supplement. D) Schematic of nematode; box indicates region of interest. Scale bar is 5  $\mu$ m.

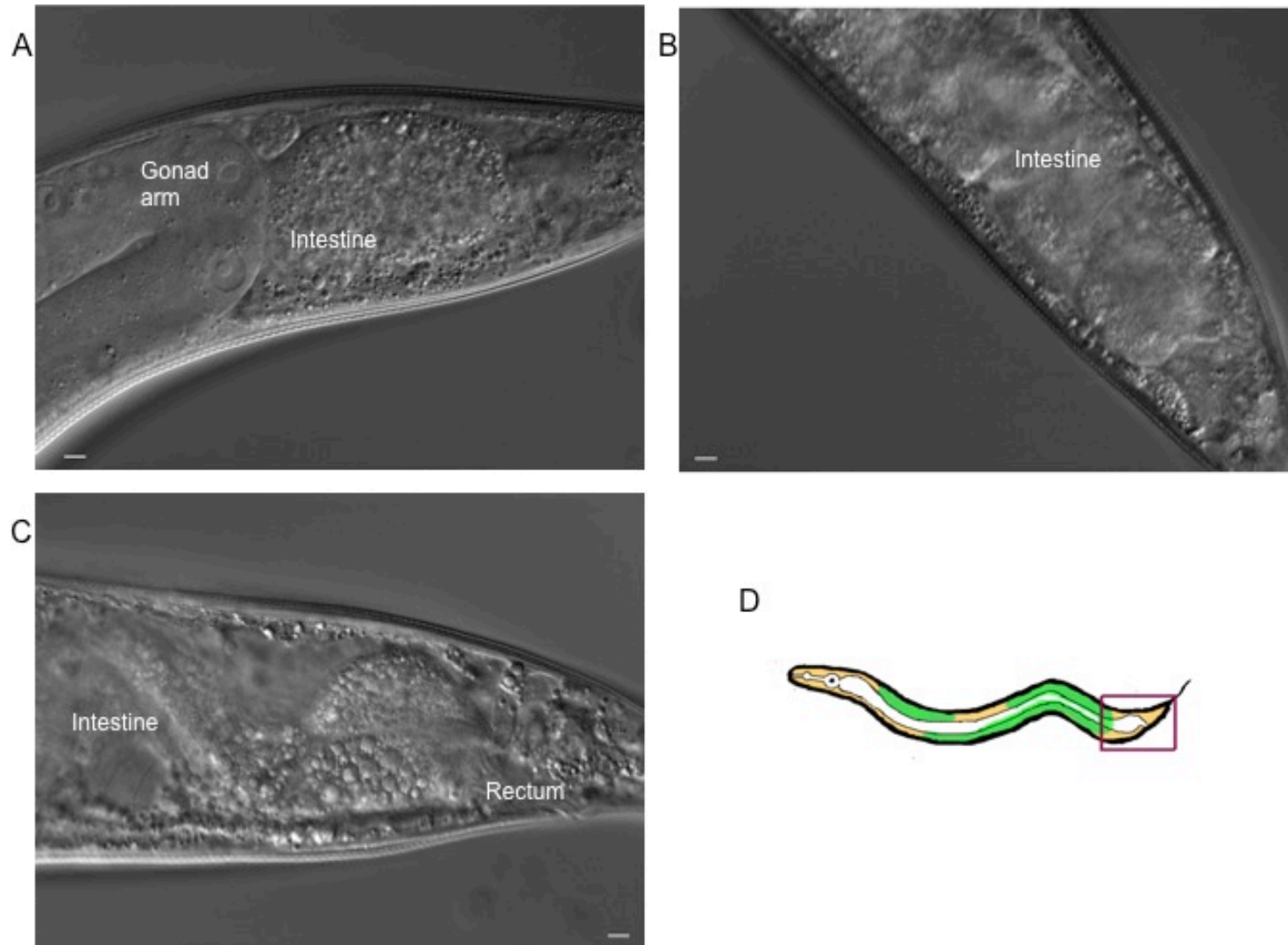


Figure 3.4 Observed morphology of the tail region of N2 *C. elegans* fed heat-killed wild-type *L. pneumophila*. Morphology observed over a period of 8 days, images taken on 1, 3 and 6 days post-infection, for A, B, and C respectively. The nematodes were incubated at 25°C on BCYE with heat-killed wild-type *L. pneumophila* as a food supplement. D) Schematic of nematode; box indicates region of interest. Scale bar is 5  $\mu$ m.

similar size throughout the infection days (Figure 3.2). The same can be said about the other controls used in the experiment (Figures 3.3. and 3.4). In all of the assays assessed, there is a lack of swelling in the lumen of the intestine. The swelling observed is seen as a natural aging process in a typical older adult nematode. The swelling seen is consistently observed over the infection period. However, there was no obvious phenotypical change in the rectum. Therefore, any morphology change in tissue structure is not due to the aging process.

### **3.2.2 Morphology of the vulva and uterus region**

The majority of the *C. elegans* body consists of two major organs one being the intestine and the other the gonadal tissue (Woods, 1988). The gonadal tissue is comprised of two gonad arms that lie in a parallel fashion to the intestinal tract along the nematode. At the midpoint of the gonad arms is the egg-laying apparatus, which houses the spermatheca, uterus, and vulva (Woods, 1988). In this region the developed oocytes travel down the gonad arms, enter the spermatheca, become fertilized and then further develop in the uterus before being expelled through the vulva (Wood, 1988). A key area of interest in pathogenic studies is the vulva and uterus area. This is because this area is the only one besides the mouth, rectum and amphids where bacteria have the ability to either exit or enter into the nematode.

The ability of the hermaphrodite nematode to generate viable embryos lasts until all the sperm are depleted. Sperm are present for an approximate period of 5.8 days, after which the nematode is able to live for 10 more days (Brenner, 1973). For the first days of imaging of the nematodes fed the control strains (heat-killed OP50 on NGM media and BCYE media, heat-

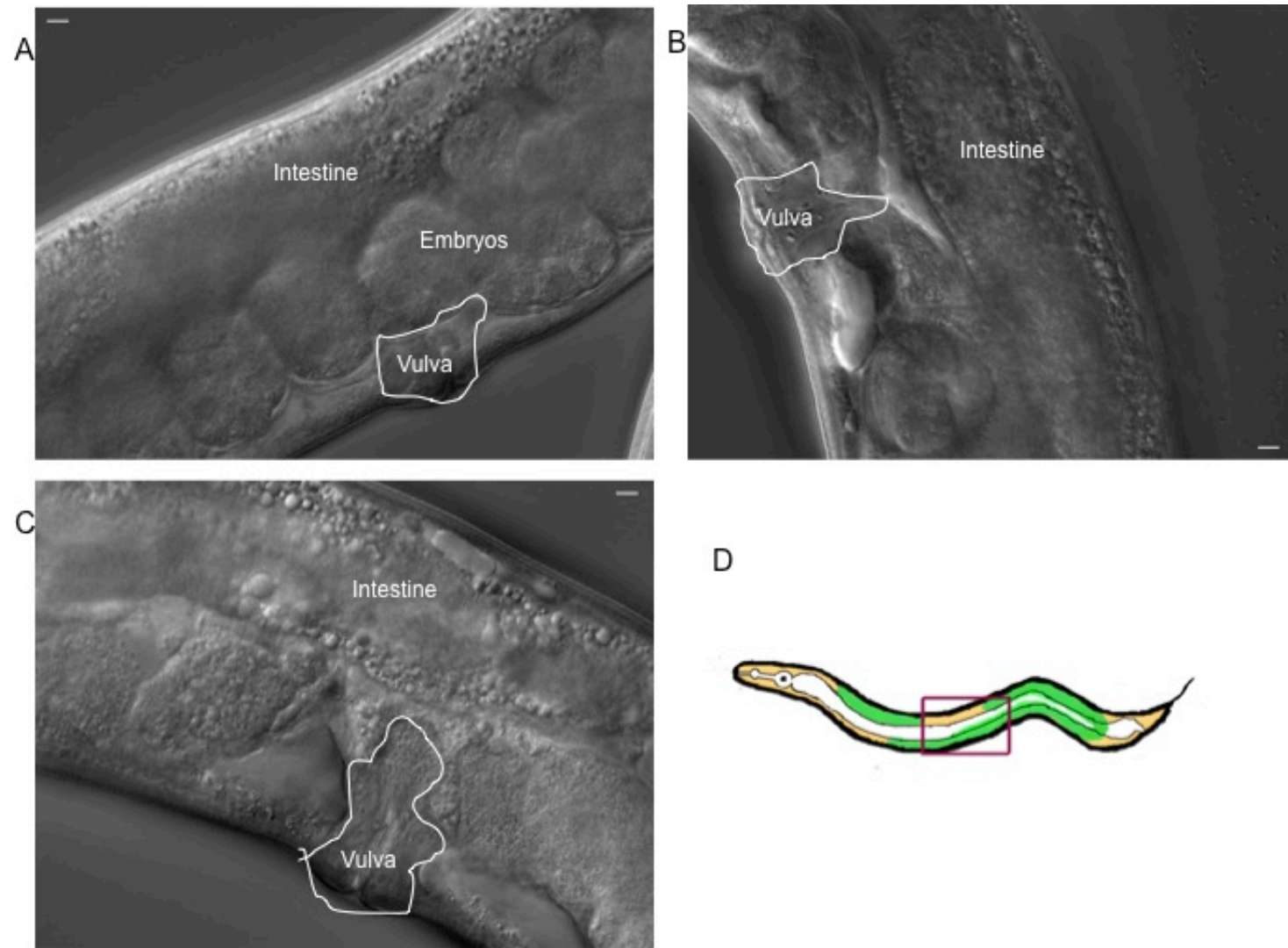


Figure 3.5 Observed morphology of the vulva and uterus region of N2 *C. elegans* fed *E. coli* OP50 on NGM. Morphology observed over a period of 8 days, images taken on 1, 3 and 6 days post-infection, for A, B, and C respectively. The nematodes were incubated at 25°C on NGM with benign *E. coli* OP50 as a food supplement. D) Schematic of nematode; box indicates region of interest. Scale bar is 5  $\mu$ m.

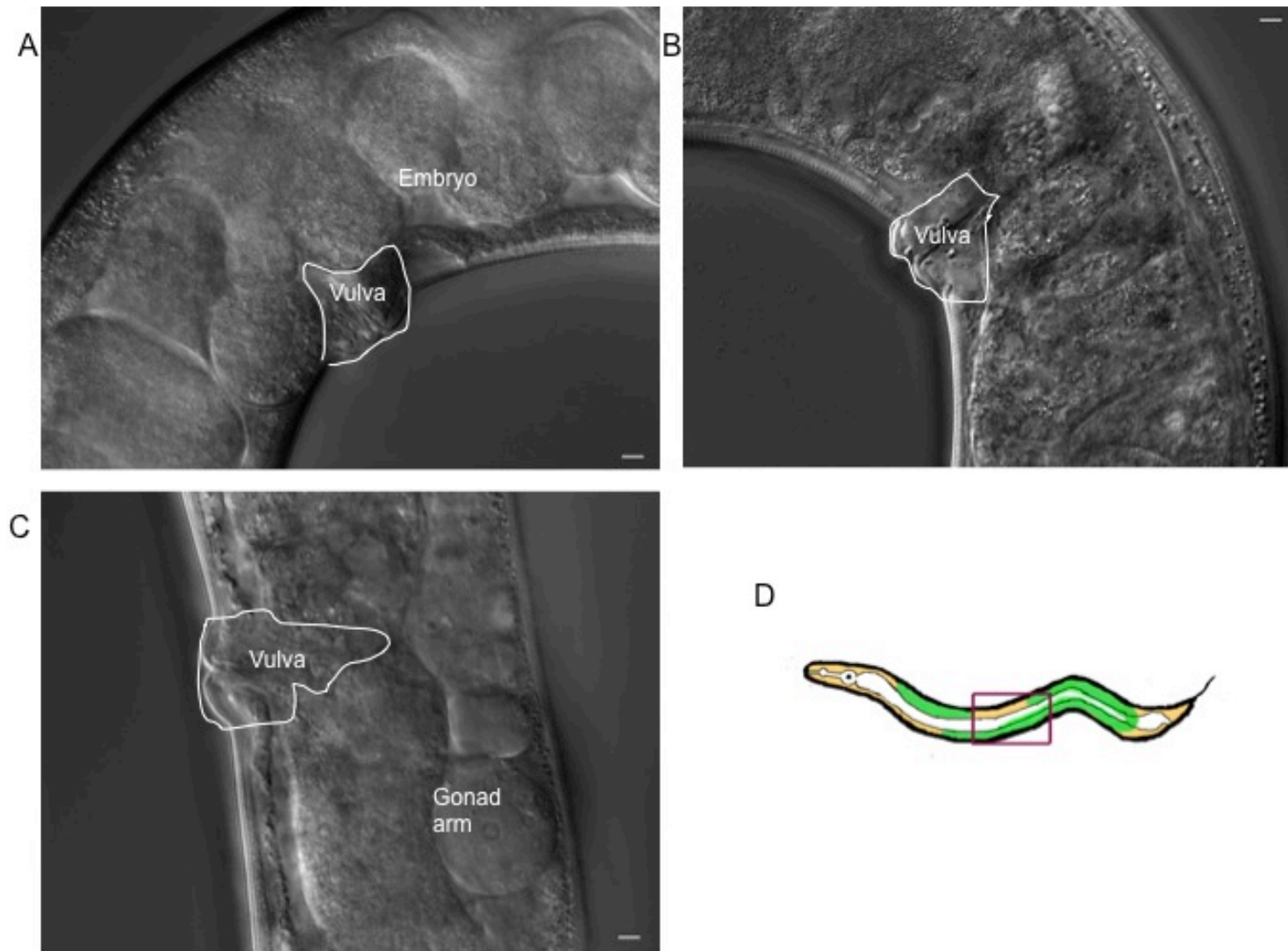


Figure 3.6 Observed morphology of the vulva and uterus region of N2 *C. elegans* fed heat-killed *E. coli* OP50 on BCYE. Morphology observed over a period of 8 days, images taken on 1, 3 and 6 days post-infection, for A, B, and C respectively. The nematodes were incubated at 25°C on BCYE with heat-killed benign *E. coli* OP50 as a food supplement. D) Schematic of nematode; box indicates region of interest. Scale bar is 5  $\mu$ m.



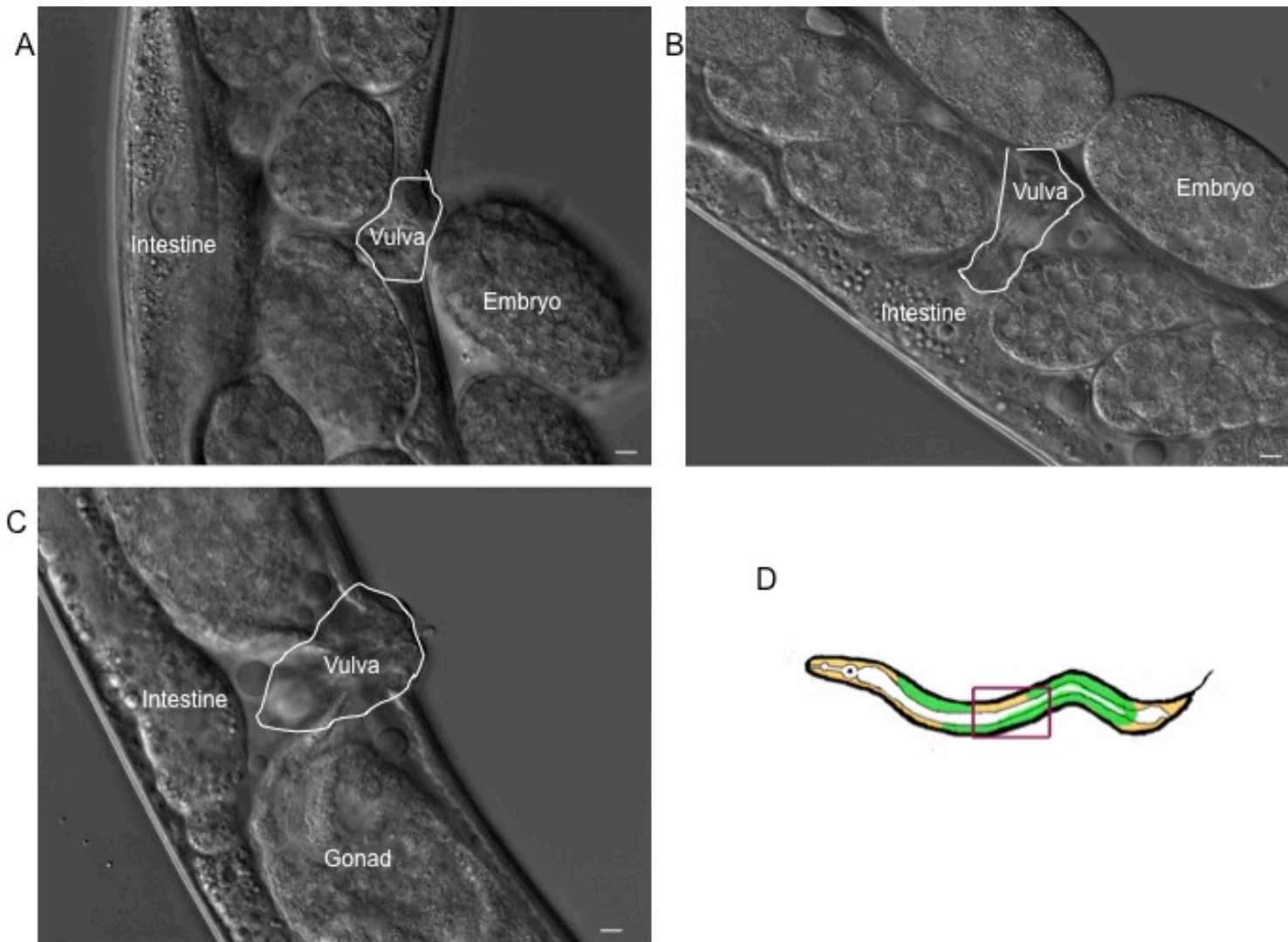


Figure 3.7 Observed morphology of the vulva and uterus region of N2 *C. elegans* fed heat-killed wild-type *L. pneumophila*. Morphology observed over a period of 8 days, images taken on 1, 3 and 6 days post-infection, for A, B, and C respectively. The nematodes were incubated at 25°C on BCYE with heat-killed wild-type *L. pneumophila* as a food supplement. D) Schematic of nematode, box indicates region of interest. Scale bar is 5  $\mu$ m.



killed *L. pneumophila* on BCYE media) embryos were observed in the vulva and uterus region (Figures 3.5, 3.6, 3.7). This is consistent with a normal fertilization period. On the third day post-infection, there was a depletion of the eggs in the uterus region with no embryos visible after the sixth day post-infection. As with the aging of the nematode, there is a tissue degradation and disfigurement (Collins *et al.*, 2008). It is assumed that after the nematode has been depleted of sperm, gonadal tissue progression arrests on significantly inhibited as the adults can lay unfertilized oocytes for a few days after sperm have been depleted (Collins *et al.*, 2008). As with the tail region, there is no swelling observed in the gonad tissue of nematodes fed the control strains through the assay. However, it is important to note that the embryos cause the gonadal tissue to swell, so there is slight swelling of the gonadal tissue after the eggs have been expelled. Nevertheless, there is no drastic phenotypic change in the vulva or uterus areas in nematodes fed the control strains.

### **3.2.3 Morphology of the intestinal tract**

The most well studied organ in host-pathogen interactions is the intestine. This is because the intestine is the major point of contact with the environmental microbes and houses the innate immune system (Schulenburg *et al.*, 2008; Ewbank 2006). Somehow, the *C. elegans* are able to recognize the existence of pathogens in their intestinal lumen and secrete antimicrobials to combat the infection (Schulenburg *et al.*, 2008). Recently, it has been found that there is strong crosstalk between intestinal innate immune response pathways that leads to a coordinated response to pathogens (Schulenburg and Ewbank, 2004). One key phenotypic observation during an immune response to a bacterial infection is the swelling of the intestinal cells. This is

indicative of antimicrobial production in the cells to combat the infection (Sifri *et al.*, 2005).

Other phenotypes of a progressive bacterial colonization infection include the increase in size of the lumen of the intestine, then a strong bacterial colonization of the lumen, followed by a decrease in size of intestinal cells (Sifri *et al.*, 2005).

In animals fed the control strains of live and heat-killed *E. coli* OP50 no swelling of the intestine is observed. There is a slight degradation of the tissue due to age and an increase in the gut granules (Figures 3.8, 3.9). All of which are normal phenotypes in an aging animal. However, in nematodes fed the heat-killed *L. pneumophila* greater morphology changes of the intestine, especially at the end of the infection period was observed. On day 6 post-infection, the intestinal tract had an extended intestinal lumen stuffed with bacteria and a clear distinction between the lumen and the intestinal cells. The intestine had decreased in size, with the presence of the gut granules not consistently surrounding the intestinal lumen (Figure 3.10 C). This may be due to non virulence effectors molecules of *L. pneumophila* and be a supporting reason in the survival rate of the nematodes fed heat-killed *L. pneumophila*.

To further investigate this finding, nematodes were fed heat-killed *L. pneumophila* for 6 days, fixed and sectioned for electron microscopic analysis. Here the bacterial forms are observed burst open (Figure 3.11 A) and nothing remains of the rod forms except of an outer shell (Figure 3.11C). Immunogold labeling with rabbit Lp1 primary antibody raised against *L. pneumophila* LPS with secondary gold-conjugated donkey anti-rabbit antibody was applied to the grids. This approach was to see if the broken forms could still be recognized as *L. pneumophila* LPS with secondary gold-conjugated donkey anti-rabbit antibody was applied to the grids. This approach was to see if the broken forms could still be recognized as *L.*

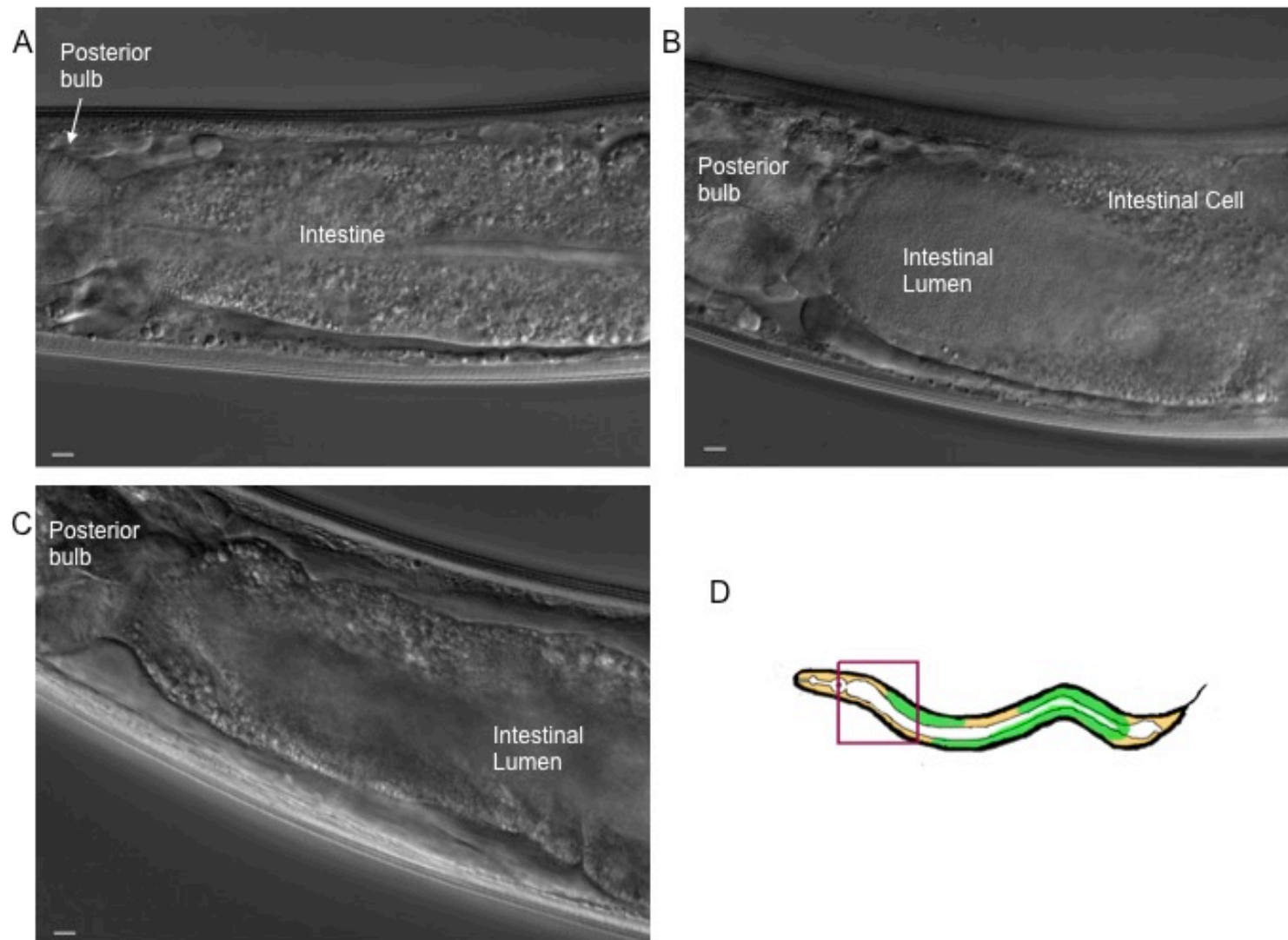


Figure 3.8 Observed morphology of the anterior intestinal region of N2 *C. elegans* fed *E. coli* OP50 on NGM. Morphology observed over a period of 8 days, images taken on 1, 3 and 6 days post-infection, for A, B, and C respectively. The nematodes were incubated at 25°C on NGM with benign *E. coli* OP50 as a food supplement. D) Schematic of nematode; box indicates region of interest. Scale bar is 5  $\mu$ m.

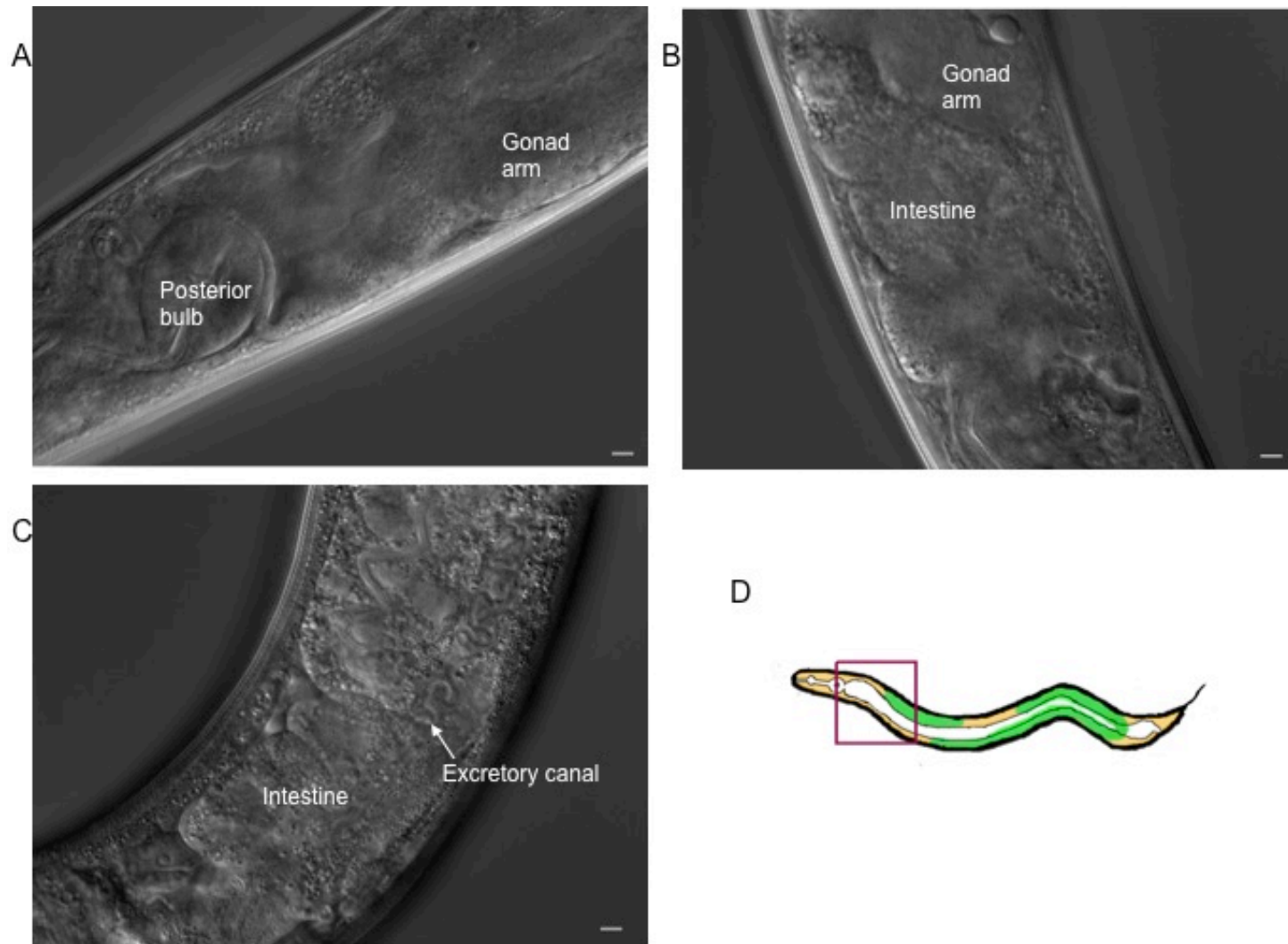


Figure 3.9 Observed morphology of the anterior intestinal region of N2 *C. elegans* fed heat-killed *E. coli* OP50 on BCYE. Morphology observed over a period of 8 days, images taken on 1, 3, and 6 days post-infection, for A, B, and C respectively. The nematodes were incubated at 25°C on BCYE with heat-killed benign *E. coli* OP50 as a food supplement. D) Schematic of nematode; box indicates region of interest. Scale bar is 5  $\mu$ m.

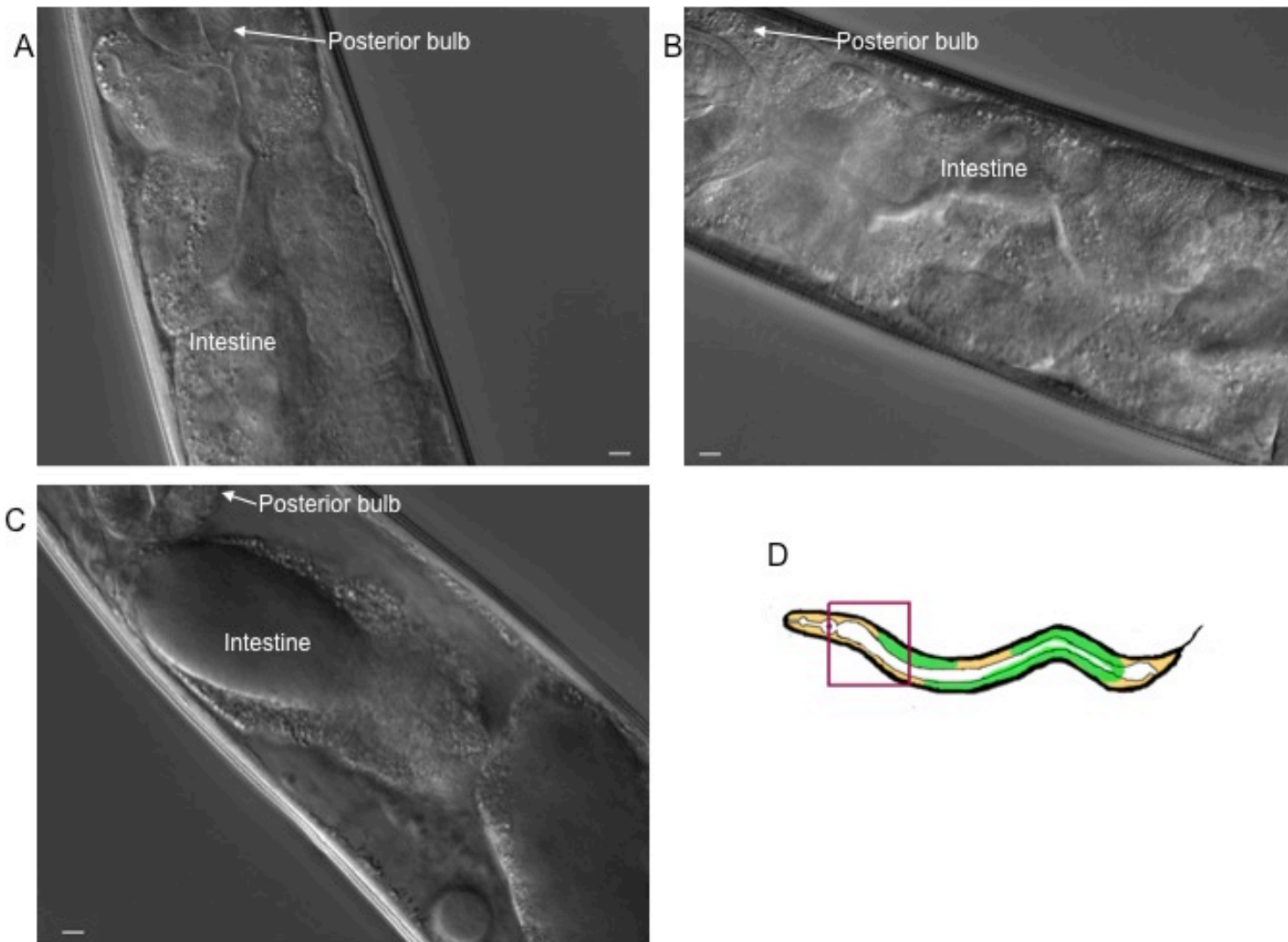


Figure 3.10 Observed morphology of the anterior intestinal region of N2 *C. elegans* fed heat-killed wild-type *L. pneumophila*. Morphology observed over a period of 8 days, images taken on 1, 3 and 6 days post-infection, for A, B, and C respectively. The nematode was incubated at 25C on BCYE with heat-killed wild-type *L. pneumophila* as a food supplement. D) Schematic of nematode; box indicates region of interest. Scale bar is 5  $\mu$ m.

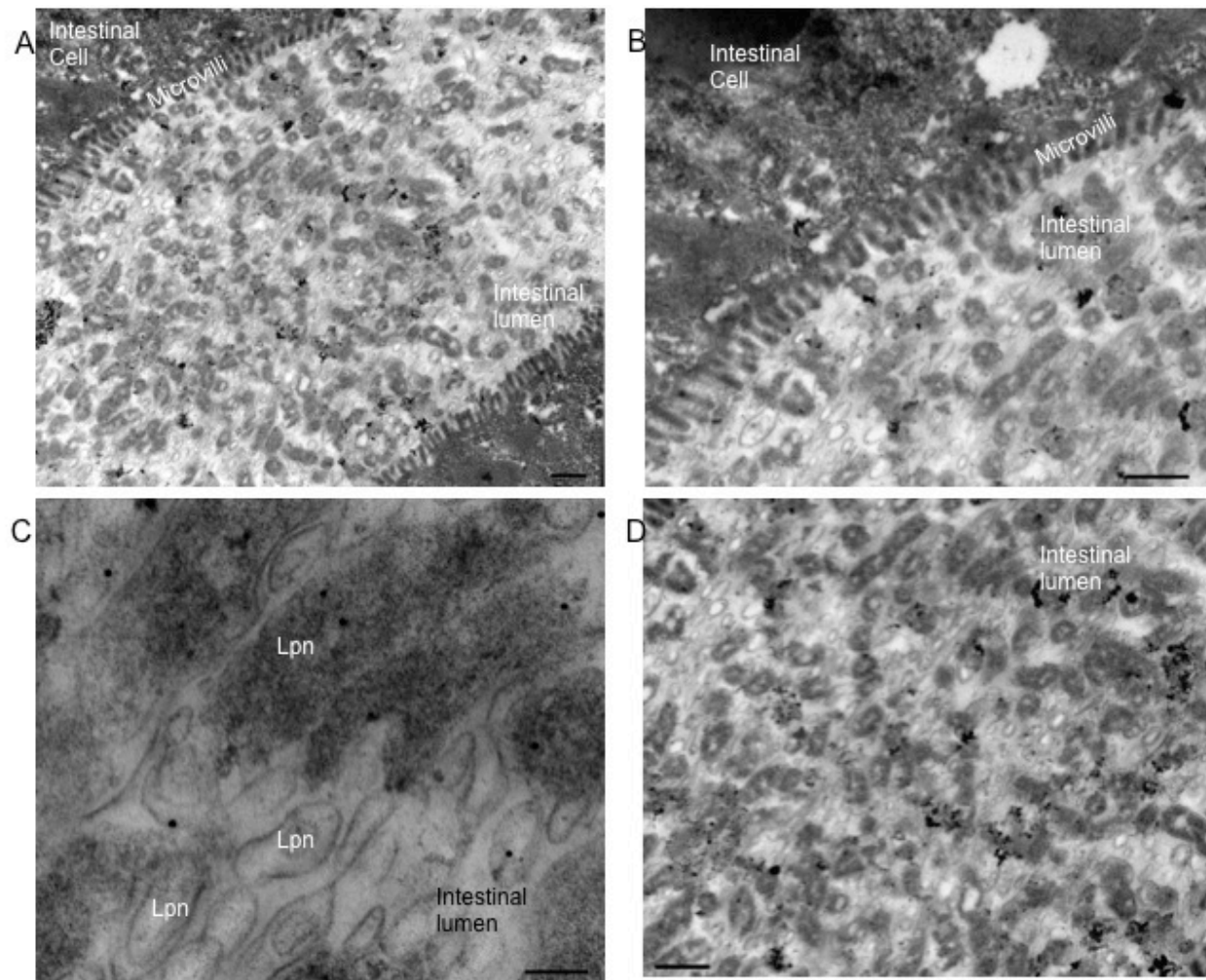


Figure 3.11 Transmission electron micrographs in the intestine of heat-killed wild-type *L. pneumophila* fed *C. elegans*. (A) Overview of the intestinal lumen with heat-killed *L. pneumophila* in the lumen. (B) Close up of the microvilli structure. (C) Close up of the bacteria forms in the intestinal lumen. (D) Zoomed in image of the bacterial forms in the intestinal lumen. Lpn: *L. pneumophila* bacteria observed. Scale bar is 500 nm for parts A, B and D. 100 nm for part C. Images were tagged with donkey anti-rabbit Lp1 antibody conjugated to gold-particle.

*pneumophila* forms. Based on the analysis of the micrographs, the antibody is specific for live and dead *L. pneumophila* bacterial forms (Figure 3.11 C). It should be noted that the microvilli of the intestinal lumen was observed to have normal morphology (Figure 3.11 B). There is packing of the heat-killed bacteria in the intestine but not to the same severity as for nematodes fed live *L. pneumophila* (Figures 3.11 and 3.13). Furthermore, no aberrations of the intestine or any physical trauma on the nematode were noted.

### **3.3 *C. elegans* Intestinal tract colonization and morphology**

With the baseline morphologic changes established for nematodes fed the control strains, nematodes fed live *L. pneumophila* can now be monitored microscopically by Nomarski optics or electron microscopy. The morphological changes observed in the nematodes are thus a result of the infectious live *L. pneumophila* bacteria. As previously noted, the morphologic changes observed in nematodes fed heat-killed and live *E. coli* OP50 bacteria were minor and otherwise associated with general aging processes. In nematodes fed heat-killed *L. pneumophila*, there were phenotypic effects that were not visualized in nematodes fed live *L. pneumophila*. These phenotypes include the lack of swelling of the intestinal lumen, constipation, and the lack of extrusion of gonadal tissue from the vulva. Therefore, the controls were valid in that the infection characteristics of nematodes fed live *L. pneumophila*, as they were not observed in any nematodes fed the control strains.

#### **3.3.1 Colonization of the intestinal tract**

Sifri *et al.* (2005) defined five different ways pathogenic bacteria are characterized to kill *C. elegans*. One of the most commonly found methods of nematode death is through the colonization of the intestine. Other killing methods involve a persistent intestinal infection and invasion of *C. elegans* tissues, or toxin induced killing or cuticle biofilm production (Sifri *et al.* 2005). The observed infection of *C. elegans* fed *L. pneumophila* was concluded to be intestinal colonization determined by Nomarski optics. At the beginning of the infectious process there are physiological similarities between nematodes fed the control strains and the nematodes fed live *L. pneumophila* (Figure 3.12 A). However, once *L. pneumophila* had time to sufficiently establish a pathogenic colonization in the intestine, other characteristics of a pathogenic infection were observed in the nematode. These characteristics are observed on the second day post-infection and include a swollen intestine, clumping of the bacteria in the intestinal lumen, and constipation indicated by rectum swelling.

In the later portion of the infection the initial pathogenic characteristics morph into more damaging and prolonged phenotypic characteristics observed. The initial swelling of the intestinal tract increases from the amount of antimicrobial products being produced and secreted in the intestinal lumen (Figure 3.12 B). The clumping of the bacteria form a blanket of colonized bacteria that pushes the intestine to fill the body cavity of the nematode (Figure 3.12 C). Lastly, the constipation of the nematode remains constant and the tissue distinction between the lumen and the intestinal cells becomes more pronounced (Figure 3.12 D). The intestine will have a varying degree of swelling from examined nematode to nematode; however, the general trend is indicative of the intestinal tract increasing in size particularly an expansion of the lumen. The



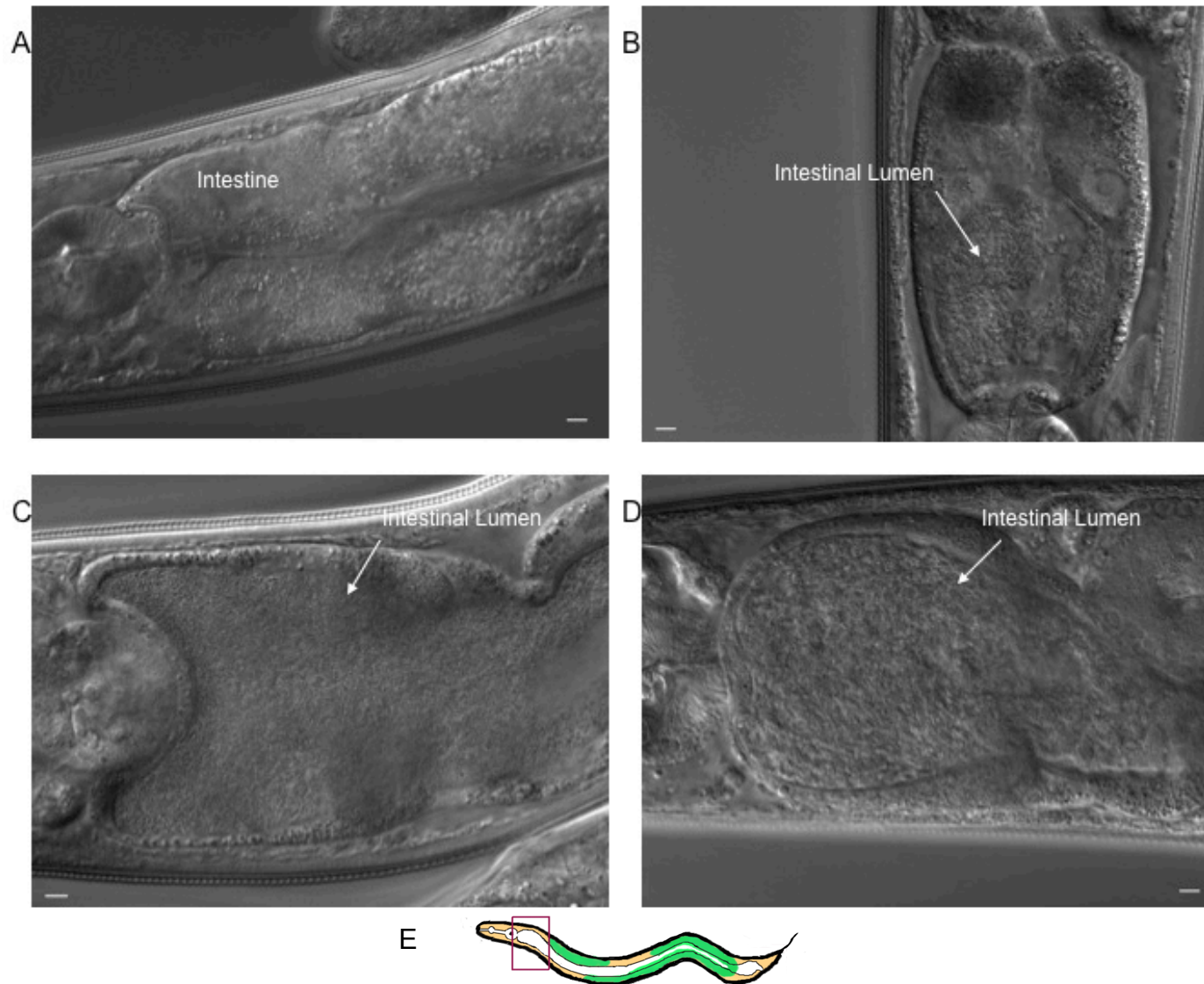


Figure 3.12 Observed morphology of the anterior intestinal lumen region of N2 *C. elegans* fed *L. pneumophila*. Infection was observed over a period of 8 days. Images taken on day 2 infection (A), day 4 infection (B), day 6 infection (C), and day 8 infection (D). (E) Schematic of nematode, box indicates region of interest. Scale bar is 5  $\mu$ m.

colonization of the nematode's intestinal lumen persists until the demise of the nematode (Figure 3.12 D).

*L. pneumophila* has various different forms depending on the stage of its life cycle (Faulkner and Garduño, 2002). Observed in the lumen of the intestine are mainly replicative forms, which can be distinguished by their typical gram-negative rod shaped form (Figure 3.13 A). Further observed in the lumen of the intestine are the bacterial forms undergoing mitosis (Figure 3.13 B). This indicates that *L. pneumophila* is able to replicate in the lumen of the intestine, and that nutrients required for bacterial replication are available in the lumen. The replicating rods further verify *L. pneumophila* ability to colonize and to establish a replicative niche in the lumen of the intestine. To verify the existence of *L. pneumophila* only in the intestinal lumen Immunogold tagging of the bacterial forms was completed through the use of the same antibody used to tag the heat-killed *L. pneumophila* bacteria forms. The nematodes were fed live *L. pneumophila* for six days then fixed and tagged as according to procedure described in material and methods. Observed is strong tagging of the bacterial form's outer membrane in the intestinal lumen (Figure 3.13 C). Also of note is the difference in replicative and transitioning forms being tagged in the same manner (Figure 3.13C). To understand the degree of colonization low magnification images were taken of *L. pneumophila* in the intestinal lumen (Figure 3.13 D). These images further support the Nomarski imaging of intestinal colonization observed.

### **3.3.2 Constipation and swelling of the intestinal tract**

A characteristic of an infection in a host is the ability of the bacteria to manipulate the

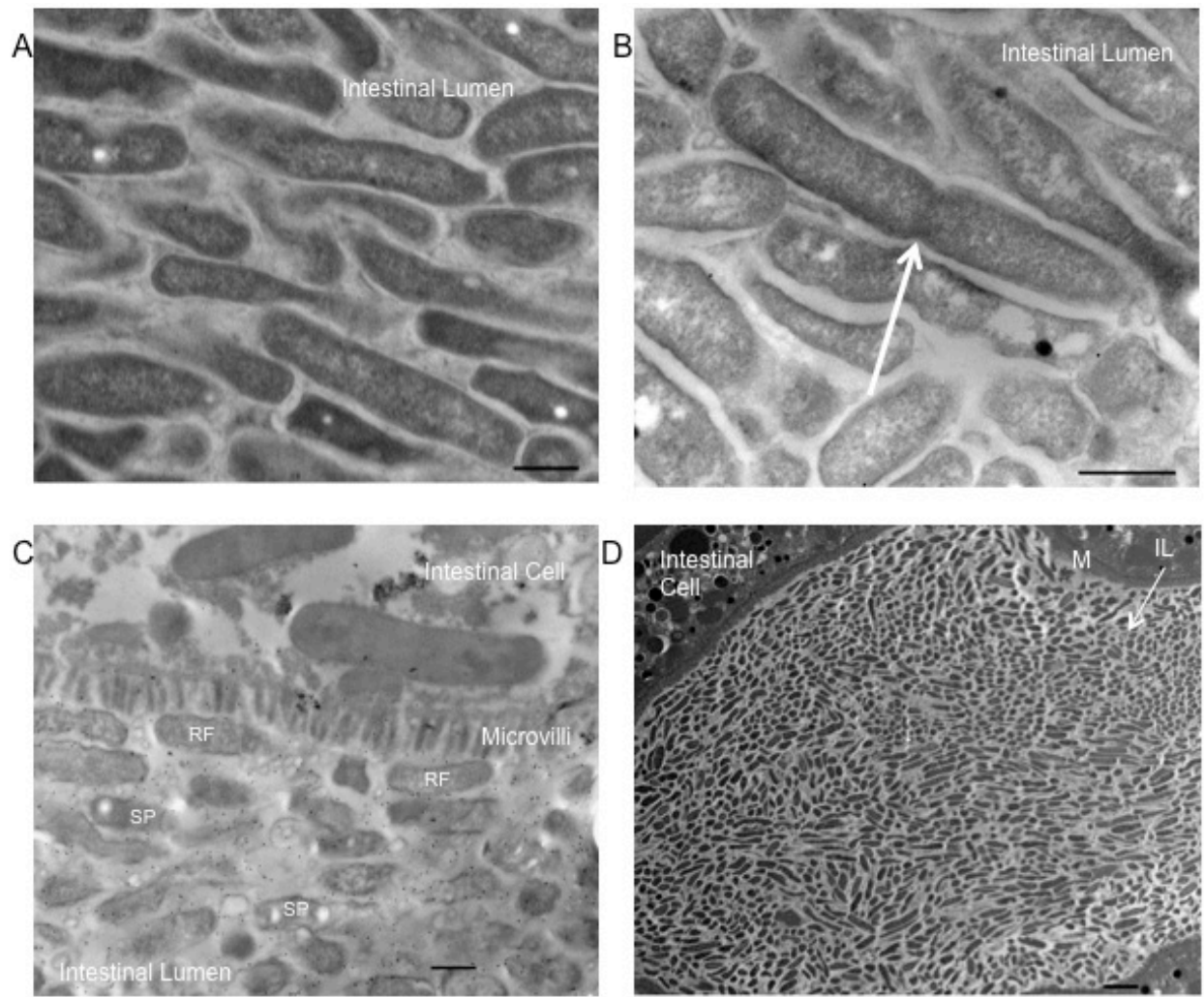


Figure 3.13 Transmission electron micrographs of *L. pneumophila* in intestinal lumen of *C. elegans*. *C. elegans* were infected with *L. pneumophila* for 6 days. (A) Scaled in image of colonized bacteria replicative forms. (B) Scaled in image of replicative forms undergoing mitosis (arrow). (C) Immunogold tagged micrograph of replicative bacteria forms. (D) Scaled out image of the intestinal lumen colonization with bacteria forms. IL: Intestinal lumen, M: microvilli. Scale bar is 500 nm (A, B, and C); 2  $\mu$ m (D).

surrounding tissues to create a better replicative niche. The *L. pneumophila* bacteria can cause constipation in the posterior portion of the intestine nematode thereby allowing the bacteria inside time to replicate and to stop the expulsion of forms via rapid peristalsis motion (Brassinga *et al.*, 2010). Some of the forms are visualized and assumed to be in the process of being expelled from the intestinal lumen (Figure 3.14 A). The constipation of the nematode is visible in the beginning of the infection process. As colonization persists the lumen of the intestine becomes distinct from the intestine and is most evident in the later portion of the infection (Figure 3.14 B).

Other portions of the intestine swell as well, but swelling is assumed to be from the production of antimicrobials in the intestinal cells (Ewbank, 2006; McGhee, 2007). Since the release of antimicrobials is in the lumen of the intestine to combat the infection, the production of the antimicrobials is generally limited to the cells that surround the lumen of the intestine. Observed at the anterior portion of the intestine, there is swelling of the intestinal cells surrounding the lumen of the intestine. In a small population of nematodes observed, there is still a presumed production of antimicrobial products to combat the infection (Figure 3.14 C). However, due to the persistent colonization infection observed on the seventh day indicates that the antimicrobial production still fails to effectively eliminate the pathogenic bacteria (Figure 3.14 C). Other portions of the intestine also swell with the anterior portion of the intestinal tract indicating, that the swelling of the intestinal tract is not specific to a portion of the intestine but rather is a primary response to the presence of a pathogen in the lumen of the intestine.

### **3.3.3. Manipulation of the intestine apical membrane**

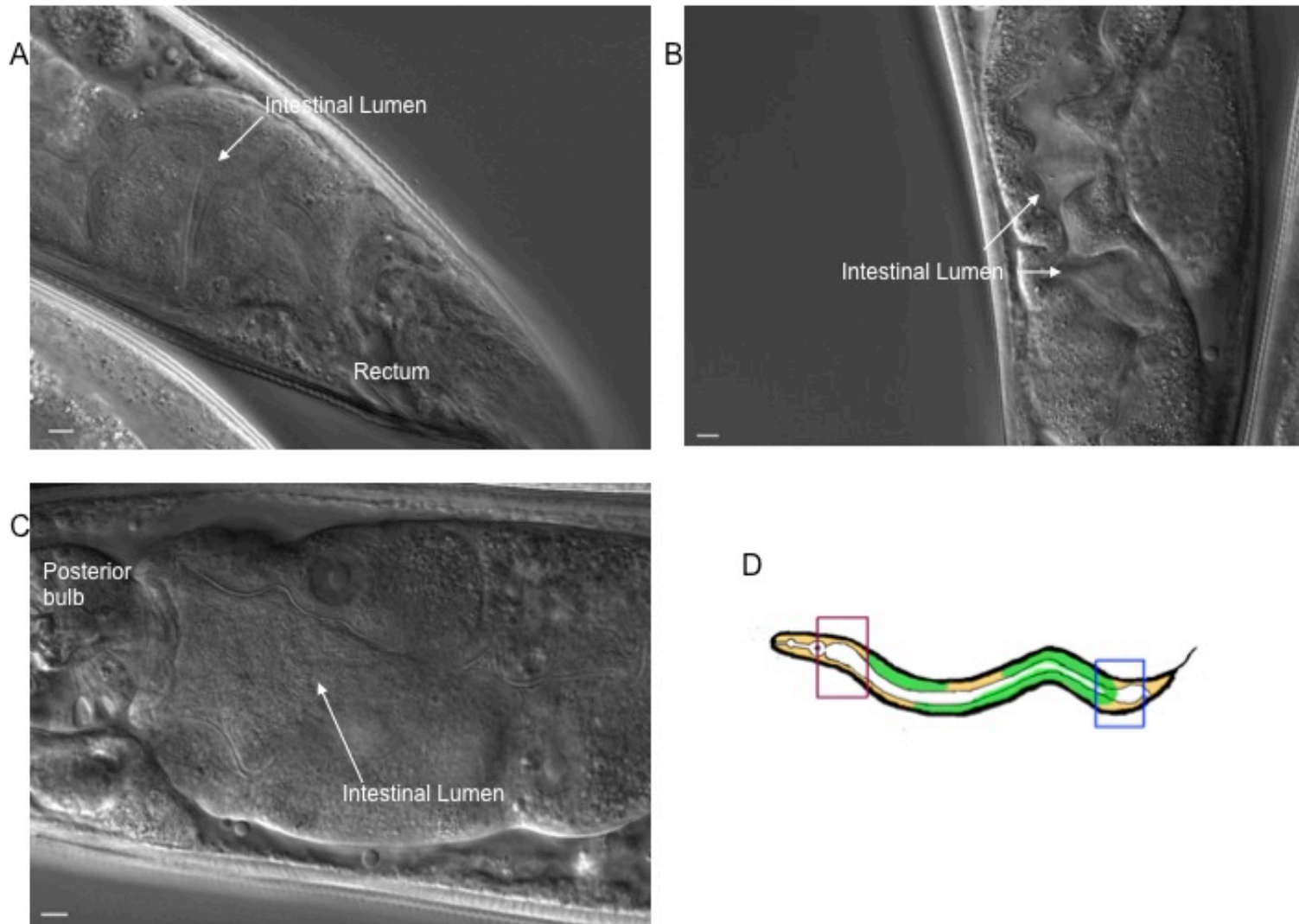


Figure 3.14 Observed morphology of the intestinal region of *C. elegans* fed *L. pneumophila*. Infection was observed over a period of 8 days. Images taken on day 4 infection (A), day 7 infection (B and C), D) Schematic of regions imaged of the *C. elegans* nematode red indicates image taken for C, blue for A and B. Scale bar is 5  $\mu$ m.

Along with the colonization of the intestinal lumen, the general swelling of the intestine and the constipation of the posterior portion of the intestine, *L. pneumophila* is able to manipulate the intestinal tract for a possible invasion of tissues. The membrane that surrounds the intestinal lumen is made up of microvilli that extend from the apical membrane to form a brush boarder (McGhee, 2007). The microvilli are anchored into a strong network of intermediate filaments called the terminal web (McGhee, 2007). Covering the microvilli is an extracellular electron-lucent coating of highly modified glycoproteins termed glycocalyx. The function of the glycocalyx is to localize digestive enzymes, protect microvilli from physical or toxic injury, or serve as a general filter of biochemical products (McGhee, 2007). The intestinal lumen is anchored by attachment to the pharyngeal and rectal valves (Woods, 1988). The bacteria are able to manipulate the lumen causing it to stretch to accommodate the mass of the replicating bacteria (Figure 3.15 D). In addition, it appears that the apical membrane is manipulated such that it protrudes into the supporting intestinal cells.

In nematodes infected with live *L. pneumophila*, an invasion of bacterial forms in the microvilli network was observed. In the microvilli network the bacterial forms presumably have the ability to bypass the glycocalyx and bind or interact with the microvilli (Figure 3.15). Imaging at the apical surface of the intestine there appears to be an embedment of the bacterial forms in the microvilli (Figure 3.15 A). Thereby suggesting that the bacteria are able to break apart microvilli individually in order to push their way out from the lumen of the intestine. A longitudinal cross section of this perceived movement strengthens the argument of bacterial rods embedding themselves within the microvilli (Figure 3.15 C). Disruption of the microvilli is further observed in the pushing of the microvilli and the apical membrane towards the intestinal

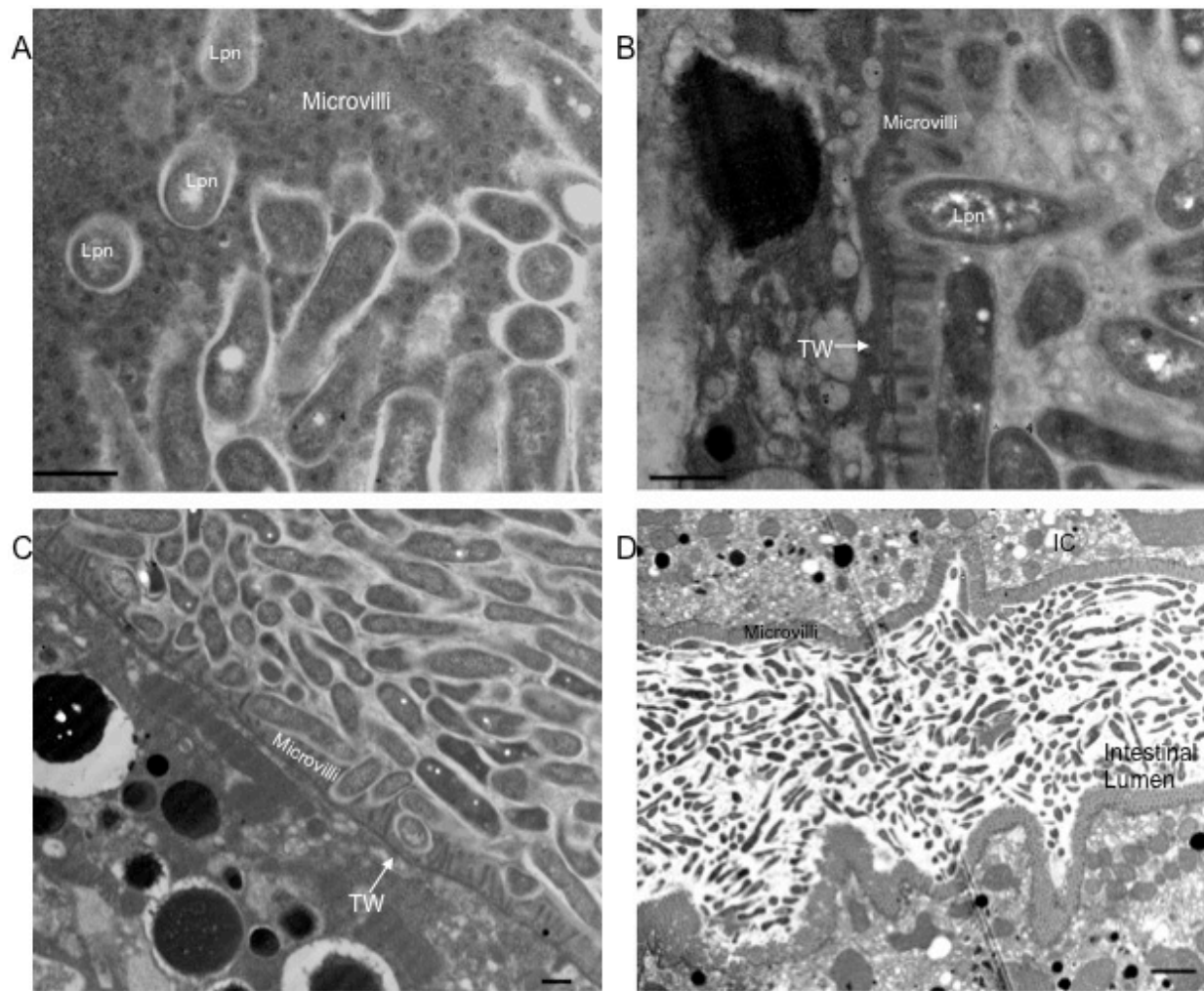


Figure 3.15 Transmission electron micrographs of *L. pneumophila* forms in various components of the brush boarder and supporting components of the intestine of *C. elegans*. Nematodes were infected with *L. pneumophila* for six days. (A) Observed is the complete embedment of the *L. pneumophila* forms in the microvilli of the intestine. (B) A bacteria form pushing both the microvilli and apical membrane. (C) *L. pneumophila* forms embedding themselves in the microvilli of the intestine. (D) The manipulation of the lumen forming bulges with the microvilli and apical surface. TW: terminal web; Lpn: *L. pneumophila*; IC: intestinal cell. Scale bar is 500 nm (A, B, and C); 2  $\mu$ m (D).

cell (Figure 3.15 B).

Further disfiguration of the apical membrane is observed by the disjoining of the microvilli from the terminal web network just under the apical surface (Figure 3.16 B). In the disjoining of the apical surface from the microvilli, there is an open space, which has the potential to be filled with bacterial forms (Figure 3.16 D). On several occasions, the open space is filled with a yolk particle and a bacterial form (Figure 3.16 C). Further observations show the microvilli disjoining from each other to form a junction, which could also allow the bacterial forms to pass through the junction into the intestinal cells (Figure 3.16 A and C). The bacterial forms observed manipulating the microvilli are seen as either transitioning or cyst-like forms. Thus, it is possible for the forms in the intestine to pass through the microvilli and the apical membrane without dismemberment of the microvilli or apical membrane. Observed in the intestinal cells there are bacterial forms present with no physical damage done to the microvilli (Figure 3.17 C). To bypass the microvilli the bacterial forms must either break down the microvilli (Figure 3.16) or else they use nematode processes to escape the intestinal lumen (Figure 3.17). The microvilli are assumed to be able to reform to a degree once the bacteria have passed through its web but there are apparent scars left behind. These scars are seen as tiny holes in the terminal web where the bacteria could have passed.

Observed in the intestinal cells the bacterial forms are present in tight vacuoles (Figure 3.17 B). A nematode was observed where the tight vacuole was completely formed around a *L. pneumophila* form in a distended portion of the intestinal lumen (Figure 3.17 A). The tight and singular bacterial forms were also observed in mammalian epithelial HeLa cells (Faulkner and Garduño, 2002). The tight vacuoles observed in the HeLa cells are said to only increase in size



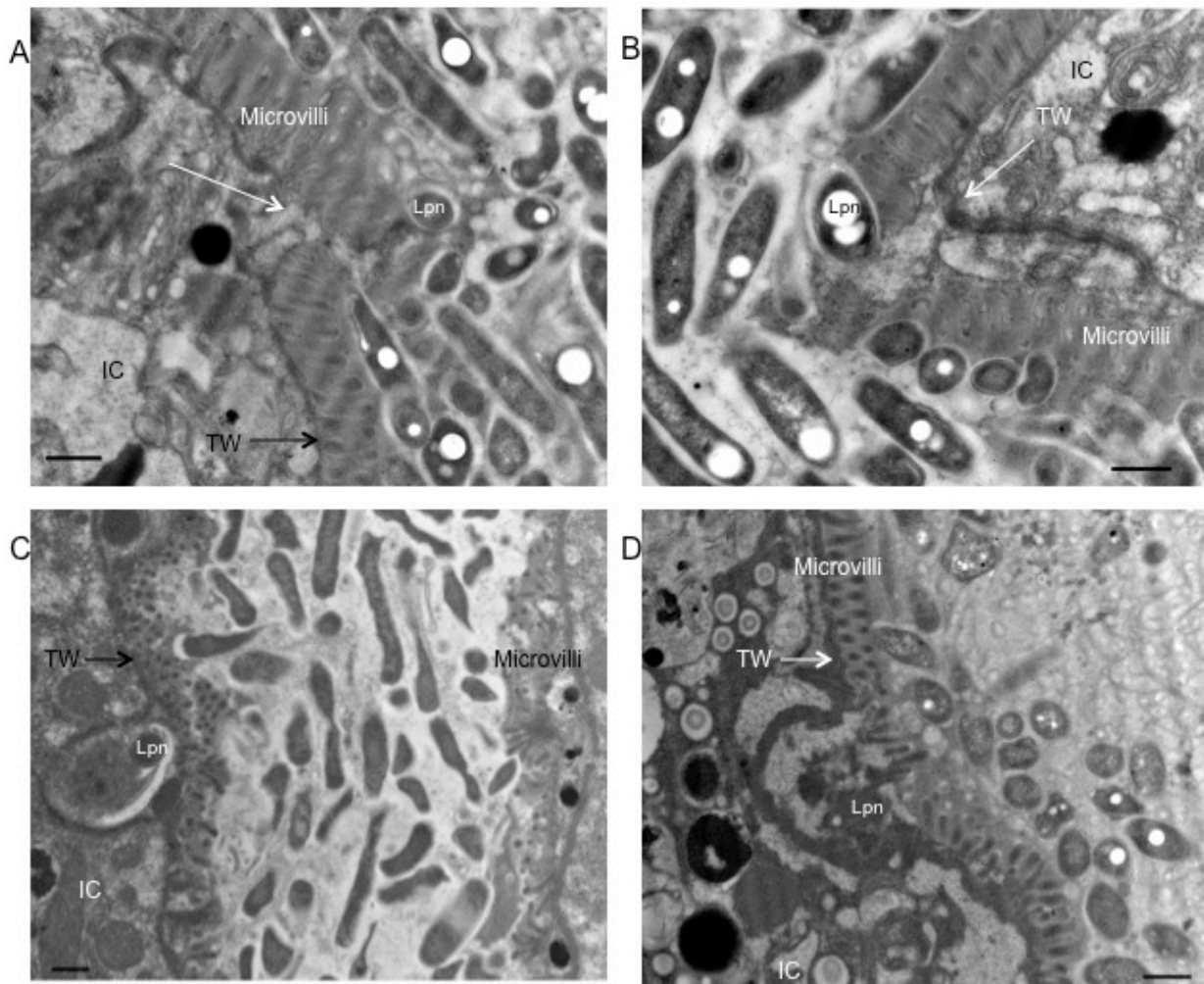


Figure 3.16 Transmission electron micrographs of *L. pneumophila* manipulating the apical membrane and microvilli of the intestine of *C. elegans*. Nematodes were infected with *L. pneumophila* for six days. (A) Is a disjoining of the microvilli with a bacterial form appearing to push on the bottom half of the microvilli (arrow) (B) The disjoining of the electron dense intermediate filaments of the terminal web of the intestine from the microvilli (arrow) (C) The disfiguration of the apical membrane from the microvilli to form a bulge, which is filled, with an unknown particle and bacteria, Lpn. (D) Similar disfiguration of the apical membrane from the microvilli: microvilli are disconnected from each other and apical membrane, Lpn is located inside of the bulge past the microvilli. IC: intestinal cell; TW: terminal web; Lpn: *L. pneumophila*. Scale bar is 500 nm.

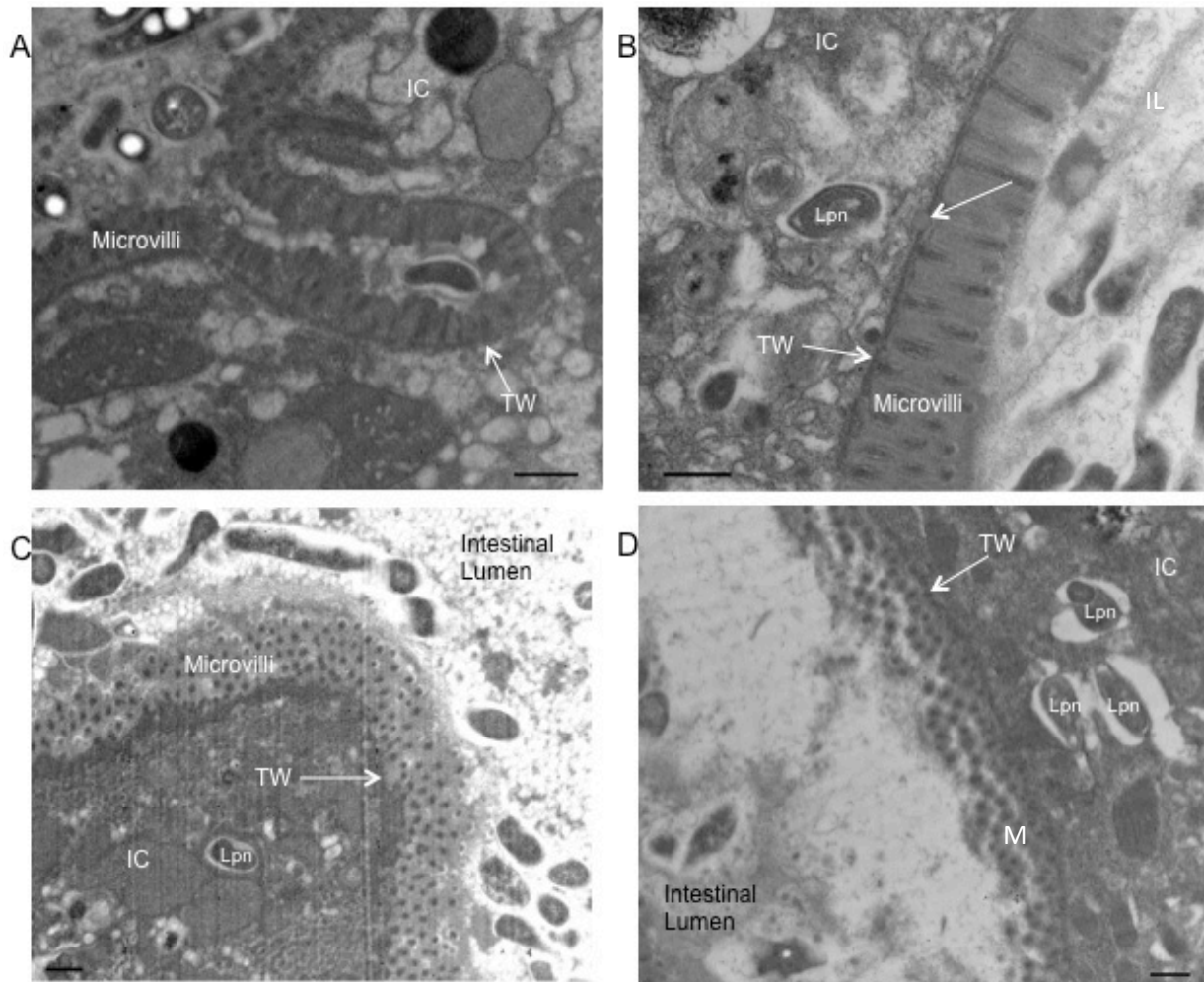


Figure 3.17 Transmission electron micrographs of *L. pneumophila* forms leaving the lumen of the intestine of *C. elegans* in tight vacuoles. Nematodes were infected with *L. pneumophila* for six days. (A) In the lumen of the intestine, there is a bulge of the lumen with a bacterial form present already in a tight vacuole. (B and C) In the intestinal cells are *L. pneumophila* forms are in tight vacuoles appearing to move through the cell. Note how the microvilli appear to be unharmed but there are small punctures in the apical membrane, see arrow in panel B. (D) Observed in low frequency is the formation of a vacuole with multiple forms, next to the intestinal lumen, from singular forms in tight vacuoles. IC: intestinal cell; IL: intestinal lumen; Lpn: *L. pneumophila*; M: microvilli; TW: terminal web. Scale bar is 500 nm.

due to the presence of bacteria inside of the vacuole (Faulkner and Garduño, 2002). In the nematode, the bacterial rods are hypothesized to move through the intestinal cells via the tight vacuoles and into other various tissues such as the gonad and the gonad arm after which the tight vacuoles join up and form a LCV vacuole. However, there is a chance that the tight vacuoles associate with each other in the intestinal cell and form the LCV in juxtaposition to the intestinal lumen (Figure 3.17 D).

### **3.4 *L. pneumophila* secondary infection site**

#### **3.4.1 *L. pneumophila* presence in the pseudocoelomic cavity**

There is no circulatory system in *C. elegans*. Instead, a pseudocoelomic cavity surrounds the tissues of *C. elegans* that helps to transport nutrients between tissues. The pseudocoelomic cavity is a fluid-filled body cavity not fully lined by mesoderm cells and does not fully extend to the cuticle. Nonetheless, it provides the *C. elegans* with a turgor-hydrostatic pressure to maintain homeostasis and contains macrophage-like coelomocytes (Wood, 1988). The pseudocoelomic cavity is a medium for intercellular signaling and nutrient transport (Hall *et al.*, 1999). During a *L. pneumophila* infection, bacteria forms are seen to congregate in the pseudocoelomic cavity leading to the hypothesis that after *L. pneumophila* is able to escape from the intestine they can then travel through the pseudocoelomic cavity to invade other tissues. The presence of *L. pneumophila* in the pseudocoelomic cavity is a delayed characteristic of the infection (Table 3.1). It has been observed that it takes a period of time for *L. pneumophila* to first colonize the intestinal lumen and then escape into the body cavity. Therefore, the LCVs first appear in the

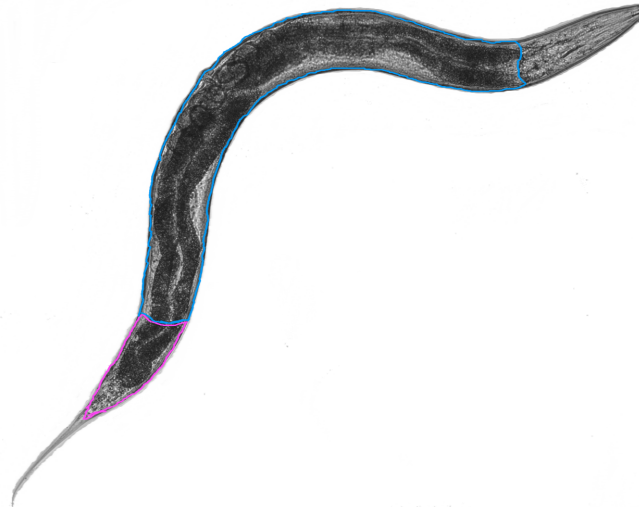


Table 3.1 Assessment of CLFs found in *C. elegans* pseudocoelomic cavity and tail during various *L. pneumophila* strain infections. The nematodes were visualized over the 8-day infection cycle. A total number of 100 nematodes were observed for each time point. The tissue was determined to be infected if LCVs or CLFs were observed. The number of nematodes with infected tissues was counted. The sum of infected tissues was divided by the total worms counted. The numbers reflect a percentage of the nematode population infected. The number was bolded if the population had more than 2/3 of the nematode population infected. Pseudocoelomic cavity outlined in blue, tail area outlined in pink.

#### Pseudocoelomic Cavity

Bacteria Strains	Day 1	Day 2	Day 3	Day 4	Day 5	Day 6	Day 7	Day 8
WT	0	0	3	5	35	45	<b>72</b>	<b>86</b>
$\Delta sdhA$	0	21	55	57	54	65	58	<b>67</b>
$\Delta sdhA$ complement	0	42	<b>64</b>	<b>79</b>	<b>95</b>	<b>89</b>	<b>97</b>	<b>100</b>
$\Delta dotA$	0	35	23	51	36	40	38	37
$\Delta dotA$ complement	0	25	34	40	<b>78</b>	<b>74</b>	<b>83</b>	<b>85</b>

#### Tail

Bacteria Strains	Day 1	Day 2	Day 3	Day 4	Day 5	Day 6	Day 7	Day 8
WT	0	1	0	9	12	25	31	32
$\Delta sdhA$	0	0	3	0	1	2	0	5
$\Delta sdhA$ complement	0	1	3	3	3	5	3	3
$\Delta dotA$	0	5	2	2	0	0	0	2
$\Delta dotA$ complement	0	1	2	13	19	8	10	21

pseudocoelomic cavity from 2 -3 days post-infection and are seen to increase in quantity until the end of the infection (Figure 3.18 D, Table 3.1).

The pseudocoelomic cavity covers all of the tissues in a fluid, which cannot mix with the luminal contents of the digestive tract nor the reproductive tract. The observation of LCVs in the pseudocoelomic cavity on day 2 post-infection is rare and usually appears around the pachytene portion of gonad arm (Figure 3.18 C). The LCVs are assumed to come from the intestinal lumen *via* intestinal cells and once in the body cavity they are able to move throughout the nematode. LCVs are also observed near the developing embryos in the uterus (Figure 3.18 A). Interestingly, in the early days of infection the LCVs are spotted as singular vacuoles with multiple long rod shaped forms present inside.

Later, in the infection process, more vacuoles are present in the cavity due to the natural movement of vacuoles from the intestine to other various tissues. It was observed that half of the vacuoles in the body cavity contained *L. pneumophila* bacterial forms. Present in the pseudocoelomic cavity are 3 pairs of coelomocytes, which have been hypothesized to have immune, scavenging and hepatic functions (Chitwood and Chitwood, 1950). However, they do not have the same phagocytic behavior seen in mammals, and lack the ability to move in through the cavity of the nematode (Ewbank, 2002). Therefore, the innate immune defenses of *C. elegans* are limited once past the intestinal lining and thus the infection can go unabated.

There is an assumption that in the early stage of infection vacuoles found in the pseudocoelomic cavity have replicative rod bacterial forms. These vacuoles with bacteria or LCVs are easier to detect in the pseudocoelomic cavity due to the lack of dense tissue in the body cavity. In the gonad tissue these vacuoles can also be present but are harder to detect due to

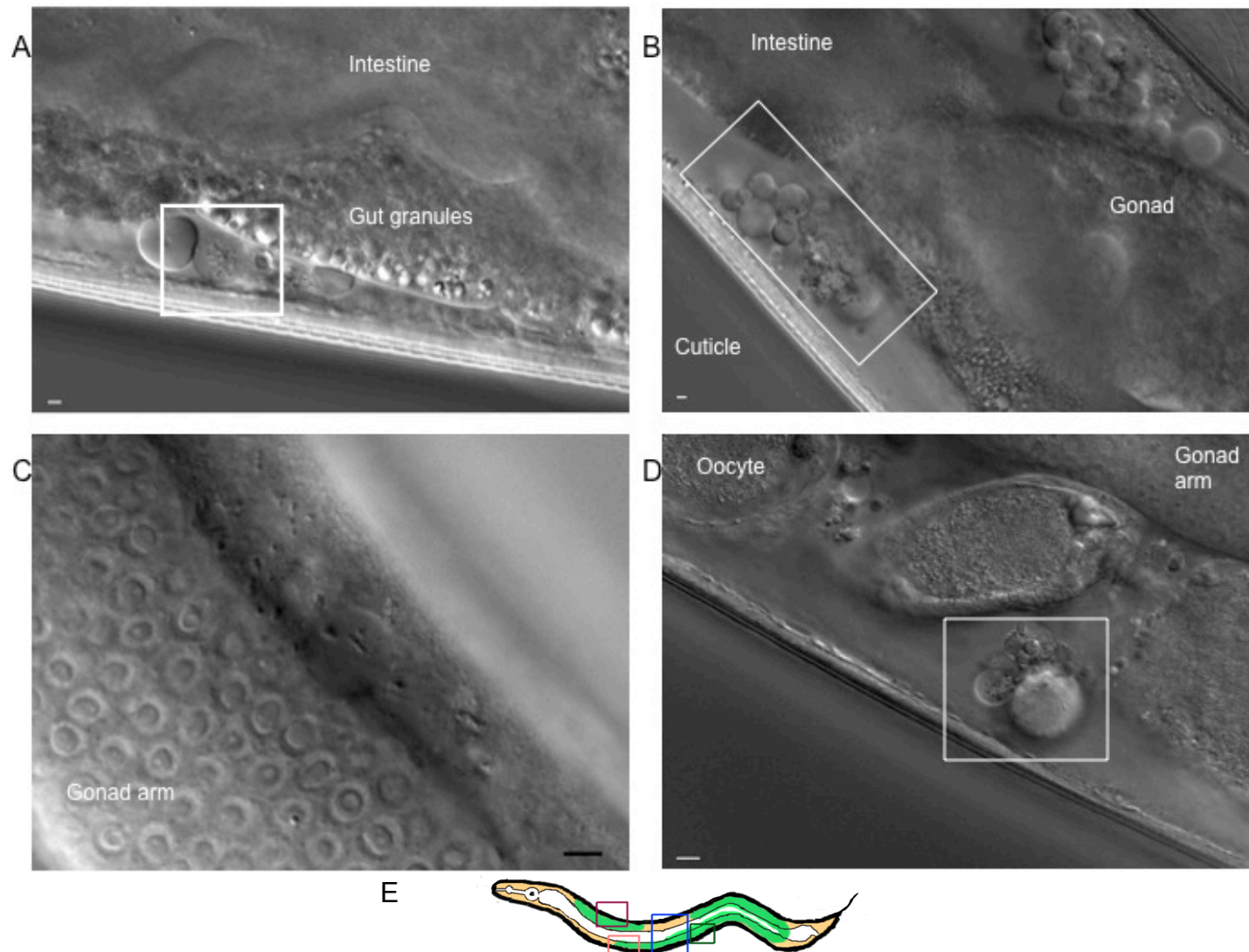


Figure 3.18 Observed morphology of the pseudocoelomic (body) cavity of *C. elegans* fed *L. pneumophila*. Infection was observed over a period of 8 days. The white boxes indicate the LCVs observed in the nematode. Images taken on day 2 infection (A and B), day 6 infection (C), day 5 infection (D), schematic of the planes imaged of the *C. elegans* nematode yellow for A, pink for B, blue for C, and green for D. Scale bar is 5  $\mu\text{m}$  (D), 2  $\mu\text{m}$  (A, B, and C).

the dense tissue surrounding the LCVs. Replicative rod-shaped bacteria are also easier to detect than motile CLF forms in a vacuole due to their length and bacterial characteristics. These replicative forms in LCVs could later infect the gonadal tissues and set up a replication niche. Similar to the lifecycle in other hosts, the bacterial forms in the LCVs are seen to shorten and become motile. This is consistent with the development and life cycle of *L. pneumophila*.

### **3.4.2 *L. pneumophila* growth in the gonadal tissue**

Besides the intestine, the most prevalent and nutrient rich tissue in the nematode is the gonad. The gonad is comprised of two gonad arms and a central egg-laying apparatus. The gonad arms contain the stem cells and the oocytes prior to fertilization (Wood, 1988). The egg-laying apparatus is the uterus, gonad, vulva and their corresponding muscles (Wood, 1988). The uterus is adjacent to the spermatheca, allowing the fertilized embryos to enter and develop before being expelled by the vulva muscles. To help with maturation of the oocytes and embryos, the gonadal tissue requires a mass import of nutrients from the intestine. Movement of nutrients and waste between the two tissues occurs through the pseudocoelomic cavity (Hall *et al.*, 1999). Therefore, the gonad tissues are an optimal secondary site for an *L. pneumophila* infection. It is assumed that the LCVs observed in the pseudocoelomic cavity can bypass the protective barriers of the gonad tissues and infect them. In support of this assumption, infection of the gonadal tissues is seen later in the infection process timeline (Table 3.2). Nomarski optic analysis of the infection in the gonad tissues gives the impression of “pothole” formation in the tissues (Figure 3.19 D). The “potholes” appear to distort the gonadal tissue, especially in the uterus, to make room for bacterial growth. Frequently, bacterial forms are present within the “potholes” of the gonadal



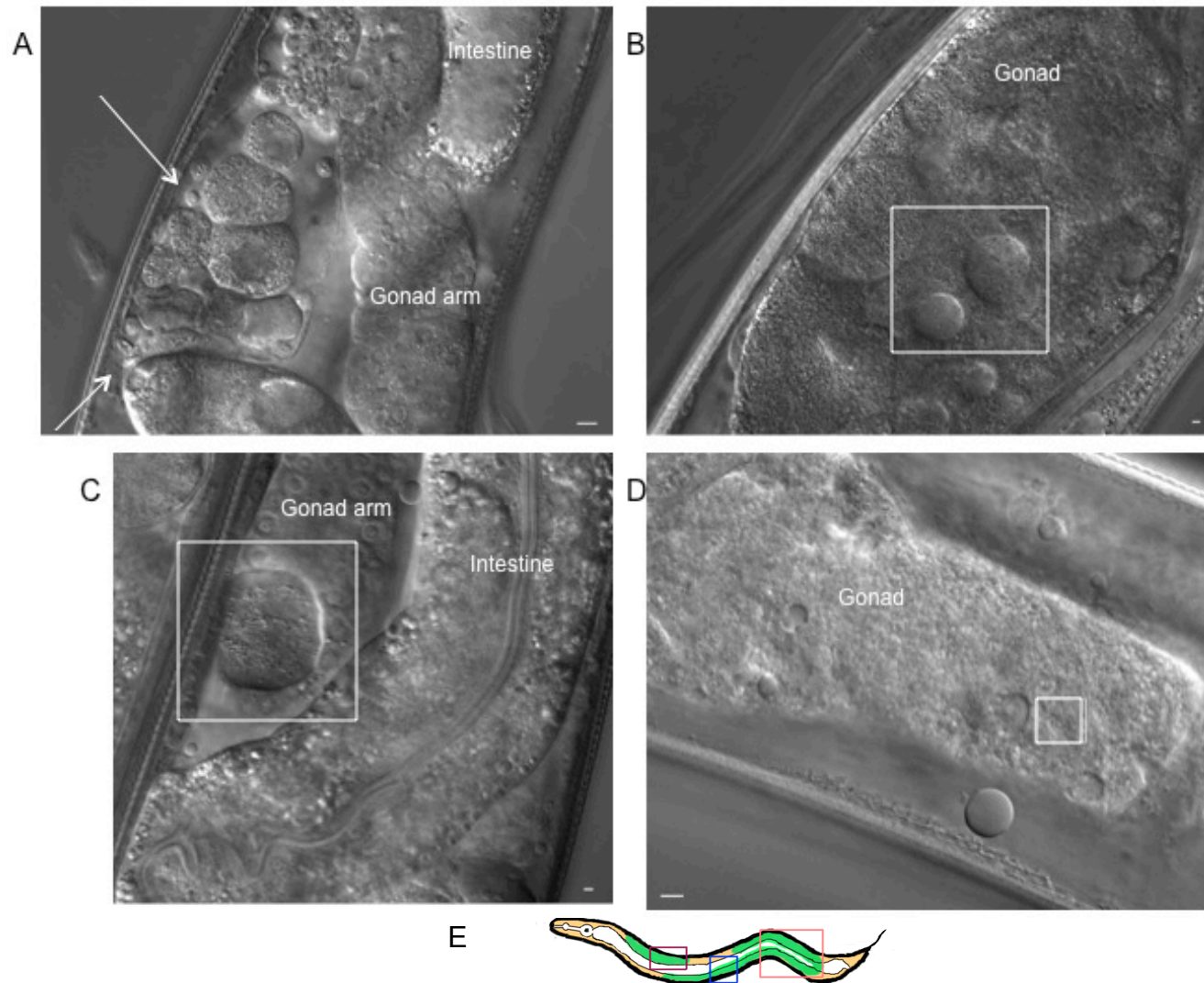


Figure 3.19 Observed morphology of the gonadal tissues of *C. elegans* fed *L. pneumophila*. Infection was observed over a period of 8 days. Images taken on day 6 infection (A) arrows indicate LCVs observed in the gaps between cells, day 7 infection (B and D) boxes indicate the “potholes” observed, day 2 infection (C) box indicates a similar “pothole” observed, schematic of the planes imaged of the *C. elegans* nematode yellow for A, pink for B, blue for C, and D. Scale bar is 5  $\mu\text{m}$  (A and D); 2  $\mu\text{m}$  (B and C).



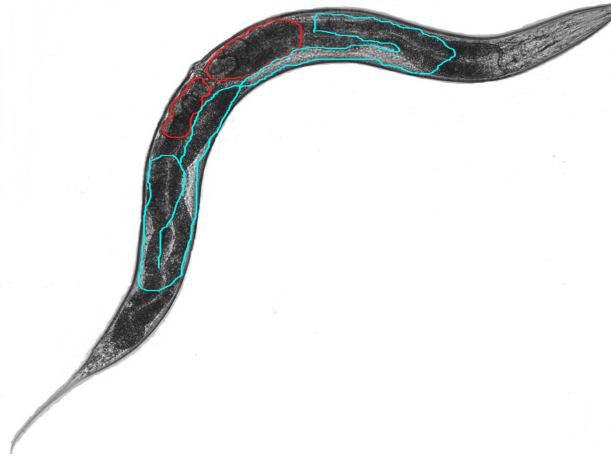


Table 3.2. Assessment of CLFs found in *C. elegans* gonad and gonad arm tissues during various *L. pneumophila* strain infections. The nematodes were visualized over the 8-day infection cycle. A total number of 100 nematodes were observed for each time point. The tissue was determined to be infected if LCVs or CLFs were observed. The number of nematodes with infected tissues was counted. The sum of infected tissues was divided by the total worms counted. The numbers reflect a percentage of the nematode population infected. The number was bolded if the population had more than 2/3 of the nematode population infected. Gonad Tissues outlined in red, Gonad arm Tissues outlined in blue.

#### Gonad Tissues

Bacteria Strains	Day 1	Day 2	Day 3	Day 4	Day 5	Day 6	Day 7	Day 8
WT	0	0	28	35	35	<b>66</b>	<b>86</b>	<b>90</b>
$\Delta sdhA$	0	0	0	0	0	0	0	10
$\Delta sdhA$ complement	0	0	8	24	<b>73</b>	<b>80</b>	<b>97</b>	<b>100</b>
$\Delta dotA$	0	0	0	11	12	11	15	2
$\Delta dotA$ complement	0	0	1	12	<b>84</b>	<b>73</b>	<b>86</b>	<b>89</b>

#### Gonad Arm Tissues

Bacteria Strains	Day 1	Day 2	Day 3	Day 4	Day 5	Day 6	Day 7	Day 8
WT	0	0	10	12	9	12	14	17
$\Delta sdhA$	0	2	3	2	5	7	5	2
$\Delta sdhA$ complement	0	4	8	21	3	7	0	2
$\Delta dotA$	0	0	2	4	7	2	5	0
$\Delta dotA$ complement	0	1	6	7	8	10	14	15

tissue (Figure 3.19 B). Later in the infection process, it was observed that these “potholes” become filled with motile bacteria forms that are similar in shape of CLFs. Thereby, the *L. pneumophila* forms appear to follow the nutrients being moved between the tissues and infect the same area with growing embryos.

Besides the egg-laying apparatus, the gonad arm also requires nutrients to help grow the oocytes for fertilization. In the Pachytene stage of the germline, nurse cells undergo apoptosis in order to give determined oocyte cells basic biochemical necessities for growth (Gartner *et al.*, 2008). However, growth of the germline into oocytes is not completely dependent on the nurse cells. Nutrients are also required which are moved from the intestine to the gonadal arm similar to the process for the gonadal tissue (Gartner *et al.*, 2008). As LCVs are observed in the pseudocoelomic cavity near the gonad arm on the second day post-infection it is assumed that the LCVs are able to bypass the sheath cells covering the germline and infect the somatic germline cells. Once in the somatic gonad cells *L. pneumophila* is able to develop similar “potholes” in the cells.

These “potholes” are phenotypically similar to the ones seen in the embryonic region of the gonad tissue. A difference in the ones observed in the gonad arm is that they appear earlier in the infection process and have more bacterial forms present (Figure 3.19 C). These “potholes” in the gonad arm could help lead to the overall demise of the gonad arm structure that is observed in the later portion of the infection (Figure 3.19 A). As seen in Figure 3.19 A the cells of the gonad arm have swollen with the generation of gaps between the swollen cells. Indicates this swelling is partially due to the lack of control over the reproductive organs after the spermatheca have been depleted (Collins *et al.*, 2008), but also from the invasion of *L. pneumophila* in the

gonad arm. Swelling of the gonad (uterus) is prevalent on day 5 post-infection and continues till the death of the nematode. It is assumed that the swelling is a cause of a lack of control over the reproductive system in combination with the infection process. As observed in the gonad the embryos swell the uterus, which remains swollen during infection (Figure 3.19 B). This may be due to the amount of bacteria present in the tissue but also it may reflect the lack of control of the nematode over its reproductive tissues.

### **3.4.3 *L. pneumophila* forms expelled from *C. elegans***

As mentioned previously, the progressive constipation of the intestinal lumen makes the defecation of CLFs to be unlikely in the later portion of the infection. In addition, the presence of CLFs in the posterior intestine cannot be confirmed *via* Nomarski imaging due to the overabundant presence of rod-shaped forms. The observation of multiple LCVs in the vulva and uterus further supports the idea of an alternative exit route for the LCVs (Figure 3.19 and 3.20 B, Table 3.3). The developing LCVs seen in the pseudocoelomic cavity have the ability to cross into the gonadal tissue and replicate. Similar to the embryos expelled by the vulva, it is hypothesized that the LCVs formed in the gonadal tissue can escape through the vulval opening. Thereby, this puts as little stress as possible on the nematode to allow maximum bacterial replication. As seen at the 90-degree twist of the intestine, there is an abundance of vacuoles with and without bacterial forms (Figure 3.18 B). As the infection progresses there is an increasing presence of vacuoles around the 90-degree twist and in the vulva region (Table 3.3). This indicates the movement of the vacuoles out of the nematode through the vulva is possible. Also



Table 3.3. Assessment of CLFs found in *C. elegans* vulva and expelled from vulva during various *L. pneumophila* strain infections. The nematodes were visualized over the 8-day infection cycle. A total number of 100 nematodes were observed for each time point. The tissue was determined to be infected if LCVs or CLFs were observed. The number of nematodes with infected tissues was counted. The sum of infected tissues was divided by the total worms counted. The numbers reflect a percentage of the nematode population infected. The number was bolded if the population had a 2 fold higher difference in values than wild-type. Vulva outlined in purple, Expelled area outlined in brown.

#### Vulva

Bacteria Strains	Day 1	Day 2	Day 3	Day 4	Day 5	Day 6	Day 7	Day 8
WT	0	0	1	2	18	5	7	3
$\Delta sdhA$	0	1	<b>9</b>	<b>11</b>	4	2	5	5
$\Delta sdhA$ complement	0	1	<b>24</b>	<b>15</b>	5	3	0	2
$\Delta dotA$	0	<b>2</b>	<b>5</b>	<b>12</b>	1	2	5	5
$\Delta dotA$ complement	0	<b>10</b>	<b>8</b>	<b>25</b>	35	51	17	8

#### Expelled Area

Bacteria Strains	Day 1	Day 2	Day 3	Day 4	Day 5	Day 6	Day 7	Day 8
WT	0	3	6	6	4	11	5	3
$\Delta sdhA$	0	0	12	<b>13</b>	<b>11</b>	6	2	2
$\Delta sdhA$ complement	0	1	7	<b>24</b>	<b>17</b>	10	5	3
$\Delta dotA$	0	5	4	<b>22</b>	<b>25</b>	10	7	6
$\Delta dotA$ complement	0	10	8	<b>20</b>	<b>14</b>	4	4	1

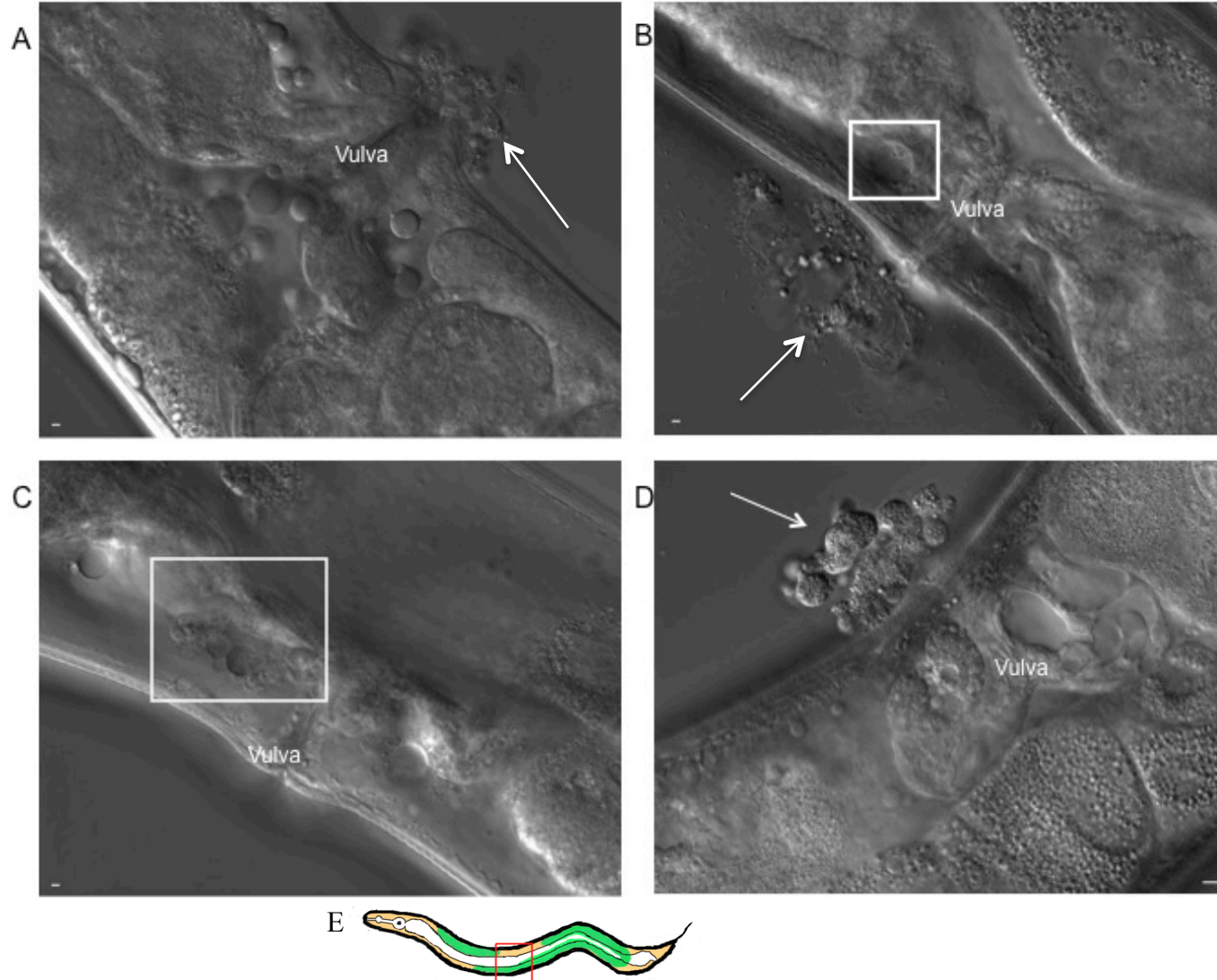


Figure 3.20 Observed morphology of the vulva region and expelled LCVs of *C. elegans* fed *L. pneumophila*. Infection observed over a period of 8 days. Images taken on day 6 infection (A, C, and D), day 8 infection (B), The boxes indicate the position of the LCVs observed in the nematode; the arrows indicate the expelled LCVs from the vulva (E) schematic of the planes imaged of the *C. elegans* nematode, box indicates region of interest. Scale bar is 2  $\mu\text{m}$  (A, B, and C) 5  $\mu\text{m}$  (D).

the vulva is the only other open port in the nematode compared to the rectum and it is bathed in the pseudocoelomic cavity whereas the cavity for expulsion while the rectum is not (Table 3.3).

Further characterization of the vacuoles was completed by electron micrographic analysis of the various secondary infection sites. Unfortunately, the expelled vacuoles could not be preserved in the fixation process of sample preparation for sectioning. Observed in the membranes that survived the fixation procedure the membrane surrounding the vacuoles is of a different composition in each site of infection (Figure 3.21). One vacuole in the uterus has an electron dense outer membrane (Figure 3.21 D). Another vacuole has a thinner or less electron dense double membrane but with greater surface area (Figure 3.21 B). In addition, this vacuole is not complete; the membrane visible is indicated by a light blue line and non-membrane bound forms in the indicated box (Figure 3.21 B). The lack of vacuole consistency between the various LCVs indicates that there is no conformed pathway out of the intestine to the secondary infection sites. Also of interest is the composition of the fluid in the vacuole components. The vacuole components in the LCV observed by the vulva has a clean non-electron dense fluid surrounding the bacteria. Whereas, a different vacuole in a similar distance away from the vulva appears in the electron microscope to be of a darker composition with a more electron dense fluid surrounding the bacteria (Figure 3.21 A). The *L. pneumophila* forms within the vacuoles are also dissimilar in that some contain the transitioning forms (Figure 3.21 D), others have the replicative forms (Figure 3.21B), and others cannot be determined (Figure 3.21A). Thus, the membrane of the vacuole is dependent on where the bacterial forms were maturing and when they joined up to form the vacuole.

#### **3.4.4 Assessment of infected tissues by wild-type *L. pneumophila***

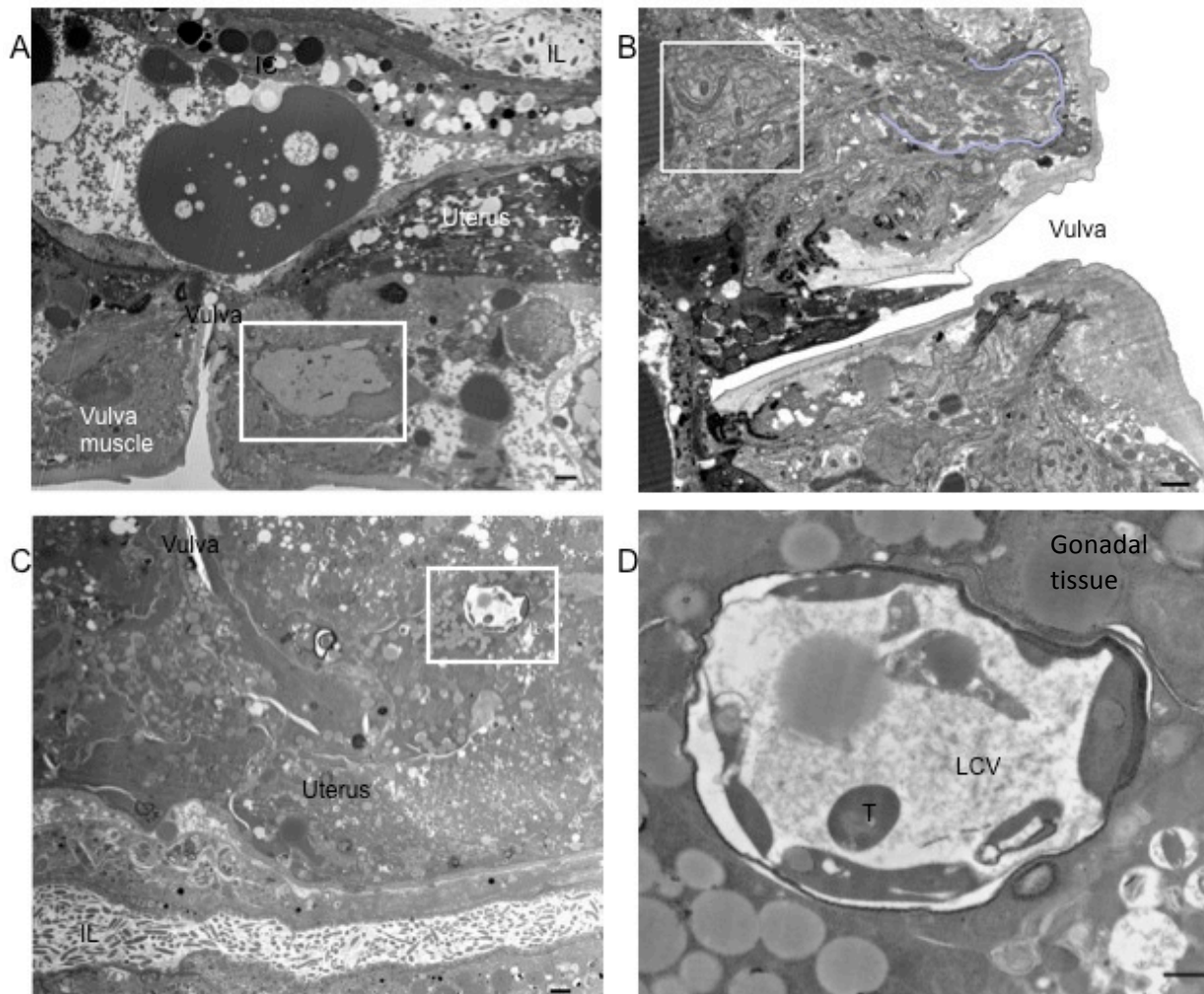


Figure 3.21 Transmission electron micrographs of *L. pneumophila* LCVs in various *C. elegans* tissues. The various LCVs observed are indicated in the boxes. The vacuoles can be observed to have both replicating *L. pneumophila* forms (B) and transitioning forms (C). The vacuoles tend to have various different components for the membrane containing the *L. pneumophila* forms. Note how the vacuole in panel B does not completely enclose the replicating *L. pneumophila*. The box indicates the lack of closure of the vacuole with replicating forms. The purple line indicates the membrane of the LCV observed (B). The LCVs can be observed in the uterus (C, and D) and in the vulva region but not in the vulval muscles (A, and B). panel D is the boxed portion of C. T: transitioning *L. pneumophila*. Scale bar is 2  $\mu$ m (A and C); 1  $\mu$ m (B); 500 nm (D).

To establish a timeline of the infectious progress in nematodes fed *L. pneumophila*, the infected nematodes were monitored on a daily basis to detect the anatomical locations that harbor the bacteria. *L. pneumophila* has the ability to evade the intestine and infect other tissues and cavities of the nematode. Replicative forms and CLFs in the nematode tissue were identified based on the comparison to the morphological characteristics of bacteria forms observed in infected protozoa (Faulkner and Garduño, 2002). Under live imaging, replicative forms had a typical Brownian motion and the CLFs were highly motile due to their polar flagellum (Fields, 1996). In addition, the bacterial forms were measured using the standard scale bar before the infection was confirmed in the tissue. Due to the lack of visible replicative forms observed outside of the intestine, these forms were not included in the assay results. However, it is important to note that the replicative forms were observed in the intestinal lumen for the duration of the infection process. The assay was assessed by Nomarski optics with a magnification of 63X. Prior to imaging, the nematodes were washed with M9 buffer to remove extracellular bacteria adhered to the cuticle of the nematode. For each time point, a hundred nematodes were imaged for identification and assessment of infected tissues within the nematodes.

Observations of nematodal tissues housing CLFs within themselves or LCVs are presented in Table 3.1. CLFs were constantly observed in the gonadal tissues, especially in the embryonic region (Table 3.1). It could not be determined if the target of the infection was in the lumen of the uterus or the growing embryos. Another key infection site was the pseudocoelomic cavity of the nematodes (Table 3.1). This cavity helps move nutrients from the lumen of the intestine to other tissues. Therefore, the ability of *L. pneumophila* to move with other nutrients in the pseudocoelomic cavity is a reasonable conclusion. This is especially true since *L.*



*pneumophila* is an intracellular pathogen with greater 200 effector cells that could have the ability to manipulate the host's systems.

The last main target where CLFs were constantly observed in the nematode was the vulva. As mentioned before, *L. pneumophila* needs to find a path out of the nematode to infect new hosts. In the vulva region there were observed LCVs surrounding the vulva. As well as surrounding the vulva, some LCVs were seen outside of the nematode in membrane bound vacuoles. The area with a 20  $\mu\text{m}$  radius surrounding the vulva was analyzed to determine if the number of LCVs would increase as more LCVs were formed in the nematode. Expulsion of the LCV was seen but not in the same constant trend as the gonadal and pseudocoelomic cavity infection was (Table 3.1). This could be because the LCVs are expelled only when the nematode dies as they lack of control over barriers between their tissues upon death and dead nematodes were not analyzed. In addition, a complete infection of other tissues not associated with the nutrient-rich gonadal tissues were not infected confirming the gonadal tissues as the target for secondary infection sites. Therefore, like the colonization of the intestinal lumen, *L. pneumophila* spreads throughout the nematode for bacterial replication, looking for niches to further intracellular replication. In addition, *C. elegans* provide a good replicate niche, as the only innate immune defense pathways are located in the intestine and the pseudocoelomic cavity and uterus supplies ample food source from nutrient filled bound vacuoles.

#### **3.4.5 *L. pneumophila* chromosomal GFP expression in *C. elegans* gonadal tissues**

The transmission electron micrographs (TEM) of the *C. elegans* tissues demonstrated the ability of *L. pneumophila* to manipulate the intestinal lining of both the apical membrane and the

basement membrane (Figure 3.16). In addition, *L. pneumophila* has the ability to infect the gonadal tissues, which can move the bacteria near the vulva to be expelled (Figure 3.21). However, the bacterial rod forms observed by Nomarski optics could not be confirmed by TEM imaging. Various Immunogold tagging of TEM sections were attempted to identify *L. pneumophila* in the gonadal tissues. However, the composition of the nematode tissue made it difficult for the antibody to penetrate the sections leading to a lack of identification. In addition, the rarity of the bacteria on the electron micrograph grids was a debilitating factor in the identification of immunotagged bacteria. Thus, an alternative approach was employed. This entailed the use of GFP-tagged *L. pneumophila* to identify the motile bacteria initially observed by Nomarski optics.

*C. elegans* have a natural autofluorescence present in their intestine. The autofluorescence stems from lipofuscin gut granules located exclusively in the intestinal cells and strengthens in intensity during a pathogenic infection (Clokey and Jacobson, 1986; Sifri *et al.*, 2005). The autofluorescence excites at a wavelength of 488 nm, similar to the excitation wavelength of GFP-tagged *L. pneumophila* thereby complicating the effectiveness of fluorescent microscopy studies in the nematodes. To circumvent this difficulty, animals carry a deletion of the *glo-3(kx94)* gene. The *glo-3(kx94)* nematodes have reduced autofluorescence due to the loss-of-function of *glo-3*, which is involved in formation of embryonic gut granules (Rabbitts *et al.*, 2008). Even with the absence of gut granules, autofluorescence is still detected from the intestine, especially localized in the posterior portion of the intestine (Figure 3.22A).

Replacing the chromosomally encoded *magA* with *gfpmut3* by allelic exchange strategy generated the GFP-tagged *L. pneumophila*. MagA is strongly expressed in the post-exponential

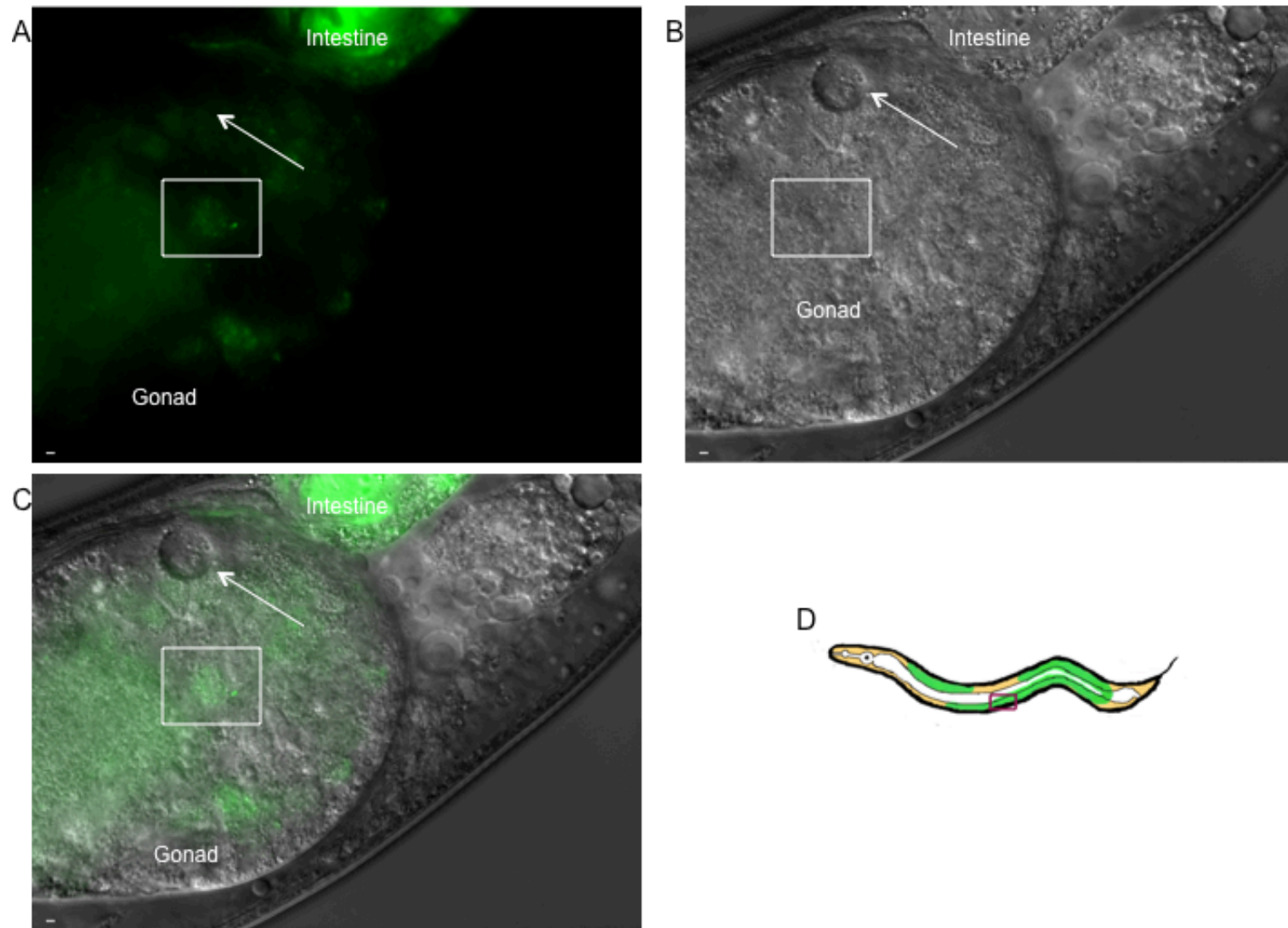


Figure 3.22 Infection day 6 epifluorescent image of  $\Delta glo-3$  (*kx94*) *C. elegans* gonadal tissue fed GFP-tagged *L. pneumophila*. GFP (*gfpmut3*) under control of the *magA* promoter. (A) GFP, (B) DIC, (C) Merged. Box indicates observed bacteria forms, arrow indicates “pothole” observed (D) Schematic of the *C. elegans* nematode, box indicates region of interest (D). Scale bar is 2  $\mu$ m.

growth stage as well as in the CLF stage (Garduño *et al.*, 2002). Thus by placing *gfpmut3* under control of the *magA* promoter there should theoretically result in a GFP expression coinciding with the transition to CLF stages. Plasmid induced GFP expression was not suitable for this approach due to constitutive expression regardless of the development stage. In nematodes infected with GFP-tagged *L. pneumophila*, GFP fluorescence could be detected in approximately half of the CLFs observed (Figure 3.23 C). It should be noted that fully developed CLFs are metabolically dormant (Garduño *et al.*, 2002). Thus, it is likely that only bacteria that are in the process of transitioning into CLFs can be identified *via* fluorescence.

On this basis, it was hypothesized that the observed motile fluorescent bacteria are not CLFs but rather late transitioning forms. Thereby observations of an earlier infection day were meant to display greater fluorescence in the gonad since the majority of forms would be transitioning into CLFs (Figure 3.22). This is true as there is a higher fluorescence observed in the gonadal tissue with various forms fluorescing throughout the tissue (box in Figure 3.22). However, as indicated by the arrow on Figure 3.22 there is a well-formed “pothole” observed with bacterial forms present with no fluorescence observed. In general, fluorescence was strongly observed in areas closest to the intestinal lumen with fluorescent decay observed as the bacteria move through the gonadal tissues (Figure 3.23). These results suggest that *L. pneumophila* is able to fully transition into the CLF in the gonadal tissue. Alternatively, there is a possibility of the *L. pneumophila* being able to replicate in the gonadal tissue.

### **3.5 *L. pneumophila* observed bacterial morphology in *C. elegans***

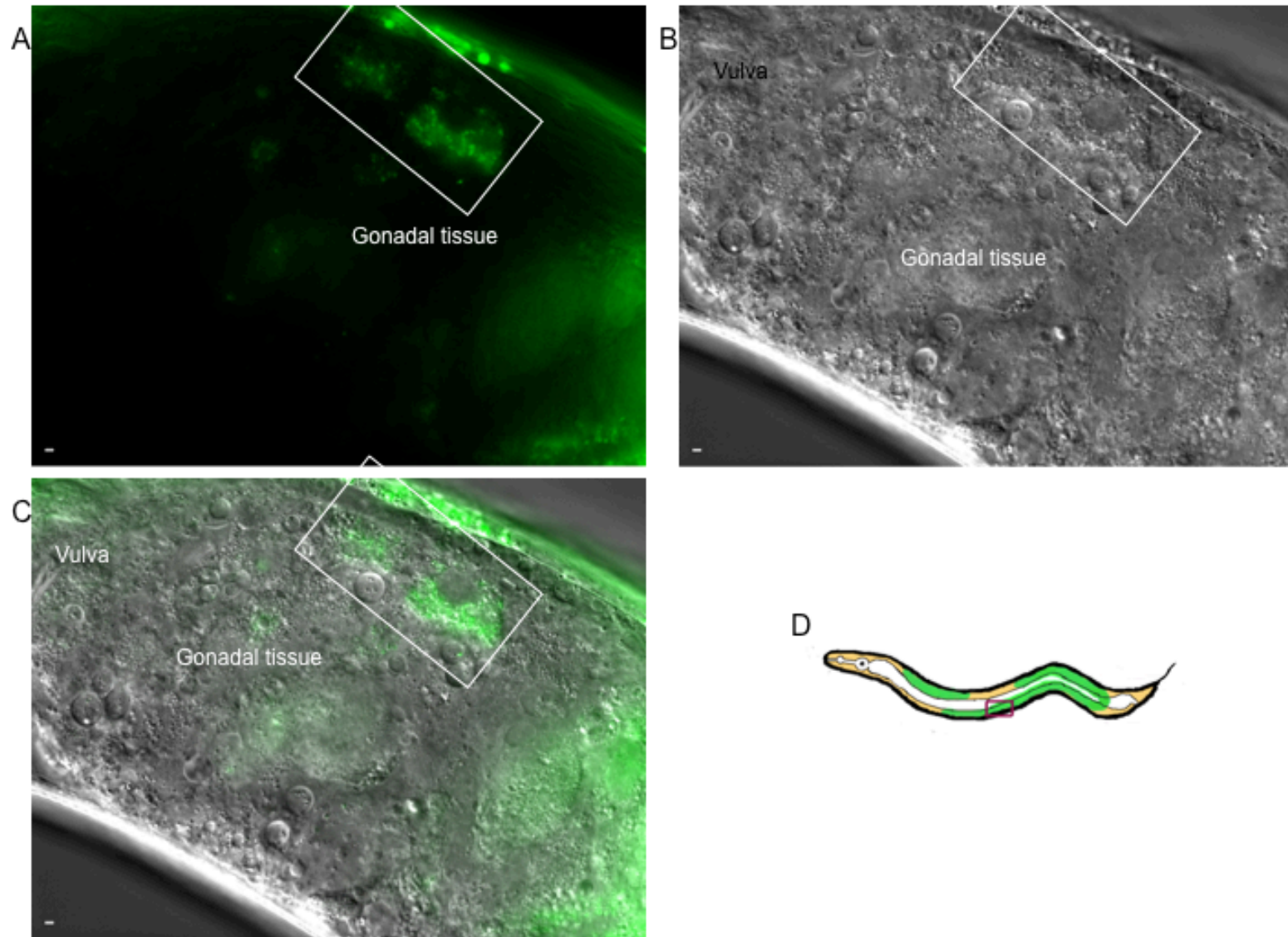


Figure 3.23 Infection day 8 epifluorescent image of  $\Delta\text{glo-3}$  (*kx94*) *C. elegans* gonadal tissue fed GFP-tagged *L. pneumophila*. GFP (*gfpmut3*) under control of the *magA* promoter. (A) GFP, (B) DIC, (C) Merged, white box indicates the observed bacteria forms (D) Schematic of the *C. elegans* nematode, box indicates region of interest. Scale bar is 2  $\mu\text{m}$

The lifecycle of *L. pneumophila* involves various bacteria forms such as replicative, transitional, and infectious CLFs all of which can be observed in a natural environmental host. Both *L. pneumophila* replicative and transitioning forms can be observed in the intestine (Figures 3.24 and 3.25) of *C. elegans* and in the secondary infection tissue sites (Figures 3.24 and 3.25). *L. pneumophila* replicative forms have a phenotype characteristic of rod Gram-negative form. These forms are found primarily in the intestinal lumen and are responsible for the colonization of the intestinal lumen. However, some replicative forms have been observed in various secondary infection sites in the *C. elegans* host model. These forms have been observed in the intestinal cell in tight vacuoles (Figure 3.24 C). It is assumed that these tight vacuoles can make their way through the nematode and could set up secondary replication niches in the gonadal tissues. However, this hypothesis has not been proven, as there is no way to track the movement of *L. pneumophila* from the intestine to the secondary tissues. Of interest there are replicative forms observed by them in the somatic gonad tissue (Figure 3.24 B). It is assumed that these replicative forms are starting to transition into CLFs, as the inner organelles of the rod form are visible. Also of interest were replicative forms observed in the gonad tissue. These forms were not in a contained membrane and no explanation for the lack of LCV is available. The same is true for the way these loose replicative forms were able to travel through the nematode and their ability to set up secondary replication niches in the gonadal tissues. However, whether membrane bound or unbound the hypothesis of *L. pneumophila* movement to the gonad should be tracked from the intestine to the secondary tissues. Of interest there are replicative forms in tight vacuoles observed by TEM in the somatic gonad tissue (Figure 3.24 B). It is assumed that these replicative forms could transition into CLFs, as the inner organelles of the rod form are

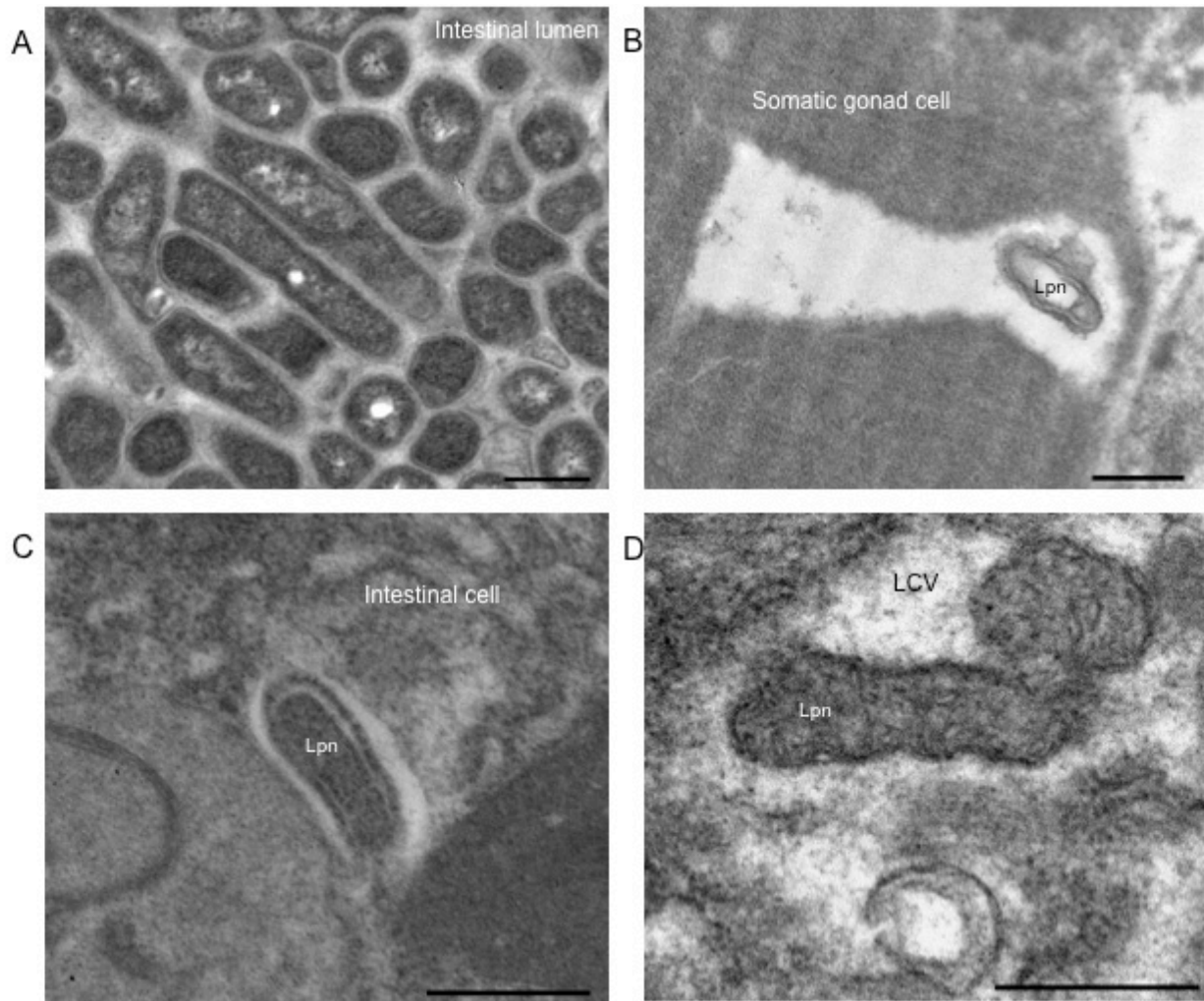


Figure 3.24 Transmission electron micrographs of replicative *L. pneumophila* in various *C. elegans* tissues. Forms were observed in the (A) intestinal lumen, (B) somatic gonad cell, (C) the intestinal cell, (D) and inside an LCV by the vulva. All forms have characteristic gram-negative rod-shaped forms. Lpn: *L. pneumophila*. Scale bar is 500 nm.

visible. Also of interest were replicative forms observed in the gonad tissue. These forms were not in a contained membrane and no explanation for the lack of membrane is available. For replicative forms are also observed in an LCV located in the vulva region of the nematode (Figure 3.24 D).

Key characteristics of the transitioning forms include the wavy outer membrane, poly-hydroxybutyrate (PHBA) inclusions, and the shortening of the bacterial form from a rod-shaped Gram-negative form to a coccid form (Garduño *et al.*, 2002). When comparing the bacteria in the secondary infection tissue sites to the bacterial forms in the intestinal lumen, it was important to compare the characteristics observed in other host models as well. *L. pneumophila* forms have been well characterized by Faulkner and Garduño in the HeLa cell-line host model (Figure 1.1) (Faulkner *et al.*, 2002; Garduño *et al.*, 2002). The replicative form was described as a typical Gram-negative envelope consisting of clearly defined outer and inner membranes of equal width. The outer membrane appears wavy, and the periplasmic region between the two membranes is electron lucent with no discernible peptidoglycan layer (Faulkner and Garduño, 2002). The same description of the replicative forms observed and characterized in the HeLa cells is seen in the intestinal lumen (Figure 3.24).

The description of a CLF is based on three main characteristics, which includes long inner membrane invaginations, a thickening of the inner leaflet of the outer membrane and an irregular shape with dense cytoplasm (Faulkner and Garduño, 2002). The description of the CLFs could be compared to many bacteria forms seen in the secondary infection sites of *C. elegans* and thus be concluded phenotypically to be similar to CLFs observed in other host models. However, key functions of CLFs include their ability to withstand extreme



environmental stresses (Faulkner *et al.*, 2002) To properly confirm the transition of intestinal replicative forms into stable CLFs extreme environmental testing should be done on the CLFs produced from the gonadal tissues. Therefore, these observations cannot alone confirm the existence of CLF forms in the gonadal tissues.

A bacterial morphology of interest is the wavy outer membrane observed in the secondary infection site of *C. elegans* (Figure 3.25 D), and in the intestine (Figure 3.25 A). The membrane of forms observed in the gonad was compared to the forms observed in HeLa cells are found to be similar as both report a pronounced amplitude outer membrane waves with respect to the bacteria form. This characteristic of many sharp high amplitude ripples is from excessive membrane invaginations on the bacterial form. Another characteristic feature of the transitional forms is a straight outer membrane (Faulkner and Garduño, 2002). This characteristic was observed in the intestinal lumen (Figure 3.25 B) and in the gonad tissue (Figure 3.25 D). Note that a membrane does not bind the forms in the gonad tissue whereas the exact same forms in the intestinal lumen are membrane bound. To further classify the bacteria as transitional a difficult to resolve inner membrane should be observed. This is seen in the electron micrographs as a dense electron body or as a dark black area on the bacteria. An example of defined inner membrane can be seen in the replicative form (Figure 3.24 C).

Lastly, prominent and well-defined inclusions of PHBA are observed. In the electron micrographs PHBA itself is not well preserved but the inclusion that contains it is. PHBA is seen as a white dot in the bacteria form with an electron dense ring surrounding it. The start of an inclusion is seen as a tiny white dot (Figure 3.25 B). A well-defined inclusion can be seen in bacterial forms in the intestinal lumen (Figure 3.25 C), in the intestinal cells (Figure 3.25 E) and

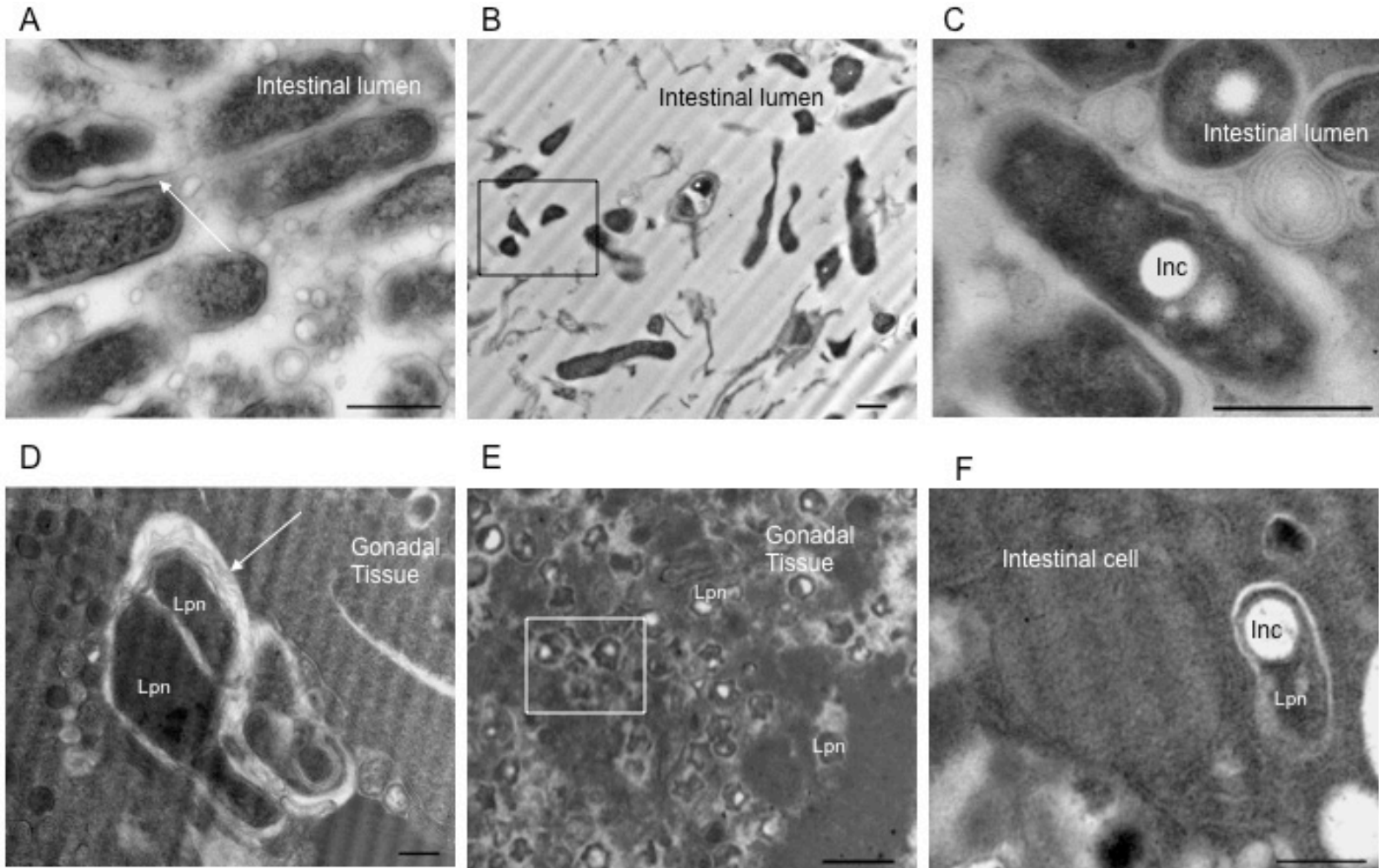


Figure 3.25 Transmission electron micrographs of transitioning *L. pneumophila* forms in various *C. elegans* tissues. The transitional forms can be seen in the intestinal lumen (A, B, and C) in the intestinal cells (F) and in the gonadal tissues (D and E). In A and D arrow indicates wavy outer membrane. In B and E box indicates irregular bacteria observed. In C and F inclusions of PHBA (Inc) are observed. Lpn: *L. pneumophila*. Scale bar is 500 nm.

in gonadal tissues (Figure 3.25 D). Due to the constipation in the posterior region of the intestinal lumen on the sixth day of infection, the lack of detectable defecation of *L. pneumophila*, and the death characteristic of gonadal tissue explosion in *C. elegans* the CLFs in the intestine cannot be determined at this time. These results indicate that *L. pneumophila* is able to transition into a proper CLF bacterial forms in *C. elegans* tissues as the transitioning forms were observed on the sixth day of infection and the nematode doesn't die for another three days.

### **3.6 Infection characteristics of *C. elegans* fed *L. pneumophila* $\Delta dotA$ and $\Delta sdhA$ mutant strains**

In other host models, the genes *dotA* and *sdhA* encode an *L. pneumophila* effector component and effector protein, respectively, that is involved in the establishment of infection. In the cell model, it was found that lack of DotA resulted in an avirulent infection process. Genetic studies show that DotA synthesis is required before macrophage uptake in order to establish an intracellular replicative niche (Roy *et al*, 1998). Therefore, DotA is an effector component required for determination of the initial phagosome trafficking decisions.

The effector protein of interest SdhA plays a role in maintenance of the membrane of the replicating vacuole. Expression of SdhA is critical in the maintenance and integrity of the LCV in the host cell (Banga *et al*, 2007). This effector protein was once thought to be involved in the evasion of the host apoptotic pathways but now only appears to act downstream of the known effector molecule SidF (Banga *et al*, 2007). There is no known interaction observed between DotA and SdhA effectors.

### 3.6.1 Survival curves of *C. elegans* fed *L. pneumophila* $\Delta dotA$ and $\Delta sdhA$ mutant strains

The survival rate of N2 *C. elegans* infected with the various mutant strains was evaluated. Given that other host models such as murine macrophages, U937 cell line, and *A. castellanii*, were able to survive for a longer period with either the *dotA* or the *sdhA* were removed (Laguna *et al.*, 2006), *C. elegans* should behave the same. Thus, the mutant strains should also affect the survival rate to increase longevity of *C. elegans* infected with the mutant strains. To this end, *C. elegans* survival assays were conducted with *L. pneumophila*  $\Delta dotA$  and  $\Delta sdhA$  mutant strains (Figure 3.26). The lack of DotA or SdhA resulted in a reduced mortality rate in comparison to nematodes fed wild-type *L. pneumophila* Lp02 (Figure 3.26). Interestingly, a similar mortality rate of both  $\Delta sdhA$  and  $\Delta dotA$  mutant strains was observed which indicates that the effector molecules have independent roles in virulence, which has been observed in other host models (Laguna *et al.*, 2006) (Figure 3.26). Thereby, a successful infection process is dependent on the initial interaction between the *L. pneumophila* and the host also, the maintenance of the LCV during intracellular replication during the infection. It should be noted that although the difference in the mortality rates is statistically significant, the biological difference is considered to be small on the organismal level.

Complementation of the mutant strains resulted in a rescued phenotype of a typical wild-type *L. pneumophila* infection in *C. elegans* for the  $\Delta sdhA$  mutant strain, but not for the  $\Delta dotA$  mutant strain. Oddly enough, the complemented  $\Delta dotA$  mutant strain appears to have a further reduced mortality rate compared to the wild-type *L. pneumophila* infection mortality rate. It is not clear why the complemented  $\Delta dotA$  mutant strain did not rescue the wild-type *L.*

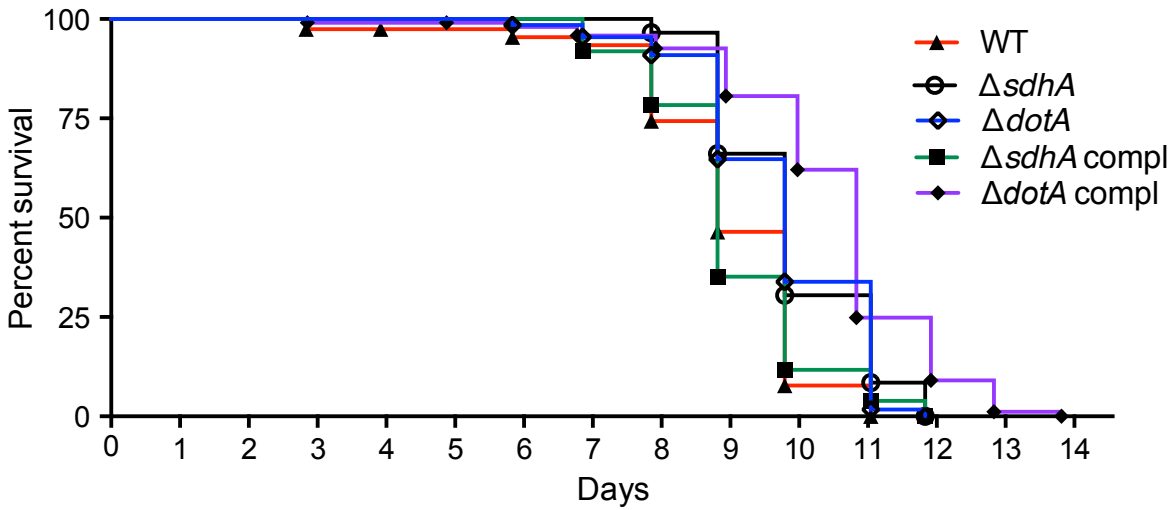


Figure 3.26 Kaplan-Meier survival curve of *L. pneumophila* wild-type,  $\Delta dotA$  and  $\Delta sdhA$  mutant strains survival assay in wild-type N2 *C. elegans*. n=90 nematodes counted for each strain in assay. A *p* value of 0.0010 and 0.0004 for  $\Delta dotA$  and  $\Delta sdhA$  strains respectively in comparison to the wild-type strain by log-rank analysis. Complements were done to restore the wild-type phenotype. A *p* value of <0.0001 and 0.9805 for  $\Delta dotA$  complement and  $\Delta sdhA$  complement strains respectively in comparison to the wild-type strain by log-rank analysis. Data is representative of three independent experiments.

*pneumophila* infection phenotype. A possible reason could be inappropriate expression levels of DotA from the complemented plasmid.

### **3.6.2 Phenotypical evaluation of *C. elegans* fed *L. pneumophila* $\Delta dotA$ mutant strain**

A key characteristic feature of the infection process by a bacterial pathogen in *C. elegans* is the colonization of the intestinal lumen. This can be observed in nematodes infected with wild-type *L. pneumophila* Lp02. During the infection of *C. elegans* with *L. pneumophila*  $\Delta dotA$  mutant strain there was a substantial bacterial presence in the lumen of the intestine. However, in contrast to observations for nematodes infected with wild-type *L. pneumophila* there was a lack of severe swelling of the intestinal cells (Figure 3.27 B) and colonization was only observed at the later portion of the infection (Figure 3.27 C). This colonization was most likely due to the age of the nematode and not from the pathogenicity of the bacteria itself. In addition, there was no severe constipation of the nematode (Figure 3.27 D). This indicates that the constipation and severity of infection is dependent on a full functioning virulent *L. pneumophila* strain.

To further characterize the infection process of nematodes by the  $\Delta dotA$  mutant strain, the secondary infection sites were evaluated for the presence of CLFs and LCVs. Evaluation was done visually with Nomarski optics (Figure 3.28) and numerically with numeration of overall infected tissues in a given population of nematodes. Visually the presence of CLFs and LCVs in the secondary infection sites were rare and occurred around day 5 of the infection process (Figure 3.28 C, Table 3.2). In addition, there was no general clumping of LCVs in the pseudocoelomic cavity as seen in nematodes infected with wild-type bacteria. There was a general phenotype of one vacuole observed in the body cavity (Figure 3.28 D). There was also a

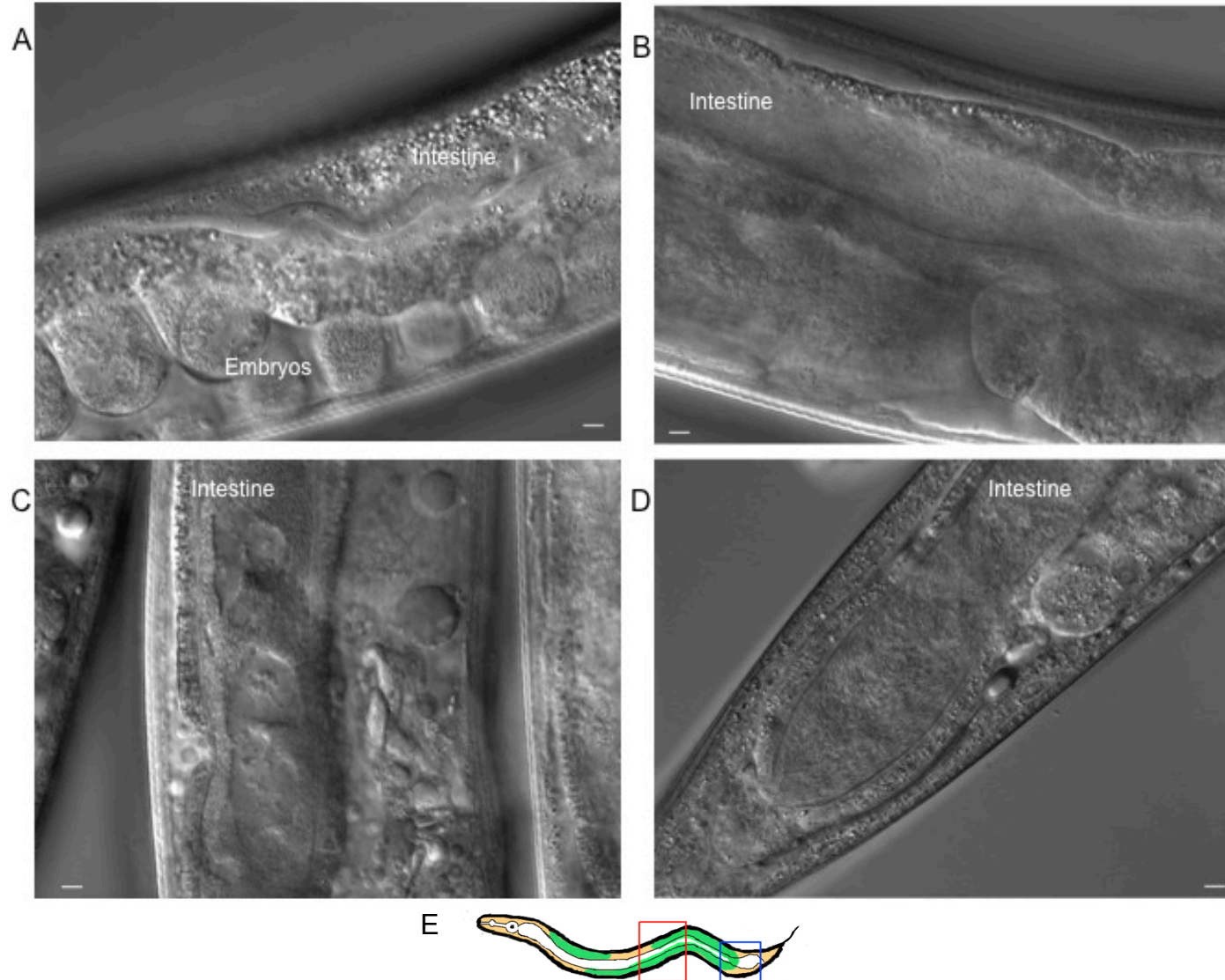


Figure 3.27 Observed morphology of the intestinal region of N2 *C. elegans* fed *L. pneumophila*  $\Delta dotA$  mutant strain. Images taken on day 1 infection (A), day 4 infection (B), day 6 infection (C), day 7 infection (D), (E) schematic of the area observed on the nematode, blue for D and red for A, B, and C. Scale bar is 5  $\mu$ m.

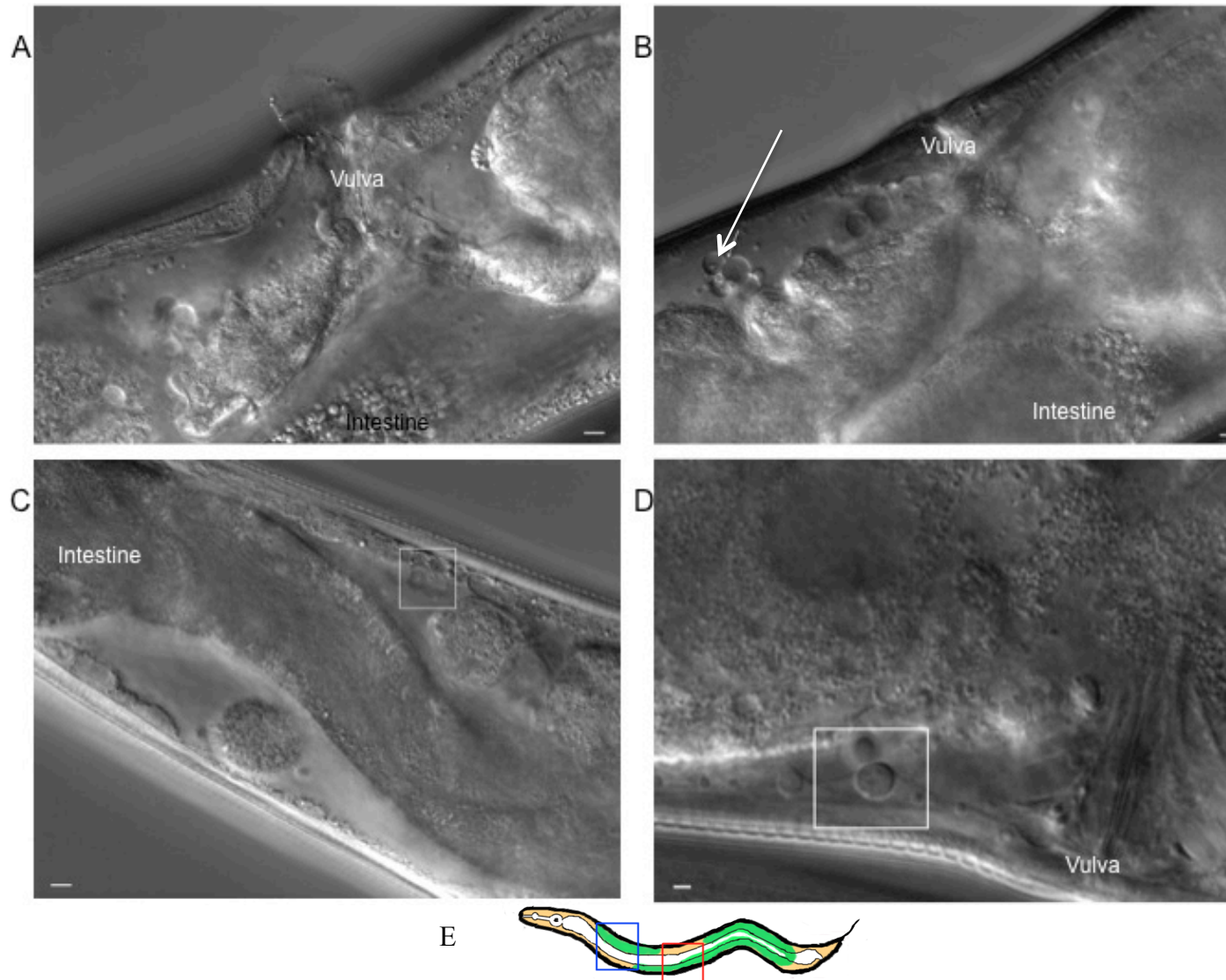


Figure 3.28 Observed morphology of the secondary infection sites of N2 *C. elegans* fed *L. pneumophila*  $\Delta dotA$  mutant strain. Images taken on day 4 infection (A and B), day 5 infection (C and D), (E) Schematic of general areas observed on the nematode, blue for C and red for A, B, and D. Boxes and arrow indicate LCVs. Scale bar is 5  $\mu$ m (A, C, and D); 2  $\mu$ m (B).



decrease in the number of infected tissues in a given population (Tables 3.1, 3.2). This was evident in the lack of a sustained infection in the gonadal tissues. A key observation is the increase in expelled LCVs from the vulva that occurs early in the infection process (Figure 3.28 A). Unfortunately, the integrity of the LCVs expelled could not be evaluated to assess the stability of the expelled LCVs. This is from the lack of stability of the LCVs upon expulsion as most of the vacuoles appeared to disintegrate after being expelled (Figure 3.28 A).

### **3.6.3 Phenotypical evaluation of *C. elegans* fed *L. pneumophila* $\Delta dotA$ complemented strain**

In the survival assay, the complemented  $\Delta dotA$  mutant strain was unable to rescue the wild-type phenotype. To investigate whether the complementation was achieved on a cellular level, nematodes were infected with the complemented strain and evaluated. Similar phenotypic characteristics were observed between nematodes infected with the complemented strain and the wild-type strain. The phenotypes of nematodes infected with the  $\Delta dotA$  mutant strain do take an additional day to develop in the given secondary infection sites but the presence and quantity of the infection is similar (Figure 3.29). The same wild-type phenotype can be observed in the pseudocoelomic cavity, especially at the 90 twist of the intestine (Figure 3.29 D).

The enumeration of infected tissues resulted in similar quantity of tissues with both CLFs and LCVs (Tables 3.1, 3.2). On the fourth day of infection there was the decrease in expelled LCVs but the number was still higher than observed in nematodes infected with the wild-type strain. These results indicate that although the mortality rate did not appear to be rescued by complementation, pathology of the infected tissues was similar to that of a nematode infected with the wild-type strain. Thus complementation was achieved on a cellular level. It should be

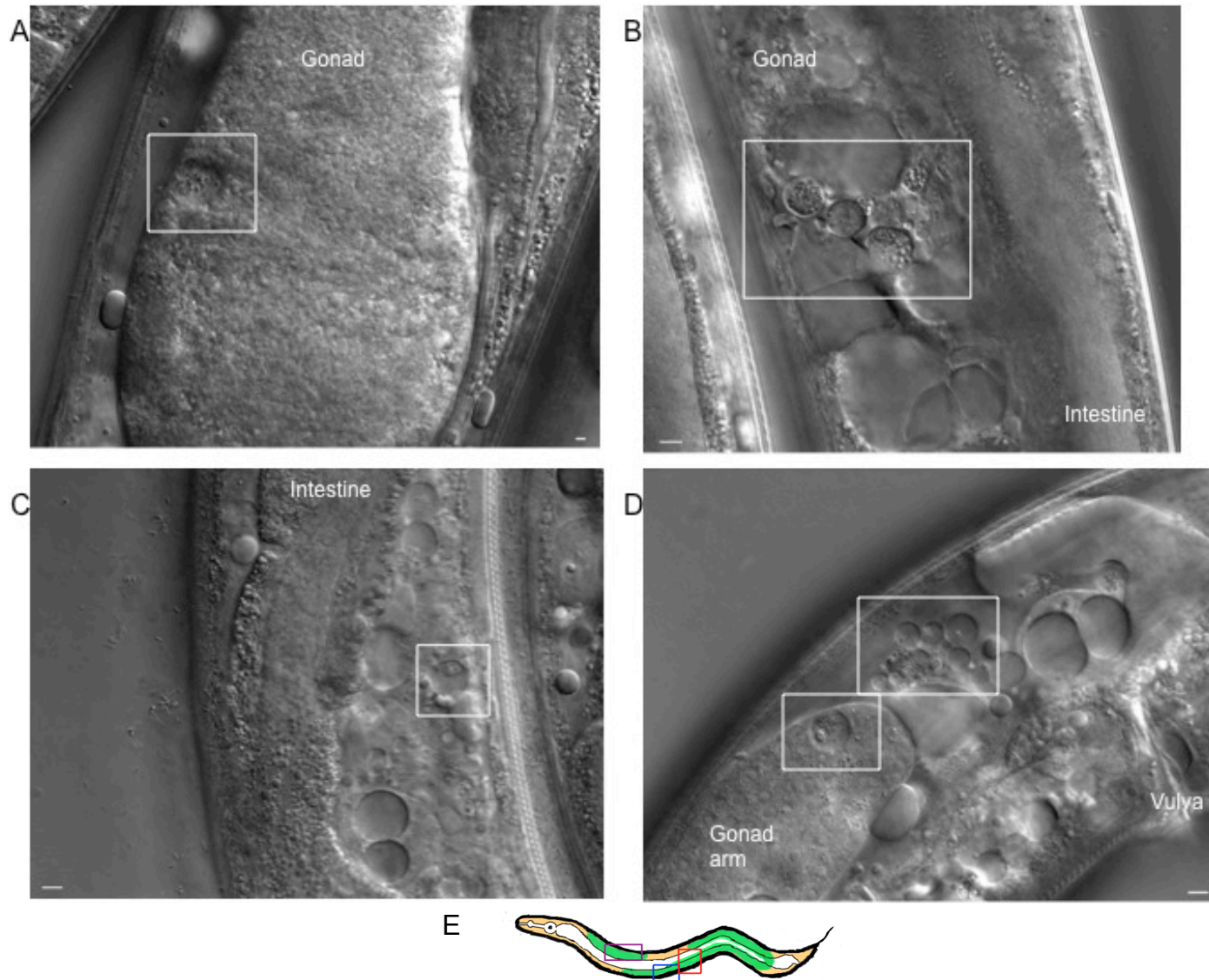


Figure 3.29 Observed morphology of secondary infection sites of N2 *C. elegans* fed *L. pneumophila*  $\Delta dotA$  complement strain. Images taken on day 7 infection (B and D), day 8 infection (A and C). (E) Schematic of the general areas on nematode observed, purple (A and C), blue (D) and red (B). Boxes indicate LCVs observed. Scale bar is 5  $\mu\text{m}$  (B, C and D); 2  $\mu\text{m}$  (A).

noted that during the survival assay the bacteria lawn became sticky and hard for the *C. elegans* to maneuver in. This may account for the lack of ability to move and digest the complemented strain and could account for the characteristic of the low mortality rate seen for the strain.

### **3.6.4 Phenotypical evaluation of *C. elegans* fed *L. pneumophila* $\Delta$ *sdhA* mutant strain**

Membrane integrity for the LCV during bacterial replication is important for infection in unicellular models, such as mammalian cells and protozoan models. Current research in the wax moth and A/J mice has concluded the importance of SdhA in maintaining the LCV integrity (Harding *et al.* 2013). Therefore, it was questioned if the lack of SdhA would result in the disruption and instability of the LCV in the *C. elegans* host model as well.

To answer this question, nematodes infected with the  $\Delta$ *sdhA* mutant strain were examined using Nomarski optics. This resulted in similar observations seen for nematodes infected with the  $\Delta$ *dotA* mutant strain. The lack of LCVs in the pseudocoelomic cavity and lack of a gonadal secondary infection site are similar characteristic features to a  $\Delta$ *dotA* mutant strain (Figure 3.30). However, it appears that there were more bacterial forms found in the intestinal lumen than in nematodes fed the  $\Delta$ *dotA* mutant strain (Figure 3.30 B, 3.27 B). Since SdhA is instrumental in maintaining the integrity of the LCV, then the colonization of the intestinal tract should be unchanged. However, there was less swelling of the nematode tissue overall which indicates that SdhA might play a role in affecting the osmolarity homeostasis process.

It should be noted that unlike the other multicellular organisms used to investigate *L. pneumophila* virulence, *C. elegans* are a highly vacuolated organism. Therefore, a complete lack of LCVs was not observed as *L. pneumophila* may have the ability to hijack host vacuoles to

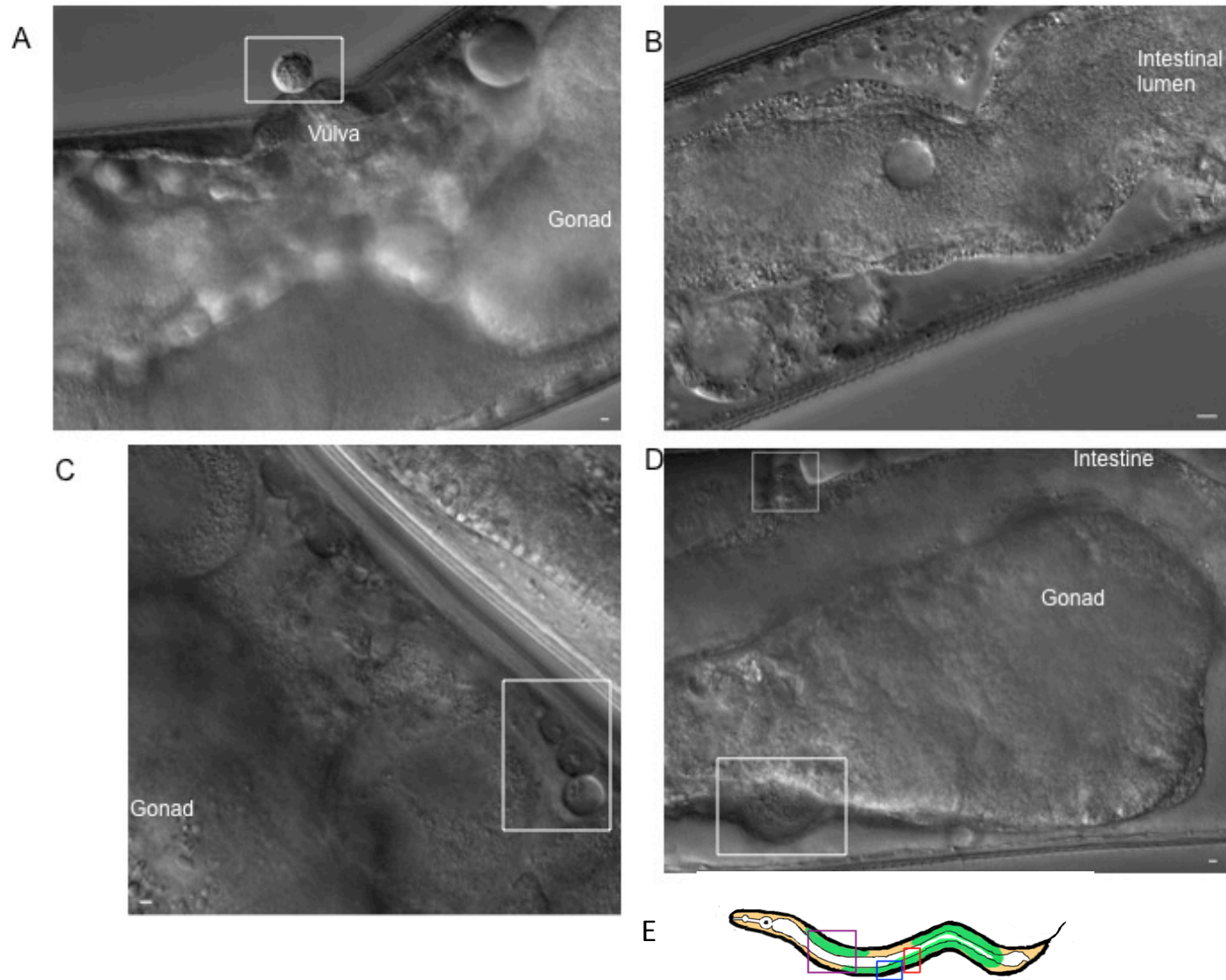


Figure 3.30 Observed morphology of secondary infection site of *C. elegans* fed *L. pneumophila*  $\Delta sdhA$  mutant strain. Images were taken on infection day 2 (C), infection day 6 (A), and infection day 8 (B and D). (E) Schematic of areas observed on the nematode, purple (B), blue (A) and red (C and D). Boxes indicate LCVs observed. Scale bar is 5  $\mu\text{m}$  (B), 2  $\mu\text{m}$  (A, C, and D).

establish a replicative niche in secondary infection sites (Figure 3.30 C, D, Table 3.2). More data is required to validate this assumption. Like the infection process of the  $\Delta dotA$  mutant strain in nematodes, the same rarity of LCVs observed in the pseudocoelomic cavity was found (Table 3.1). The rarity of LCVs was that the vacuoles were singular and less populated in the pseudocoelomic cavity (Figure 3.30 D, Table 3.1).

### **3.6.5 Phenotypical evaluation of *C. elegans* fed *L. pneumophila* $\Delta sdhA$ complement strain**

The  $\Delta sdhA$  complement strain was able to restore the wild-type infection phenotype (Figure 3.31). This was accomplished to a degree based on the survival assay (Figure 3.26). Some time points indicated a higher mortality rate, but overall the wild-type phenotype was restored. This indicates that all of the phenotypic observations in the  $\Delta sdhA$  mutant strain were based on the removal of that gene alone. With the complemented strain, there was an increase in gonadal tissue infections (Table 3.5) as well as a destruction of the gonad arm, which may be due to an inappropriate expression of SdhA from the complement plasmid (Figure 3.31 C). LCVs were once again present in the pseudocoelomic cavity (Figure 3.31 A). Also, the constipation of the posterior region of the intestine returned (Figure 3.31 D). There was no drastic increase observed in expelling of vacuoles in nematodes infected with either of the  $\Delta sdhA$  mutant strain or the  $\Delta sdhA$  complement strain, this indicates that the phenotype may be specific to the lack of DotA.

### **3.7 Germline Apoptosis**

Germline apoptosis is similar to somatic apoptosis in that both rely on the key

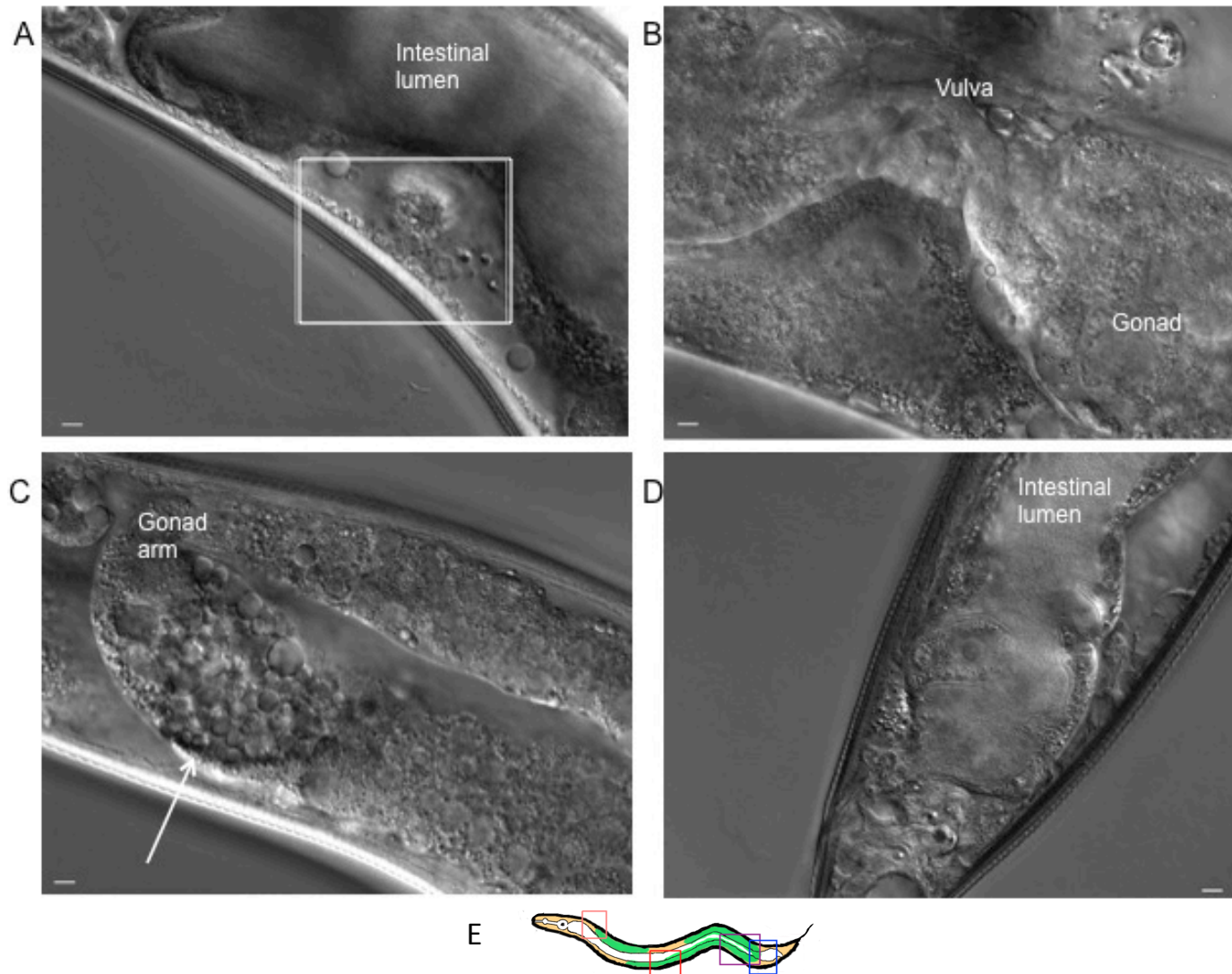


Figure 3.31 Observed morphology of secondary infection sites of *C. elegans* fed *L. pneumophila*  $\Delta sdhA$  complement strain. Images taken on day 3 infection (A), day 5 infection (D), day 7 infection (B), day 8 infection (C). (E) Schematic of areas observed on the nematode, pink (A), red (B), purple (C) and blue (D). Box indicates LCV, arrow tissue degradation. Scale bar is 5  $\mu\text{m}$ .

components of the core apoptotic machinery, CED-3 and CED-4 (Gartner *et al*, 2008). However, unlike germline apoptosis, somatic apoptosis is developmentally programmed by a cell lineage and is activated by a different set of regulator factors (Gartner *et al*, 2008). Germline apoptosis is involved in oogenesis and contains two different categories. One of these is the natural “physiological” germline apoptosis that helps with oogenesis and is independent of the BH3-only apoptosis effector EGL-1 (Gartner *et al*, 2008). The second category of germline apoptosis is the “stress-induced” apoptosis, which is triggered by a genomic integrity checkpoint (Gartner *et al*, 2008). Cells under “stress-induced” apoptosis if the DNA is damaged or in some cases if the nematode is exposed to certain environmental insults or pathogens that induce germ cell apoptosis (Gartner *et al*, 2008). The germ cells of a nematode are both pluripotent to give rise to all cell types, and immortal to produce all subsequent generations (Gartner *et al*, 2008). The germline is the only adult tissue that is maintained by stem cells, which constantly replenish the cellular population. Lastly, the germline is the only tissue in which apoptosis is not controlled by an invariant cell lineage (Gartner *et al*, 2008).

A sensitive method to detect a germ cell undergoing apoptosis is by fluorescent imaging of apoptotic or corpse cells with GFP tagged CED-1. The CED-1::GFP is a fusion protein that highlights the cell that surrounds around each apoptotic germ cell during the phagocytosis engulfment (Schumacher *et al*, 2005). This method is best for the detection of low-to-moderate apoptotic cell counts, but not for high apoptotic cell counts due to the appearance of diluted apoptotic cells making detection of individual cells difficult. The germ cells of interest are found in the death zone, which includes the transition zone, pachytene zone, and the loop of the gonad arm. Normally the germ cells undergo apoptosis only in the death zone to form viable oocytes.

However, when the nematode is infected with a bacterial pathogen, increased numbers of corpse cells can be seen along the entire gonad arm except for in the distal tip cell area where the stem cells lie.

In a previous study, it was reported that apoptotic cell count levels at the 24-hour infection time point were unusually low in nematodes infected with wild-type *L. pneumophila*. This suggests that secreted effectors may be interacting with the germline apoptosis pathway (Brassinga *et al.*, 2010). To confirm that the CED-1::GFP nematodes followed the same trend at the 24 hour infection time point a time lapse study was done to compare the CED-1::GFP nematodes to the previously documented nematodes. These nematodes were infected with *E. coli* OP50, wild-type *L. pneumophila* and *S. Typhimurium* SL1344. At time points 0 h, 12h, 24h, and 36h the nematodes were assessed for the apoptotic counts. It is important to note that *E. coli* OP50 was grown on the nutrient rich BCYE agar plate making an anaerobic environment that can be considered to be infectious to the nematodes. Like the previous study, the 24h time point indicated the strongest difference between the three bacterial strains tested (Figure 3.32).

### **3.7.1 Germline apoptosis assay of known apoptotic *L. pneumophila* mutant strains**

The ability of *L. pneumophila* to secrete over 300 effector molecules by a Type IV secretion system facilitates infection of the host cell (Richards *et al.*, 2013). The effector molecules modify the host cell environment to make a suitable replication niche. Effector molecules with known anti- and pro-apoptotic function in the macrophage cell were studied to verify the function of these molecules in *C. elegans* infected with *L. pneumophila*. It should be



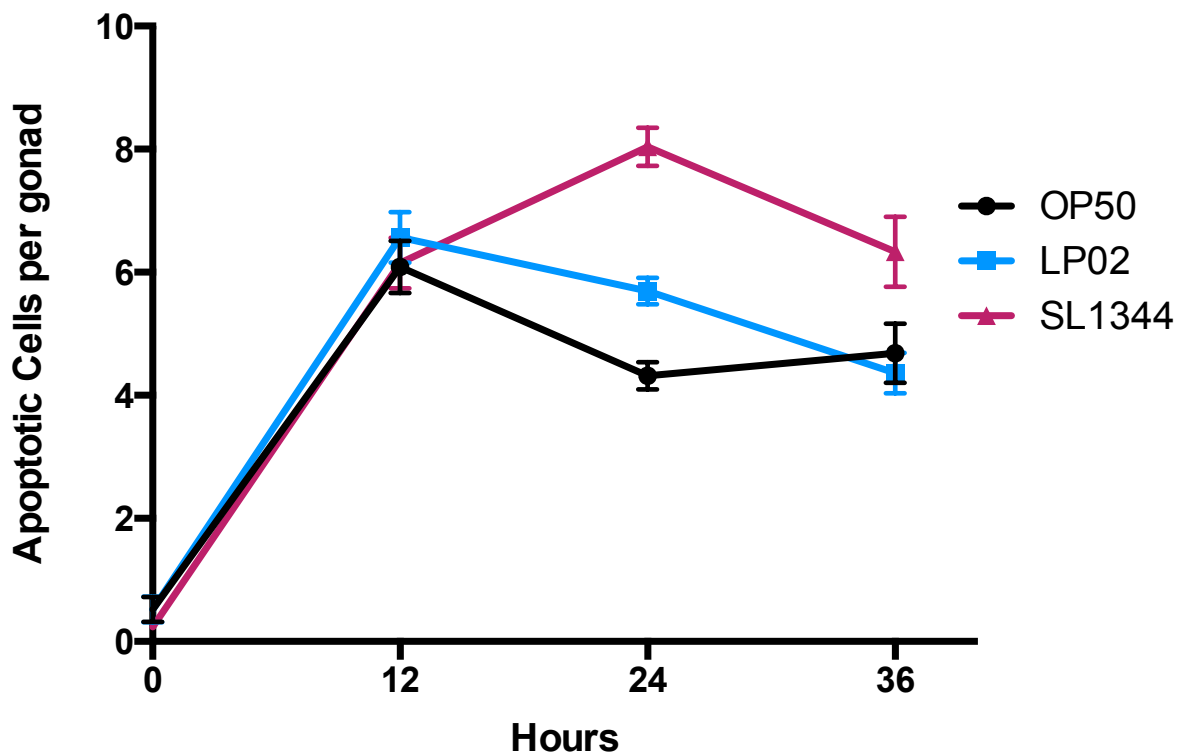


Figure 3.32 Timeline of Apoptotic cell counts in CED-1::GFP nematodes infected with various bacterial strains. *E. coli* OP50 (OP50) was grown on BCYE for 24h. Wild-type *L. pneumophila* (LP02) was grown on BCYE (thy 100) for 48h. *S. Typhimurium* (SL1344) was grown on BCYE for 24h. At 12h intervals the apoptotic cells were counted under epifluorescence. Significance was observed at the 24h time point between all strains. At 24 hours  $p$  values of  $<0.0001$  for LP02 SL1344; 0.0002 for LP02 and OP50 were obtained by a paired T-test.

noted that components of the *C. elegans* germline apoptosis pathway are functionally conserved with components of the macrophage apoptosis pathways.

The study of an *L. pneumophila* infection on the germline apoptosis was first conducted with the  $\Delta dot/icm$  mutant strain fed to the nematodes. The genotype of the  $\Delta dot/icm$  mutant strain is the complete deletion of the 27 *dot/icm* genes that encode the Type IV Dot/Icm secretion system (Isberg *et al.*, 2009). The complete deletion of the system should theoretically result in an increase in apoptotic cell counts due to the inability of *L. pneumophila* to block germline apoptosis. This was observed in the mutant strain with a *p* value of  $<0.0001$  (two-tailed paired T-test) compared to nematodes infected with the wild-type strain (Figure 3.33). To help validate this finding, the effector molecule DotA was next targeted due to its ability to affect the Dot/Icm Secretion system of *L. pneumophila*. With DotA mutated the Dot/Icm becomes dysfunctional and no longer properly secretes effector molecules, the specific function of DotA is still unknown. With the  $\Delta dotA$  mutant strain there was an increase in apoptotic counts almost as high as the super null  $\Delta dot/icm$  secretion system strain (Figure 3.32). The *p* value between the wild-type *L. pneumophila* strain and  $\Delta dotA$  mutant strain was  $<0.0001$  (two-tailed paired T-test).

Effector molecules with described direction interaction with the apoptotic machinery in the macrophage cell were also included in the germline apoptosis assays. The molecules of interest would include the already described SdhA and SidF effector molecules. SdhA was originally proposed to interact with the infection-induced type 1 interferon response, which plays a role in counteracting the host defense system (Ge and Shao, 2011). However, SdhA has since been determined to maintain the integrity of the LCV in the macrophage host cell (Langua *et al.*, 2006; Harding *et al.*, 2013). The lack of SdhA may result in an increase in the germline apoptosis

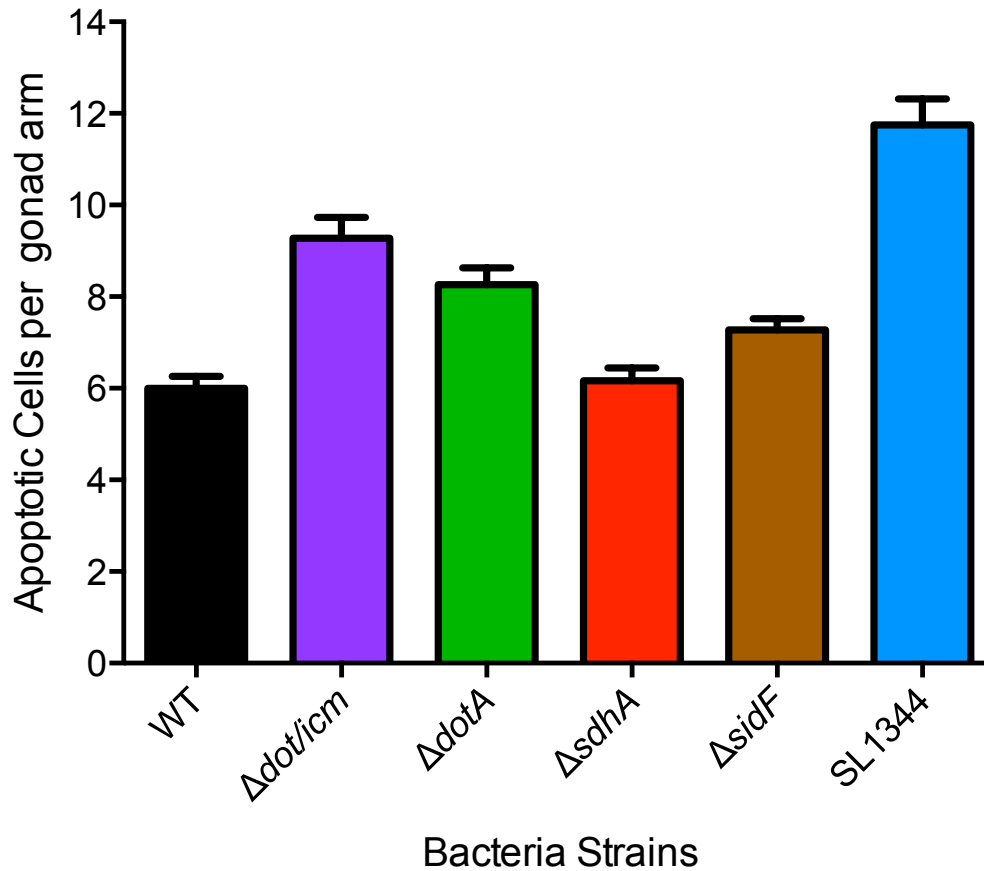


Figure 3.33 Germline Apoptotic Counts of infected transgenic CED-1::GFP *C. elegans* with various *L. pneumophila* effector molecule mutant strains at 24 hour time point. Approximately 20-30 nematodes were analyzed (2 gonad arms per nematode) for a total of 40-60 gonad arms counted for apoptotic cells. Two-tailed student's statistical analyses determined p values of <0.0001 for  $\Delta dot/icm$  and  $\Delta dotA$  and 0.0013 for  $\Delta sidF$  in comparison to wild-type *L. pneumophila*. *S. Typhimurium* SL1344 was used as a positive control for apoptotic cell counts.

as access of the effector molecules to the germline apoptotic pathway may be compromised. Lack of SdhA resulted in no significant difference between the mutant strain the wild-type strain (Figure 3.33). Therefore, the lack of significant cell death indicates that the germ line apoptosis is not as critical in the infection process as it is in a macrophage host. Also these results suggest that the effector molecules are still able to interact with the germline apoptosis pathway and that SdhA is not an essential part of this interaction.

The second effector molecule SidF has direct interaction with the macrophage apoptosis pathways. SidF is specifically stated to interact with the pro-apoptosis Bcl-2 family proteins, which includes BNIP3 and Bcl-rambo (Banga *et al.*, 2007). The direct interaction with these proteins is to delay cell death since both proteins are involved with the mitochondrial release of cytochrome c to activate various caspases inducing cell death. The effect of SidF on the germ line apoptosis should be consistent with the macrophage host model as there is homology between *C. elegans* CED-9 to the Bcl-2 protein family (Tan *et al.*, 2001). As expected apoptotic cell count levels were significantly elevated in nematodes fed bacteria lacking SidF (Figure 3.33). In nematodes fed  $\Delta$ *sidF* mutant strain in comparison to apoptotic levels in nematodes fed the wild-type strain there was a *p* value of 0.0013 (two-tailed paired t-test) (Figure 3.33).

Thereby, the apoptotic effect is similar but not identical to the assumed apoptotic effect on the macrophage cell. The difference is so that *L. pneumophila* is able to infect and evade multiple different hosts, protozoan, ciliates, and macrophages, using various effector molecules. Some key effector molecules overlap but not all effector molecules are the same for every host model; even when comparing different cell lines of the same host such as U937 and murine macrophage cells.

### 3.7.2 Germline apoptosis assay of *L. pneumophila* Dot/Icm component mutant strains

Select components of the Dot/Icm secretion system (DotB, DotF, DotG and DotH) with unknown function in the infection process in *C. elegans* were also investigated. The focus of the assay was to determine if one or more of the components interacted with the *C. elegans* apoptosis pathway and could be related back to the macrophage apoptosis pathway. The next targets of the germline apoptosis assay were effector molecules with unknown function with the macrophage apoptosis pathway (Figure 3.34). The idea was to identify any *C. elegans* specific effector molecules for interaction with the apoptotic machinery (Figure 3.34).

The targets included various dot effector molecules: DotB, DotF, DotG and DotH. The function of all the effector molecules has been concluded in the macrophage cell. DotB is an ATPase, which provides energy to the Dot/Icm secretion system, and functions in protein export (Sexton *et al.*, 2005). DotF is a protein known to span the inner and outer bacterial membranes (Isberg *et al.*, 2009). It interacts with four other Dot/Icm proteins: DotC, D, G and H. The exact function of DotF is to interact with substrates/major components of Dot/Icm channel (Isberg *et al.*, 2009). DotG interacts with DotF for the bacterial envelope-associated core complex. There is a critical partnership between effector molecules DotG and DotH in that in the absence of DotG DotH fails to localize in the outer membrane. Like DotF, DotG is assumed to be a major component of the channel (Isberg *et al.*, 2009). It has been reported that either inner membrane proteins DotF or DotG are critical for an interaction with substrates that pass through the core complex, and that this interaction is mediated through the DotL/DotM ATPase (Isberg *et al.*,

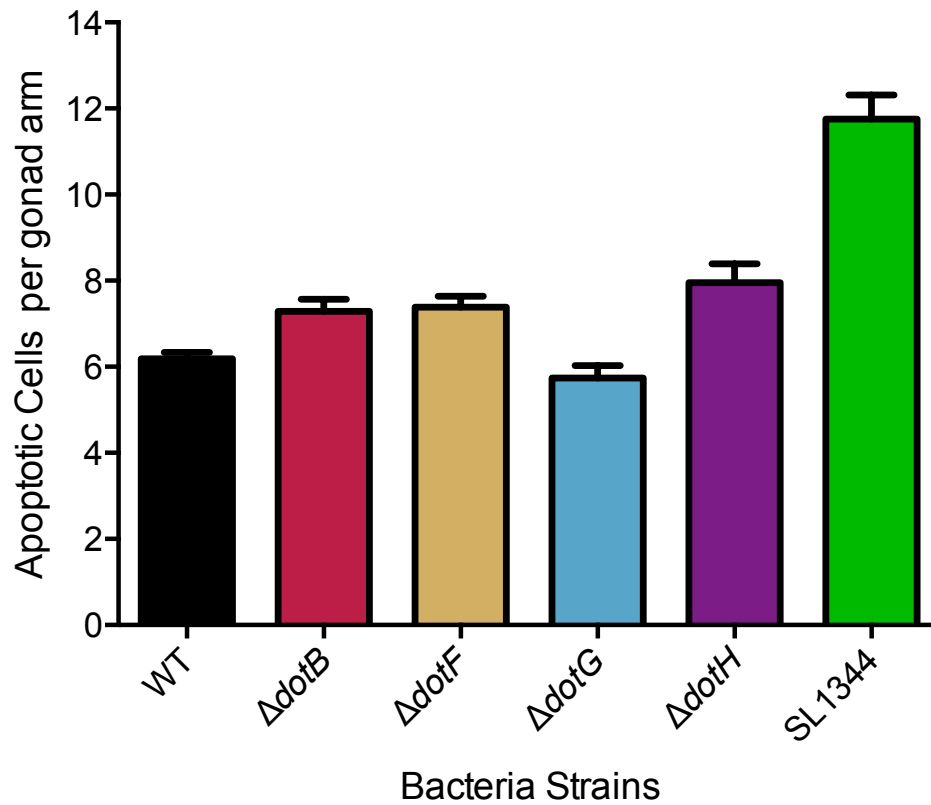


Figure 3.34 Germline apoptotic cell counts of infected transgenic CED-1::GFP *C. elegans* with various Dot/Icm *L. pneumophila* mutant strains at 24 hour time point. Approximately 20-30 nematodes were analyzed (2 gonad arms per nematode) for a total of 40-60 gonad arms counted for apoptotic cells. Two-tailed student's statistical analyses determined *p* values of 0.0009 for  $\Delta dotH$ , 0.0024 for  $\Delta dotB$ , and 0.0028 for  $\Delta dotF$ , in comparison to wild-type *L. pneumophila*; *S. Typhimurium* SL1344 was used as a positive control for apoptotic cell counts.

2009). DotH is the outer membrane channel that interacts with the DotF/DotG inner membranes to allow substrates transit (Isberg *et al*, 2009).

In general, the apoptotic cell counts were elevated slightly to show low significant differences for nematodes infected with  $\Delta dotB$ ,  $\Delta dotF$ ,  $\Delta dotG$  or  $\Delta dotH$  mutant strains in comparison to apoptotic levels of the wild-type strain. From the determined function of the effector molecules in other host models, it is unlikely that the effector molecules have a direct interaction with the core apoptotic machinery (Figure 3.34). However, it is possible that the inability of effective secretion of the various effector molecules to directly interact with the *C. elegans* apoptotic machinery may be the cause of the seen increase in germline apoptosis. The low effect of the germline apoptosis indicates again that the germline apoptotic death rate is not a key target for the *L. pneumophila*; it appears to be secondary especially when compared to the infection in macrophages.

### 3.7.3 Germline Apoptosis assay of CED-3

To further analyze the interactions between the known Dot/Icm effector molecules and the *C. elegans* germline apoptosis pathway, RNAi of *C. elegans* apoptotic pathway genes was done. RNAi nematodes were fed *E. coli* HT115, which had specific gene of interest in the bacteria's plasmid (Fire *et al.*, 1998). By feeding the nematode with this strain, the bacteria were able to create both RNA and dsRNA of the gene of interest. The *E. coli* strain fed to the nematodes will generate a dsRNA by the T7 polymerase on the pL4440 of *E. coli* HT115 that is induced by IPTG (Grishok, 2005). The nematode will process the dsRNA into an intermediate siRNA. The siRNA interacts with the nematode's RISC complex, with the anti-sense siRNA

binding to the complex to target the sense RNA of the genes of interest (Grishok, 2005). With the binding of the anti-sense RNA to the sense RNA creates a dsRNA, which is then degraded by the complex. The RNA in the RISC complex will target the gene of interest and degrade the complementary mRNA (Fire *et al.*, 1998; Grishok, 2005). The siRNA corresponds to the heritable factor of RNAi in *C. elegans* as well as a template to generate more RNA to target the same gene of interest giving the RNAi its systemic effect on the nematodes (Grishok, 2005). The systemic effect is of value as the nematode population can be fed or soaked in the dsRNA instead of having to individually inject each nematode with dsRNA (Grishok, 2005). A gravid nematode population was fed RNAi and their progeny were scored for the defect. RNAi-treated nematodes were then infected with *L. pneumophila* strains for apoptotic cell count assays as described previously.

CED-3 was targeted because of it has orthologous function to macrophage caspases 3 and its directly responsible for activating apoptosis in the nematode. Upstream of CED-3 both CED-4 and CED-9 interact with each other to control the activation of CED-3. Lack of CED-3 should result in no apoptotic counts observed in the *C. elegans* germline even during a bacterial infection (Aballay and Ausubel, 2001). One key affect of RNAi is the knockdown of gene expression, in that the gene is not mutated but rather the post-transcriptional process is disrupted. RNAi is not 100% effective and varying expression levels are often observed even with different RNAi constructs targeted for the same gene. Therefore, all RNAi experimental trends were taken out of a higher number of biological replicates.

The RNAi CED-3 nematodes had a drastically reduced number of apoptotic cells in *E. coli* fed and *L. pneumophila* infected *C. elegans* (Figure 3.35). Interestingly, the loss of function



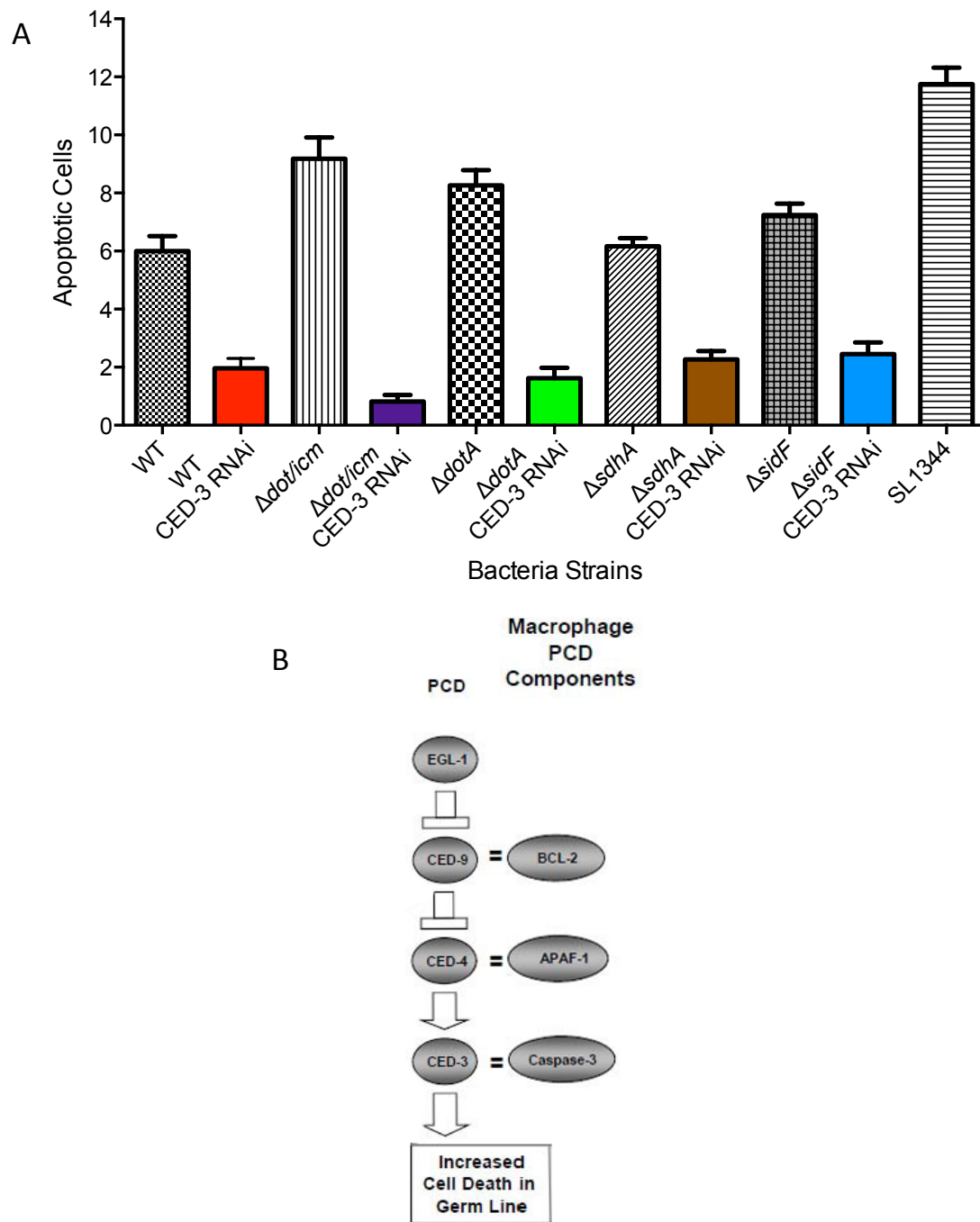


Figure 3.35 Germline apoptotic cell counts of RNAi *ced-3* CED-1::GFP *C. elegans* infected with various *L. pneumophila* strains at 24 hour time point. (A) Approximately 20-30 nematodes were counted (2 gonad arms per nematode) for a total of 40-60 gonad arms counted for apoptotic cells. Two-tailed student's statistical analyses determined *p* values of <0.0001 for all strains between the RNAi CED-3 nematodes in comparison to the untreated nematodes. (B) Schematic of the core apoptosis machinery with mammalian counterparts.

of the Dot/Icm secretion system with the knockdown of CED-3 resulted in the lowest apoptotic counts (Figure 3.35). Thereby, CED-3 is required for germline apoptosis seen of *C. elegans* during a bacterial infection. This is an expected result and henceforth the counts of apoptotic counts in RNAi CED-3 nematodes infected with wild-type *L. pneumophila* will be used as a control for all future germline apoptosis involving RNAi.

### 3.7.4 Germline Apoptosis assay of SEK-1

To further assess the involvement of the pathways that activate germline apoptosis, the p38 MAPK pathway was investigated (Figure 3.36 B). It is known that the p38 MAPK pathway works upstream of the PCD pathway. SEK-1 activates PMK-1, which will suppresses the anti-apoptotic component CED-9 (Gartner *et al.*, 2008). The presence of the bacterial pathogen in the intestinal lumen is detected by receptors lining the lumen and signal for a specific innate immune response (Sifri *et al.*, 2005). The RNAi SEK-1 should confirm the activation of the p38 MAPK pathway in the intestinal lumen. This can be accomplished if there is a decreased level of germline apoptosis for RNAi SEK-1.

The knock down RNAi of SEK-1 was done by the previously described RNAi feeding process (Section 3.7.3). It was observed in the knockdown of SEK-1 that there was little to no significant difference between all of the *E. coli* feed mutant strains, and the wild-type *L. pneumophila* fed strains. There was significance between the RNAi CED-3 and RNAi SEK-1 nematodes infected with wild-type *L. pneumophila* ( $p$  0.0006 by two-tailed paired t-test) (Figure 3.36). There was also great significance between the apoptotic counts between the CED-1::GFP nematodes and the RNAi SEK-1 nematodes ( $p$  < 0.0001 by two-tailed paired t-test) (Figure

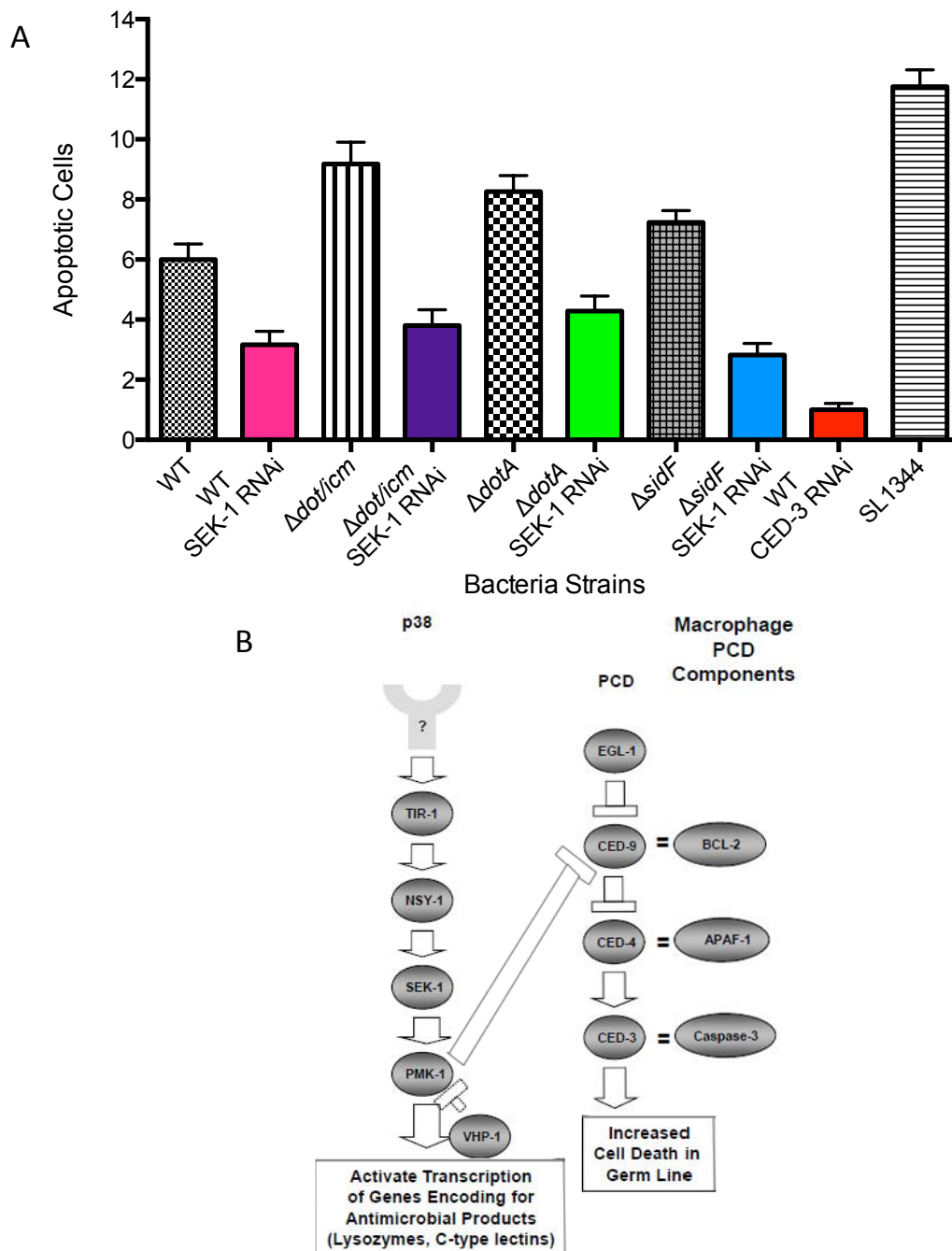


Figure 3.36 Germline apoptosis cell counts of RNAi *sek-1* CED-1::GFP *C. elegans* infected with various *L. pneumophila* strains at 24 hour time point. (A) Approximately 20-30 nematodes were counted (2 gonad arms per nematode) for a total of 40-60 gonad arms counted for apoptotic cells. p values of <0.0001 for WT,  $\Delta dot/icm$ , and  $\Delta sidF$  strains; and 0.0002 for  $\Delta dotA$  strain in comparison between the RNAi SEK-1 nematodes to the untreated nematodes. (B) Schematic of the p38 MAPK innate immune pathway proteins that regulate core apoptosis machinery with mammalian counterparts.

3.36). Possible reasons for the higher apoptotic cell counts in the *sek-1* RNAi nematodes include insufficient knockdown expression of SEK-1 or activation of PMK-1 by MEK-1. In any event, it appears that the p38 MAPK pathway is involved in the activation of germline apoptosis. To further verify this result other proteins involved in the MAPK pathway should be analyzed for consensus.

### 3.7.5 Germline Apoptosis assay of VHP-1

To help understand the interaction between PMK-1 and CED-9, the expression of VHP-1, an inhibitor of PMK-1, was knocked down by RNAi in the same fashion as described previously (Section 2.9.2) (Figure 3.37 B). Reduced expression of VHP-1 should remove the inhibitory effect of PMK-1, which in turn increases the inhibitory effect on CED-9 leading to an increase in germline apoptosis.

Interestingly, the opposite effect on apoptotic cell counts was observed in RNAi VHP-1 nematodes to the CED-1::GFP nematodes. There was a significant difference between the RNAi VHP-1 nematodes and the untreated nematodes that were infected with both *dot/icm* and wild-type *L. pneumophila* (Figure 3.37). There was no significant difference between RNAi VHP-1 nematodes infected with *dot/icm* mutant strain and wild-type *L. pneumophila* strain (Figure 3.37). However, there was a significant difference between the RNAi VHP-1 nematodes infected with  $\Delta dotA$  mutant strain and wild-type *L. pneumophila* ( $p < 0.0001$  by a two-tailed t-test) (Figure 3.37). Little difference in apoptotic counts was observed in RNAi VHP-1 nematodes and untreated nematodes infected with the  $\Delta dotA$  mutant strain. It is not clear the reason for this unexpected result; perhaps reduced expression of VHP-1 resulted in additional inhibitory

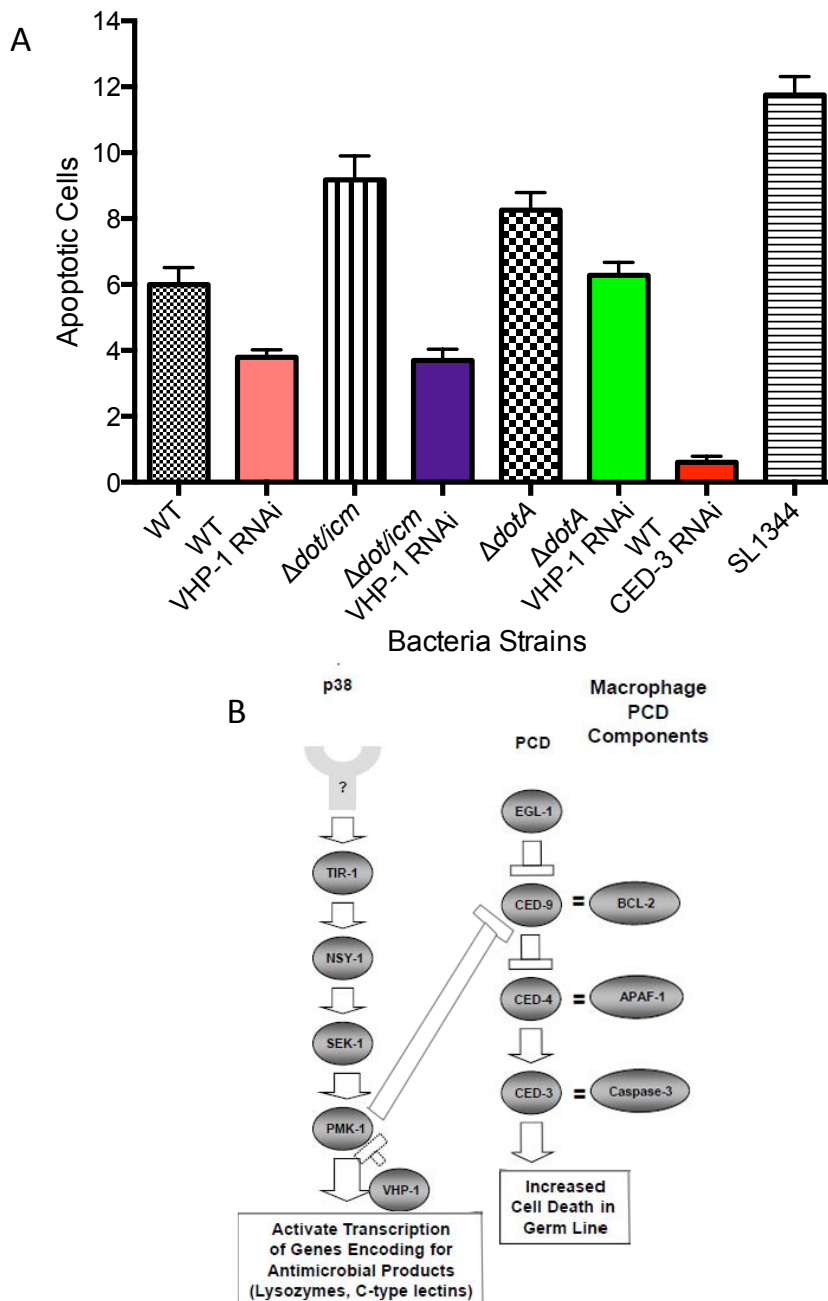


Figure 3.37 Germline Apoptosis Cell Counts of RNAi *vhp-1* CED-1::GFP *C. elegans* infected with various *L. pneumophila* strains at 24 hour time point. (A) Approximately 20-30 nematodes were counted (2 gonad arms per nematode) for a total of 40-60 gonad arms counted for apoptotic cells. Two-tailed student's statistical analyses determined *p* values of 0.0002 for wild-type, <0.0001 for  $\Delta dot/icm$  strain, and 0.0210 for  $\Delta dotA$  strain between the RNAi VHP-1 knockdown nematodes to the untreated nematodes. (B) Schematic of the p38 MAPK innate immune pathway proteins that regulate core apoptosis machinery with mammalian counterparts.

activities on the activation of germline apoptosis through another unknown component of the innate immune system.

### **3.8 Effects of the Oocyte Endocytosis pathway during an *L. pneumophila* infection**

The *L. pneumophila* infection process is specific in the *C. elegans*, similar to other host models. *L. pneumophila* has the ability to manipulate the host cellular processes to create replicative niches. Characteristic features of *L. pneumophila* infection in *C. elegans* include the constipation of the posterior intestinal lumen, observed gonadal tissue infection sites and the inhibition of germline apoptosis. However, the movement of *L. pneumophila* and its various interactions within multiple tissues is not known. *C. elegans* are highly vacuolar organisms, relying on the intestinal lumen to supply nutrients to various organs via endocytosis pathways. The manipulation of the endocytosis pathway to the other organs appears to be a prime target for *L. pneumophila* to facilitate a further bacterial spread throughout the nematode. Various exocytosis and endocytosis pathways are involved in moving various nutrients in *C. elegans*. Each different endocytosis and exocytosis have specific regulators, recognition receptors, and proteins that coat the vacuoles and help the nutrients to be incorporated into the target cell (Sato *et al.*, 2014) The *L. pneumophila* secondary infection site is observed to be the gonadal tissues as confirmed by microscopic examination. Thus, it is hypothesized that the oocyte endocytosis pathway may be utilized by *L. pneumophila* to gain access to the gonadal tissue.

The oocyte endocytosis pathway is responsible for the movement of nutrients from the intestine to the growing oocytes and the uterine bound embryos. The endocytosis pathway is able to deliver nutrients to the germline cells in the pachytene area where the germline cells are

starting to develop and undergo various changes. One of these many changes is the accumulation of cytoplasmic nutrients from the nurse cells that undergo apoptosis to feed the growing oocytes. To further help the growing cell to develop into oocytes, nutrients are required from the intestinal lumen. This pathway has been under intense study in the past decade, and new targets and functions of proteins involved in this pathway are currently being found and characterized (Grant *et al.*, 2006; Sato *et al.*, 2014).

Some of the best-characterized components of this pathway are the various RME (receptor mediated endocytosis) proteins. The first general endocytosis regulators studied and characterized were RME-1 and RME-8 (Grant *et al.*, 2006). RME-1 is an EH domain protein and is associated with recycling of endosomes and is thought to contribute to the formation of membrane tubules that recycle receptors from endosomes to the cell surface (Grant *et al.*, 2001). RME-8 is a large DNA-J domain protein that is known to bind to HSP-1/Hsc70, a protein folding chaperone (Zhang *et al.*, 2001; Sato *et al.*, 2014). It is proposed that rme-8 functions to help uncoat the clathrin-coated vesicles in the oocytes (Grant *et al.*, 2001). Another rme gene of interest is RME-2 which is an LDL-receptor related molecule expressed specifically in the oocytes (Grant and Hirsh, 1999). The mutation of RME-2 leads to accumulation of yolk in the pseudocoelom of adult hermaphrodites (Sato *et al.*, 2014).

All of the rme genes were identified to play a role in endocytosis through screens of the major yolk protein YP170 fused to GFP (Grant *et al.*, 2001). YP170-GFP is an LDL that is synthesized in the intestine of adult hermaphrodites and is secreted basolaterally into the pseudocoelomic cavity (Grant and Hirsh, 1999). The Nomarski optic analysis of the yolk uptake in mutants defective in YP170-GFP uptake identified 11 rme genes, including the ones already

discussed, which are required components in endocytic transport (Grant and Hirsh, 1999). Thereby the screening provided a genetically tractable system for the study of clathrin and Rab dependent transport processes.

### **3.8.1 Survival Proportion of $\Delta rme-1(b1045)$ *C. elegans* during infection with various *L. pneumophila* strains**

A survival assay was done to assess the survival rate of wild-type and  $\Delta rme-1(b1045)$  nematodes infected with wild-type *L. pneumophila* (Figure 3.38). The mortality rate of the  $\Delta rme-1(b1045)$  was decreased significant compared to the wild-type nematodes ( $p$  value of 0.0072 Log-rank (Mantel-Cox) test) (Figure 3.38). Therefore, the lack of infection in the gonadal tissue resulted in a prolonged life expectancy. Therefore the infection is dependent on the *L. pneumophila* bacterial forms moving from the intestine to the gonadal tissues in an oocyte endocytosis dependent manner. Furthermore the infection in the gonadal tissue is significant in the characteristics and attribute to the longevity of *C. elegans* infected with wild-type *L. pneumophila*.

The survival assay with  $\Delta rme-1(b1045)$  nematodes was expanded to include infections with *L. pneumophila*  $\Delta dotA$  and  $\Delta sdhA$  mutant strains (Figure 3.39). Interestingly, it appears that the *L. pneumophila*  $\Delta dotA$  and  $\Delta sdhA$  mutant strains further prolonged the lifespan of the nematodes compared to wild-type nematodes infected with the wild-type strain. However, the observed longevity of the  $\Delta sdhA$  mutant strain did not result in a statistically significant difference to the nematodes fed the wild-type strain. There was a statistical significance between the  $\Delta dotA$  mutant strain and the wild-type *L. pneumophila* strain ( $p$  value of 0.0046 Log-rank



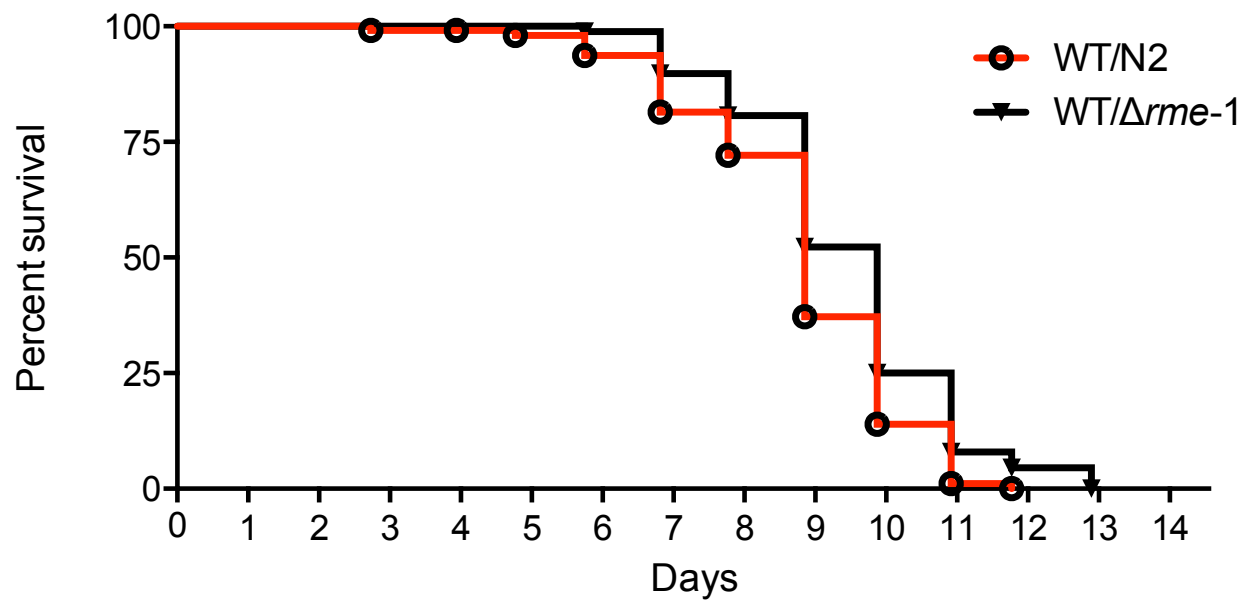


Figure 3.38 Kaplan-Meier survival curve of  $\Delta rme-1(b1045)$  *C. elegans* infected with wild-type *L. pneumophila*. n=90 nematodes counted for each strain in assay. A p value of 0.0072 was observed between the two strains.

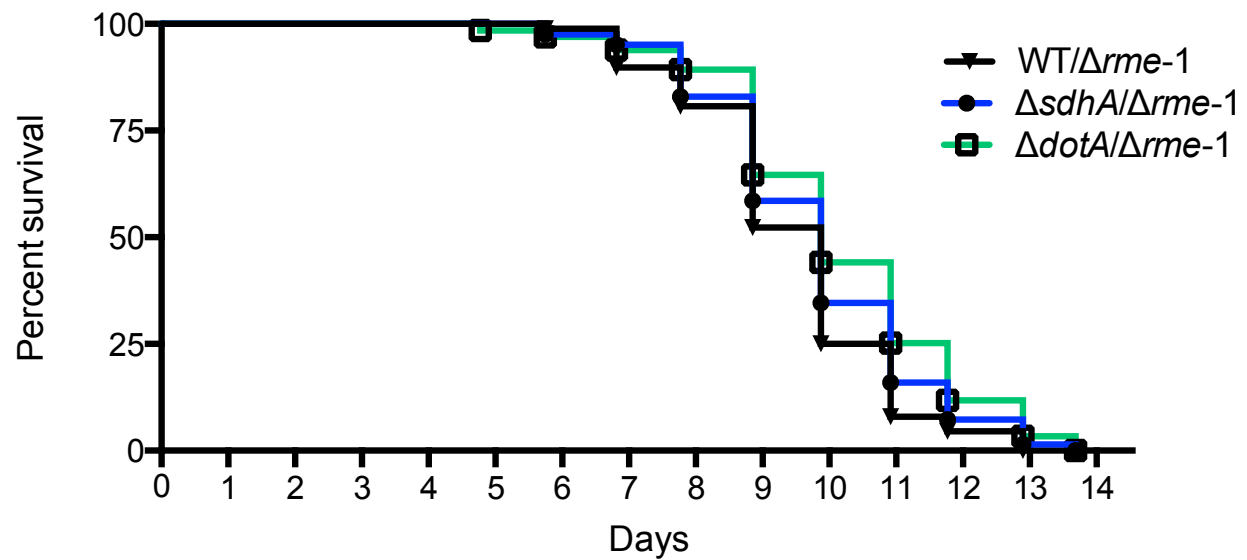


Figure 3.39 Kaplan-Meier survival curve of  $\Delta rme-1(b1045)$  *C. elegans* infected with wild-type  $\Delta dotA$  and  $\Delta sdhA$  mutant *L. pneumophila* strains. n=90 nematodes counted for each strain in assay. A *p* value of 0.0046 was observed between wild-type and  $\Delta dotA$  strain. No significance was determined between  $\Delta sdhA$  and wild-type strain.

(Mantel-Cox) test) (Figure 3.39). These results indicate that there could be an interaction between various effector molecules involved in virulence and LCV integrity and the oocyte endocytosis pathway.

### **3.8.2 Phenotype of $\Delta rme-1(b1045)$ *C. elegans* during a wild-type *L. pneumophila* infection**

The phenotype of  $\Delta rme-1(b1045)$  mutant nematodes is that endosomes accumulate basolaterally with endocytosed fluid in grossly enlarged endosomes (Grant and Caplan, 2008). The phenotype was verified in  $\Delta rme-1(b1045)$  nematodes fed *E. coli* OP50 as endosomes are visible in the pseudocoelomic cavity as well as swollen endosomes in the intestinal lining (Figure 3.40 A). Similar to the infectious process of wild-type *L. pneumophila* in wild-type nematodes a distension of the intestinal lumen was observed. However, the distension of the intestinal lumen in the  $\Delta rme-1(b1045)$  nematodes was due to a larger bacterial mass present in the intestinal lumen than in the wild-type nematodes (Figure 3.40 B). Similar to the known phenotype of the  $\Delta rme-1(b1045)$  mutant nematodes are the ghastly-enlarged endosomes, which is also present during an infection with *L. pneumophila* indicating that the infection doesn't change the observed non-pathogenic phenotype of the nematode (Grant *et al.*, 2001) (Figure 3.40 C). A final observation was in the osmotic pressure observed in the body cavity of the nematode in that there was a swelling of the cavity of the nematode along with the complete degradation of the intestinal lumen by the endosomes. The endosomes can be seen to take up most of the intestinal lumen (Figure 3.40 D and Figure 3.41 D).

The phenotypic presence of LCVs in the secondary infections sites was similar to those nematodes affected by both  $\Delta dotA$  and  $\Delta sdhA$  mutant strains. As there were multiple vacuoles

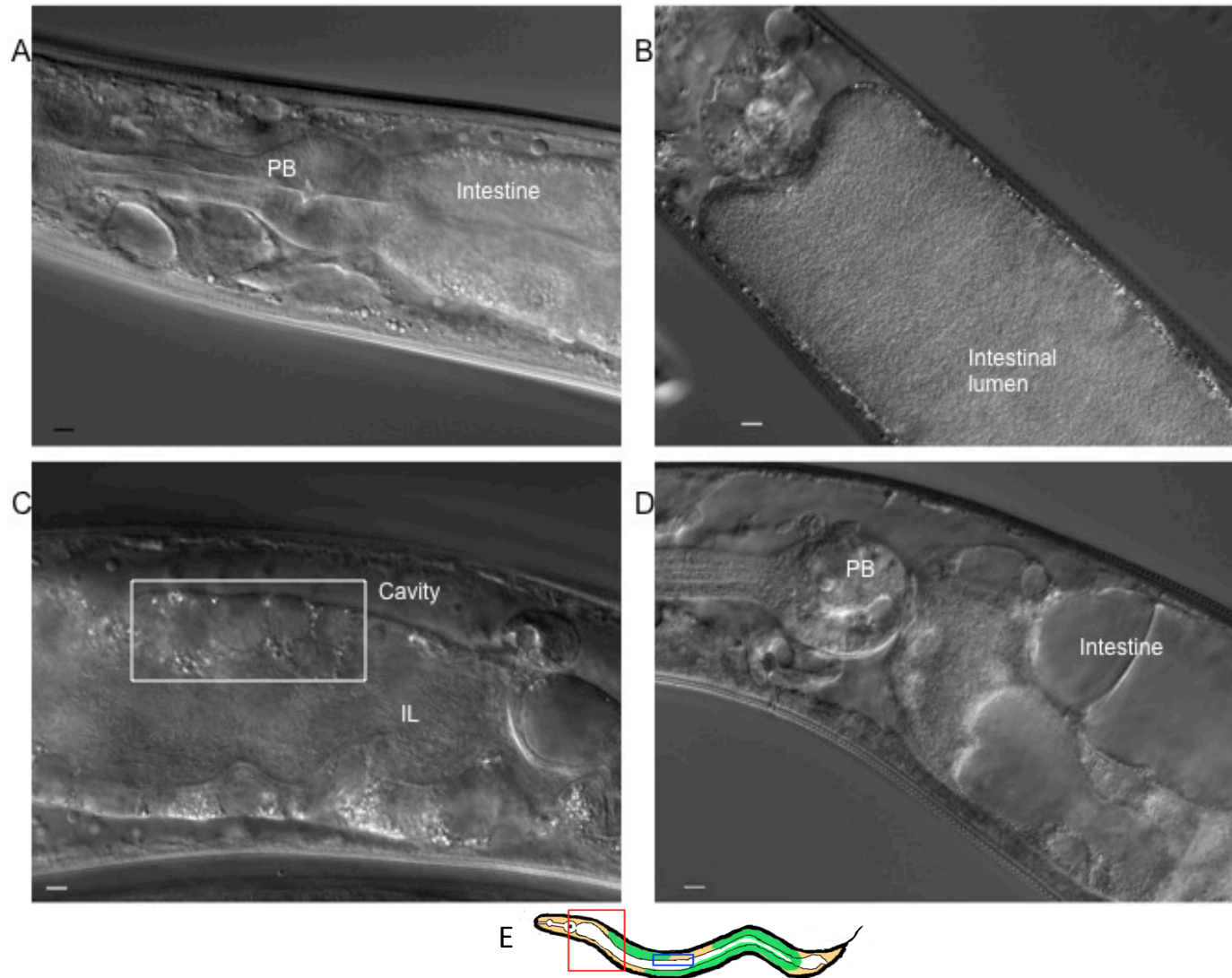


Figure 3.40 Observed morphology of intestinal region of  $\Delta rme-1(b1045)$  *C. elegans* fed wild-type *L. pneumophila*. Images taken on day 5 infection (C), day 6 infection (B and D), and day 1 adult  $\Delta RME-1$  nematodes fed *E. coli* benign food source on NGM were imaged. Schematic of general areas observed on the nematode red (A, B, and D), blue (C). Box indicates vacuoles observed. Scale bar of 5  $\mu m$ .

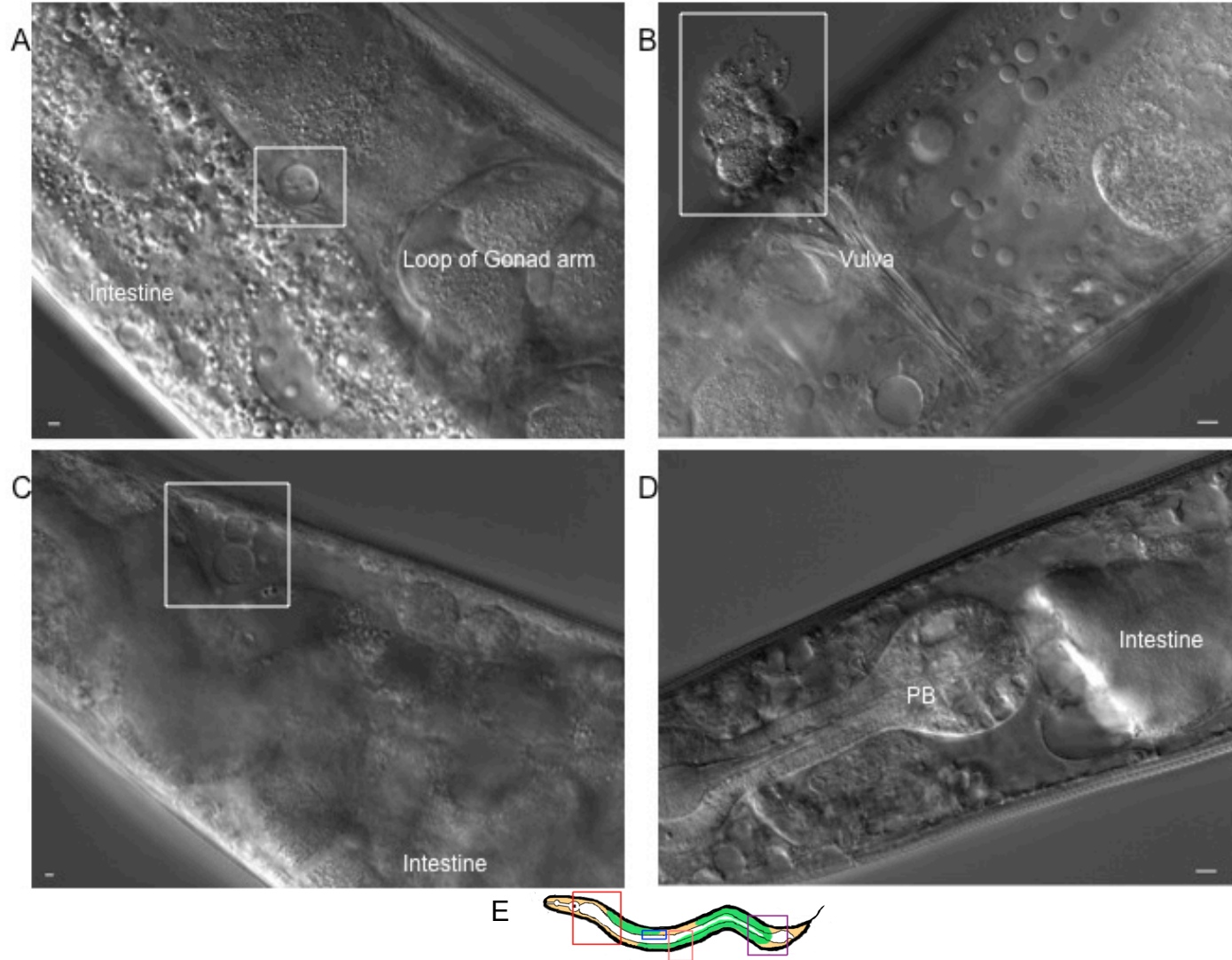


Figure 3.41 Observed morphology of intestinal region and secondary infection sites of  $\Delta rme-1(b1045)$  *C. elegans* fed wild-type *L. pneumophila*. Images taken on day 2 infection (A), day 4 infection (B), day 5 infection (C) and day 6 infection (D). (E) Schematic of general areas observed on the nematode red (D), blue (A), pink (B) and purple (C). Boxes indicate LCVs. Scale bar of 5  $\mu\text{m}$  (B and D); 2  $\mu\text{m}$  (A and C).

present in the cavity of the nematode, but there was an absence of LCVs in the gonadal tissues. Unlike the mutant strains there was an increase in presence of LCVs in the pseudocoelomic cavity (Figure 3.41 C). The expelling of LCVs from the vulva is similar to nematodes infected with wild-type *L. pneumophila*. However, the integrity of the vacuoles expelled appears to be less stable as the vacuoles soon combust and the forms inside the vacuoles are released into the environment (Figure 3.41 B). A further note was the placement of the LCVs in that most of these LCVs were observed in the intestinal lining or the intestinal cells (Figure 3.41 A). As mentioned before the  $\Delta rme-1(b1045)$  mutant nematodes fed wild-type *L. pneumophila* have a similar infection phenotypic characteristic to the  $\Delta dotA$  and  $\Delta sdhA$  *L. pneumophila* mutant strains. The number of LCVs observed in the secondary gonadal tissues is rare (Figure 3.42 A and B). However, unlike the  $\Delta dotA$  and  $\Delta sdhA$  *L. pneumophila* mutant strains there is still a possibility of infection in the gonadal tissues and when infection occurs in the gonadal tissue it is similar to the phenotype of wild-type *L. pneumophila* infected in wild-type nematodes (Figure 3.42 C). Another observation is that the vacuoles that contain bacterial forms are seen touching the gonadal tissues but not infecting the tissue (Figure 3.42 D). Indicating that a functioning endocytosis pathway is needed for *L. pneumophila* vacuoles to penetrate the gonadal tissue. Also in conclusion is that the gonadal tissues as the primary target for a secondary infection site as the vacuoles appear to dock at the gonadal tissue but lack the ability to enter.

### **3.8.3 Survival Proportions of RME-2 knockdown gene expression in *C. elegans***

The *rme-2* gene is an LDL receptor on the oocytes. The survival rate of knockdown RNAi RME-2 nematodes compared to wild-type nematodes both infected with wild-type *L.*

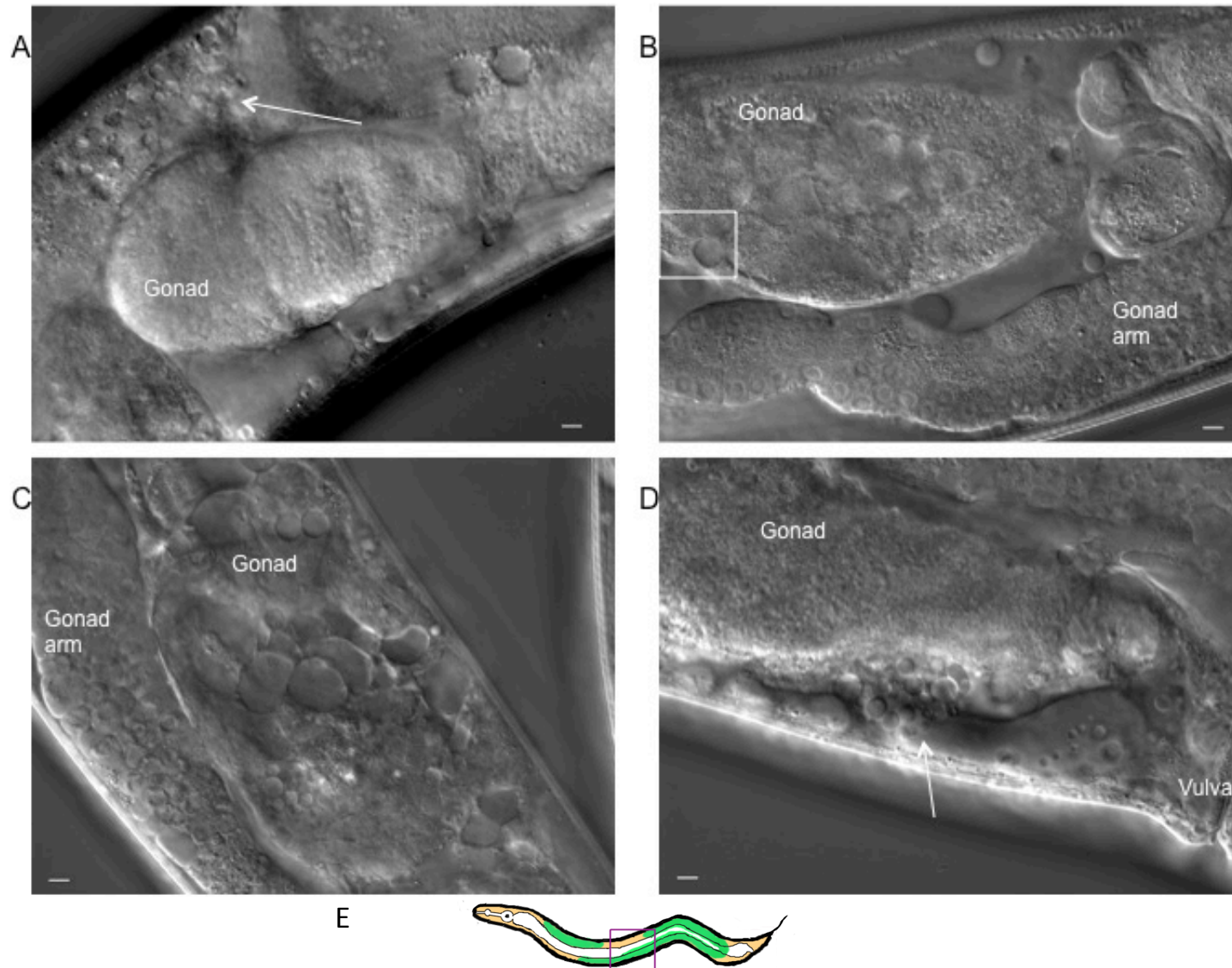


Figure 3.42 Observed morphology of secondary gonad infection site of  $\Delta rme-1(b1045)$  *C. elegans* fed wild-type *L. pneumophila*. Images taken on day 3 infection (B), day 6 infection (C), day 7 infection (D), and day 8 infection (A). (E) Schematic of general area observed on the nematode. Box and arrows indicate LCVs. Scale bar of 5  $\mu$ m.

*pneumophila* appears to prolong the longevity of the nematodes (Figure 3.43). The survival rate of the infection only appears during the later part of the infection process. This result strongly suggests that the secondary infection site of the gonadal tissue is important for the observed mortality rate of wild-type *C. elegans* during a wild-type *L. pneumophila* infection process.

#### **3.8.4 Germline Apoptosis assay of RNAi RME-2**

To further characterize the infection of wild-type *L. pneumophila* in RNAi RME-2 nematodes, a germline apoptosis assay was completed with the CED-1::GFP nematodes. It was observed that the knockdown expression of RME-2 did not play a significant role in the germline apoptosis indicating that the endocytosis process is not playing a role in germline apoptosis (Figure 3.44). Thereby the effector molecules do not use the oocyte endocytosis pathway to interact with the germline apoptosis.



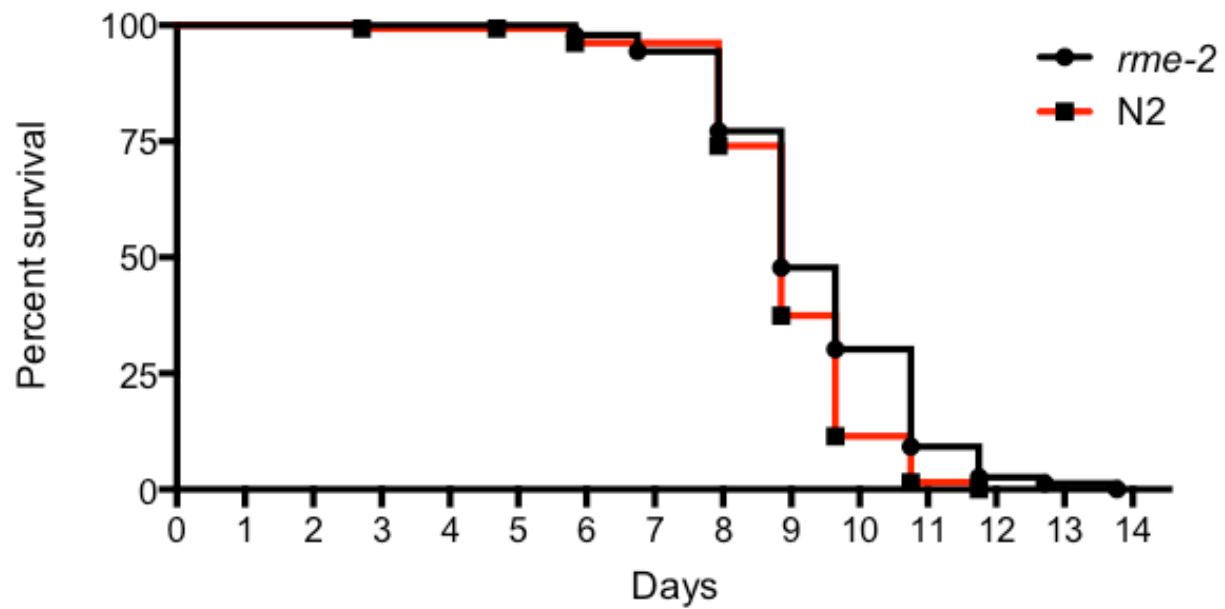


Figure 3.43 Kaplan-Meier survival curve of RNAi *rme-2* knockdown *C. elegans* infected with wild-type *L. pneumophila*. n=90 nematodes counted for each strain in assay. A *p* value of 0.0045 was observed between the two nematode strains.

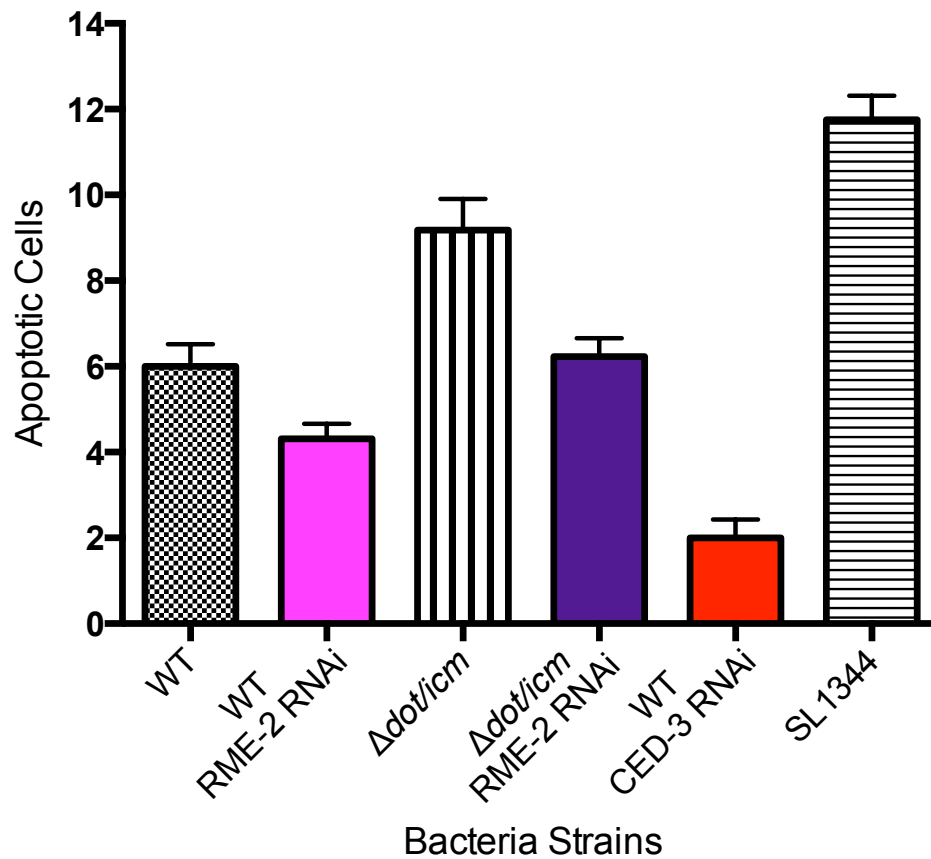


Figure 3.44 Germline apoptotic cell counts of RNAi *rme-2* CED-1::GFP *C. elegans* infected with various *L. pneumophila* strains at 24 hour time point. Approximately 20-30 nematodes were counted (2 gonad arms per nematode) for a total of 40-60 gonad arms counted for apoptotic cells. Two-tailed student's statistical analyses determined *p* values of 0.0032 for wild-type, 0.0067 for  $\Delta dot/icm$  between the RME-2 CED-1::GFP knockdown nematodes to CED-1::GFP nematodes.

## Chapter 4: Discussion

*C. elegans* have recently become an important model for understanding host-pathogen interactions especially in the study of the innate immune response. The first pathogen of study was *P. aeruginosa* PA14, which can kill *C. elegans* by either a fast-kill toxin mechanism or through a slow-kill intestinal colonization mechanism. However, the initial act of colonization in the intestinal lumen is only a characteristic of the infection and cannot be the cause of death (Sifri *et al.*, 2005). The cause of death for a nematode with an intestinal colonization is from the accumulation of bacteria in the intestine from indigestion and bacterial replication (Alegado *et al.*, 2003). Pathogenic bacteria utilize other mechanisms to kill *C. elegans*, which include a persistent intestinal infection, invasion of nematode cells and cuticle biofilm formation. Each mechanism of killing nematodes is specific to the pathogenic bacteria.

*L. pneumophila*, an intracellular pathogen of human macrophages has been established as a pathogen to *C. elegans* (Brassinga *et al.*, 2010). Thereby, there are general similarities between microorganisms that use the same mechanism to kill *C. elegans*. The exact pathways activated during a *L. pneumophila* infection are not known. *L. pneumophila* was first described as pathogenic in other host models such as HeLa cells, protozoa, mouse and human macrophage cells. In these models the *L. pneumophila* replicates until the cell becomes overloaded with bacteria and undergoes lysis (Faulkner and Garduño, 2002). Only in the environment are CLFs observed in protozoan cells (Faulkner and Garduño, 2002). As mentioned before, the CLFs expelled from the protozoan cell are capable of infecting new hosts.

Recently, new cases Legionnaires disease has been traced back to contaminated potting soil with increasing number of cases every year (Fields, 1996). With the work done to indicate

the presence of CLFs in the intestinal lumen of *C. elegans* it was suggested that the soil nematodes might also be natural reservoirs of *L. pneumophila* in the environment (Brassinga *et al.*, 2010). To become the soil environmental host *C. elegans* must produce CLFs similar to the ones found in protozoan cells as they must be able to be secreted successfully from the dying host, infect new hosts, and the CLFs must be able to survive in harsh conditions. Thus, this study was undertaken to further investigate the *L. pneumophila* infectious process in the *C. elegans* host model. It was determined that *L. pneumophila* was able to form LCVs containing differentiated CLFs in the gonadal tissue and pseudocoelomic cavity.

#### **4.1 Pathology of *L. pneumophila*-infected nematodes**

The innate immune system receptors of *C. elegans* line in the intestinal lumen recognize and interact with pathogenic bacteria and set off one of the various innate immune pathways. These pathways produce antimicrobial products such as C-type lectins, p450 cytochromes, and lysosomes. To combat the innate immune system, *L. pneumophila* overwhelms the intestinal lumen through bacterial load and colonizes the intestine (Figures 3.12 and 3.14). *L. pneumophila* is able to establish a persistent infection in the intestinal lumen and remains long after the nematodes are removed from the infectious bacteria (Brassinga *et al.*, 2010). To rule out the use of toxin-like substances to kill the nematode the mortality rate was observed under dead bacteria. If a toxin is used in the killing mechanism then the nematode should die in the same fashion whether it was fed live or dead bacteria (Sifri *et al.*, 2005). However, this was not observed and therefore *L. pneumophila* is an infectious bacteria that colonizes the intestinal lumen, and display characteristics similar to other bacteria that colonize the intestine (Figure 3.1).

The colonization of the nematode is important but release of infectious bacteria is also necessary for *C. elegans* to be considered an environmental host. Severe constipation in the posterior section of the nematode is observed early in the infection process (Figure 3.14 A). Based on the time needed for CLF formation in the intestinal lumen there would not be any CLFs present within 96 hours, (Figure 3.12 A and C), as the nematode still is not fully colonized during that time. Also any bacteria that are moved through the nematode starts in the replicative or stationary form as CLFs cannot grow on BCYE agar. Constipation is further confirmed by Nomarski optics (Figure 3.14). It is also important to note that the frequency of pharyngeal pumping was observed coordinating with a lack of movement of the nematodes on the infection agar plates. By Electron Microscopy we do see some *L. pneumophila* forms transitioning into the CLF state in the intestinal lumen (Figure 3.13). These transitioning forms observed in the intestinal lumen possess the same characteristics described by Faulkner and Garduño, 2002, in the protozoan and HeLa cell models. The ability to lyse the nematode through bacterial mass presence is not seen in *C. elegans* instead the bacteria must find an escape route out of the nematode. With the swollen intestinal tract of *C. elegans* it is hypothesized that the intestinal lumen CLF forms cannot be excreted. This conclusion is further proven from DIC observations made on the posterior portion of the nematode during a *L. pneumophila* infection.

As *L. pneumophila* is an intracellular pathogen, it interacts with cellular processes in both the macrophage and protozoa host cell models. This has not been completed in the *C. elegans* model as the infection has only been described as an extracellular infection. However, new evidence has shown that *L. pneumophila* is able to invade *C. elegans* tissues and could possibly interact with the intracellular pathways in a similar fashion to those described in the other host

models. As such the colonization of the nematode is only one characteristic of the infection process. To understand if there are other phenotypical effects similar to the other host models other *C. elegans* tissues should be examined for signs of intracellular manipulation.

#### **4.2 *L. pneumophila* infection affects on Germline PCD**

The effect of a bacterial pathogen on the germline PCD pathway has been studied in the intracellular pathogen *Salmonella* Typhimurium SL1344 strain. This strain is determined to kill the nematode through the mechanism of a persistent infection in the intestine (Aballay and Ausubel *et al.*, 2001). Aballay and Ausubel *et al.*, 2001, concluded that SL1344 infected *ced-3(n717)* mutant nematodes lead to a decrease in apoptotic counts in the germline and had a higher mortality rate. In this study, the analysis of the mortality rate of the same *ced-3(n717)* mutant nematodes was not conducted but RNAi of CED-3 was conducted for germline apoptosis. By RNAi the *ced-3* gene in the nematodes it was observed that there was a significant decrease in apoptotic cell counts during an *L. pneumophila* infection (Figure 3.34). Indicating that apoptosis of the germline during a *L. pneumophila* infection is dependent on the *ced-3* gene in a similar fashion to *S. Typhimurium* infection. Therefore, *ced-3(n717)* mutant nematodes under a *L. pneumophila* infection would exhibit the same fraction of change in their mortality rate.

Past analysis of the nematode's core apoptotic genes led to understanding genes that regulate the pathway through CED-9, an anti-apoptotic gene, and regulated by the p38 MAPK pathway, PMK-1 (Aballay *et al.*, 2003). PMK-1 however could not be studied directly due to lack of resources and time; the genes that directly interact with PMK-1 were available to be studied. These genes are SEK-1 and VHP-1, are an activator and inhibitor of PMK-1,

respectively (Ewbank, 2006 Salinas *et al.*, 2006). SEK-1 is activated during intestinal colonization of multiple bacteria, and decrease in germline apoptosis is seen in *sek-1* mutants (Ewbank, 2006; Aballay *et al.*, 2003). SEK-1 RNAi nematodes had decreased germline apoptotic counts during an *L. pneumophila* infection, keeping with the trend observed in *S. Typhimurium* fed *sek-1(km4)* mutants (Aballay *et al.*, 2003). A similar but not as drastic a decrease in apoptotic germline counts was observed for VHP-1 RNAi nematodes fed wild-type *L. pneumophila*. This latter observation was contradictory to the trend observed previously as the inhibitor was predicted to increase the apoptotic cell counts. There is no sound assumption or judgment to justify the contradictory result. Regardless of the result from the VHP-1 germline assay, activation of germline apoptosis during an infection is dependent on the activation of SEK-1 and the PCD pathway is dependent on PMK-1 interaction. The other gene of interest in nematodes was VHP-1, the regulator of PMK-1. It should be noted that the effect on germline apoptosis levels by a bacterial infection appears to be a pathogen-specific response as germline apoptosis levels were unaffected by *P. aeruginosa* PA14 (Aballay *et al.*, 2003).

The other side of the story in germline apoptosis concerns the effect of the effectors secreted by *L. pneumophila* during infection and their interaction with the apoptotic machinery. The alteration of germline apoptosis levels in *L. pneumophila* infected nematodes implies that the bacterial effectors are able to directly interact with the apoptotic machinery. Than any removal of the effectors that directly interacts with machinery would alter the apoptotic counts. Since *L. pneumophila* inhibits the PCD pathways in the macrophage host cell than any mutation in effectors interacting with the homologous machinery in *C. elegans* would result in increased germline apoptosis. To support this hypothesis, the supernull *dot/icm* *L. pneumophila* mutant

strain cause an increased in germline cell deaths observed (Figure 3.35). This result indicates that either a *dot/icm* component or effectors or both interact with the *C. elegans* directly interact with the PCD pathway.

The effector protein SidF is known to interact with macrophage apoptosis pathway Bcl-2 protein family (Banga *et al.*, 2007) was mutated and fed to *C. elegans*. A slight increase in apoptosis was observed in the nematodes fed  $\Delta$ *sidF* *L. pneumophila* (Figure 3.33) thereby SidF is more important in macrophage apoptosis interactions than with nematode apoptosis machinery. There could also be a weaker interaction between the *C. elegans* Bcl-2 homolog, CED-9, and the SidF effector molecule (Gartner *et al.*, 2008). An assay to verify this effect is to assay the germline apoptosis counts of the  $\Delta$ *sidF* mutant *L. pneumophila* strain in a *ced-9* mutant nematode. The outcome of this future assay would hope to shed light on the matter of host specific *L. pneumophila* immune responses and the redundancy of the effectors secreted in the host cell.

*L. pneumophila* effector components were analyzed to determine if they could play a role in delay of the *C. elegans* PCD in the germline. The first component tested was DotA which when mutated leads to an avirulent phenotype. *C. elegans* infected with  $\Delta$ *dotA* *L. pneumophila* showed great significance in apoptotic cell counts compared to wild-type *L. pneumophila*. Indicating that somehow DotA is involved in the interaction between *L. pneumophila* and the germline PCD pathway. The precise function of DotA in virulence is not known as any mutation in *dotA* leads to an avirulent function inhibiting study on direct interactions to on its apoptotic effect on the host pathways (Roy *et al.*, 1998). Others Dot/Icm components analyzed that showed weak significance difference in apoptotic counts to wild-type *L. pneumophila* were DotB, DotF,



and DotH; with DotG showing no significant change in apoptotic counts. It is assumed that since the components DotB, F, and H plays no direct role in macrophage apoptosis pathways these results are valid. The function of the components is in formation of a channel for secretion of molecules into the host cell the lack of an effective channel may have been the cause of the raised *C. elegans* germline apoptotic counts.

The effectors that showed the greatest significance between the mutant *L. pneumophila* and wild-type *L. pneumophila* were tested in RNAi nematodes with various known MAPK genes that interact with the PCD pathway. Similar to the results observed for *L. pneumophila* mutant strains there was general increase in apoptotic counts even with core *C. elegans* genes under RNAi influence. As with the wild-type nematodes the increase in apoptosis levels indicates that either a dot/icm component or an effector molecule or both could interact with the PCD pathway. Due to time the effector molecule SidF could not be analyzed in the RNAi MAPK nematodes. Taken together, the absence of the Dot/Icm system removes the suppression of germline apoptosis. However, while SidF appears to interact with the PCD, other effectors and/or Dot/Icm components may also participate, directly or indirectly, in altering germline apoptosis levels.

#### **4.3 Secondary *L. pneumophila* Infections Sites in *C. elegans***

The formation of CLFs in the protozoa host is needed for *L. pneumophila* survival in the environment. For *C. elegans* to be considered as an additional environmental host model, particularly the soil host, the formation and the expelling of CLFs must occur. The formation of CLFs has already been observed in the intestinal lumen of *C. elegans*. However, what was not seen were the CLFs being successfully expelled and how the expelled CLFs able to infect new

hosts. Still the ability to infect new hosts has not been analyzed, but the formation of CLFs and the expelling from the host was. TEM observations on the sixth day of infection were transitioning forms with stable PHBA inclusions present in the intestinal lumen (Figure 3.13). Also observed was the manipulation of the microvilli in the intestinal lumen as well as the destruction of the strong network web that holds the microvilli together (Figures 3.15 and 3.16). Note how there was no manipulation of the microvilli or of the intestinal apical membrane in the heat-killed wild-type *L. pneumophila* fed *C. elegans* (Figure 3.11). The *L. pneumophila* that cross the intestinal apical membrane are morphologically different, as they are assumed to be *L. pneumophila* in stationary phase. There has yet to be a direct or common mechanism determined for how *L. pneumophila* is able to escape the intestinal lumen and infect *C. elegans* tissues. Since *L. pneumophila* is an intracellular pathogen the ability to infect *C. elegans* cells should be of a similar virulence factors *L. pneumophila* utilizes to infect protozoan and macrophage cells, however, the exact mechanism in the case of *C. elegans* intestinal cells are not known. *L. pneumophila* is assumed to use its intracellular capabilities including its various effectors to manipulate host pathways and cross the barrier into intestinal cells. Further work on the mechanism or mechanisms *L. pneumophila* can use to cross the apical membrane will shed light on its infection of it and other intracellular pathogens seen only to colonize the *C. elegans* intestinal lumen.

Following the path of *L. pneumophila* traveling through the nematodal tissue, it was observed that the bacteria were either replicating or transitioning forms. Both of these forms were seen in either tight vacuoles and vacuoles containing two to three bacteria in the intestinal cell (Figure 3.17). The tight vacuoles are also observed in the infection of HeLa cells (Faulkner

and Garduño, 2002). Based on this comparison, it was assumed that these tight vacuoles become functional replication vacuoles containing multiple bacteria forms. These functioning vacuoles are often observed in the gonadal tissue of *C. elegans* (Figure 3.21), which also corresponds to the observed DIC imaging done as well (Figure 3.19). It is assumed that the bacteria exit the intestinal lumen in the tight vacuole based on their ability to move faster and easier through *C. elegans* tissues. Once in the gonadal tissue, the tight vacuoles are assumed to accumulate and join membranes to form LCVs. However, large replicating vacuoles similar to the LCVs observed in the gonadal tissue and other hosts are observed in the pseudocoelomic cavity (Figure 3.18). It is unclear if these LCVs are capable of infecting the gonadal tissue or if they are expelled through other openings.

The movement of the bacteria to the gonadal tissues required passage through the pseudocoelomic cavity. The vacuoles were first observed in the nematode on the third to fourth infection day, the quantity of vacuoles found in the cavity would increase drastically as the infection progressed (Table 3.1). With the bacteria always present in the pseudocoelomic cavity in the later portion of the infection, we were unable to track the individual vacuoles in the cavity to understand their movement to new tissues or they were considered expellable by the host. Also of loss the biochemical composition of the LCVs membrane in the gonadal tissue was observed to be drastically different, there was no study done to identify the composition of the membrane. The answer to this question may shed light onto where the LCV develops and how it is able to infect the gonadal tissue. Under the assumption of the vacuole characteristics, specifically the bacteria's movement and size, the "potholes" in the gonadal tissue are thought to be generated from the movement of these vacuoles in the pseudocoelomic cavity. These

collective results indicate the gonadal tissue and the pseudocoelomic cavity as a secondary infection sites.

In the gonadal tissue, *L. pneumophila* either transition fully in the CLFs gonadal tissue or *L. pneumophila* move out of the intestinal lumen as transitional forms (Figure 3.17). The CLFs are then capable of being expelled from the vulva once they form LCVs in the gonadal tissue. An alternative hypothesis is that the bacteria are able to create replication niches as the bacteria enter back into the replication phase as there are replicative forms observed in the gonadal tissue (Figure 3.13, part D). The evidence for the expelling of bacteria from the vulva is based on the observed LCVs near the opening of the vulva (Figure 3.20). Therefore, CLFs are not only formed in *C. elegans* but they have an exit route from the host to infect others. The ultrastructural characteristics of the bacteria in the intestinal lumen and in the gonadal tissue are similar to those characteristics observed in the protozoa host model (Figure 3.24 and 3.25). Also the bacteria have the same ultrastructure as those in the intestinal lumen of *C. elegans*. Therefore, the pathways that *L. pneumophila* uses to infect other tissues is varies on the manner of escape from the intestinal lumen, which tissue it chooses to infect and the time of infection. Unlike the simple infection process in the unicellular host models, the movement of *L. pneumophila* to different tissues is complicated but it could also shed light on how *L. pneumophila* is able to infect a wide variety of hosts.

As seen with other bacteria the colonization of the intestine, the colonization is often referred to as the sore of killing but it is not sufficient for the death of the nematode (Sifri *et al.*, 2005). The colonization of the intestine in this case leads to *L. pneumophila* being trapped along the brush border of the intestine and therefore it pushes past the intestinal apical membrane

invading new tissues to further replicate. Hence many bacteria that leave the intestinal lumen are in transitional forms presumably due to the lack of nutrients. Earlier in the infectious process, it is assumed that replicative forms could be leaving the intestinal lumen in tight vacuoles as well. However, those forms that invade the gonad tissue must be supplied nutrients from the intestine to support replication. There is a time where *L. pneumophila* can replicate feed on the nutrients present in the gonad cells and growing embryos. However, the nutrient supply in these cells is finite, as the intestine will no longer supply the gonadal tissue with nutrients when the nematode is no longer reproductive. It is hypothesized that the bacteria transition into CLFs and are expelled from the nematode.

#### **4.3.1 Effector protein and component involved in intracellular replication**

The ability to invade the gonadal tissue and move through *C. elegans* plus *L. pneumophila* requirement for effector proteins and components to achieve both was of interest. Furthermore, the effector molecule SdhA and Dot/Icm component DotA were investigated to determine if *L. pneumophila* or *C. elegans* are responsible for the production of the vacuoles observed. SdhA maintains the integrity of LCVs and DotA is essential for virulence (Roy *et al.*, 1998; Langua *et al.*, 2006). It was hypothesized that a lack of SdhA would lead to defective LCV biogenesis in *C. elegans* since a knockout of this effector molecule produced a drastic affect on LCV formation in other models (Langua *et al.*, 2006; Harding *et al.*, 2013). Lack of DotA or SdhA resulted in the observation of little to none gonadal tissue infection (Figures 3.28 and 3.30). LCVs were observed in the pseudocoelomic cavity, but to a lesser extent (Table 3.1). Thus, the vacuoles in the pseudocoelomic cavity are assumed to be host derived. In addition

there was a decreased mortality rate of nematodes fed  $\Delta dotA$  and  $\Delta sdhA$  mutant *L. pneumophila* strains compared to nematodes fed wild-type *L. pneumophila*. Therefore, attenuated virulence for both mutant strains were observed, similar to observations in other host models (Harding *et al.*, 2013; Garduño *et al.*, 2002). Thus, it appears that the secondary infection sites help kill the nematode faster by overloading the host with bacteria.

#### **4.3.2 Oocyte Endocytosis proteins involved in intracellular replication**

To further understand the derivation of the LCVs, the oocyte endocytosis pathway was analyzed based on the assumption that it is utilized in moving *L. pneumophila* from the intestine to the gonadal tissues. When infected with *L. pneumophila* the  $\Delta rme-1(b1045)$  nematodes showed an increase in survival rate (Figure 3.38). As well as the RNAi *rme-2* nematodes had an increase in survival rate (Figure 3.43). Therefore, the movement of the infectious process may be dependent on the movement of the vacuoles using the oocyte endocytosis pathway. Detailed microscopic analyses showed that the  $\Delta rme-1(b1045)$  nematodes resulted in a decrease in infected gonadal tissues (Figure 3.42). However, there was a small population of infected gonads observed in the  $\Delta rme-1(b1045)$  nematodes (Figure 3.42 C). This may be due to a spontaneous infection, as generally only one of the two gonads in these nematodes would be affected. Since RME-1 and RME-2 are components of the oocyte endocytosis pathway, the results indicate that *L. pneumophila* may be utilizing this pathway to facilitate the bacterial spread throughout the nematode tissues. The movement of *L. pneumophila* out of the intestinal lumen is not dependent on the oocyte endocytosis pathway as many vacuoles are observed in the pseudocoelomic cavity. Furthermore, the lack of movement into the gonadal tissues had the greatest effect on the

integrity of the intestine. In the  $\Delta rme-1(b1045)$  nematodes, the intestine appears to be under stress from the accumulation of vacuoles in the intestinal cells (Figure 3. 40 C). The mutant nematodes have an observed stronger colonization, and an increased presence of LCVs in the head and what appears to be a start of a grinder infection (Figures 3.40A and D). Thereby, the secondary infections sites are needed for *L. pneumophila* to replicate, and the bacteria do not have intentions to deteriorate the nematode tissues. Thereby the movement of *L. pneumophila* into the gonad is dependent on the effectors that stabilize the replication vacuole and the genes that help move vacuoles between tissues.

#### **4.4 Proposed Lifecycle of *Legionella pneumophila* in *C. elegans***

This study has provided more insight into the lifecycle of *L. pneumophila* in *C. elegans*. The ultrastructure characteristics of the bacteria have been identified as replicative forms that transition into infectious forms similar to the characteristics of *L. pneumophila* lifecycle observed in protozoa. Further, the characteristics of *L. pneumophila* observed in *C. elegans* are the manipulation and the crossing of the apical membrane of the intestine then the invasion of the surrounding intestinal cells. Finally the oocyte endocytosis pathway is used by the nematode to move nutrients from the intestine to gonad were observed to be manipulated by *L. pneumophila*.

The proposed lifecycle of *L. pneumophila* in *C. elegans* is that the bacteria cause a primary infection in the intestinal lumen and continue to proliferate. Bacterial colonization of the intestinal lumen triggers the innate immune system to activate antimicrobial products, which over time proves to be ineffective against the virulence bacteria. The bacterial colonization causes stress on the microvilli and the membrane that surrounds the intestinal lumen. The

breaking down of the intestinal lining allows multiple bacteria to cross the border (Figure 4.1). However, long before the membrane is broken, singular bacteria are secreted through the intestinal cells in tight vacuoles. The tight vacuoles may or may not be the result of the endocytosis pathway. Once the bacteria are in the intestinal cell, they must then be transported through the cell, through the pseudocoelomic cavity before crossing the membrane of the gonadal tissues (Figure 4.1). The transport across the gonad membrane is where the endocytosis pathway is most critical. The movement out of the intestine is not fully endocytosis based, but rather the intake by the gonadal tissue. This is confirmed by the LCVs observed the pseudocoelomic cavity in the  $\Delta rme-1(b1045)$  nematodes. Therefore, any mutation of the endocytosis genes involved in transportation or recognition of the vacuoles in the oocytes leads to a severe decrease in *L. pneumophila* presence in secondary infection sites.

#### 4.5 Conclusions

The manipulation of the phylogenetically conserved innate immune system by *L. pneumophila* can be modeled using *C. elegans*. Colonization and invasion of nematode tissues are the mechanisms utilized by *L. pneumophila* to kill *C. elegans*. Colonization is in the primary infection site and the secondary sites are considered to be the gonadal tissue and the pseudocoelomic cavity. *L. pneumophila* is able to invade the gonadal tissues by manipulating the apical membrane of the intestinal lumen passing through the intestinal cell and pseudocoelomic cavity, and then entering into the gonadal tissue. The manner in which *L. pneumophila* employs to get into the gonadal tissue is the oocyte endocytosis pathway, which is also responsible for movement of nutrients to the growing embryos. The bacterial escape from the intestine could be



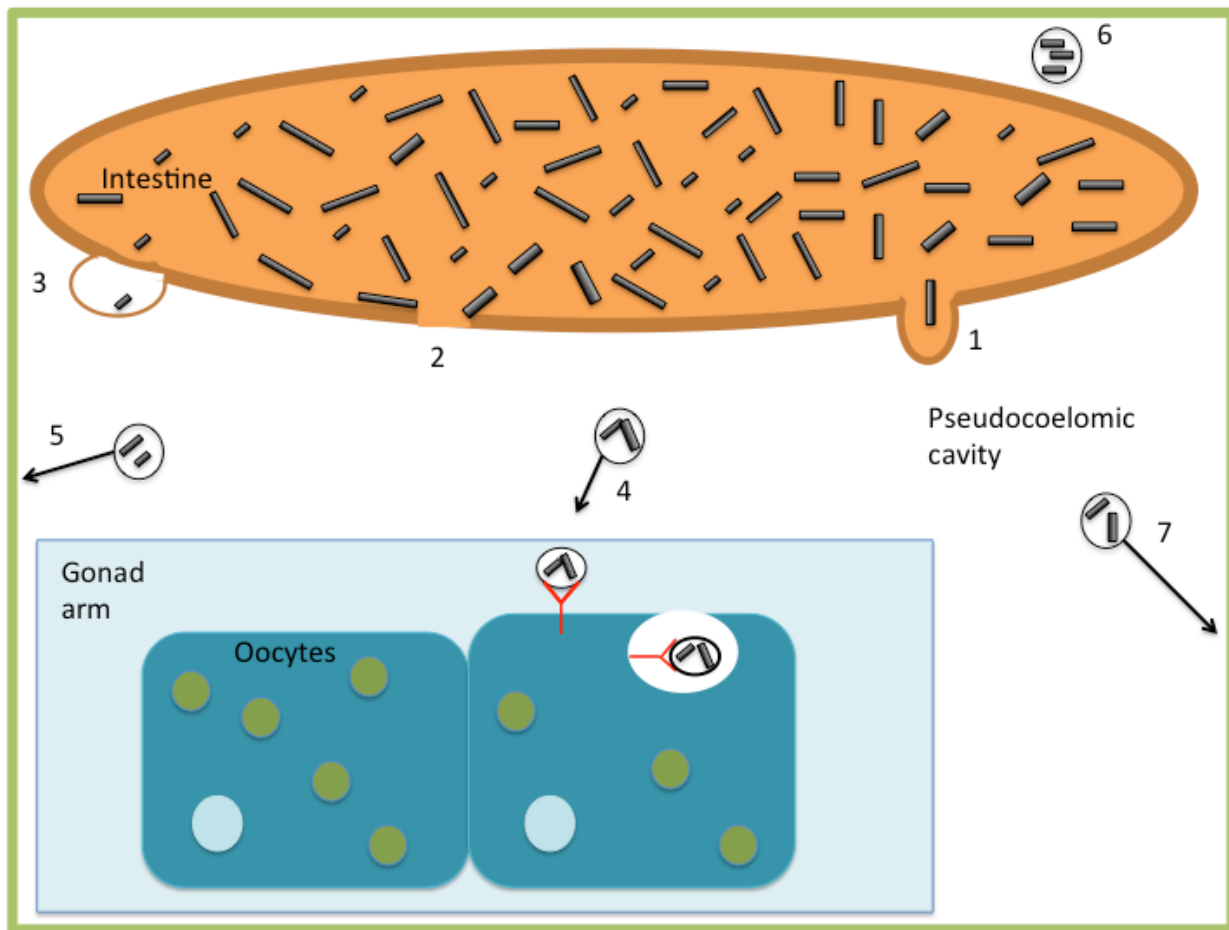


Figure 4.1 Schematic of *L. pneumophila* movement in the *C. elegans* host model. It is proposed that the bacteria either escape 1) in a tight vacuole and causing a bulge in the apical membrane, or 2) separated/disconnected the apical membrane from itself, or 3) the terminal web has separated from the microvilli and bacteria forms are seen in the bulge created. Once past the intestinal lumen and intestinal cells, LCVs are seen in the pseudocoelomic cavity. Once in this cavity the bacteria 4) move to the oocytes and use the endocytosis RME-2 receptor to enter the oocytes, or 5) move to other cells in the gonad arm and gonad, or 6) move around freely in the pseudocoelomic cavity, or 7) move towards the vulva for expulsion. The green outer membrane is indicative of the pseudocoelomic cavity surrounding all tissues in *C. elegans*. Note that the oocytes are growing in the gonad arm and all organs are not anatomically to size or in correct ratio to each other.

dependent and independent of the oocyte endocytosis pathway. Key to the secondary infection site is the escape route through the vulva that it provides. With the prolonged time in the nematode, *L. pneumophila* is able to fully go through its life cycle and enter into the CLF stage and then be expelled to infect new hosts through the vulva of the nematode. Upon death, there is a general expulsion of material from the vulva, providing a new opportunity to leave the spent host and infect new hosts.

The effectors that control apoptosis in the macrophage infection also affect *C. elegans* core apoptotic machinery. The p38 MAPK pathway has a role in apoptosis regulation, as well as effectors SidF, and DotA. The exact *C. elegans* proteins triggering the response and mechanism of interaction with the effectors is unknown.

#### **4.6 Future Directions**

To further study the pathogenesis of *L. pneumophila* in *C. elegans*, work needs to be done to identify and characterize effectors that interact with the PCD pathway. Also, further study is required to understand the interaction between *C. elegans* PCD components and effector molecule SidF. The exact regulation of p38 MAPK pathway on germline apoptosis should be studied as well as other key proteins from the other innate immune signaling pathways.

In understanding the life cycle of *L. pneumophila* in *C. elegans* the resilient infectious qualities of the expelled CLFs should be assessed for various environmental conditioning including chlorine testing, heat shock and the infectiousness of the CLFs. To further understand the involvement of the endocytosis pathway components should be investigated on an individual basis using the fluorescence protein, YP170::GFP. Also the movement of *L. pneumophila* in the

gonadal tissue the fluorescent *L. pneumophila* should be analyzed with fluorescence tagged to components of interest of *C. elegans* endocytosis pathways to confirm the use of the endocytosis pathway. Also, TEM or epifluorescence studies on the tracking of vacuole locations in the nematode should be completed to characterize their method of movement. Studies should also be done to analyze nematodes on earlier infection days to fully understand the manipulation of the intestinal membranes. The functional roles of DotA and SdhA will need to be further investigated in the RNAi *rme-2* nematodes and the  $\Delta rme-1(b1045)$  nematodes.

## References

- Aballay, A., and Ausubel, F.M. (2001). "Programmed cell death mediated by ced-3 and ced-4 protects *Caenorhabditis elegans* from *Salmonella typhimurium*-mediated killing." *PNAS* **98**(5): 2735-39
- Aballay, A., Drenkard, E., Hilbun, L.R., Ausubel, and Frederick M. (2003). "*Caenorhabditis elegans* innate immune response triggered by *Salmonella enterica* requires intact LPS and is mediated by a MAPK signaling pathway." *Curr Biol* **13**(1): 47-52
- Abu Khweek, A., Fernández Dávila, N.S., Caution, K., Akhter, A., Abdulrahman, B.a., Tazi, M., Hassan, H., Novotny, L.a., Bakaletz, L.O., and Amer, A.O. (2013). "Biofilm-derived *Legionella pneumophila* evades the innate immune response in macrophages." *Front in Cell and Infect Micro* **3**(5): 1-8
- Abu-Zant, A., Jones, S., Asare, R., Suttles, J., Price, C., Graham, J., and Kwaik, Y.A. (2007). "Anti-apoptotic signalling by the Dot/Icm secretion system of *L. pneumophila*." *Cell Microbiol* **9**(1): 246-64
- Alegado, R.A., Campbell, M.C., Chen, W.C., Slutz, S.S., and Tan, M.-W. (2003). "Characterization of mediators of microbial virulence and innate immunity using the *Caenorhabditis elegans* host-pathogen model." *Cell Micro* **5**(7): 435-44
- Alper, S., McBride, S. J., Lackford, B., Freedman, J. H. and Schwartz, D. A. (2007). "Specificity and complexity of the *Caenorhabditis elegans* innate immune response." *Mol Cell Biol* **27**: 5544-53
- Altun, Z.F., Herndon, L.A., Crocker, C., Lints, R. and Hall, D.H. (2009). "Handbook of *C. elegans* anatomy." In *WormAtlas* <http://www.wormatlas.org>
- Altun, Z.F. and Hall, D.H. (2009). "Introduction." In *WormAtlas*. [doi:10.3908/wormatlas.1.1](https://doi.org/10.3908/wormatlas.1.1)
- Altun, Z.F. and Hall, D.H. (2009). "Pericellular structures." In *WormAtlas*. [doi:10.3908/wormatlas.1.20](https://doi.org/10.3908/wormatlas.1.20)
- Andrews, H.L., Vogel, J.P., and Isberg, R.R. (1998). "Identification of linked *Legionella pneumophila* genes essential for intracellular growth and evasion of the endocytic pathway." *Infect. Immun.* **66**(3): 950-8
- Avery D.G. and Thomas, J.H. (1997). "Feeding and defecation." In *C. elegans* Volume II. Ed.s Riddle D.L., Blumenthal, T., Meyer B.J. and Priess J.R. 679-716. Cold Spring Harbor Laboratory Press

- Austin, J., and Kimble, J. (1987). “*glp-1* is required in the germ line for regulation of the decision between mitosis and meiosis in *C. elegans*.” Cell **51**: 589-99
- Balklava, Z., Pant, S., Fares, H., and Grant, B.D. (2007). “Genome-wide analysis identifies a general requirement for polarity proteins in endocytic traffic.” Nat. Cell Biol **9**:1066-1073
- Bandyopadhyay, P., Xiao, H., Coleman, H.A., Price-Whelan, A., and Steinman, H.M. (2004). “Icm / Dot-Independent Entry of *Legionella pneumophila* into Amoeba and Macrophage Hosts.” Infect. Immun. **72**(8): 4541-51
- Banga, S., Gao, P., Shen, X., Fiscus, V., Zong, W.-X., Chen, L., and Luo, Z.-Q. (2007). “*Legionella pneumophila* inhibits macrophage apoptosis by targeting pro-death members of the Bcl2 protein family.” PNAS **104**(12): 5121-6
- Berk, S.G., Ting, R.S., Turner, G.W., Ashburn, J., Ashburn, R.J. (1998). “Production of Respirable Vesicles Containing Live *Legionella pneumophila* Cells by Two *Acanthamoeba spp.*” Appl. Environ. Microbiol. **64**(1): 279-86
- Brassinga, A.K.C., Kinchen, J.M., Cupp, Meghan E., Day, Shandra R., Hoffman, Paul S., and Sifri, Costi D. (2010). “*Caenorhabditis* is a metazoan host for *Legionella*.” Cell Microbiol **12**(3): 343-61
- Brenner, S. (1973). “The genetics of behavior.” Br Med Bull **29**: 269-271
- Brenner, S. (1974). “The genetics of *Caenorhabditis elegans*.” Genetics **77**: 71-94
- Brodsky, F.M., Chen, C.Y., Knuehl, C., Towler, M.C., and Wakeham, D.E. (2001). “Biological basket weaving: formation and function of clathrin-coated vesicles.” Annu. Rev Cell Dev Biol **17**: 517-68
- Byerly, L., Cassada, R.C., and Russell, R.L. (1976). “The life cycle of the nematode *Caenorhabditis elegans*.” Dev Biol **51**: 23-33
- Cassada, R.C. and Russell, R.L. (1975). “The dauer larva, a postembryonic developmental variant of the nematode *Caenorhabditis elegans*.” Dev Biol **46**: 326-342
- C. elegans* Sequencing Consortium. (1998). “Genome sequence of the nematode *C. elegans*: a platform for investigating biology.” Science **282**(5396): 2012-8.
- Chitwood, B.G. and Chitwood, M.B. 1950. Somatic musculature, connective tissue, body cavity, and organs of body cavity. In An introduction to nematology. Chapter 4. pp 48-56. Baltimore, University Park Press
- Cianciotto, N.P. (2001). “Pathogenicity of *Legionella pneumophila*.” Int J Med Microbiol

**291:** 331-343.

Chávez, V., Mohri-Shiomi, A., Maadani, A., Vega, L.A., and Garsin, D.A. (2007). "Oxidative stress enzymes are required for DAF-16-mediated immunity due to generation of reactive oxygen species by *Caenorhabditis elegans*." Genetics **176**(3): 1567-77

Church, D.L., Guan, K.L., and Lambie, E.J. (1995). "Three genes of the MAP kinase cascade, *mek-2*, *mpk-1/sur-1* and *let-60* ras, are required for meiotic cell cycle progression in *Caenorhabditis elegans*." Development **121**(8): 2525-35

Collins, J.J., Huang, C., Hughes, S., and Kornfeld, K. (2007) "The measurement and analysis of age-related changes in *Caenorhabditis elegans*." *WormBook*, ed. The *C. elegans* Research Community, WormBook, doi/10.1895/wormbook.1.137.1, <http://www.wormbook.org>.

Conradt, B., and Horvitz, H.R. (1999). "The TRA-1A sex determination protein of *C. elegans* regulates sexually dimorphic cell deaths by repressing the *egl-1* cell death activator gene." Cell **98**: 317-27

Crofton, H.D. (1966). "Nematodes." Hutchinson, London

de Felipe, K.S., Glover, R.T., Charpentier, X., Anderson, O.R., Reyes, M., Pericone, C.D., and Shuman, H.a. (2008). "*Legionella* eukaryotic-like type IV substrates interfere with organelle trafficking." PLoS Pathog **4**(8): e1000117

Edelstein, P.H., and Edelstein, M.A. (1993). "Intracellular growth of *Legionella pneumophila* serogroup 1 monoclonal antibody type 2 positive and negative bacteria." Epidemiol Infect. Dec **111**(3): 499-502

Ellis, H.M., and Horvitz, H.R. (1986). "Genetic control of programmed cell death in the nematode *C. elegans*." Cell **44**: 817-29

Ensminger, A. W. and Isberg, R. R. (2009). "*Legionella pneumophila* Dot/Icm translocated substrates: a sum of parts." Curr Opin Microbiol **12**: 67-73

Ermolaeva, M., and Schumacher, B. (2014). "Insights from the worm: The *C. elegans* model for innate immunity." Semin Immunol <http://dx.doi.org/10.1016/j.smim.2014.04.005>

Ewann, F. and Hoffman, P. S. (2006). "Cysteine metabolism in *Legionella pneumophila*: characterization of an L-cysteine-utilizing mutant." Appl Environ Microbiol **72**: 3993-4000.

Ewbank J.J. (2002). "Tackling both sides of the host-pathogen equation with *Caenorhabditis elegans*." Microbes Infect. **4**: 247-256

Ewbank, J. J. (2006). "Signaling in the immune response." *WormBook*, ed. The *C. elegans* Research Community, WormBook, doi/10.1895/wormbook.1.83.1, <http://www.wormbook.org>

Faulkner, G., and Garduño, R.A., (2002). "Ultrastructural Analysis of Differentiation in *Legionella pneumophila*." *J. Bacteriol* **184**(24): 7025-41

Faulkner, G., Berk, S.G., Garduño, E., Ortiz-Jiménez, M.A., and Garduño, R.A. (2008). "Passage through *Tetrahymena tropicalis* triggers a rapid morphological differentiation in *Legionella pneumophila*." *J. Bacteriol* **190**(23): 7728-38

Faulkner, G., and Garduno, R.A. (2013) "Electron microscopy of *Legionella* and *Legionella*-infected cells" *Methods Mol Biol* **954**: 279-307

Fields, B.S. (1996). "The molecular ecology of *Legionellae*." *Trends Microbiol* **4**(7): 286-90.

Fields, B. S., Benson, R.F., and Besser, R.E. (2002). "*Legionella* and Legionnaires' disease: 25 years of investigation." *Clin Microbiol Rev* **15**: 506-26.

Fire A., Xu S., Montgomery, M.K., Kostas, S.A., Driver, S.E., Mello, C.C. (1998). "Potent and specific genetic interference by double-stranded RNA in *Caenorhabditis elegans*." *Nature* **391**: 806-11

Fontana, M.F., Banga, S., Barry, K.C., Shen, X., Tan, Y., Luo, Z.-Q., and Vance, R.E. (2011). "Secreted bacterial effectors that inhibit host protein synthesis are critical for induction of the innate immune response to virulent *Legionella pneumophila*." *PLoS Pathog* **7**(2): e1001289

Fontana, M.F., Shin, S., and Vance, R.E. (2012). "Activation of host mitogen-activated protein kinases by secreted *Legionella pneumophila* effectors that inhibit host protein translation." *Infect Immun* **80**(10): 3570-5

Garduño, R.A., Garduño, E., Hiltz, M., and Hoffman, P.S., (2002). "Intracellular Growth of *Legionella pneumophila* Gives Rise to a Differentiated Form Dissimilar to Stationary-Phase Forms." *Infect Immun* **70**(11): 6273-83

Garduño, R.A. (2008). "Life Cycle, Growth Cycles and Developmental Cycle of *Legionella pneumophila*." *Legionella pneumophila: Pathogenesis and Immunity*. **Ch 4**: 65-84 Springer Protocols

Gartner, A., Milstein, S., Ahmed, S., Hodgkin, J., and Hengartner, M.O. (2000). "A conserved checkpoint pathway mediates DNA damage-induced apoptosis and cell cycle arrest in *C. elegans*." *Mol Cell* **5**: 435-43

Gartner, A., MacQueen, A.J., and Villeneuve, A.M. (2004). "Methods for analyzing checkpoint responses in *Caenorhabditis elegans*." *Methods Mol Biol* **280**: 257-74

- Gartner, A., Boag, P.R., and Blackwell, T. K. (2008). "Germline Survival and Apoptosis." *WormBook*, ed. The *C. elegans* Research Community, WormBook, doi/10.1895/wormbook.1.145.1 <http://www.wormbook.org>
- Ge, J., and Shao, F. (2011). "Manipulation of host vesicular trafficking and innate immune defence by *Legionella* Dot/Icm effectors." *Cell Microbiol* **13**(12): 1870-80
- Ge, J., Xu, H., Li, T., Zhou, Y., Zhang, Z., Li, S., Liu, L., and Shao, F. (2009). "A *Legionella* type IV effector activates the NF-kappaB pathway by phosphorylating the IkappaB family of inhibitors." *PNAS* **106**(33): 13725-30
- Grant, B., and Hirsh, D. (1999). "Receptor-mediated endocytosis in the *Caenorhabditis elegans* oocyte." *Mol Biol Cell* **10**: 4311-26
- Grant, B., Zhang, Y., Paupard, M.C., Lin, S.X., Hall, D.H., and Hirsh, D. (2001). "Evidence that RME-1, a conserved *C. elegans* EH-domain protein, functions in endocytic recycling." *Nature Cell Biol* **3**(6): 573-9.
- Grant, B.D., and Sato, M. (2006). "Intracellular Trafficking" *WormBook*, ed. The *C. elegans* Research Community, WormBook, doi/ 10.1895/wormbook.1.77.1 <http://www.wormbook.org>
- Grant, B.D., and Caplan, S. (2008). "Mechanisms of EHD/RME-1 protein function in endocytic transport." *Traffic* **9**(12): 2043-52
- Gumienny, T.L., Lambie, E., Hartweg, E., Horvitz, H.R., and Hengartner, M.O. (1999). "Genetic control of programmed cell death in the *Caenorhabditis elegans* hermaphrodite germline." *Development* **126**(5): 1011-22
- Grishok, A. (2005). "RNAi mechanisms in *Caenorhabditis elegans*." *FEBS Letters* **579**:5932-9.
- Hall, D.H. (1995). "Electron microscopy and three-dimensional image reconstruction." *Methods Cell Biol* **48**:395-436
- Hall, D.H., Winfrey, V.P., Blaeuer, G., Hoffman, L.H., Furuta, T., Rose, K.L., Hobert, O., and Greenstein, D. (1999). "Ultrastructural features of the adult hermaphrodite gonad of *Caenorhabditis elegans*: relations between the germ line and soma." *Dev Biol* **212**(1): 101-23
- Hardiman, C.A., McDonough, J.A., Newton, H.J., and Roy, C.R. (2012). "The role of Rab GTPases in the transport of vacuoles containing *Legionella pneumophila* and *Coxiella burnetii*." *Biochem Soc Trans* **40**(6): 1353-9
- Harding, C.R., Stoneham, C.A., Schuelein, R., Newton, H., Oates, C.V., Hartland, E.L., Schroeder, G.N., and Frankel, G. (2013). "The Dot/Icm effector SdhA is necessary for virulence



of *Legionella pneumophila* in *Galleria mellonella* and A/J mice.” Infect. Immun. **81**(7): 2598-605

Hedgecock, E.M., Sulston, J.E., and Thomson, J.N. (1983). “Mutations affecting programmed cell deaths in the nematode *Caenorhabditis elegans*.” Science **220**: 1277–9

Hilbi, H., Segal, G., Shuman, H.A. (2001). “Icm/dot-dependent upregulation of phagocytosis by *Legionella pneumophila*.” Mol Microbiol **42**(3): 603-17

Hirsh, D., Oppenheim, D. and Klass, M. (1976). “Development of the reproductive system of *Caenorhabditis elegans*.” Dev Biol **49**: 200-19

Horvitz, H.R. (2003). “Worms, life, and death (Nobel lecture).” Chembiochem **4**: 697–711

Horwitz, M.A. (1983). “Formation of a novel phagosome by the Legionnaires’ disease bacterium (*Legionella pneumophila*) in human monocytes.” J. Exp. Med **158**: 1319–1331

Hsu, F., Zhu, W., Brennan, L., Tao, L., Luo, Z.-Q., and Mao, Y. (2012). “Structural basis for substrate recognition by a unique *Legionella* phosphoinositide phosphatase.” PNAS **109**(34): 13567-72

Irazoqui, J.E., Troemel, E.R., Feinbaum, R.L., Luhachack, L.G., Cezairliyan, B.O., and Ausubel, F.M. (2010). “Distinct pathogenesis and host responses during infection of *C. elegans* by *P. aeruginosa* and *S. aureus*.” PLoS Pathog **6**(7): e1000982

Isberg, R.R., O'Connor, T.J., and Heidtman, M. (2009). “The *Legionella pneumophila* replication vacuole: making a cosy niche inside host cells.” Nature Rev Microbiol **7**(1): 13-24

Kim, D.H., Liberati, N.T., Mizuno, T., Inoue, H., Hisamoto, N., Matsumoto, K., and Ausubel, F.M. (2004). “Integration of *Caenorhabditis elegans* MAPK pathways mediating immunity and stress resistance by MEK-1 MAPK kinase and VHP-1 MAPK phosphatase.” Proc Natl Acad Sci USA **101**:10990–4

Kimble, J.E., and Hirsh, D. (1979). “The postembryonic cell lineages of the hermaphrodite and male gonads in *Caenorhabditis elegans*.” Dev Biol **70**: 396-417

Koubar, M., Rodier, M.-H., Garduño, R.A., and Frère, J. (2011). “Passage through *Tetrahymena tropicalis* enhances the resistance to stress and the infectivity of *Legionella pneumophila*.” FEMS Microbiol Lett **325**(1): 10-5

Kurz, C.L., and Tan, M.W. (2004). “Regulation of aging and innate immunity in *C. elegans*.” Aging Cell **3**:185–93

Kwaik, Y.A., Gao, L., Stone, B.J., Venkataraman, C., and Harb, O.S., (1998). "Invasion of protozoa by *Legionella pneumophila* and its role in bacterial ecology and pathogenesis." Appl Environ Micro **64**(9): 3127-33

Laguna, R.K., Creasey, E.A., Li, Z., Valtz, N., and Isberg, R.R. (2006). "A *Legionella pneumophila*-translocated substrate that is required for growth within macrophages and protection from host cell death." PNAS **103**(49): 18745-50

Lettre, G., Kritikou, E.A., Jaeggi, M., Calixto, A., Fraser, A.G., Kamath, R.S., Ahringer, J., Hengartner, M.O. (2004). "Genome-wide RNAi identifies p53-dependent and -independent regulators of germ cell apoptosis in *C. elegans*." Cell Death Differ **11**(11): 1198-203

Lewis, J.A. and Fleming J.T. (1995). "Basic culture methods." In *Caenorhabditis elegans*, Modern biological analysis of an organism (ed. Epstein, H.F. and Shakes, D.C.). **Ch 1**. 4-27. Academic Press, California

Lints, R. and Hall, D.H. (2009). Reproductive system, somatic gonad. In *WormAtlas*. [doi:10.3908/wormatlas.1.22](https://doi.org/10.3908/wormatlas.1.22) Edited for the web by Laura A. Herndon. Last revision: February 5, 2013.

Luo, Z.-Q., and Isberg, R.R. (2004). "Multiple substrates of the *Legionella pneumophila* Dot/Icm system identified by interbacterial protein transfer." PNAS **101**(3): 841-6

Maddox, A.S. and Maddox, P.S. (2012). "High-resolution imaging of cellular processes in *Caenorhabditis elegans*." Methods Cell Biol **107**: 1-34

McGhee J. (2007). "The *C. elegans* Intestine" *WormBook*, ed. The *C. elegans* Research Community, WormBook, doi/10.1895/wormbook.1.133.1 <http://www.wormbook.org>

Menzel, R., Yeo, H.L., Rienau, S., Li, S., Steinberg, Christian E.W., and Stürzenbaum, S.R. (2007). "Cytochrome P450s and short-chain dehydrogenases mediate the toxicogenomic response of PCB52 in the nematode *Caenorhabditis elegans*." J Mol Biol **370**(1): 1-13

Millet, A.C.M., and Ewbank, J.J. (2004). "Immunity in *Caenorhabditis elegans*." Curr Opin Immunol **16**(1): 4-9

Mizuno, T., Hisamoto, N., Terada, T., Kondo, T., Adachi, M., Nishida, E., Kim, D.H., Ausubel, F.M., and Matsumoto, K. (2004). "The *Caenorhabditis elegans* MAPK phosphatase VHP-1 mediates a novel JNK-like signaling pathway in stress response." EMBO J **23**: 2226–34

Molmeret, M., Santic', M., Asare, R., Carabeo, R.A., and Abu Kwaik, Y. (2007). "Rapid escape of the dot/icm mutants of *Legionella pneumophila* into the cytosol of mammalian and protozoan cells." Infect Immun **75**(7): 3290-304

Molofsky, A.B. and Swanson, M.S. (2004). "Differentiate to thrive: lessons from the *Legionella pneumophila* life cycle." Mol Microbiol **53**: 29-40.

Newton, H. J., Ang, D. K. Y, van Driel, I. R. and Hartland, E. L. (2010). "Molecular pathogenesis of infections caused by *Legionella pneumophila*." Clin Microbiol Rev **23**: 274-298  
Nicholas, H.R., and Hodgkin, J. (2004). "The ERK MAP kinase cascade mediates tail swelling and a protective response to rectal infection in *C. elegans*." Curr Biol **14**(14):1256-61

O'Rourke, D., Baban, D., Demidova, M., Mott, R. and Hodgkin, J. (2006). "Genomic clusters, putative pathogen recognition molecules, and antimicrobial genes are induced by infection of *C. elegans* with *M. nematophilum*." Genome Res **16**: 1005-16

Palmer, C.J., Tsai, Y.L., Paszko-Kolva, C., Mayer, C., and Sangermano, L.R. (1993). "Detection of *Legionella* species in sewage and ocean water by polymerase chain reaction, direct fluorescent antibody, and plate culture methods." Appl Environ Micro **59**(11): 3618-24

Partridge, F.A., Gravato-Nobre, M.J., and Hodgkin, J. (2010). "Signal transduction pathways that function in both development and innate immunity." Dev Dynam **239**(5): 1330-6

Pinette, M.M. (2011). "Evaluating the Survival and Germline Apoptosis Levels in *C. elegans* Exposed to *L. pneumophila*" Co-op report

Rauta, P.R., Samanta, M., Dash, H.R., Nayak, B., and Das, S. (2013). "Toll-like receptors (TLRs) in aquatic animals: signaling pathways, expressions and immune responses." Immun Lett **158**(1-2): 14-24

Richards, A.M., Von Dwingelo, J.E., Price, C.T., and Abu Kwaik, Y. (2013). "Cellular microbiology and molecular ecology of *Legionella*-amoeba interaction." Virulence **4**(4): 307-14  
Riddle, D.L. (1988). "The dauer larva." In *The nematode C. elegans* (ed. W.B. Wood). **Ch 12**. 393-412. Cold Spring Harbor Laboratory Press, Cold Spring Harbor, New York

Rourke, D.O., Baban, D., Demidova, M., Mott, R., and Hodgkin, J. (2006). "Genomic clusters , putative pathogen recognition molecules , and antimicrobial genes are induced by infection of *C. elegans* with *M. nematophilum*." Letter **16**: 1005-16

Roy, C.R., Berger, K.H., and Isberg, R.R. (1998). "*Legionella pneumophila* DotA protein is required for early phagosome trafficking decisions that occur within minutes of bacterial uptake." Mol Microbiol **28**(3): 663-74

Sahu, S.N., Anriany, Y., Grim, C.J., Kim, S., Chang, Z., Joseph, S.W., and Cinar, H.N. (2013). "Identification of virulence properties in *Salmonella typhimurium* DT104 using *Caenorhabditis elegans*." PloS one **8**(10): e76673

Salinas, L.S., Maldonado, E., and Navarro, R.E. (2006). "Stress-induced germ cell apoptosis by a p53 independent pathway in *Caenorhabditis elegans*." Cell Death Diff **13**(12): 2129-39

Sato, K., Norris, A., Sato, M., and Grant, B.D. (2014). "*C. elegans* as a model for membrane traffic." *WormBook*, ed. The *C. elegans* Research Community, WormBook, doi/10.1895/wormbook.1.77.2 <http://www.wormbook.org>

Savage-Dunn, C. (2005) "TGF- $\beta$  signaling" *WormBook*, ed. The *C. elegans* Research Community, WormBook, doi/10.1895/wormbook.1.22.1, <http://www.wormbook.org>

Schulenburg, H., and Ewbank, J.J. (2004). Diversity and specificity in the interaction between *Caenorhabditis elegans* and the pathogen *Serratia marcescens*. BMC Evol Biol **4**: 49

Schulenburg, H., Hoepfner, M.P., Weiner, J., and Bornberg-Bauer, E. (2008). "Specificity of the innate immune system and diversity of C-type lectin domain (CTLN) proteins in the nematode *Caenorhabditis elegans*." Immunobiol **213**(3-4): 237-50

Schumacher, B., Hanazawa, M., Lee, M.-H., Nayak, S., Volkmann, K., Hofmann, E.R., Hofmann, R., Hengartner, M., Schedl, T., and Gartner, A. (2005). "Translational repression of *C. elegans* p53 by GLD-1 regulates DNA damage-induced apoptosis." Cell **120**(3): 357-68

Sexton, J.A., Yeo, H.-J., Vogel, J.P. (2005). "Genetic analysis of the *Legionella pneumophila* DotB ATPase reveals a role in type IV secretion system protein export." Mol Microbiol **57**(1): 70-84

Shaye, D.D., and Greenwald, I. (2011). "OrthoList: a compendium of *C. elegans* genes with human orthologs." PLoS one **6**(5): e20085

Shin, S., and Roy, C.R. (2008). "Host cell processes that influence the intracellular survival of *Legionella pneumophila*." Cell Microbiol **10**(6): 1209-20

Sifri, C.D., Begun, J., and Ausubel, F.M. (2005). "The worm has turned--microbial virulence modeled in *Caenorhabditis elegans*." Trend Microbiol **13**(3): 119-27

Steinert, M., Hentschel, U. and Hacker, J. (2002). "*Legionella pneumophila*: an aquatic microbe goes astray." FEMS Microbiol Rev **26**: 149-62

Sulston, J.E., and Horvitz, H.R. (1977) "Post-embryonic cell lineages of the nematode, *Caenorhabditis elegans*." Dev Biol **56**(1): 110-56

Sulston, J.E., Schierenberg, E., White J.G., and Thomson, J.N. (1983). "The embryonic cell lineage of the nematode *Caenorhabditis elegans*." Dev Biol **100**: 64-119

Sulston, J. & Hodgkin, J. (1988). "Methods. in: Wood, W.B. (ed.) The Nematode *Caenorhabditis elegans*." Cold Spring Harbor Laboratory, Cold Spring Harbor: 587-606

Tan, F.J., Zuckerman, J.E., Wells, R.C., and Hill, R.B. (2011). "The *C. elegans* B-cell lymphoma 2 (Bcl-2) homolog cell death abnormal 9 (CED-9) associates with and remodels LIPID membranes." Prot Sci **20**(1): 62-74

Tan, M.W., Mahajan-Miklos, S., and Ausubel, F.M. (1999). "Killing of *Caenorhabditis elegans* by *Pseudomonas aeruginosa* used to model mammalian bacterial pathogenesis." PNAS **96**(2): 715-20

Tan, M.W., Rahme, L.G., Sternberg, J.A., Tompkins, R.G., and Ausubel, F.M. (1999). "*Pseudomonas aeruginosa* killing of *Caenorhabditis elegans* used to identify *P. aeruginosa* virulence factors." PNAS **96**(5): 2408-13

Tenor, J.L., McCormick, B.A., Ausubel, F.M., Aballay, A., and Carolina, N. (2004). "*Caenorhabditis elegans* -Based Screen Identifies *Salmonella* Virulence Factors Required for Conserved Host-Pathogen Interactions." Curr Biol **14**: 1018-24

Troemel, E.R., Chu, S.W., Reinke, V., Lee, S.S., Ausubel, F.M. and Kim, D. H. (2006). "p38 MAPK regulates expression of immune response genes and contributes to longevity in *C. elegans*." PLoS Genet **2**: e183

Urwyler, S., Brombacher, E., and Hilbi, H. (2009). "Endosomal and secretory markers of the *Legionella*-containing vacuole." Commun Integrat Biol **2**(2): 107-9

Vincent, C.D., Friedman, J.R., Jeong, K.C., Buford, E.C., Miller, J.L., and Vogel, J.P. (2006). "Identification of the core transmembrane complex of the *Legionella* Dot/Icm type IV secretion system." Mol Microbiol **62**(5): 1278-91

Welsh, C. T., Summersgill, J. T. and Miller, R. D. (2004). "Increases in c-Jun N-Terminal kinase/stress-activated protein kinase and p38 activity in monocyte-derived macrophages following the uptake of *Legionella pneumophila*." Infect Immun **72**: 1512-1518

Woo, A.H., Goetz, A., and Yu, V.L. (1992). "Transmission of *Legionella* by respiratory equipment and aerosol generating devices." Chest **102**: 1586-90

Wood, W.B. (1988). "Introduction to *C. elegans* biology." In The nematode *C. elegans* (ed. W.B. Wood). **Ch 1**. 1-16. Cold Spring Harbor Laboratory Press, Cold Spring Harbor, New York

Zhang, Y., Grant, B., and Hirsh, D. (2001). "RME-8, a conserved J-domain protein, is required for endocytosis in *Caenorhabditis elegans*." Mol Biol Cell **12**: 2011-21

Zhou, Z., Hartwig, E., and Horvitz, H.R. (2001). "CED-1 is a transmembrane receptor that mediates cell corpse engulfment in *C. elegans*." Cell **104**(1): 43-56

Zink, S.D., Pedersen, L., Cianciotto, N.P., and Kwaik, Y.A. (2002). "The Dot / Icm Type IV Secretion System of *Legionella pneumophila* Is Essential for the Induction of Apoptosis in Human Macrophages." Infect Immun **70**(3): 1657-63